ISTANBUL TECHNICAL UNIVERSITY ★ INSTITUTE OF SCIENCE AND TECHNOLOGY

LUMPED PARAMETER MODELS FOR LOW-TEMPERATURE GEOTHERMAL RESERVOIRS

Ph.D. Thesis by

Hülya SARAK, M.Sc.

(505972121)

Date of submission : 9 February 2004

Date of defence examination: 19 April 2004

Supervisor (Chairman): Prof. Dr. Abdurrahman SATMAN

Members of the Examining Committee Prof.Dr. Mustafa ONUR (ITU)

Prof.Dr. Argun GÜRKAN (ITU)

Prof.Dr. Hasan YAZICIGİL (ODTU)

Assist. Prof.Dr. Niyazi AKSOY (DEU)

APRIL 2004

İSTANBUL TEKNİK ÜNİVERSİTESİ ★ FEN BİLİMLERİ ENSTİTÜSÜ

DÜŞÜK SICAKLIKLI JEOTERMAL REZERVUARLAR İÇİN BOYUTSUZ REZERVUAR MODELLERİ

DOKTORA TEZİ

Y. Müh. Hülya SARAK

(505972121)

Tezin Enstitüye Verildiği Tarih : 9 Şubat 2004

Tezin Savunulduğu Tarih : 19 Nisan 2004

Tez Danışmanı : Prof. Dr. Abdurrahman SATMAN

Diğer Jüri Üyeleri : Prof.Dr. Mustafa ONUR (İTÜ)

Prof.Dr. Argun GÜRKAN (İTÜ)

Prof.Dr. Hasan YAZICIGİL (ODTÜ)

Yrd. Doç.Dr. Niyazi AKSOY (DEÜ)

NİSAN 2004

ACKNOWLEDGEMENTS

I would like to present my endless thanks to my advisor, Prof. Dr. Abdurrahman Satman, for his encouragement, guidance, support and patience during my Ph.D. study. He had given useful criticism and assistance during all stages of this dissertation. It was a great honor working with him.

My deepest appreciation goes to Prof. Dr. Mustafa Onur for providing Levenberg-Marquardt optimization procedure in a Fortran code and for his useful comments on all kinds of problems involved during my Ph.D. study.

I address my sincere gratitude to Balcova Jeotermal Ltd. and especially to Assist. Prof. Niyazi Aksoy for providing the field data about Balcova-Narlidere Geothermal System.

Also my very special thanks are addressed to the Department of Petroleum and Natural Gas Engineering at Istanbul Technical University for providing sources during my Ph.D. study. Financial support was provided by the Istanbul Technical University Research Foundation and is acknowledged.

I would also like to thank the Geothermal Institute of Auckland University for introducing me into World of Geothermal Energy.

At last but not least I would like to say my grateful thanks to my family and my husband for their support and patience during my graduate studies.

April 2004 **Hülya SARAK**

TABLE OF CONTENTS

LIST OF TABLES

LIST OF FIGURES

SYMBOLS

C : Specific heat at constant volume
c : Compressibility
E : Internal energy of total system
f : Model function
h : Enthalpy
J : Objective function
M : Total number of model function
n : Number of observations
p : Pressure
Q : Net heat conducted to reservoir
T : Temperature
t : Time
V : Volume
v : Specific volume
W : Mass
w : Mass rate
$w_{j,i}$: Positive weight
x : Steam quality
y : Measured value

Greek Symbols:
ϕ : Porosity, %
ρ : Density
α : Recharge constant
κ : Storage capacity
χ : l-Dimensional column vector
Δ : Difference

Subscripts:
a : Aquifer
$a1$: Inner aquifer
$a2$: Outer aquifer
c : Current condition
e : Water influx
g : Steam
i : Initial condition
inj : Reinjection
L : Loss
p : Production
p,net : Net production (production-reinjection)
$p,net1$: Net production of shallow reservoir
$p,net2$: Net production of deep reservoir

r : Reservoir
$r1$: Shallow reservoir
$r2$: Deep reservoir
ss : Steady state flow
t : Reservoir formation and contained fluid
w : Water

Superscripts:
T : Transpose of a matrix
$\rightarrow$: Vector
$'$: Derivative

LUMPED PARAMETER MODELS FOR LOW-TEMPERATURE GEOTHERMAL RESERVOIRS

SUMMARY

Lumped parameter modeling which is also known as zero-dimensional modeling, is used most commonly at the beginning of the life of a field, when relatively little information is available for the field. Generally, in all lumped parameter models, the reservoir is described as a single homogeneous tank with average properties. The pressure (and/or water level) changes in the reservoir are modeled by using mass and energy balances and therefore, the potential of the field can be predicted under various production/reinjection scenarios.

The main objective of this dissertation is to model pressure (or water level) behavior of the low-temperature liquid dominated geothermal reservoirs. The tools with the objectives are to be achieved by a simpler approach known as lumped parameter models and analytical models are obtained by well known material balance equations. Since no boiling takes place during the production of low temperature – high pressure liquid dominated geothermal reservoirs, the actual path would be essentially isothermal. Therefore, in our lumped models valid for low-temperature liquid dominated geothermal reservoirs, only mass balance is applied and energy balance is neglected.

In this study, reservoir and aquifer are represented by different tanks and the effect of recharge on the performance is studied. The reservoir in which the production/reinjection occurs represents the innermost part of the geothermal system. The changes in pressure and/or water level are monitored and production/reinjection rates are recorded. The aquifer in which neither production nor reinjection occurs, recharges the reservoir. The production causes the pressure in the reservoir to decline, which results in water influx from the aquifer to the reservoir. The recharge source represents the outermost part of the geothermal system and recharges the aquifer.

Tank systems used in modeling to represent the geothermal system can be classified as; (a) 1 reservoir with recharge source (1-Tank Model), (b) 1 reservoir-1 aquifer with/without recharge source (2-Tank Model), (c) 1 reservoir-2 aquifers with/without recharge source (3-Tank Model), (d) 1 shallow reservoir-1 deep reservoir with recharge source (2 Reservoir Tanks Without Aquifer Model), (e) 1 shallow reservoir-1 deep reservoir-1 aquifer with recharge source (2 Reservoir Tanks With Aquifer Model).

The outer aquifer boundary is investigated in 2- and 3-tank models. If the aquifer tank is supported by a constant pressure recharge source the system is called as "Open System" and if it has no flow boundary the system is called as "Closed System". The model equations are obtained for both open and closed systems.

Moreover, unsteady-state flow behavior of recharge is modeled by using more than 1 aquifer tank (e.g. 2- and 3-tank models).

The advantage of the 2 reservoir tank models, in which the reservoir is represented by 1 shallow and 1 deep reservoir tanks, over the 1-, 2- and 3-tank models, in which the reservoir is represented by 1 reservoir tank, is that the shallow and deep parts of the field can be treated separately. Therefore, several production and reinjection scenarios such as 1) production and reinjection for both zones, 2) production from the deeper one and reinjection into the shallow one, or vice versa, can be investigated.

Natural recharge is taken into account by applying Schilthuis steady-state water influx model between the tanks (aquifer-reservoir, recharge source-aquifer, and recharge source-reservoir).

The early-time and the late-time reservoir pressure behavior can be easily handled by asymptotic expressions of the analytical solutions, since the governing equations are obtained as simple analytical expressions. During the early-time production period, the reservoir pressure decreases linearly with the production time as a function of production/reinjection rate and, reservoir storage capacity. The reservoir pressure during the long-term production in closed systems continuous to decline as a function of production/reinjection rate and, the system (aquifer + reservoir) storage capacities. However, in open systems the reservoir pressure stabilizes at a constant value as a function of production/reinjection rate, and aquifer and reservoir recharge constants.

Model results for constant production/reinjection flow rates are given in the form of analytical expressions and variable flow rate case is modeled by Duhamel's Principle.

The models are used to match the long-term measured water level or pressure response to a given production/reinjection history. For history matching purposes, Levenberg-Marquardt optimization algorithm is used to minimize an objective function based on weighted least-squares for estimating relevant aquifer/reservoir parameters. In addition, standard 95% confidence intervals are computed to assess uncertainty in the estimated parameters. Moreover, the standard deviation of errors as well as the root mean square errors (RMS) are also computed for each data set matched to show the matching quality as quantitatively.

Four field examples (Laugarnes, Glerardalur and Svartsengi geothermal fields located in Iceland and the Balcova-Narlidere geothermal field located in Turkey) are studied to demonstrate the applicability and validity of the models and optimization algorithm. The measured and simulated water level changes obtained from the models are discussed. The modeling results for the field cases (especially Balcova-Narlidere geothermal field case) show that the inaccuracy as well as the discontinuity of the input data such as the production/reinjection flow rates and the water level measurements greatly affect the confidence intervals and RMS values computed from the matching analysis of the model. A longer and continuous history of production/reinjection and water level data with accuracy definitely increases the reliability of the matching procedure. Moreover, reliability of the selected model increases by considering available geologic, geophysical, hydraulic data.

DÜŞÜK SICAKLIKLI JEOTERMAL REZERVUARLAR İÇİN BOYUTSUZ MODELLER

ÖZET

Yeni bulunan jeotermal sahalar için elde yeterli miktarda veri bulunmaması nedeniyle sıfır-boyutlu modelleme olarak da bilinen boyutsuz rezervuar modellemesi sıkça kullanılan bir yöntemdir. Boyutsuz rezervuar modellerinde rezervuar ve akifer homojen tanklar olarak tanımlanmakta ve bu tanklarda rezervuar ve akiferin ortalama özellikleri kullanılmaktadır. Rezervuarın basıncı (veya su seviyesi) tanklarda kütle ve enerji dengesi kurularak modellenmektedir. Böylece çeşitli üretim/tekrar-basma senaryoları için sahanın potansiyeli tahmin edilebilmektedir.

Bu doktora çalışmasının başlıca amacı düşük sıcaklıklı sıvının etken olduğu jeotermal rezervuarların basınç (veya su seviyesi) davranışını modellemektir. Bu amaçla boyutsuz rezervuar modelleri kullanılmakta ve bilinen kütle denge denklemleri kullanılarak analitik modeller geliştirilmektedir. Düşük sıcaklıklı ve yüksek basınçlı sıvının etken olduğu jeotermal rezervuarlarda üretim dönemi süresince rezervuar iki faza geçmediği için sistem içinde izotermal koşullar geçerlidir. Bu nedenle bu çalışmada sadece kütle dengesi kullanılarak, enerji dengesi ihmal edilmektedir.

Bu çalışmada, jeotermal sistemi oluşturan rezervuar ve akifer ayrı ayrı tanklar olarak temsil edilmekte ve beslenme kaynağının etkisi incelenmektedir. Rezervuar üretim ve tekrar-basmanın gerçekleştiği jeotermal sistemin iç bölgesini temsil etmektedir. Basınç ve/veya su seviyesindeki değişiklikler gözlemlenerek, üretim/tekrar-basma debileri kayıt edilmektedir. Üretim ve tekrar-basma yapılmayan bölge olan akifer ise rezervuarı beslemektedir. Rezervuardan yapılan üretim nedeniyle rezervuar basıncı düşmekte ve akiferden rezervuara su girişi olmaktadır. Jeotermal sistemin dış bölgesini temsil eden beslenme kaynağı ise akiferi beslemektedir.

Modellemede kullanılan tank sistemleri: (a) 1 rezervuar tankı ve beslenme kaynağı (1-Tank Modeli), (b) 1 rezervuar, 1 akifer ve beslenme kaynağı (2-Tank Modeli), (c) 1 rezervuar, 2 akifer ve beslenme kaynağı (3-Tank Modeli), (d) 1 sığ rezervuar, 1 derin rezervuar ve beslenme kaynağı (Akifersiz 2 Rezervuar Tankı Modeli), (e) 1 sığ rezervuar, 1 derin rezervuar, 1 akifer ve beslenme kaynağı (Akiferli 2 Rezervuar Tankı Modeli) şeklinde sıralanabilmektedir.

Yukarıdaki modellerde akifer tankının dış sınırından sabit basınçlı bir beslenme kaynağından beslenmesi (Açık Sistem) ve dış sınırından beslenme olmaması (Kapalı Sistem) durumları da göz önünde bulundurulmakta ve model çözümleri bu iki farklı durum için sunulmaktadır. Ayrıca, birden fazla akifer tankının kullanılması (2- ve 3-tank modelleri) beslenmenin kararsız akışını modellenmeye olanak sağlamaktadır.

Rezervuarın 1 sığ ve 1 derin rezervuar tankı olarak temsil edildiği 2 rezervuar tankı modellerinin rezervuarın bir rezervuar tankı ile temsil edildiği 1-, 2- ve 3- tank

modellerine göre en büyük avantajı, sahadaki sığ ve derin üretim tabakalarının ayrı ayrı incelenmesine olanak sağlamasıdır. Böylece her iki üretim tabakasından (sığ ve derin) üretim/tekrar-basma yapılması veya herhangi birinden üretim ve diğerinde tekrar-basma yapılması durumunda sahanın davranışını modellemek olasıdır.

Tanklar arasındaki (akifer-rezervuar, beslenme kaynağı-akifer ve beslenme kaynağı-rezervuar) doğal beslenme için Schilthuis kararlı akış su girişi modeli kullanılmaktadır.

Model denklemleri basit analitik ifadeler şeklinde elde edildiğinden modellerin erken ve geç zaman davranışları kolaylıkla incelenebilmektedir. Zamanın erken dönemlerinde rezervuar basıncı üretim/tekrar-basma debisi ve rezervuarın depolama kapasitesinin bir fonksiyonu olarak zamanla doğrusal olarak azalmaktadır. Zamanın geç dönemlerinde ise kapalı sistemlerde rezervuar basıncı üretim/tekrar-basma debisi ve sistemin (rezervuar + akifer) depolama kapasitesine bağlı olarak azalmaya devam etmekte ancak açık sistemlerde üretim/tekrar-basma debisi ve akifer ve rezervuarın beslenme katsayısının bir fonkisyonu olarak sabit bir değerde sabitlenmektedir.

Model sonuçları sabit debide üretim/tekrar-basma durumunda analitik ifadeler şeklinde verilmekte ve daha genel değişken debili üretim/tekrar-basma durumları geliştirilen sabit debili analitik çözümlere Duhamel ilkesinin uygulanmasıyla modellenmektedir.

Geliştirilen modelerden elde edilen basınç (veya su seviyesi) verileri uzun dönem ölçülmüş basınç (veya su seviyesi) verileri ile çakıştırılmakta akifer/rezervuar özellikleri tahmin edilmektedir. Geçmiş zamanlara ait verilere çakıştırma yapmak amacıyla, optimizasyon yöntemlerinden Levenberg-Marquardt yöntemi kullanılarak doğrusal olmayan ağırlıklı en küçük-kareler yöntemi üzerine kurulu hedef fonksiyonu minimize edilmektedir. Tahmin edilen parametrenin güvenilirliğini belirlemek amacıyla standart %95 güvenilirlik aralığı hesaplanmaktadır. Ayrıca, çakışmanın uyum derecesini niteliksel olarak olarak değerlendirmek için çakışmaya ait RMS (sapmaların karelerinin toplamının ortalamasının karakökü) değeri hesaplanmaktadır. RMS değeri küçüldükçe, model sonuçları ile saha verilerinin çakışması iyileşmekte ve parametreler için elde edilen %95 güvenilirlik aralıkları küçüldükçe parametreler daha güvenilir hesaplanmaktadır.

İzlanda'da bulunan Laugarnes, Glerardalur ve Svartsengi jeotermal sahaları ile Türkiye'de bulunan Balçova-Narlıdere jeotermal sahasına ait veriler kullanılarak bu çalışmada geliştirilen modellerin ve optimizasyon tekniğinin uygulaması yapılmaktadır. Modellerden elde edilen su seviyesi değişimlerinin ölçülen su seviyesi değişimleri ile gösterdiği uyum tartışılmaktadır. Yapılan saha uygulamaları (özellikle Balçova-Narlıdere uygulaması) üretim/tekrar-basma debileri ve su seviyesi ölçümlerinin sürekliliğinin, %95 güvenilirlik aralıklarını ve RMS değerlerini oldukça fazla etkilediğini göstermektedir. Modellere giriş verileri olan üretim/tekrar-basma debileri ve su seviyesi ölçümlerinin uzun dönemde ve sürekli yapılmış olması model ile saha verileri arasındaki çakışmanın güvenilirliğini kesinlikle arttırmaktadır. Ayrıca, modelleme çalışmasından bulunan sonuçların eldeki diğer veriler ve bilgilerle (jeolojik, jeofizik, hidrolojik vb) desteklenmesi seçilen modele olan güvenilirliği arttıracaktır.

1. INTRODUCTION

Geothermal energy has been known and used for centuries. Records show that the Chinese, Romans, Turks, Japanese, Icelanders, Central Europeans and the Maori people of New Zealand have used the geothermal resources for heating, bathing and cooking. Commercial utilization of geothermal resources for energy production only started in the early 1900's. Electricity production was initiated in Larderello, Italy, in 1904 and operation of the largest geothermal district heating system in the world in Reykjavik, Iceland, started in 1930.

Utilization of geothermal energy depending on their temperature has increased steadily since the natural forms of energy are readily available at low development cost. With respect to reservoir temperature at economic depths (1000 m), geothermal reservoirs can be classified as (Axelsson and Gunnlaugsson, 2000; Satman, 2003);

- Low-temperature geothermal reservoirs; the reservoir temperature is below 150°C. They are used dominantly in direct utilization (district heating, etc.) plants.
- High-temperature geothermal reservoirs; the reservoir temperature is above 200°C. They are commonly used to generate electricity.

It should be suitable to describe some definitions related with geothermal energy:

1) Geothermal Field usually indicates an area of geothermal activity at the earth's surface. In cases without surface activity this term may be used to indicate the area at the surface corresponding to the geothermal reservoir below.

2) Geothermal System refers to all parts of the hydrological system involved, including the recharge zone, all subsurface parts and the outflow of the system. Figure 1.1 shows a schematic of a geothermal system. A geothermal reservoir is usually surrounded by colder rocks that are hydraulically connected with the reservoir. Hence, water may move from colder rocks outside (recharge) towards the reservoir, where hot fluids move under the influence of buoyancy forces towards a

discharge area. The whole volume of rocks in which fluids move both inside and outside the reservoir, together with the heat source and the natural discharge, constitute a geothermal system. In some reservoirs, natural recharge may be induced by exploitation; in others, recharge can be provided artificially by injection of cold water.

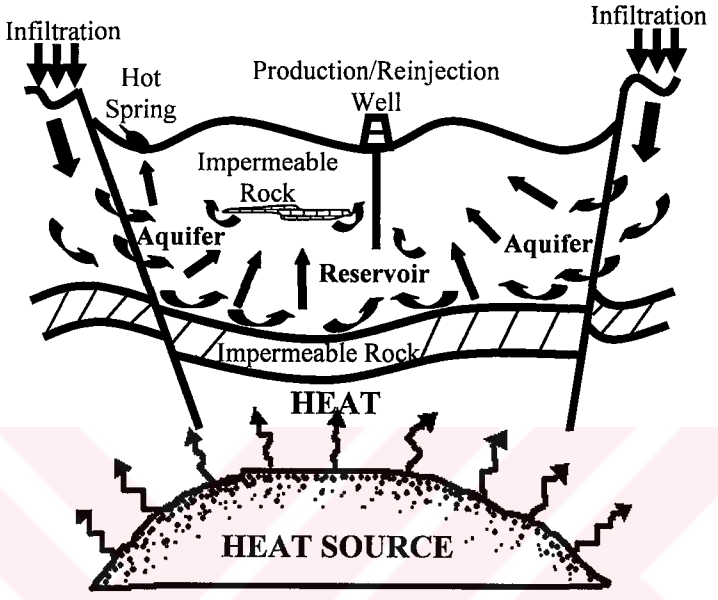

Figure 1.1 Schematic of a geothermal system.

3) Geothermal Reservoir describes a volume of rocks where geothermal fluids are stored and produced. The main properties of a geothermal reservoir are porosity and permeability. The porosity of a reservoir rock is used to assess the volume of fluids stored in a reservoir and the permeability controls flow rate of the produced fluid. In Turkey, most of the geothermal reservoirs consist of fractured and faulted zones, which occur often as a result of recent tectonic activities. Deeply-penetrating meteoric waters sweep some heat from the deeper part of the fractured and faulted zone and then, due to its low gravity, the heated fluids ascend within a segment of the fracture zone.

Geothermal reservoirs are more commonly classified depending on their physical state as;

- Liquid-dominated geothermal reservoirs: Figure 1.2 shows a pressure-temperature diagram for pure water, indicating critical point and boiling point curve. The water temperature is at, or below, the boiling point curve at the

prevailing pressure and the water phase controls the pressure in the reservoir. Some steam may be present, however. Pressure in the reservoir is close to hydrostatic pressure.

- Two-phase geothermal reservoirs: The two phases co-exist and the temperature and pressure follow boiling point curve.
- Vapor-dominated geothermal reservoirs: The water temperature is at, or above, the boiling point curve at the prevailing pressure and the steam phase controls the pressure in the reservoir. Some water may, however, be present. Pressure in the reservoir is close to steam-static pressure.

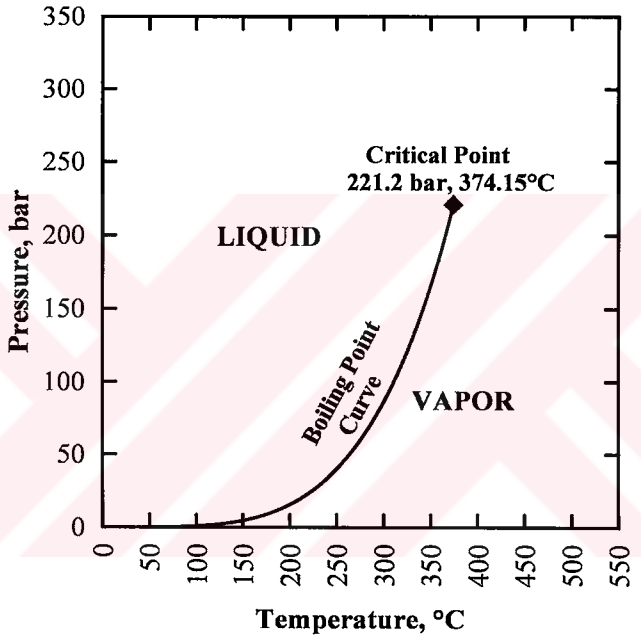

Figure 1.2 Pressure – temperature diagram for pure water.

4) Aquifer is an underground stratum that will yield water in sufficient quantity as a source supply. Geothermal reservoirs are bounded by aquifers. In response to the production, the reservoir pressure drops and the aquifer reacts to offset or retard pressure decline by natural recharge. Natural recharge occurs by expansion of the water and/or compressibility of the aquifer rock. How much, and how fast, the natural recharge is determined by the rate of production, on one hand, and the size and properties of the aquifer, on the other hand.

As a result of the growing need throughout the world for increasing utilization of geothermal energy in many different sectors such as generating electricity, district heating, etc., the reservoir management has become a significant step. Some

important questions of reservoir management, such as production capacity of the geothermal field, the rate of the pressure decline, the effect of recharge and reinjection on the field performance, are primary objectives of geothermal reservoir modeling.

Typically, a reservoir model describes the change in reservoir pressure as a function of time or cumulative fluid production. Mainly, three methods are currently available in literature for modeling the behavior of geothermal reservoirs. They are decline curve analysis, lumped parameter models, and numerical models.

Decline Curve Analysis is used to predict future well decline and cumulative production by fitting algebraic equations to observed flow rate decline data from wells. The predicted flow decline can then be used to estimate the number of makeup (additional) wells that will be needed in the future.

Lumped Parameter Models generally use two blocks to represent the entire system. One of the blocks represent the main reservoir and the other acts as a recharge block or an aquifer. Average properties are assigned to reservoir and aquifer blocks, and the changes of reservoir pressure, temperature, and production are monitored. The material and/or heat entering and leaving are used in material and/or energy balance equations. The governing equations under idealized conditions can sometimes be reduced to ordinary differential equations that can be solved semi-analytically. Lumped parameter models are generally calibrated against a pressure history. After a history match is obtained, the model is used to predict future average reservoir pressure. The main advantage of the lumped parameter models is their simplicity. Some of the disadvantages are that (1) they do not consider fluid flow within the reservoir and neglect spatial variations in thermodynamic conditions and reservoir properties, (2) they cannot simulate fronts such as phase or thermal fronts because of coarse space discretization, and (3) they cannot consider questions of well spacing or injection well locations.

Numerical Models are very general models that can be used to simulate reservoirs with few or many (>100 to 1000) gridblocks. They can be used to simulate entire geothermal system, including reservoir, caprock, bedrock, shallow cold aquifers, recharge zones, etc. They allow spatial variations in rock, fluid, and well properties and thermodynamic conditions. The principal advantage of numerical models is that they have all mathematics built into computer code and allow the user to decide how

detailed the simulation should be and what physical processes should be considered. Disadvantage of the numerical models is the need for more input data.

Reservoir assessment is a continuous process from the time a geothermal field is discovered to the time its development is completed. The various methods are most applicable at different stages of the project. It is generally advisable to start with the simplest method such as a lumped parameter model, since relatively little information is known at the beginning of the life of a reservoir. On the other hand, numerical models which require more information are appropriate at late stages, since great amount and quality of field data are available.

1.1 Literature Review

This part reviews pertinent literature on the subject of water influx (or recharge) models, geothermal reservoir modeling, and lumped parameter models.

1.1.1 Water influx models

Geothermal and petroleum reservoirs are in some respects similar. One of their similarities is the recharge or water influx from the aquifers and the other one is material balance. Methods developed for petroleum reservoirs involving water influx and material balance can be adopted for geothermal reservoirs. In this part of the literature survey, water influx and material balance methods in petroleum engineering are investigated as a first step.

Schilthuis (1936) analyzed the reservoir pressure decline as related to production of oil and gas production. He pointed out that the lowering pressure in the oil and gas reservoirs which have a good connection with strata containing water, causes water encroachment and that retards the decline in reservoir pressure. Schilthuis steady-state water influx model states that the rate of water influx is proportional to the pressure gradient that exists between the water-bearing strata and the oil and gas reservoir. For practical purposes, the value of this gradient would be the difference between the value of the original reservoir pressure and any subsequent value.

As different from Schilthuis steady-state model, van Everdingen and Hurst (1949) studied unsteady-state water influx. They included a time-dependent term in the calculations for water influx. The tables which present dimensionless pressure and

water influx as a function of dimensionless time, were constructed for two inner boundary (constant terminal rate and constant terminal pressure) and two outer boundary (finite and infinite reservoirs) conditions as a result of their work.

Chatas (1970) indicated a method for estimating aquifer parameters such as the size of the aquifer, its mobility, and a characteristic constant, from an investigation of the reservoir performance. To achieve this objective he analyzed the material balance and diffusivity equations considering unsteady-state water influx. The least squares method was applied to determine three aquifer parameters.

An approach that utilizes pseudosteady-state aquifer productivity index and an aquifer material balance to simulate water influx was presented by Fetkovich (1971). In his model, water influx problem was separated into a rate equation and a material balance equation, therefore superposition was not required and this made the concepts and calculations quite simple and easy to apply.

Fanchi (1985) developed some simple analytical expressions for the van Everdingen and Hurst aquifer influx influence functions by using linear regression analysis. Regression results were presented for a variety of aquifer radius/reservoir radius ratios.

Allard and Chen (1988) suggested a new water influx model that differs from traditional approaches in that it includes the effect of vertical flow at the reservoir/aquifer interface. The results were introduced in the form of dimensionless groups, which makes the model readily applicable to a wide range of systems.

Six sets of simple polynomials that provide a fast, simple method to determine van Everdingen and Hurst dimensionless variables for finite or infinite radial aquifers, were reported by Klins et al. (1988).

Brigham (1998) investigated two inner boundary conditions-constant pressure or constant flow rate, and three outer boundary conditions-infinite, closed and constant pressure, and three geometries - linear, radial and spherical as a point of view of water influx. The solutions were presented in the form of infinite series, and as well as in very simple closed form equations.

Permadi et al. (1998) have modeled multiphase flow of oil and water in reservoirs with water influx by modifications of single-phase semi-analytical solutions. To

calculate water influx, they used the Fetkovich method instead of using an analytical solution restricted by a specified condition at the outer reservoir boundary.

Nishikioriand Hayashida (1999) described the multi-disciplinary approach to investigate and model complex water influx into water driven sandstone reservoir in Khafji Oil Field in Arabian Gulf. They mentioned two kinds of water influx – one is conventional edge water and another is supplemental water invasion from the aquifer of the lower reservoir through conductive faults – depending on the geological description of this field. The complex nature of water influx were accurately modeled by use of precise classification of rock type and adoption of pseudo relative permeability accounting for upward increasing or decreasing trend of permeability.

1.1.2 Numerical models

A number of different methods for modeling the behavior of geothermal reservoirs have been reported in the reservoir engineering literature.

Horne and O'Sullivan (1977) considered the problem of a hypothetical geothermal reservoir that depletes the fluid saturating its upper regions during production. The objective of their study was to achieve a better understanding of the Wairakei geothermal reservoir in New Zealand and of other similar type. They mentioned that the depletion leads to the characteristic depressurization and drawdown of liquid level observed at Wairakei. The model they described was the end result of a sequence of numerical models, each building on the conclusions of the last, and was a single-phase axisymmetric representation in which fluid was withdrawn through bores grouped around the axis and replaced at the surface.

Zyvoloski and O'Sullivan (1980) described a model to simulate gas-dominated, two-phase geothermal reservoirs. The basic equations governing the behavior of a two-phase mixture of carbon dioxide and water were discussed. A Newton-Raphson scheme, based on the alternating direction implicit method for multidimensional problems, was used to solve the nonlinear finite difference approximation of the governing nonlinear system of partial differential equations. As conclusion, sample calculations showing the behavior of hypothetical reservoirs with varying carbon dioxide contents were presented.

Goyal and Kassoy (1981) reported a two-dimensional vertical planar model of the East Mesa system in the Imperial Valley of California. Their primary goal was to

show that the concept of fault zone controlled charging of a geothermal reservoir like that hypothesized at East Mesa was plausible. They calculated the recharge rate to the fault, vertical variations of horizontal velocities within the aquifer, temperature fields in the aquifer and caprock, and surface heat flows.

One of the studies on fault-charged reservoirs was presented by Bodvarsson et al. (1982). The model was fully transient and included conductive heat transfer to the caprock and bedrock. Since vertical variations in temperature and velocity within the aquifer were ignored, the model is most applicable to relatively thin aquifer systems.

Marcou and Gudmundsson (1986) used a geothermal development model to study the effect of reservoir deliverability and different power plant schemes on the economics of geothermal electric power. They pointed out that how the development cost of geothermal electric power projects can be estimated. The deliverability of liquid-dominated reservoirs were investigated in terms of reservoir performance, inflow performance, and wellbore performance. The inflow performance was given in terms of a linear productivity index for liquid-only flow, and a solution-gas drive relationship for two-phase flow. The production histories of the liquid-dominated Ahuachapan in El Salvador and Wairakei in New Zealand reservoirs were successfully matched using the radial form of Hurst's simplified water influx method.

State-of-the-art reviews of geothermal modeling have been made by various authors (Bodvarsson et al., 1986; Pruess, 1990; Sanyal et al., 2000). Bodrasson et al. (1986) pointed out that no universal modeling strategy is applicable to all of the geothermal systems since geothermal systems are very complex, exhibiting such features as fracture-dominated flow, phase change, chemical reactions, and thermal effects. He summarized the kinds of geothermal models and emphasized their applicabilities. The various modeling tasks – including natural-state, exploitation, injection, multicomponent, and subsidence modeling – were illustrated with geothermal field examples.

Pruess (1990) concerned that how good the available simulation technology is , and what we have learned from applications of simulators, both in terms of improved understanding of geothermal reservoir dynamics, and in terms of improved engineering of geothermal energy projects. He examined some applications of

numerical modeling to studies of reservoir dynamics, well test design and analysis, and modeling of specific fields.

Bullivant et al. (1991) worked on speeding up the geothermal simulator MULKOM by using fast conjugate solver. Also a graphics package for preparing data for, and processing output from MULKOM was discussed.

Richards and Wallroth (1995), and Kohl and Hopkirk (1995) reviewed a number of current hot dry rock modeling approaches.

1.1.3 Lumped parameter models

Several lumped parameter models have been reported in the literature. These models allow to simulate reservoirs where there is little history of production and a minimum knowledge of the reservoir parameters.

Sanyal et al. (1976) suggested a simplified analytical approach for fluid flow and heat transfer in a geothermal reservoir with a circular array of production wells surrounded by a circular array of injection wells. The model was assumed to be a vertical stack of horizontal layers, permeable and impermeable layers alternating. The heat transfer problem was handled by a modification of the solution to the problem of heat extraction from fractured dry rocks proposed by Gringarten. The pressure distribution in various layers were calculated by spatial superposition of the continuous line source solution for the given geometry and assuming average fluid properties within the system. As a result of this approach, the breakthrough time of injected water in each layer, the pressure distribution in space and time, and the temperature of the produced water over time were modeled by semi analytical solutions.

Whiting and Ramey (1969), and Brigham and Ramey (1981) developed lumped parameter models by using material and energy balances. Water influx models for hemispherical, linear, and radial flow were used. In all three cases, flow was assumed to be isothermal liquid water of constant viscosity, compressibility, and enthalpy. Viscous flow, such that Darcy's law applies, was also assumed. They pointed out that the governing equations are useful for estimating the initial reservoir conditions and for matching the past performance and predicting the future performance of reservoirs.

Castanier et al. (1980), and Castanier and Brigham (1983) described an analytical model for simulation of geothermal reservoirs. Their model can be applied to any type of geothermal reservoirs such as all liquid, all steam or two phase. The model assumes radial geometry with three distinct zones: (1) an innermost, circular production zone, (2) an intermediate, concentric zone subjected to fluid flow, (3) an outermost, radially infinite (finite) aquifer zone. The innermost zone was treated as a homogeneous tank and lumped parameter model derived by Whiting and Ramey (1969) was used to predict the production of mass and energy. The surrounding intermediate zone was considered as a zone in which neither production nor injection occurs. This zone was subjected to heat and mass transfer that occurs from periphery toward the innermost zone. The water entering from the outer zone cools part of the intermediate zone. To maintain a proper heat balance, the amount of heat received by the innermost zone during a time step is computed using the differences seen in the temperature profiles of the intermediate zone before and after each time. The outermost zone was subjected to mass transfer only. During each depletion step, a mass of fluid leaves the outermost zone to enter the intermediate zone. This is either equal to the amount of fluid injected or it is the natural water influx calculated using van Everdingen and Hurst method.

Olsen (1984), and Gudmundsson and Olsen (1987) derived and presented depletion models for liquid-dominated geothermal reservoirs. The depletion models were divided into two categories: confined and unconfined. For both cases depletion models with recharge and no recharge were used to match field data from the Svartsengi high temperature geothermal field in Iceland. The match to production data from Svartsengi Field was improved when influx was included. The influx was modeled by the steady-state Schilthuis, the finite aquifer method of Fetkovich, the unsteady-state method of Hurst, and Hurst simplified method for infinite linear and radial aquifer geometries. The best match was obtained using an infinite linear aquifer model with Hurst simplified solution.

Axelsson (1989), Axelsson and Dong (1998), and Axelsson and Gunnlaugsson (2000) described a method of lumped parameter modeling to simulate data from several low-temperature geothermal reservoirs in Iceland. This model is based on a general capacitor/conductor network. In their formulation, the basic system of

equations was derived in matrix form and, thus, the solution is presented in implicit form.

Alkan and Satman (1990) developed a lumped parameter model for geothermal reservoirs in the presence of carbon dioxide. The effects of carbon dioxide on important thermodynamic variables were considered and mathematically formulated. Application of the model to well-known geothermal fields such as Cerro Prieto Field in Mexico, Ohaaki Field in New Zealand, Bagnore Field in Italy, and Kizildere Field in Turkey were also discussed.

1.2 Statement of Problem

Fluid extraction from geothermal reservoir causes some decline in reservoir pressure which is reflected in the lowering of the water level in boreholes. The only exception is when production from a reservoir is less than its natural recharge. The recharge water flows from aquifer to reservoir in response to the lowered pressure or water level as a result of production. The pressure drop can be small or large, slow or fast, all depending on the rate of production, the size and properties of the geothermal system, and the recharge characteristics of the system. In many systems the pressure continues to drop with time as geothermal fluid production continues. This is because recharge to these system is limited.

The main objective of this dissertation is to model the pressure or water level behavior of low-temperature liquid dominated geothermal reservoirs. For this purpose, a simpler approach known as lumped parameter simulation is used in this study. The lumped parameter models presented in this study are similar in concept to Axelsson's model (Axelsson, 1989; Axelsson and Dong, 1998; Axelsson and Gunnlaugsson, 2000). As in Axelsson's work, the solutions presented in our work are valid for the low-temperature liquid dominated geothermal reservoirs only and assume that variations in temperature within the system can be neglected. As different from Axelsson's study, model equations are in the term of the well-known material balance equations, and the governing solutions are in the form of explicit analytical expressions. Early-time and late-time reservoir pressure behavior can be easily handled by asymptotic expressions of the analytical solutions.

In this study, the analytical solutions are presented for different types of geothermal systems such as 1 reservoir with recharge, 1 reservoir - 1 aquifer with/without recharge, 1 reservoir - 2 aquifers with/without recharge, 1 shallow reservoir - 1 deep reservoir with recharge, and 1 shallow reservoir - 1 deep reservoir - 1 aquifer with recharge (Figure 1.3).

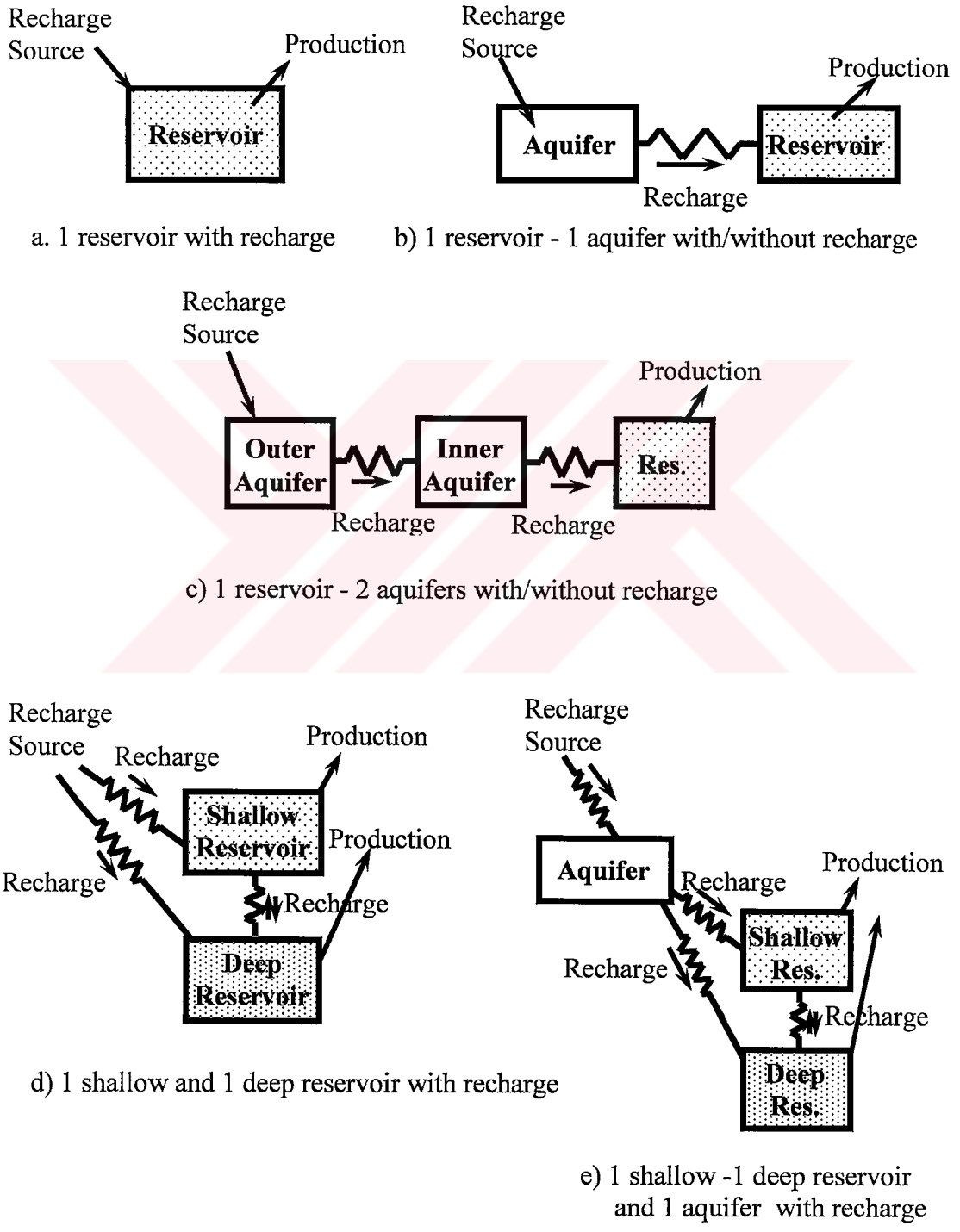

Figure 1.3 Tank systems used in modeling.

The reservoir simulates the innermost (production) part of the geothermal system, and the aquifers simulate the outer parts of the system. The outer aquifer can either be closed or can be connected to a recharge zone (constant pressure source). The rate of water influx (or recharge) between the aquifer and reservoir or between the aquifers is expressed by using Schilthuis's steady-state equation with water influx constant. Furthermore, Duhamel's Principle is applied to handle variable mass flow rate. For all types of geothermal systems, described above, the reservoir and aquifer parameters are estimated by making history matching. For this purpose, the Levenberg-Marquardt optimization method, based on weighted least-squares, is performed.

This study has focused on the following objectives:

1. to develop analytical models of the pressure behavior of the low-temperature geothermal reservoirs,
2. to examine the importance of various parameters on the behavior of the models developed,
3. to relate these models to field data available to test their validity,
4. to investigate the problems involved in field applications,
5. to study the possibility of using new models to predict the production performance of the field cases.

The thesis is organized as follows. In Chapter 2, the general aspects of lumped parameter modeling, relevant water recharge models and flow characteristics are discussed. Some of the lumped parameter models in the literature are presented. In Chapter 3, new lumped parameter models developed for the low-temperature geothermal systems are discussed in detail. Analytical solutions are presented in Chapter 3 and the detailed formulations are given in Appendices A-J. The early time and late time solutions obtained by the asymptotic approaches are given. The optimization procedure used to estimate the model parameters by history matching and the approach to handle the variable flow rate observed in field applications are presented. In Chapter 4, four field applications (Laugarnes, Glerardalur, Svartsengi and Balcova-Narlıdere geothermal fields) are performed and the results are discussed in detail. The major conclusions obtained are presented in Chapter 5.

2. GENERAL ASPECTS OF LUMPED PARAMETER MODELING AND WATER RECHARGE MODELS

In this section lumped parameter modeling and relevant water influx models will be presented as a prior knowledge of the further study.

2.1 Lumped Parameter Modeling

Lumped parameter modeling which is known as zero-dimensional modeling, is used most commonly at the beginning of the life of a field, when relatively information is known. Generally, in all lumped parameter models, the reservoir is described as a single homogeneous block with the production/injection rate and recharge flow specified. The pressure (and/or water level) changes in the reservoir are modeled by using mass and energy balances and therefore, the potential of the field can be predicted under various production/injection scenarios.

In this study, the geothermal system is considered as consisting of mainly with three parts. These are; (1) the reservoir, (2) the aquifer, and (3) the recharge source. First two are treated as homogeneous tanks with the average properties. The recharge source connected to the aquifer or directly to the reservoir is treated as a point source supplying recharge into the system. These three parts could be considered from the center to the periphery as Castanier et al. (1980) and Castanier and Brigham (1983) described (Figure 2.1). It is also possible to consider these parts as series of connected tanks (Figure 2.2).

The reservoir in which the production/injection occurs represents the innermost part of the geothermal system. The changes in pressure and/or water level are monitored and production/injection rates are recorded. These data are important for evaluation of changes in the reservoir and are important for simulations. Information on the nature, properties and size of a geothermal reservoir are obtained by careful monitoring and modeling of its production and reservoir history.

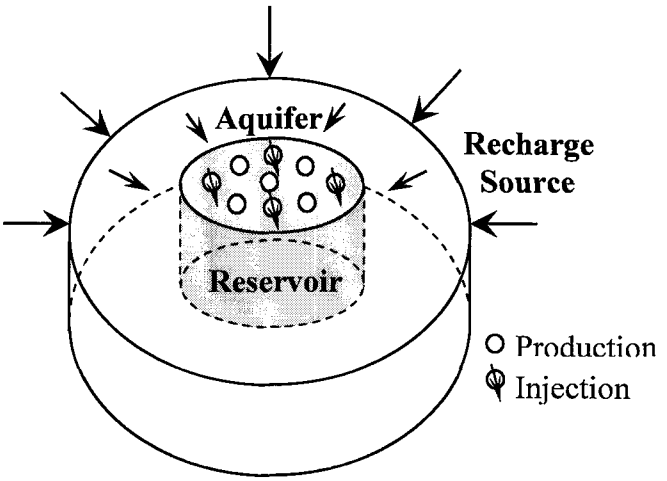

Figure 2.1 Parts of a geothermal system from the center to the periphery.

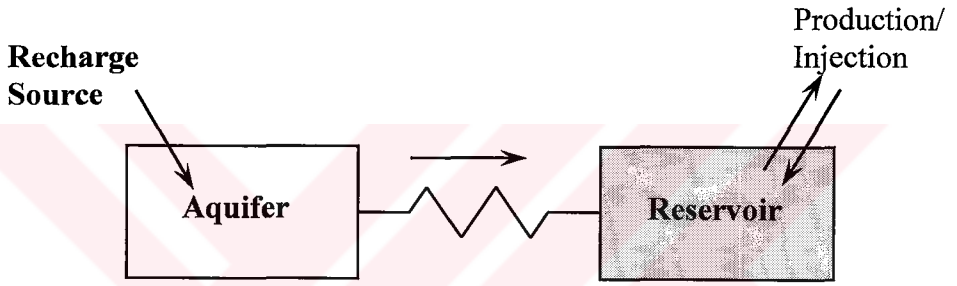

Figure 2.2 Parts of a geothermal system considered as series connected.

The aquifer in which neither production nor injection occurs, recharges the reservoir. The production causes the pressure in the reservoir to decline, which results in water influx from the aquifer to the reservoir.

The recharge source represents the outermost part of the geothermal system. It recharges the aquifer.

If the system is modeled by tanks, the water influx between the tanks (aquifer-reservoir, recharge source-aquifer, and recharge source-reservoir) can be modeled by various methods given in the literature (Schilthuis, 1936; van Everdingen and Hurst, 1949; Fetkovich, 1971).

One of the most important and basic approaches to petroleum reservoir engineering is the mass balance. Since the non-isothermal effects can be much larger for water than for hydrocarbon systems, in the case of geothermal reservoir engineering, it is usually necessary to add an energy balance to the mass balance.

The production of geothermal fluid may or may not be under isothermal conditions, while production of petroleum reservoirs is normally considered to be isothermal. Whiting and Ramey (1969) consider both isothermal and non-isothermal fluid flow in the lumped parameter model. The following equation derived for non-isothermal two-phase fluid flow by combining mass and energy balances.

$$W_p(h_p - E_c) + W_L(h_L - E_c) + Q = W_i\left\{E_i - E_c + \left(\frac{1-\phi}{\phi}\right)\left[x\,v_{gi} + (1-x)v_{wi}\right]\rho_t\, C_t(T_i - T_c)\right\} + (h_e - E_c)W_e \quad (2.1)$$

This equation states that for a given geothermal reservoir the total energy loss due to production (the first term on the left hand side), fluid leakage (the second term on the left hand side) and conductive heat transfer (the third term on the left hand side) should be equal to the heat transferred from the rock and the enthalpy change due to the change of fluid mass in the reservoir. The conductive heat loss term Q is negligible, assuming that the heat transferred to the bottom of the reservoir is equal to the loss from the top. The last term on the right-hand side of the equation includes the energy change term due to water influx. It is assumed that enthalpy of the water influx would remain constant.

If the reservoir contains only liquid water, the thermodynamic path is isothermal and Equation 2.2 is obtained which is similar to that employed for petroleum production above bubble point (Whiting and Ramey, 1969).

$$(W_p + W_L)v_w = W_i(v_w - v_{wi}) + W_e v_e \quad (2.2)$$

In our lumped models which are valid for low-temperature liquid dominated geothermal reservoirs, only mass balance is applied and energy balance is neglected. The reason for ignoring energy balance in the models could be explained by pressure-temperature behavior of the geothermal reservoirs. Figure 2.3 is a pressure-temperature diagram for the liquid-vapor region for pure water, showing critical point and three other points representing possible initial conditions for a geothermal reservoir.

First consider that a reservoir initially existed at state "A", entirely within the vapor region. The temperature is above the boiling point curve at the prevailing pressure

and the steam phase controls the pressure in the reservoir. The production causes the reservoir pressure to decline, and the pressure follows the dashed line 1. The actual path for production of such a reservoir would not be truly isothermal, but temperature decline should be so small to measure with normal field instruments. The initial conditions corresponding to point "A" represent a vapor-dominated geothermal reservoir in which no hot water is formed during the production.

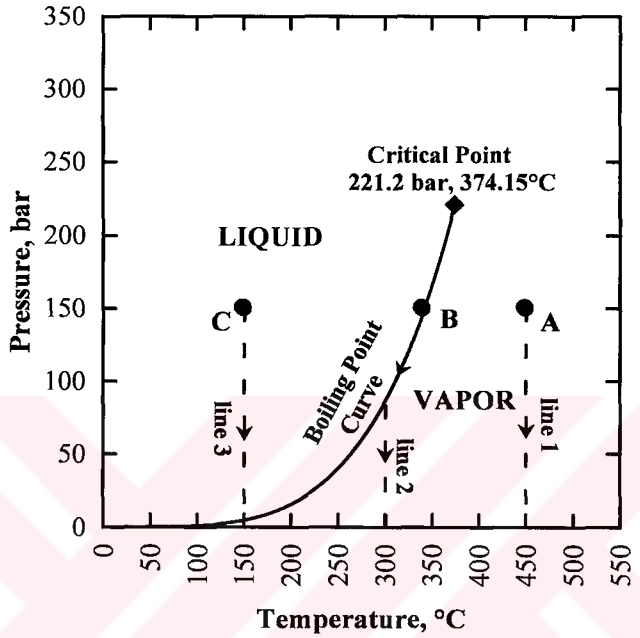

Figure 2.3 Pressure-temperature diagram for pure water.

Point "B" in Figure 2.3 lies on the boiling point curve and both hot water and steam exist in the reservoir which is known as two phase geothermal reservoir. As production proceeds, the temperature and pressure decline along the boiling point curve. The produced steam-hot water ratio continues to increase until all water has been boiled away. The temperature then departs from the boiling point curve and its decline essentially stops (line 2).

Point "C" in Figure 2.3 corresponds to a low-temperature liquid-dominated geothermal reservoir (Brigham and Ramey, 1981). The water temperature is below the boiling point curve at the prevailing pressure and the water phase controls the pressure in the reservoir. The pressure declines as production proceeds, and it moves down along line 3. Although it is expected that line 3 intersects the boiling point curve, in practice two-phase internal steam drive does not begin until the reservoir

pressure has declined to a small fraction of its initial value. The actual path would be essentially isothermal since no boiling takes place during the production.

Figure 2.4 presents the variations of the reservoir pressure with the percent of initial fluid mass produced. A comparison of the Reservoirs "A", "B", and "C" shows the effect of the total system compressibility on the fluid production. The total system compressibility may be defined as:

$$c_t = c_{fluid} + c_{formation} \tag{2.3}$$

and it is essentially the reciprocal of the slope of the curves on Figure 2.4. The compressibility of the vapor phase ($c_{Reservoir\ A}$) is greater than that of liquid phase ($c_{Reservoir\ C}$) since the expansion of the steam is much greater than the liquid expansion. On the other hand, the two-phase system has a compressibility ($c_{Reservoir\ B}$) greater than that of single phase vapor system ($c_{Reservoir\ B} > c_{Reservoir\ A} > c_{Reservoir\ C}$).

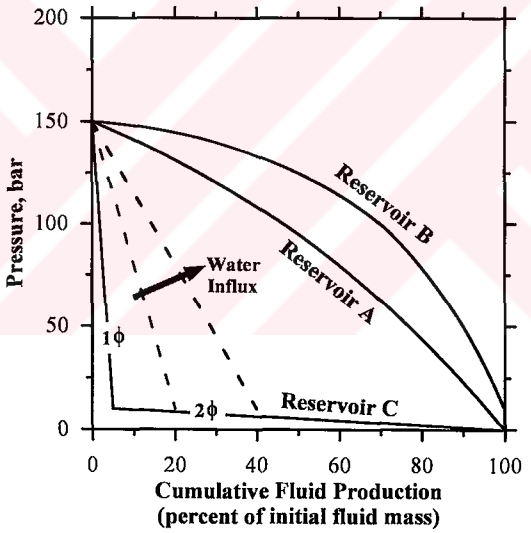

Figure 2.4 Pressure vs. cumulative fluid production for Reservoirs A, B, and C.

In case of Reservoir "C" unless a strong water drive exists, the reservoir pressure initially declines rapidly with production, since only liquid expansion and rock compaction supply the driving force. If the reservoir has a water recharge, the production of Reservoir "C" follows the dashed lines depending on the amount of the water recharge.

Axelsson (Axelsson, 1989; Axelsson and Dong, 1998; Axelsson and Gunnlaugsson, 2000) described a method of lumped parameter modeling to simulate pressure response data from low temperature geothermal reservoirs in Iceland. The energy

balance is neglected in his model since the model simulates low temperature geothermal reservoirs. A general lumped network of the sketched in Figure 2.5 is considered and the network consists of a total of N capacitors and resistors. The capacitors represent the reservoir and aquifer parts of the geothermal system. The capacitors are pair wise connected by resistors which simulates the flow resistance. Each capacitor has the mass, m, storage coefficient, κ, and pressure, $p = m/\kappa$. The mass flow from the k' th to the i' th capacitor is given by Equation 2.4.

$$q_{ik} = \sigma_{ik}\,\Delta p = \sigma_{ik}\,(p_k - p_i) \tag{2.4}$$

Applying conservation of mass, the basic system equation is obtained in matrix form below;

$$K\,d\vec{p}/dt + A\vec{p} = \vec{f} \tag{2.5}$$

where the vectors and matrices are defined as follows.

$$K = [\kappa_i \delta_{ik}]\,, \quad A = \left[\left(\sum_j \sigma_{ij} + \sigma_i\right)\delta_{ik} - \sigma_{ik}\right], \quad \vec{p} = (p_i), \quad \vec{f} = (f_i) \tag{2.6}$$

where f_i represents an external source mass flow into the i' th capacitor. The terms in Equations 2.4 to 2.6 are defined in Axelsson's (Axelsson, 1989; Axelsson and Dong, 1998; Axelsson and Gunnlaugsson, 2000) work.

Consequently, his model is valid for low temperature liquid dominated reservoirs. The system equation is derived in matrix form and thus, the solution is presented in implicit form. An iterative non-linear least-squares technique is applied to fit model results to the observed data and to estimate the model parameters.

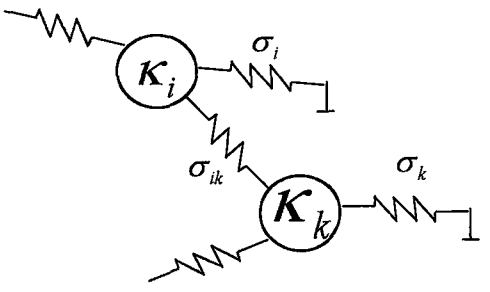

Figure 2.5 General lumped capacitor/resistor network.

2.2 Water Influx Models

The aquifer surrounding and recharging the reservoir is an important criterion to determine the geothermal reservoir production performance. Generally in all geothermal systems, the aquifer is so large compared to the reservoir and outcrops at one or more places where it replenishes by surface waters.

In response to a pressure drop in the reservoir due to production, the aquifer reacts to offset or retard pressure decline by providing a source of water influx. From an analytical point of view, the amount of water that has influxed into the reservoir from the aquifer should be calculated to determine the effects of the aquifer on the pressure or water level behavior of the geothermal reservoir.

In petroleum engineering literature, several models (Schilthuis, 1936; van Everdingen and Hurst, 1949; Fetkovich, 1971) are studied to calculate water influx. These models can be generally categorized by a time dependence. In this chapter, flow regimes such as steady-state, unsteady-state, and pseudosteady-state will be discussed by their features.

The production causes the pressure decline in the reservoir and consequently the pressure drops at the reservoir-aquifer boundary. At very late time, pressure response is affected by the influence of aquifer boundary, but prior to those late times the pressure response does not feel the effect of the aquifer boundary, and aquifer acts as if it were infinite in extent. This response is known as "Unsteady-State Flow" period.

Eventually the effects of the aquifer boundary might be felt at the well. The time at which the boundary effect is noticed is dependent on several factors, including the distance to the boundary and the properties of the permeable formation and the fluid that fills it. The two types of aquifer boundary that are most commonly considered are (1) closed and (2) constant pressure.

A closed boundary (also known as a no flow boundary) occurs where the aquifer is not connected to a recharge source. No flow boundary can also arise when the influx from the recharge source is negligible as compared to the production. When a reservoir-aquifer system has no flow boundary, the pressure transient is transmitted outwards until it reaches the outer boundary, which the reservoir-aquifer depletion enters a state known as "Pseudosteady-State". In this stage, the pressure declines at the same rate everywhere in the reservoir-aquifer region.

When the reservoir-aquifer system is supported by a strong recharge source, then a constant pressure boundary presents. The effect of constant pressure boundary causes the pressure response to achieve "Steady-State", at which the reservoir-aquifer pressure remains constant for all production period.

The pressure behavior of these flow regimes is given by Figure 2.6. Hydraulic analogs and mathematical expressions of the flow regimes are discussed in the following sections.

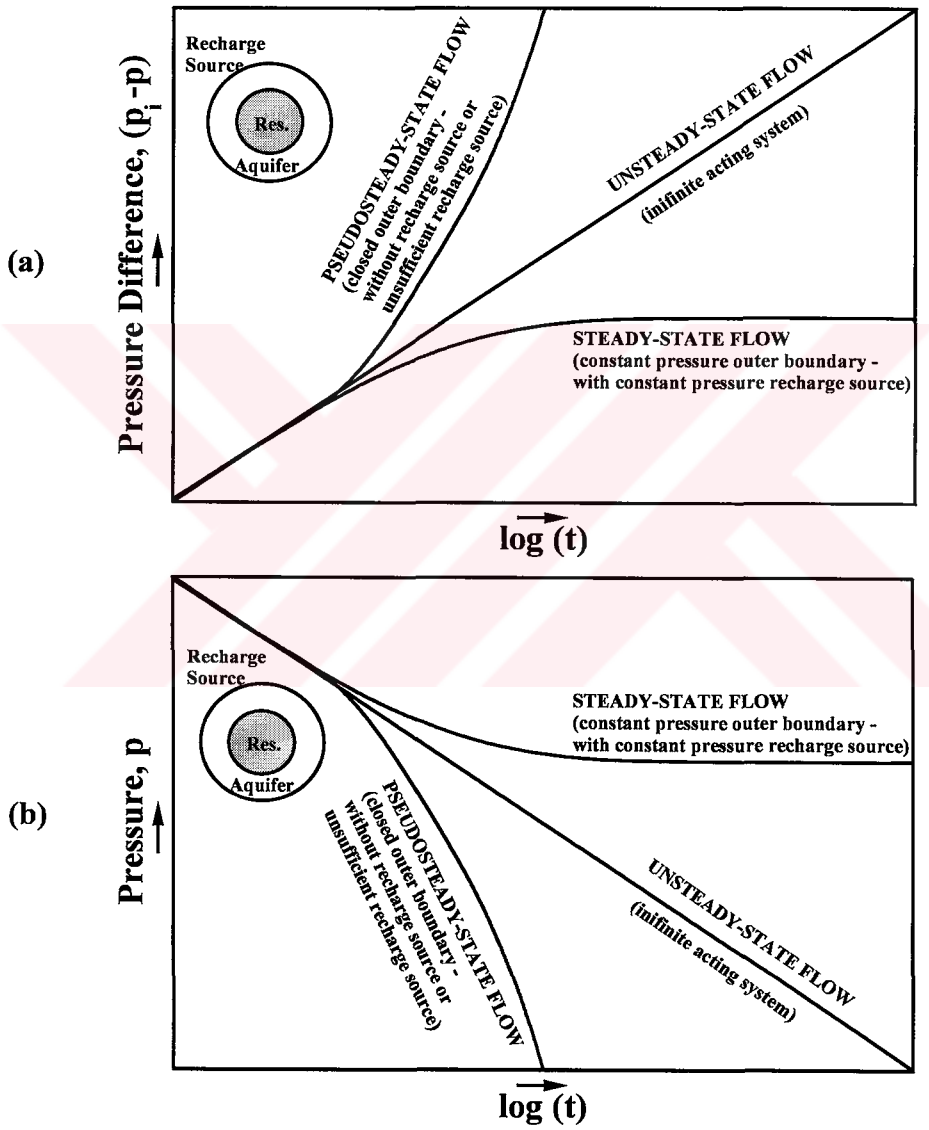

Figure 2.6 (a) Pressure difference, (b) pressure behavior of the flow regimes.

2.2.1 Steady-state flow

Water influx from the aquifer to the reservoir could be modeled as shown in Figure 2.7 by considering the aquifer and the reservoir by tanks. The aquifer and the

reservoir tanks are connected to the each other through a sand-filled pipe. Initially both tanks are filled to the same level and have the same pressure, p_i. When the fluid production started from the reservoir, reservoir pressure drops from the value of p_i to the value of p. In that case, water influx occurs from the aquifer to the reservoir as expected. The rate of water influx by Darcy's Law is proportional to the permeability of the sand in the pipe, the cross-sectional area of the pipe, and the pressure drop $(p_i - p)$; and inversely proportional to the water viscosity and the length of the pipe. Aquifer pressure remains constant where the water efflux from the aquifer is replenished, or the aquifer tank is quite large compared with the reservoir tank. If the rate of influx is equal to the reservoir voidage rate, the reservoir pressure stabilizes. In other words, the amount of the water influx into the reservoir is equal to the amount of the produced mass from the reservoir. Therefore, the reservoir pressure does not decline with the production.

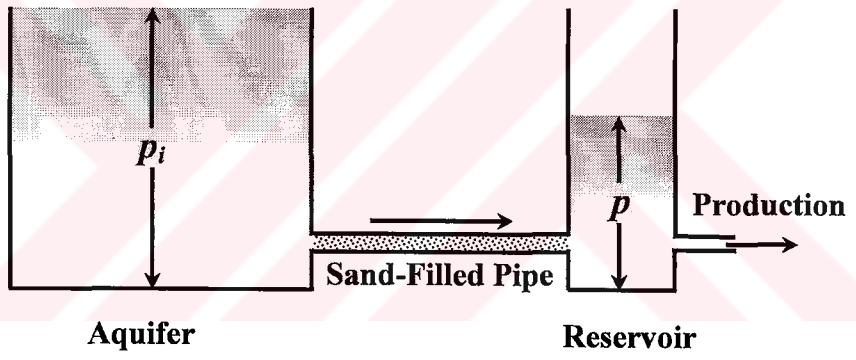

Figure 2.7 Hydraulic analog of steady-state flow (Craft and Hawkins, 1959).

In literature, steady-state flow is expressed analytically (Equation 2.7) by Schilthuis (1936). Schilthuis model assumes that the pressure at the external boundary of the aquifer is maintained at the initial value p_i and that flow to the reservoir is proportional to the pressure differential $(p_i - p)$, assuming that water viscosity, average permeability, and aquifer geometry remain constant.

$$\left.\begin{aligned} W_e &= \alpha \int_0^t (p_i - p)dt \\ \frac{dW_e}{dt} &= \alpha (p_i - p) \end{aligned}\right\} \qquad (2.7)$$

where;

W_e : water influx mass, kg

$\frac{dW_e}{dt}$: rate of water influx, kg/sec

α : recharge constant, kg/bar-sec

$(p_i - p)$: boundary pressure drop, bar

Steady-state refers to a situation in which the pressure and the rate distribution in the reservoir remain constant with time. Figure 2.8 represents the pressure distribution and rate distribution during radial flow that exhibits the characteristics of steady-state flow. Water influx rate at the outer boundary of the aquifer, r_e, equals to the production rate at the wellbore, r_w, gives a pressure and rate history almost identical to the one described in Figure 2.8.

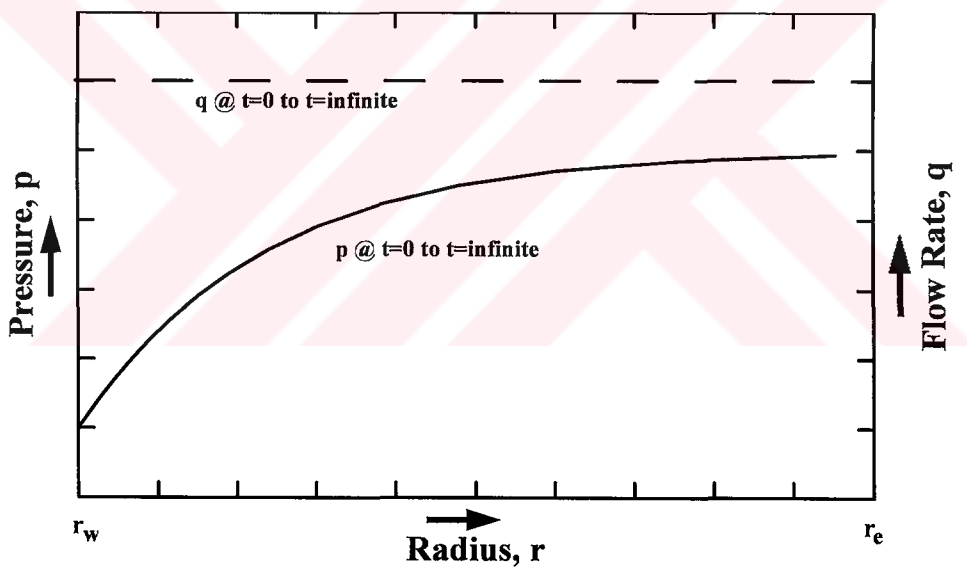

Figure 2.8 Pressure and rate distribution of steady-state flow in the reservoir-aquifer system (Slider, 1983).

2.2.2 Unsteady-state flow

Hydraulic analog of an unsteady-state flow is shown in Figure 2.9 where the reservoir tank is connected to a series of aquifer tanks as different from Figure 2.7. The volumes of aquifer tanks are increasing as the distance increasing from the reservoir tank. Aquifer tanks are connected to each other by sand-filled pipes of constant diameter and sand permeability, but of decreasing length between larger tanks.

To understand the reason of using increasing aquifer tank volumes and decreasing sand-filled pipe lengths, cylindrical elements such as shown in Figure 2.10 are considered. As it is seen from Figure 2.10, the cylindrical element volumes are increasing while the diameters are increasing. Therefore, the volumes of the tanks are selected by increasing volumes. On the other hand, as the resistance to flow between elements are decreasing because of the increasing cross-sectional areas, the lengths of the sand-filled connecting pipes vary inversely with the radii of tanks.

Initially all tanks (Figure 2.9) are filled to a same level and have the same pressure (p_i). As production proceeds, the reservoir pressure drops and water influx occurs from aquifer tank 1 to the reservoir tank. This causes a pressure drop in aquifer tank 1 which induces flow from aquifer tank 2 to tank 1, and so on. It is evident that pressure drop in the aquifer tanks are not uniform but varies with time and production rate changes in a manner such as that shown in Figure 2.11 for a constant reservoir production rate, and Figure 2.12 for constant well pressure.

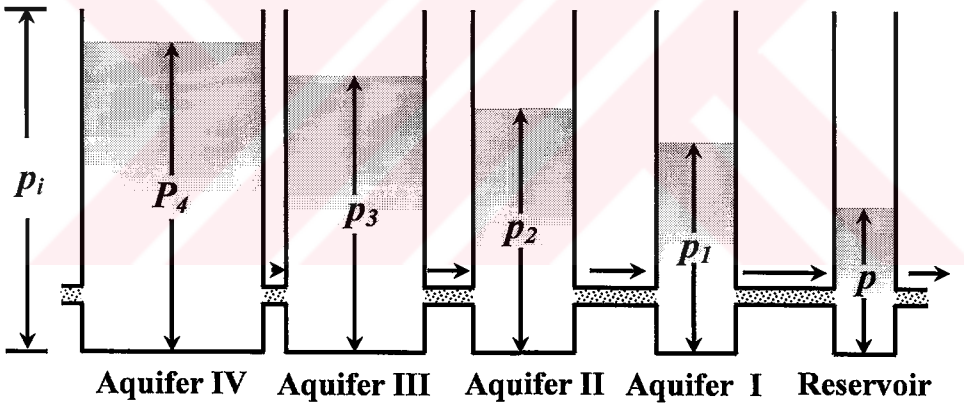

Figure 2.9 Hydraulic analog of unsteady-state flow (Craft and Hawkins, 1959).

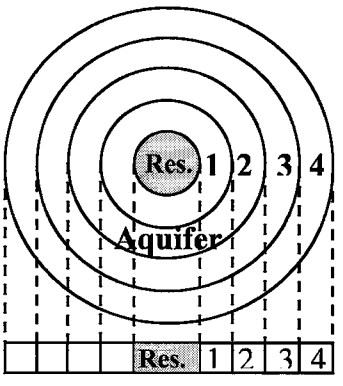

Figure 2.10 Cylindrical elements in an aquifer surrounding a circular reservoir.

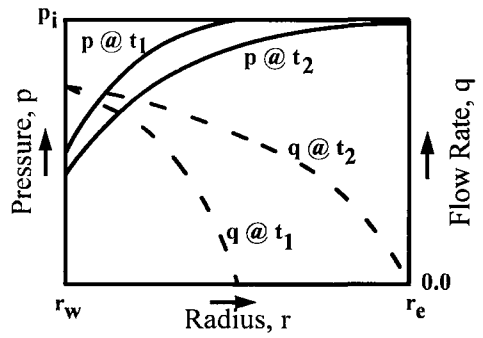

Figure 2.11 Unsteady-state flow for constant production rate (Slider, 1983).

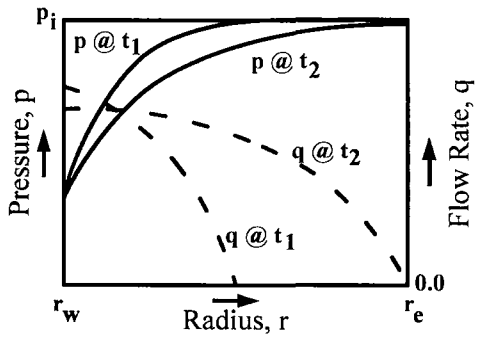

Figure 2.12 Unsteady-state flow for constant well pressure (Slider, 1983).

Until the pressure in the entire reservoir-aquifer system is affected by the outer aquifer boundary, r_e, the only energy causing the fluid flow is the expansion of the fluids themselves.

In Figures 2.11 and 2.12, after some short period of production, a small portion of the reservoir near the production well is affected and a considerable pressure drop occurs. The pressure and rate distributions move on through these positions immediately as the production continues to affect more and more of the reservoir-aquifer region. That is subjected to flow, until the entire reservoir-aquifer region is affected as shown by the pressure at t_2.

Since the flow is taking place due to expansion of the fluid, the rate at r_e is zero and it increases with a reduction in radius until the maximum rate in the reservoir is obtained at r_w.

In the literature, van Everdingen and Hurst (1949), Klins et al. (1988) and Edwardson et al. (1962) give the mathematics of unsteady-state flow for constant pressure and constant rate case as a function of time and the radius. Moreover, the flow geometries are the parameters have to be considered. In the case of infinite acting aquifers, water influx could be calculated for semi-spherical, radial and linear flow (Whiting and Ramey, 1969).

2.2.3 Pseudosteady-state flow

Pseudosteady-state is a special case of unsteady-state flow. At time t=0 the pressure throughout the reservoir is uniform at p_i. After some short production time t_1 at a constant rate only a small portion of the reservoir is affected and the entire reservoir-

aquifer system is experienced a significant pressure drop as production continues (Figure 2.13). After the closed boundary effect is noticed (p at t_2), the change of the pressure with time at all radii in the reservoir-aquifer system becomes uniform. So that the pressure distributions at subsequent times are parallel as illustrated by the pressure distributions at times t_3, and t_4. This situation continues with constant changes in pressure with time at all radii and with subsequent parallel pressure distributions until the reservoir is no longer able to sustain a constant flow rate at the wellbore.

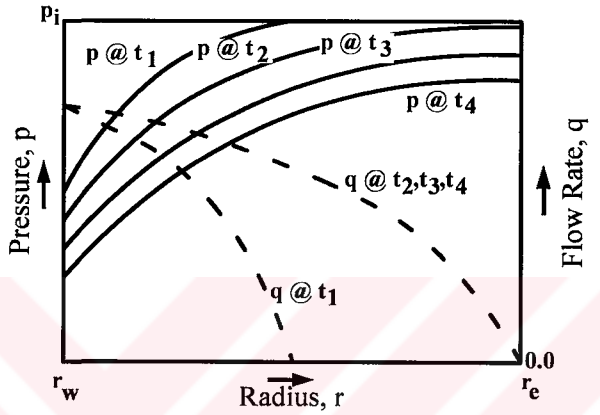

Figure 2.13 Pseudosteady-state flow (Slider, 1983).

In the literature, Fetkovich (1971) discusses pseudosteady-state flow independent of flow geometries by using productivity index of aquifer and mass balance equation.

3. LUMPED PARAMETER MODELS FOR LOW-TEMPERATURE LIQUID DOMINATED GEOTHERMAL RESERVOIRS

The geothermal fluid production causes the pressure in a geothermal system to decline, which is reflected in the lowering of the water level in boreholes. The rate of pressure or water level decline is determined by the rate of production and/or reinjection, the size and properties of the geothermal system, and the recharge characteristics of the system.

For reservoirs with liquid only, the production path is for all practical purposes isothermal. The energy balance thus can be omitted. During the drawdown history of a geothermal reservoir, the recharge water invades the system in response to the lowered pressure or water level, and it maintains the reservoir pressure by replacing the produced liquids. A term of influx mass has to be added to the mass balance equations and the mass balance becomes,

$$W_c = W_i - W_p + W_a + W_{inj} \tag{3.1}$$

where the current mass, W_c, equals that initially in the reservoir, W_i, minus what has been produced, W_p, plus any water influx, W_a, and plus reinjected mass, W_{inj}.

The initial fluid in place in a liquid-dominated reservoir may be compressed water. In this case, when the reservoir is produced, the water expands because of its compressibility. This is called a confined reservoir. For a reservoir of volume V_r, the liquid mass in place is given by

$$W_c = V_r \phi_r \rho_w \tag{3.2}$$

where ϕ_r is reservoir porosity, and ρ_w is liquid density. When this relationship and Equation 3.1 are differentiated with respect to time and the definition of isothermal compressibility is used, the following equation in terms of mass flow rates, w, results,

$$w_a - w_p + w_{inj} = V_r \phi_r \rho_w c_t \frac{dp}{dt} \tag{3.3}$$

where c_t is the total (fluid+formation) compressibility $\left(c_t = c_f + c_r\right)$ for the reservoir system where $c_f = 1/\rho_w (d\rho_w / dp)_T$ and $c_r = 1/\phi_r (d\phi_r / dp)_T$. We assume c_f and c_r are constants so that slightly compressible fluid and rock assumptions are valid. The production and reinjection terms could be defined as "*Net Production Term*" as given in Equation 3.4.

$$w_{p,net} = w_p - w_{inj} \tag{3.4}$$

Therefore Equation 3.3 becomes as follows.

$$w_a - w_{p,net} = V_r \phi_r \rho_w c_t \frac{dp}{dt} \tag{3.5}$$

The steady-state Schilthuis (1936) water-influx method is used to describe the recharge rate from the recharge source to reservoir tank (or from the aquifer to the reservoir, or from the recharge source to the aquifer). This method assumes that the recharge is proportional to the pressure difference between the reservoir tank and the recharge source, and it is given by

$$w_a = \alpha_r (p_i - p_r) \tag{3.6}$$

where α_r is the reservoir recharge constant, p_i is the pressure of the recharge source and p_r is the pressure of the reservoir.

The models are developed for constant pressure aquifer outer boundary (open system) and for no flow aquifer boundary (closed system). In cases where a closed system is modeled, $w_a = 0$ is set in Equation 3.5.

Although the equations and solutions given in this study are in the form of pressure, they can be represented in terms of water level *h(t)* by using the relation $p_r(t) = \rho_w g h(t)$.

Several variations of geothermal systems using the tank model approach are studied and explicit analytical solutions are obtained to describe the reservoir pressure behavior. The systems studied in detail are;

1. 1 reservoir with recharge source (1-Tank Model),
2. 1 reservoir - 1 aquifer with/without recharge source (2-Tank Open/Closed Model),
3. 1 reservoir - 2 aquifers with/without recharge source (3-Tank Open/Closed Model),
4. 1 shallow reservoir - 1 deep reservoir with recharge source (2 Reservoir Tanks Without Aquifer Model),
5. 1 shallow reservoir - 1 deep reservoir - 1 aquifer with recharge source (2 Reservoir Tanks With Aquifer Model).

3.1 1 Reservoir With Recharge Source (1-Tank Model)

Consider a geothermal system sketched in Figure 3.1 consisting of a reservoir and a recharge source. The system (reservoir and recharge source) is in equilibrium at $t = 0$. Reservoir is produced at a mass rate of $w_{p,net}$ and the recharge source at a constant pressure of p_i supplies water.

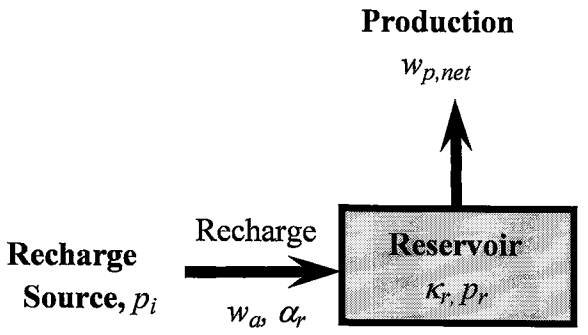

Figure 3.1 Schematic of a single tank model with recharge source.

Using Equations 3.6 in Equation 3.5 and rearranging the resulting equation gives

$$w_{p,net} = \alpha_r (p_i - p_r) - \kappa_r \frac{dp}{dt} \tag{3.7}$$

where, κ_r could be called as reservoir storage capacity and defined as,

$$\kappa_r = V_r \phi_r \rho_w c_t \tag{3.8}$$

Because p_i is constant, we can recast Equation 3.7 in terms of $\Delta p_r = p_i - p_r$ as

$$\frac{d\Delta p_r}{dt} + \frac{\alpha_r}{\kappa_r}\Delta p_r = \frac{w_{p,net}}{\kappa_r} \tag{3.9}$$

Equation 3.9 is a first order ordinary differential equation and the solution can be obtained by using an initial condition which can be written as;

$$p_r(t=0) = p_i \quad \text{or} \quad \Delta p_r(t=0) = 0 \tag{3.10}$$

and the solution of Equation 3.9 in terms of pressure difference is given by (Sarak et al., 2003a)

$$\Delta p_r(t) = \frac{w_{p,net}}{\alpha_r}\left[1 - exp\left(-\frac{\alpha_r t}{\kappa_r}\right)\right] \tag{3.11}$$

or in terms of reservoir pressure is

$$p_r(t) = p_i - \frac{w_{p,net}}{\alpha_r}\left[1 - exp\left(-\frac{\alpha_r t}{\kappa_r}\right)\right] \tag{3.12}$$

Equations 3.11 and 3.12 give the pressure behavior of a geothermal system as a function of production time under the conditions of a constant production rate and a constant recharge pressure. Equation 3.11 (or 3.12) is first presented by Grant et al., 1982). Later Onur (2001) extended the solution for variable rate history. For the completeness, the detailed solution is given in Appendix-A for the 1-tank model.

For early-time behavior, the exponential term in Equations 3.11 and 3.12 can be approximated as,

$$exp(-\alpha_r t / \kappa_r) \approx 1 - \alpha_r t / \kappa_r \qquad \text{for } t << \kappa_r / \alpha_r \tag{3.13}$$

For all practical purposes, Equation 3.13 becomes valid for $t < 0.1\frac{\kappa_r}{\alpha_r}$. Thus, Equations 3.11 and 3.12 become, respectively,

$$\Delta p_r(t) = \frac{w_{p,net}}{\kappa_r} t \tag{3.14}$$

$$p_r(t) = p_i - \frac{w_{p,net}}{\kappa_r} t \tag{3.15}$$

which clearly indicates that reservoir pressure will decline linearly with time, and recharge to reservoir will be negligible over these early times. In other words, reservoir pressure is dependent on reservoir storage capacity, κ_r, and independent of reservoir recharge constant, α_r. So, when Equations 3.14 and 3.15 apply, one can be able to determine only κ_r. Notice that the early-time solution, Equations 3.14 or 3.15, corresponds to the pseudosteady-state behavior of the reservoir.

For late-time behavior, the exponential term in Equations 3.11 and 3.12 can be approximated as,

$$exp(-\alpha_r t / \kappa_r) \cong 0 \qquad \text{for } t >> \kappa_r / \alpha_r \tag{3.16}$$

Equations 3.11 and 3.12 reduce to

$$\Delta p_{rss} = \frac{w_{p,net}}{\alpha_r} = const. \tag{3.17}$$

$$p_{rss} = p_i - \frac{w_{p,net}}{\alpha_r} = const. \tag{3.18}$$

It is worth noting that for all practical purposes, Equation 3.16 becomes valid for $t \geq 5\kappa_r / \alpha_r$. So Equations 3.17 and 3.18 indicate that for all t such that $t \geq 5\kappa_r / \alpha_r$, the reservoir pressure stabilizes at a value determined by a balance with the recharge. The pressure decline becomes independent of reservoir storage coefficient, κ_r, but dependent on the reservoir recharge constant, α_r. So, when Equations 3.17 and 3.18 apply, it is possible to determine α_r, but not κ_r.

For constant production rate, Figure 3.2 shows 1-tank modeling results obtained from Equation 3.12 with $\kappa_r = 2 \times 10^7$ kg/bar, $\alpha_r = 50$ kg/bar-s and $w_{p,net} = 100$ kg/s. The slope of the reservoir pressure drop vs. t plot, which is valid for

$t < 0.1\kappa_r / \alpha_r = 40000$ s $\cong$ 0.46 days, is calculated as 5×10^{-6} bar/s $\cong$ 0.43 bar/days by using the early-time solution (Equation 3.14), and the reservoir pressure stabilizes at $\Delta p_{rss} = 2$ bars for late times, $t \geq 5\kappa_r / \alpha_r = 2 \times 10^6$ s $\cong$ 23 days (Equation 3.17). On the other hand, the slope is obtained from Figure 3.2 as 0.43 bar/days for $t < 0.46$ days, and Δp_{rss} is obtained as 2 bars for $t \geq 23$ days. The asymptotic solutions given by Equations 3.14 and 3.17 are justified by the results of Figure 3.2.

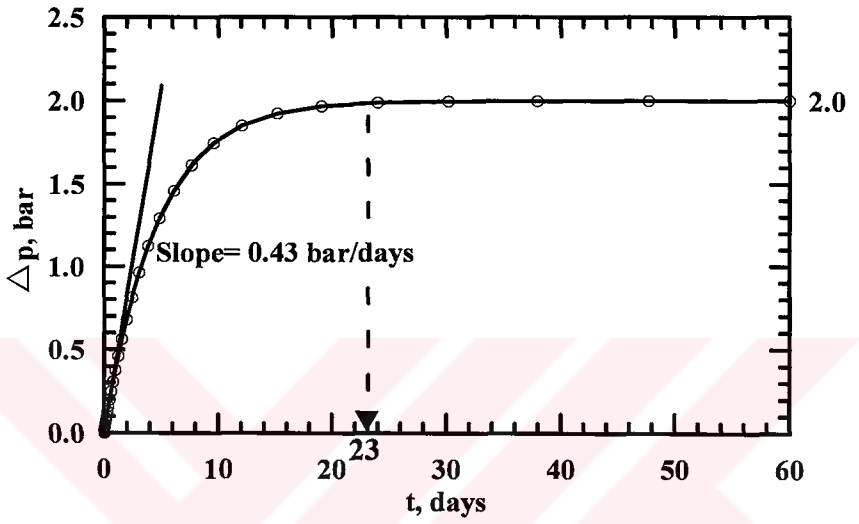

Figure 3.2 Δp vs t graph for 1-tank modeling with $\kappa_r = 2\ 10^7$ kg/bar, $\alpha_r = 50$ kg/bar-s and $w_{p,net} = 100$ kg/s

3.2 1 Reservoir – 1 Aquifer System (2-Tank Model)

The second lumped parameter model considered in this work consists of two tanks. A schematic of the 2-tank lumped model is shown in Figure 3.3. The first tank represents the reservoir, the inner or central part of the geothermal system, where the production/reinjection occurs. The second tank, is connected to the first tank, simulates the outer part of the system (aquifer) recharging the reservoir. The aquifer may be treated as a closed one with a closed outer boundary or an open one with a constant pressure source.

Hot water is pumped out of the first tank (reservoir), which causes the pressure and water level to decline. This in turn causes the decline of pressure and water level in the second tank (aquifer). Thus the total geothermal system is affected by the production.

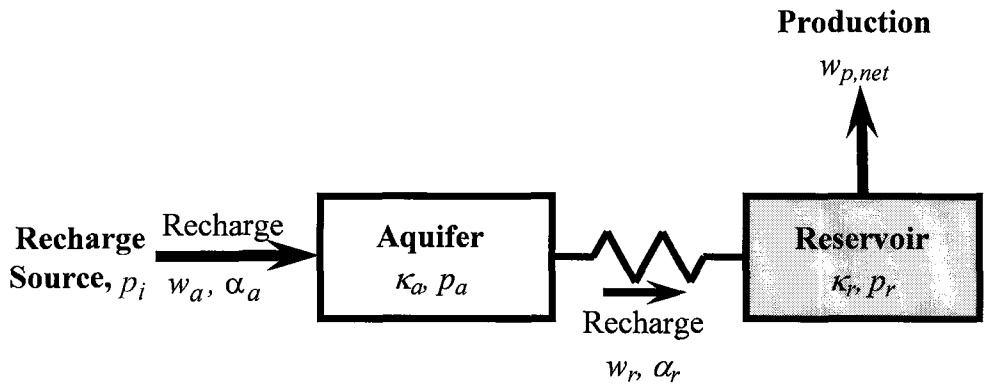

Figure 3.3 Schematic of a 2-tank model.

It should be noted that the pressure or water level decline in the system is influenced from the recharge characteristics of the system, and initial pressures of the system parts which will be discussed in the following sections.

3.2.1 1 reservoir – 1 aquifer with recharge source (2-tank open system)

If the second tank (aquifer tank) is connected to a constant pressure source (recharge source in Figure 3.3), then the system is described as an open system, and the recharge source supplies water with a rate of $w_a = \alpha_a(p_i - p_a)$ to the geothermal system.

The mass balances written for the 2-tank open system shown in Figure 3.3 yield the following differential equations describing the flow:

For Aquifer:

$$w_a - w_r = \kappa_a \frac{dp_a}{dt} \qquad \text{or} \qquad \alpha_a(p_i - p_a) - \alpha_r(p_a - p_r) = \kappa_a \frac{dp_a}{dt} \tag{3.19}$$

For Reservoir:

$$w_r - w_{p,net} = \kappa_r \frac{dp_r}{dt} \qquad \text{or} \qquad \alpha_r(p_a - p_r) - w_{p,net} = \kappa_r \frac{dp_r}{dt} \tag{3.20}$$

where $\kappa_a = V_a \phi_a \rho_a c_t$ and $\kappa_r = V_r \phi_r \rho_r c_t$

Initial Condition:

$$\Delta p_a(t=0) = \Delta p_r(t=0) = 0 \tag{3.21}$$

According to this formulation (Equation 3.21), we assume that hydraulic equilibrium exists between the tanks.

The solutions describing the aquifer and reservoir pressure behaviors can be obtained from Equations 3.19 - 3.21 by the use of Laplace transformation (Sarak, 2003a). Details of the solution procedure can be found in Appendix-B. Here, only the solution describing the reservoir pressure behavior, $\Delta p_r(t) = p_i - p_r(t)$ is recorded,

$$\Delta p_r(t) = \frac{w_{p,net}}{\kappa_r}\left[\frac{d}{\mu_1\mu_2} + \frac{\mu_1 - d}{\mu_1(\mu_2 - \mu_1)}exp(-\mu_1 t) + \frac{\mu_2 - d}{\mu_2(\mu_1 - \mu_2)}exp(-\mu_2 t)\right] \tag{3.22}$$

where $d = \dfrac{\alpha_a + \alpha_r}{\kappa_a}$, and μ_1 and μ_2 are the roots of

$$s^2 + \left[\frac{\alpha_a + \alpha_r}{\kappa_a} + \frac{\alpha_r}{\kappa_r}\right]s + \frac{\alpha_a\alpha_r}{\kappa_a\kappa_r} = (s + \mu_1)(s + \mu_2) = 0 \tag{3.23}$$

$$\left.\begin{aligned}\mu_1 &= \frac{\left[\frac{(\alpha_a + \alpha_r)}{\kappa_a} + \frac{\alpha_r}{\kappa_r}\right] + \sqrt{\left[\frac{(\alpha_a + \alpha_r)}{\kappa_a} + \frac{\alpha_r}{\kappa_r}\right]^2 - 4\frac{\alpha_a\alpha_r}{\kappa_a\kappa_r}}}{2} \\ \mu_2 &= \frac{\left[\frac{(\alpha_a + \alpha_r)}{\kappa_a} + \frac{\alpha_r}{\kappa_r}\right] - \sqrt{\left[\frac{(\alpha_a + \alpha_r)}{\kappa_a} + \frac{\alpha_r}{\kappa_r}\right]^2 - 4\frac{\alpha_a\alpha_r}{\kappa_a\kappa_r}}}{2}\end{aligned}\right\} \tag{3.24}$$

For sufficiently small production times, t, the exponential terms in Equation 3.22 can be approximated as,

$$exp(-\mu_1 t) \approx 1 - \mu_1 t \quad \text{and} \quad exp(-\mu_2 t) \approx 1 - \mu_2 t \qquad \text{for } t < 0.1/\mu_1 \tag{3.25}$$

Thus, Equation 3.22 reduces to,

$$\Delta p_r(t) = \frac{w_{p,net}}{\kappa_r}t \tag{3.26}$$

which is exactly the same with the early-time solution obtained for 1-tank model and describes the pseudosteady-state behavior of the reservoir tank alone.

The analytical solution of the 2-tank problem, Equation 3.22, yields the magnitude of the reservoir pressure decline and as well as the time at which the steady-state pressure drop occurs. The steady-state pressure drop is given by

$$\Delta p_{rss} = \left(\frac{\alpha_a + \alpha_r}{\alpha_a \alpha_r} \right) w_{p,net} = \left(\frac{1}{\alpha_a} + \frac{1}{\alpha_r} \right) w_{p,net} \tag{3.27}$$

Since $|\mu_1| > |\mu_2|$, $\exp(-\mu_1 t)$ term approaches to zero before $\exp(-\mu_2 t)$ term does, and the time at which the steady-state pressure drop occurs (denoted by t_{ss}, steady-state or stabilization time) is found from $\mu_2 t > 5$ as follows,

$$t_{ss} = \frac{10(\kappa_a \kappa_r)}{[\kappa_r(\alpha_a + \alpha_r) + \kappa_a \alpha_r] - \sqrt{[\kappa_r(\alpha_a + \alpha_r) + \kappa_a \alpha_r]^2 - 4\alpha_a \alpha_r \kappa_a \kappa_r}} \tag{3.28}$$

It is interesting to note from Equation 3.27 that the steady-state reservoir pressure drop, Δp_{rss}, is a function of the harmonic average of recharge constants of reservoir and aquifer, and the net production rate ($\alpha_r, \alpha_a, w_{p,net}$), whereas the stabilization time, t_{ss}, is dependent on aquifer and reservoir properties and independent of the net production rate. These results are similar to the ones obtained from the 1 reservoir tank with recharge source case.

3.2.2 1 reservoir – 1 aquifer without recharge source (2-tank closed system)

If no recharge is allowed then the system is called as a closed system. For this case, we set $w_a = 0$ or equivalently $\alpha_a = 0$ for the mass balance on aquifer tank (Equation 3.19). Then we obtain

$$-w_r = \kappa_a \frac{dp_a}{dt} \tag{3.29}$$

then the resulting system of equations is solved for p_a and p_r by using Laplace transformation (Appendix-C). The pressure change solution for the reservoir, i.e, $\Delta p_r(t)$, for the case of constant production rate (i.e., $w_{p,net}$ is constant) is given by

$$\Delta p_r(t) = \frac{w_{p,net}}{(\kappa_a + \kappa_r)} t + \frac{w_{p,net}}{\alpha_r} \left(\frac{\kappa_a}{\kappa_a + \kappa_r} \right)^2 \left[1 - exp\left(-\alpha_r \frac{\kappa_a + \kappa_r}{\kappa_a \kappa_r} t \right) \right] \tag{3.30}$$

It can be shown that for sufficiently small values of time such that

$$t < 0.1 \frac{\kappa_a \kappa_r}{\alpha_r (\kappa_a + \kappa_r)} \tag{3.31}$$

the exponential term in Equation 3.30 is approximated as

$$exp\left(-\alpha_r \frac{\kappa_a + \kappa_r}{\kappa_a \kappa_r} t \right) \approx 1 - \alpha_r \frac{\kappa_a + \kappa_r}{\kappa_a \kappa_r} t \tag{3.32}$$

Equation 3.30 reduces to

$$\Delta p_r(t) = \frac{w_{p,net}}{\kappa_r} t \tag{3.33}$$

which indicates that the pressure drop in the reservoir increases linearly with time with a slope equals to $w_{p,net} / \kappa_r$.

Similarly for sufficiently large times such that

$$exp\left(-\alpha_r \frac{\kappa_a + \kappa_r}{\kappa_a \kappa_r} t \right) \cong 0 \quad \text{for} \quad t > 5 \frac{1}{\alpha_r} \frac{\kappa_a \kappa_r}{\kappa_a + \kappa_r} \tag{3.34}$$

in Equation 3.30, then it can be shown that Equation 3.30 becomes

$$\Delta p_r(t) = \frac{w_{p,net}}{(\kappa_a + \kappa_r)} t + \frac{w_{p,net}}{\alpha_r} \frac{\kappa_a^2}{(\kappa_a + \kappa_r)^2} \tag{3.35}$$

which indicates that the pressure drop in the reservoir increases linearly with time with a slope equals to $w_{p,net} / (\kappa_a + \kappa_r)$. Equation 3.35 corresponds to the pseudosteady-state equation for the aquifer and reservoir system.

3.2.3 A comparison of behavior of the 2-tank open and closed systems

Figure 3.4 shows early-time and late-time reservoir pressure drawdown for the open and closed 2-tank lumped models for the case of constant production rate. As long as

the production rate is constant the early-time pressure response of a closed system is the same as of an open system. The pressure drop increases linearly with the production time and is given by Equations 3.26 and 3.33. This corresponds to pseudo-steady state flow behavior of the reservoir itself.

After some transition time the pressure (or water level) continues to decline steadily with time in the case of closed system. The pressure drop during this long-term production is given by Equation 3.35, which corresponds to pseudo-steady state behavior of the total system of reservoir and aquifer.

However, in the case of an open system, the late-time pressure stabilizes at a value which is given by Equation 3.27. This pressure behavior corresponds to steady-state flow behavior of the total system.

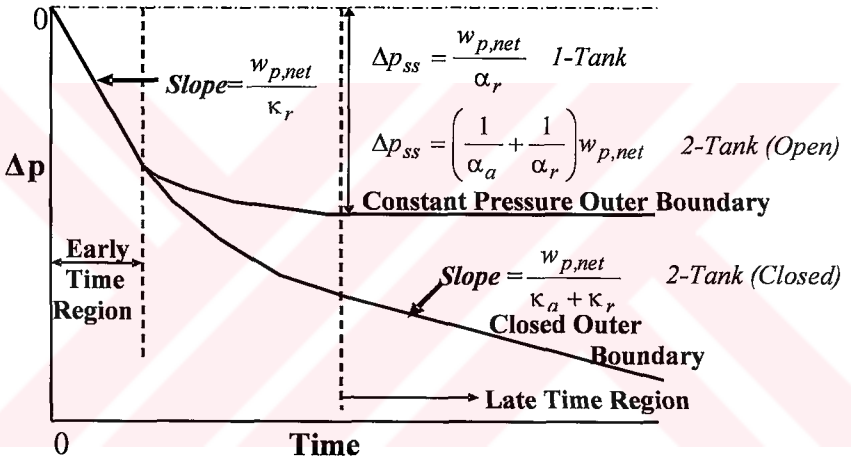

Figure 3.4 A comparison of early time and late time reservoir pressure drawdown in 2-tank open and closed lumped models for constant production rate.

As discussed earlier the pressure drop - time behavior of all models exhibit three district regions. The first region, the early-time region, reflects the pseudosteady-state behavior of the reservoir tank itself and yields a cartesian plot of Δp versus t straight line with slope of $w_{p,net} / \kappa_r$. This early-time pseudosteady-state behavior occurs for all models. The last region, the late-time region, reflects the pseudosteady-state behavior of the total system (reservoir + aquifer) for the closed model, whereas it exhibits the steady-state behavior of the total system for the open model. The pseudosteady-state behavior of the closed model is characterized by a straight line on a Δp versus t plot and the slope of the straight line is given by $w_{p,net} / (\kappa_a + \kappa_r)$.

The steady-state behavior of the open model is identified when Δp reaches a constant value which is given by $w_{p,net}(1/\alpha_a + 1/\alpha_r)$ for a 2-tank open model.

For both models, the duration of the transition region between the early-time region and the late-time region is mainly dependent on $\alpha_r, \alpha_a, \kappa_r$ and κ_a values. It lasts longer if the ratio of κ_a / κ_r gets larger. Figure 3.5 gives the pressure drop versus time graphs for the 2-tank open and closed models. The graphs show the pressure behavior of models for different time scales. For open and closed models the values of $\alpha_r, \alpha_a, \kappa_r$ and $w_{p,net}$ were assumed to be the same. Only the value of κ_a is changed.

As Figure 3.5-a indicates all models show the same behavior at early times up to 0.2 days. The early-time straight line has a slope of $w_{p,net} / \kappa_r$. All cases reach to the transition region after 0.2 days of production time. The open and closed models with $\kappa_a = 2 \times 10^7$ kg/bar deviates from each other and the closed one enters into the late time pseudosteady-state behavior (see Figure 3.5-b and c). However, the open and closed models with $\kappa_a = 2 \times 10^8$ kg/bar exhibit the same Δp versus t behavior until 20 days when open and closed models for this case deviate from each other (Figure 3.5-c and d). Interestingly, a straight line relationship can develop for $\kappa_a = 2 \times 10^8$ kg/bar case between 6 and 20 days (Figure 3.5-c). Existence of such a straight line relationship is also seen for $\kappa_a = 2 \times 10^9$ kg/bar case between 6 and 200 days (Figure 3.5-c and d) and for $\kappa_a = 2 \times 10^{10}$ kg/bar case between 10 and 1000 days (Figure 3.5-c, d, e, and f). The straight line relationship in the transition region is given by

$$\frac{d\,\Delta p}{dt} = \frac{w_{p,net}}{\kappa_a + \kappa_r} \tag{3.36}$$

which is the pseudosteady-state relationship for the closed model. The κ_a values in cases which exhibit such relationship are much larger than the κ_r values so that the equation above reduces to

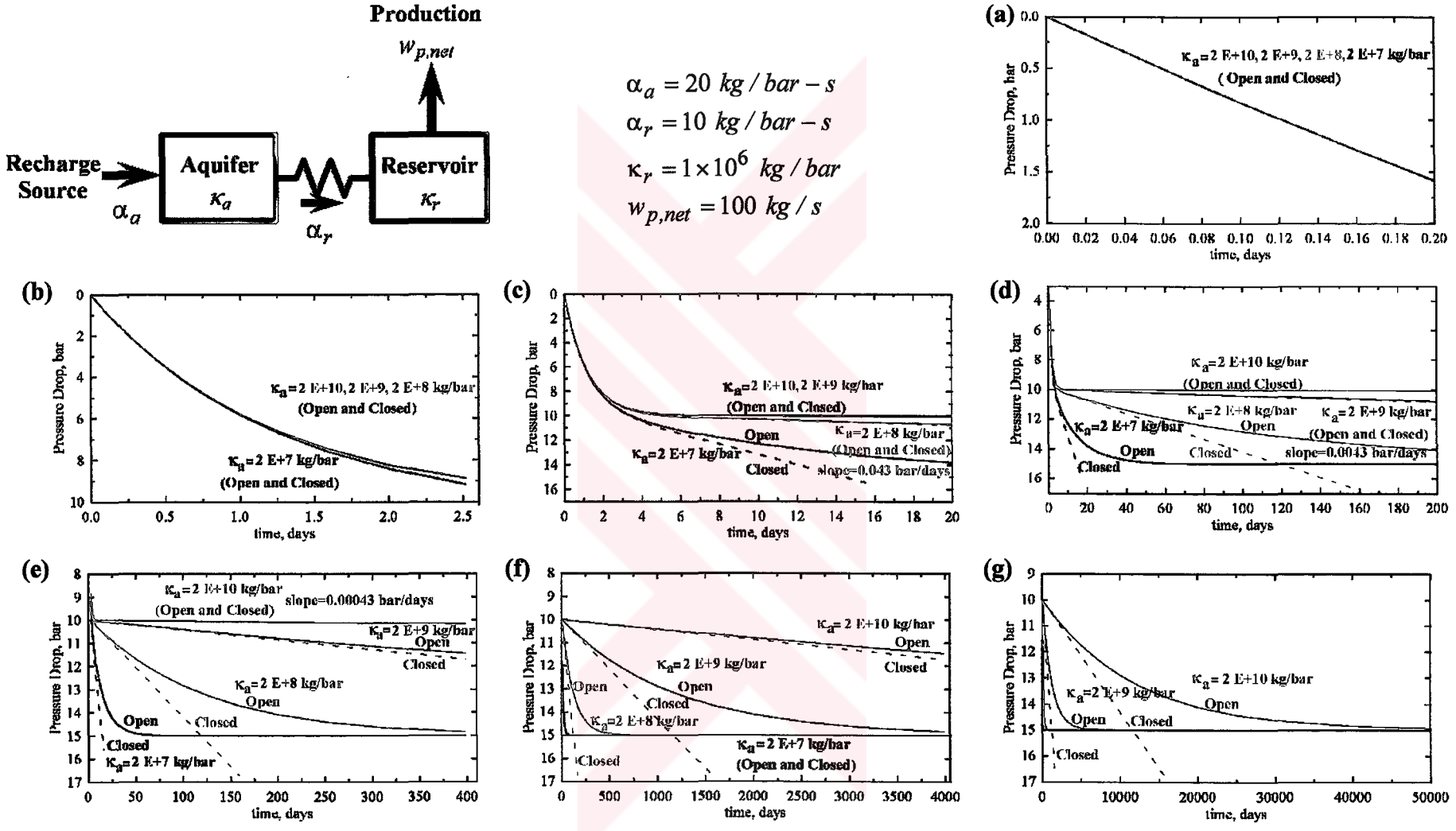

Figure 3.5 Transition region behavior of 2-tank open system

$$\frac{d\,\Delta p}{dt} \cong \frac{w_{p,net}}{\kappa_a} \tag{3.37}$$

In conclusion; whenever $\kappa_a >> \kappa_r$ holds, the open and close models show the pseudosteady-state straight line relationship in the transition region. The duration of this relationship gets longer when κ_a is larger or α_a is smaller. In other words, before feeling the effects of the recharge source the open model exhibits the pseudosteady-state behavior similar to the closed model as long as $\kappa_a >> \kappa_r$.

3.2.4 1 reservoir–1 aquifer with recharge source (without initial hydraulic equilibrium)

In this case, the system is similar to the system considered in Chapter 3.2.1, the constant pressure recharge source supplies the aquifer tank which recharges the reservoir tank as production proceeds. However, it is assumed that the initial pressures of the reservoir and the aquifer tanks are different from the recharge source initial pressure, p_i. Such an assumption is valid when the recharge source is not in hydraulic equilibrium with the reservoir and aquifer system at $t = 0$. Although the mass balances on the aquifer and the reservoir tanks are the same (Equations 3.19 and 3.20), initial condition is expressed as below:

$$\text{Initial Condition} \quad : \quad p_a(t=0) = p_r(t=0) = p_o \neq p_i \tag{3.38}$$

The resulting equation is expressed by adding a term including initial pressure difference between the recharge source and the reservoir or aquifer tanks $(p_i - p_o)$ to the solution (Equation 3.22) obtained in Chapter 3.2.1. The pressure change solution for the reservoir, $\Delta p_r(t)$, for the case of constant production rate is given by

$$\left.\begin{aligned} \Delta p_r(t) = \overbrace{\frac{w_{p,net}}{\kappa_r}\left[\frac{d}{\mu_1\mu_2} + \frac{(\mu_1 - d)}{\mu_1(\mu_2 - \mu_1)}exp(-\mu_1 t) + \frac{(\mu_2 - d)}{\mu_2(\mu_1 - \mu_2)}exp(-\mu_2 t)\right]}^{Equation\ 3.22} \\ + \frac{\alpha_a\,\alpha_r}{\kappa_a\,\kappa_r}(p_i - p_o)\frac{[(\mu_2 - \mu_1) - \mu_2\,exp(-\mu_1 t) + \mu_1\,exp(-\mu_2 t)]}{\mu_1\,\mu_2(\mu_1 - \mu_2)} \end{aligned}\right\} \tag{3.39}$$

The detailed solutions describing the aquifer and reservoir pressure behaviors are given in Appendix-D.

By using the early- and the late-time approximations of the exponential terms in Equation 3.39, the solution reduces to the equations given below, respectively.

For early-time : $$\Delta p_r(t) = \frac{w_{p,net}}{\kappa_r} t \tag{3.40}$$

For late-time : $$\Delta p_{rss} = \left[\frac{1}{\alpha_a} + \frac{1}{\alpha_r}\right] w_{p,net} - (p_i - p_o) \tag{3.41}$$

As it can be seen from Equation 3.40, the early time solution, for this case, is exactly the same with one obtained in Chapter 3.2.1 (Equation 3.26), the reservoir pressure declines with production time as a function of production rate, $w_{p,net}$, and reservoir storage capacity, κ_r. On the other hand, the late-time solution (Equation 3.41) is obtained by subtracting a term of $(p_i - p_o)$ from the solution obtained in Chapter 3.2.1 (Equation 3.27).

3.3 1 Reservoir – 2 Aquifers System (3-Tank Model)

Lumped parameter models containing more than two tanks have also been considered. Figure 3.6 shows a system containing 1 reservoir and 2 aquifers. The system is represented by three tanks. The main purpose to model such a system is to model the unsteady-state behavior of flow from the aquifer tanks to the reservoir tank (see the discussion related to Figures 2.7 and 2.8).

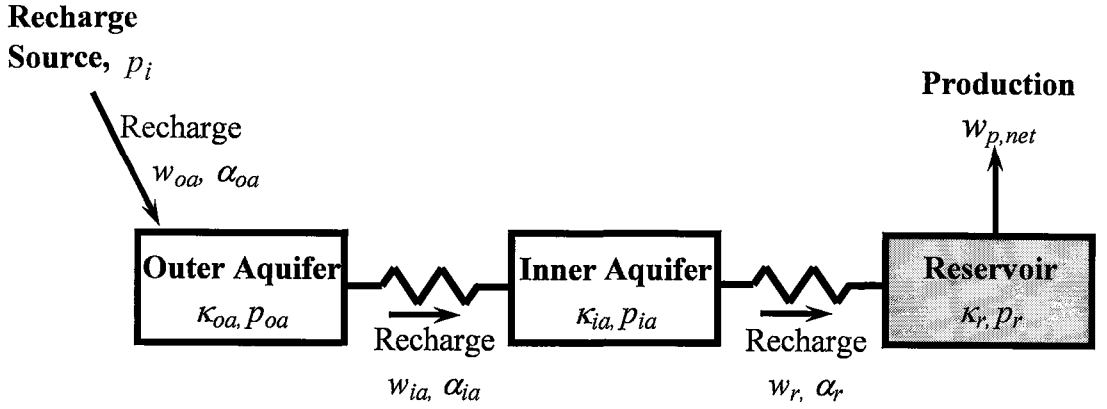

Figure 3.6 Schematic of a 3-tank model.

The pressures of the reservoir and the aquifer tanks are assumed to be the same throughout the system when production initiated. Due to the fluid production from the reservoir tank, the reservoir pressure drops hence fluid flows from the inner aquifer tank to the reservoir tank to maintain the reservoir pressure. This flow causes a pressure drop in the inner aquifer tank and a corresponding expansion of the remaining fluid in the inner aquifer tank. When enough flow takes place from the inner aquifer to cause a significant pressure drop in the inner aquifer, a pressure difference exists between the outer aquifer tank and the inner aquifer tank. Flow takes place from the outer aquifer to the inner aquifer tank. This flow tends to maintain the inner aquifer pressure and eventually causes a pressure drop in the outer aquifer tank. If the outer aquifer tank is connected to a recharge source, the fluid flow initiates from the recharge source to the outer aquifer tank.

Two outer boundary conditions namely the constant pressure outer aquifer boundary and no flow outer aquifer boundary, are considered similar to 2-tank modeling. If the outer aquifer tank is connected to a recharge source at a constant pressure of p_i, the system is called 3-tank open system, whereas if the outer aquifer has no flow boundary then the system is called as 3-tank closed system.

3.3.1 1 reservoir - 2 aquifers with recharge source (3-tank open system)

In this chapter, the analytical solution is obtained for the system shown in Figure 3.6 by using mass balance equations on the reservoir and the aquifer tanks which yields the following differential equations below:

For Outer Aquifer:

$$w_{oa} - w_{ia} = \kappa_{oa} \frac{dp_{oa}}{dt} \quad \text{or} \quad \alpha_{oa}(p_i - p_{oa}) - \alpha_{ia}(p_{oa} - p_{ia}) = \kappa_{oa} \frac{dp_{oa}}{dt} \tag{3.42}$$

For Inner Aquifer:

$$w_{ia} - w_r = \kappa_{ia} \frac{dp_{ia}}{dt} \quad \text{or} \quad \alpha_{ia}(p_{oa} - p_{ia}) - \alpha_r(p_{ia} - p_r) = \kappa_{ia} \frac{dp_{ia}}{dt} \tag{3.43}$$

For Reservoir:

$$w_r - w_{p,net} = \kappa_r \frac{dp_r}{dt} \quad \text{or} \quad \alpha_r(p_{ia} - p_r) - w_{p,net} = \kappa_r \frac{dp_r}{dt} \tag{3.44}$$

where $\kappa_{oa} = V_{oa}\phi_{oa}\rho_{oa}c_t$, $\kappa_{ia} = V_{ia}\phi_{ia}\rho_{ia}c_t$ and $\kappa_r = V_r\phi_r\rho_r c_t$

Initial Condition:

$$\Delta p_{oa}(t=0) = \Delta p_{ia}(t=0) = \Delta p_r(t=0) = 0 \tag{3.45}$$

The solutions describing the outer and inner aquifers, and reservoir pressure behaviors can be obtained from Equations 3.42 - 3.45 by the use of Laplace transformation. Details of the solution procedure are given in Appendix-E. The solution of the reservoir pressure behavior is as follows:

$$\Delta p_r(t) = \frac{w_{p,net}}{\kappa_r}\left[A + B\,exp(-\mu_1 t) + C\,exp(-\mu_2 t) + D\,exp(-\mu_3 t)\right] \tag{3.46}$$

where

$$\left.\begin{aligned} A &= \frac{a_2}{\mu_1\mu_2\mu_3} \quad , \quad B = -\frac{\mu_1^2 - a_1\mu_1 + a_2}{\mu_1(\mu_2-\mu_1)(\mu_3-\mu_1)} \\ C &= -\frac{\mu_2^2 - a_1\mu_2 + a_2}{\mu_2(\mu_1-\mu_2)(\mu_3-\mu_2)} \quad , \quad D = -\frac{\mu_3^2 - a_1\mu_3 + a_2}{\mu_3(\mu_1-\mu_3)(\mu_2-\mu_3)} \end{aligned}\right\} \tag{3.47}$$

μ_1, μ_2, and μ_3 are the roots of cubic equation given in Appendix-E,

$$\left.\begin{aligned} \mu_1 &= 2\sqrt{Q}\,cos\left(\frac{\theta}{3}\right) + \frac{a_3}{3} \quad , \quad \mu_2 = 2\sqrt{Q}\,cos\left(\frac{\theta+2\pi}{3}\right) + \frac{a_3}{3} \\ \mu_3 &= 2\sqrt{Q}\,cos\left(\frac{\theta+4\pi}{3}\right) + \frac{a_3}{3} \end{aligned}\right\} \tag{3.48}$$

where

$$Q = \frac{a_3^2 - 3a_4}{9} \quad , \quad R = \frac{2a_3^3 - 9a_3a_4 + 27a_5}{54} \quad , \quad \theta = arc\,cos\left(\frac{R}{\sqrt{Q^3}}\right) \tag{3.49}$$

$$
\left.
\begin{aligned}
a_1 &= \frac{\kappa_{ia}(\alpha_{ia}+\alpha_{oa})+\kappa_{oa}(\alpha_{ia}+\alpha_r)}{\kappa_{ia}\kappa_{oa}} \\
a_2 &= \frac{\alpha_{ia}\alpha_r+\alpha_{oa}\alpha_r+\alpha_{ia}\alpha_{oa}}{\kappa_{ia}\kappa_{oa}} \\
a_3 &= \frac{\kappa_{oa}\kappa_r(\alpha_{ia}+\alpha_r)+\kappa_{ia}\kappa_r(\alpha_{ia}+\alpha_{oa})+\kappa_{ia}\kappa_{oa}\alpha_r}{\kappa_{ia}\kappa_{oa}\kappa_r} \\
a_4 &= \frac{\kappa_r(\alpha_{ia}\alpha_{oa}+\alpha_{ia}\alpha_r+\alpha_{oa}\alpha_r)+\kappa_{ia}(\alpha_{ia}\alpha_r+\alpha_{oa}\alpha_r)+\kappa_{oa}(\alpha_{ia}\alpha_r)}{\kappa_{ia}\kappa_{oa}\kappa_r} \\
a_5 &= \frac{\alpha_{ia}\alpha_{oa}\alpha_r}{\kappa_{ia}\kappa_{oa}\kappa_r}
\end{aligned}
\right\} \qquad (3.50)
$$

For early and late production times, the reservoir pressure behavior (Equation 3.46) can be simplified by using the polynomial approximation of exponential expression.

For early production times, $t < 0.1/\mu_1$, the exponential terms in Equation 3.46 can be approximated as,

$$exp(-\mu_1 t) \approx 1-\mu_1 t, \quad exp(-\mu_2 t) \approx 1-\mu_2 t, \text{ and } \quad exp(-\mu_3 t) \approx 1-\mu_3 t \qquad (3.51)$$

Thus, Equation 3.46 becomes,

$$\Delta p_r(t) = \frac{w_{p,net}}{\kappa_r}[A+B(1-\mu_1 t)+C(1-\mu_2 t)+D(1-\mu_3 t)] \qquad (3.52)$$

Substituting the terms of *A, B, C, D,* μ_1, μ_2 ,and μ_3 (these constants are given in Appendix E) in Equation 3.52 gives

$$\Delta p_r(t) = \frac{w_{p,net}}{\kappa_r} t \qquad (3.53)$$

Equation 3.53 is the same with the other early-time solutions of the models investigated earlier and it indicates that reservoir pressure declines linearly with production time.

The exponential terms in Equation 3.46 approximate to zero for late production times and Equation 3.46 reduces to

$$\Delta p_{rss} = \frac{w_{p,net}}{\kappa_r}[A] \qquad \text{or} \qquad \Delta p_{rss} = w_{p,net}\left[\frac{\alpha_{ia}(\alpha_{oa}+\alpha_r)+\alpha_{oa}\alpha_r}{\alpha_{ia}\alpha_{oa}\alpha_r}\right] \qquad (3.54)$$

The reservoir pressure stabilizes at a value determined by Equation 3.54 and the stabilization time, t_{ss}, is determined from $\mu_2 t > 5$ (since $|\mu_1| > |\mu_3| > |\mu_2|$) as follows,

$$t_{ss} = \frac{5}{2\sqrt{Q}\cos\left(\frac{\theta + 2\pi}{3}\right) + \frac{a_3}{3}} \tag{3.55}$$

3.3.2 1 reservoir – 2 aquifers without recharge source (3-tank closed system)

If the outer aquifer tank has no flow boundary (outer aquifer tank is not connected to a constant pressure source), $\alpha_{oa} = 0$ is set and mass balance on the outer aquifer tank can be written as,

For Outer Aquifer:

$$-w_{ia} = \kappa_{oa}\frac{dp_{oa}}{dt} \qquad \text{or} \qquad -\alpha_{ia}(p_{oa} - p_{ia}) = \kappa_{oa}\frac{dp_{oa}}{dt} \tag{3.56}$$

Thus, the reservoir pressure behavior in terms of pressure difference, $\Delta p_r(t)$, is obtained as follows (Appendix-F):

$$\begin{aligned}\Delta p_r(t) = {} & \frac{w_{p,net}}{\kappa_r} a_2 \left\{ \frac{t}{\mu_1\mu_2} + \frac{1}{\mu_2 - \mu_1}\left[\frac{exp(-\mu_1 t) - 1}{\mu_1^2} - \frac{exp(-\mu_2 t) - 1}{\mu_2^2} \right] \right\} \\ & + \frac{w_{p,net}}{\kappa_r} a_1 \left\{ \frac{1}{\mu_2 - \mu_1}\left[\frac{1 - exp(-\mu_1 t)}{\mu_1} - \frac{1 - exp(-\mu_2 t)}{\mu_2} \right] \right\} \\ & + \frac{w_{p,net}}{\kappa_r} \left\{ \frac{1}{\mu_2 - \mu_1}\left[exp(-\mu_1 t) - exp(-\mu_2 t) \right] \right\}\end{aligned} \tag{3.57}$$

where

$$\mu_1 = \frac{a_3 + \sqrt{a_3^2 - 4a_4}}{2} \quad , \quad \mu_2 = \frac{a_3 - \sqrt{a_3^2 - 4a_4}}{2} \tag{3.58}$$

$$a_1 = \frac{\kappa_{oa}(\alpha_{ia} + \alpha_r) + \kappa_{ia}\alpha_{ia}}{\kappa_{ia}\kappa_{oa}}$$

$$a_2 = \frac{\alpha_{ia}\alpha_r}{\kappa_{ia}\kappa_{oa}}$$

$$a_3 = \frac{\kappa_{oa}\kappa_r(\alpha_{ia} + \alpha_r) + \kappa_{ia}\kappa_r\alpha_{ia} + \kappa_{ia}\kappa_{oa}\alpha_r}{\kappa_{ia}\kappa_{oa}\kappa_r} \tag{3.59}$$

$$a_4 = \frac{(\kappa_{ia} + \kappa_{oa} + \kappa_r)\alpha_{ia}\alpha_r}{\kappa_{ia}\kappa_{oa}\kappa_r}$$

By using the early- and late-time approximations of the exponential terms in Equation 3.57, the solution reduces to the equations given below, respectively.

For early-time : $$\Delta p_r(t) = \frac{w_{p,net}}{\kappa_r} t \tag{3.60}$$

For late-time : $$\Delta p_r(t) = \frac{w_{p,net}}{(\kappa_{ia} + \kappa_{oa} + \kappa_r)} t + w_{p,net}\left[\frac{(\kappa_{ia} + \kappa_{oa})^2\alpha_{ia} + \kappa_{oa}^2\alpha_r}{\alpha_{ia}\alpha_r(\kappa_{ia} + \kappa_{oa} + \kappa_r)^2}\right] \tag{3.61}$$

For early-time, the reservoir pressure declines with time and after some transition time reservoir pressure reaches steady-state flow and it stabilizes with a constant value. The stabilization time is obtained by $\mu_2 t > 5$, since $|\mu_1| > |\mu_2|$.

$$t_{ss} = \frac{10\kappa_{ia}\kappa_{oa}\kappa_r}{\kappa_{oa}\kappa_r(\alpha_{ia} + \alpha_r) + \kappa_{ia}\kappa_{oa}(\alpha_r) + \kappa_{ia}\kappa_r(\alpha_{ia}) - SQRT} \tag{3.62}$$

$$SQRT = \sqrt{\begin{matrix}[\kappa_{oa}\kappa_r(\alpha_{ia} + \alpha_r) + \kappa_{ia}\kappa_{oa}(\alpha_r) + \kappa_{ia}\kappa_r(\alpha_{ia})]^2 \\ - 4\alpha_{ia}\alpha_r\kappa_{ia}\kappa_{oa}\kappa_r(\kappa_{ia} + \kappa_{oa} + \kappa_r)\end{matrix}} \tag{3.63}$$

3.4 1 Shallow Reservoir – 1 Deep Reservoir With Recharge Source (2 Reservoir Tanks Without Aquifer Model)

It is assumed that the reservoir consists of two parts; 1 shallow (upper) reservoir and 1 deep (lower) reservoir. Both are interconnected and supplied by the same recharge source. A schematic of the model discussed is presented in Figure 3.7.

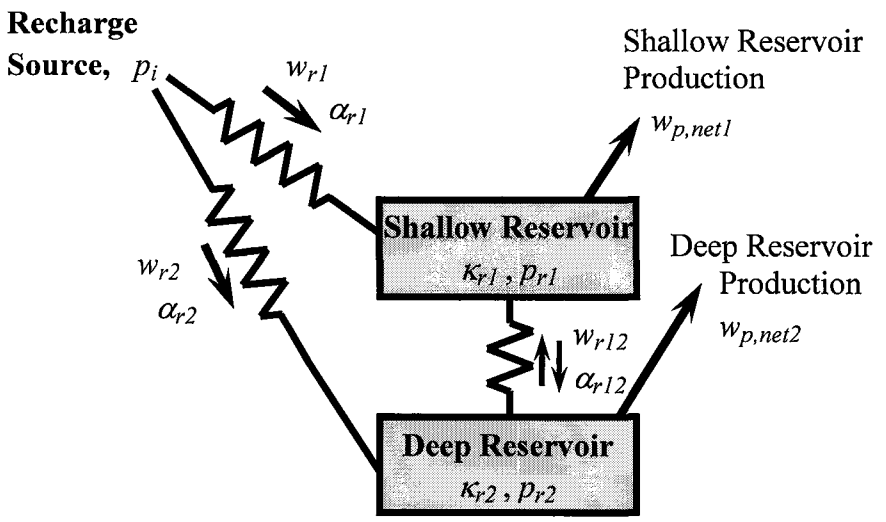

Figure 3.7 Schematic of a 2 reservoir tanks without aquifer model.

Depending on the production rates, $w_{p,net1}$, $w_{p,net2}$, and the recharge rates of the shallow and deep reservoirs, w_{r1}, w_{r2}, the fluid flow occurs between the reservoirs.

Two cases are considered: (1) There is hydraulic equilibrium initially between the reservoir tanks, and (2) There is no hydraulic equilibrium initially between the reservoir tanks.

3.4.1 2 reservoir tanks without aquifer model (with initial hydraulic equilibrium)

It is considered that the shallow and deep reservoirs and the recharge source all are in a hydraulic equilibrium. Mass balances on both reservoirs and the initial conditions can be expressed as below:

For Shallow Reservoir :

$$w_{r1} + w_{r12} - w_{p,net1} = \alpha_{r1}(p_i - p_{r1}) + \alpha_{r12}(p_{r2} - p_{r1}) - w_{p,net1} = \kappa_{r1}\frac{dp_{r1}}{dt} \qquad (3.64)$$

For Deep Reservoir :

$$w_{r2} - w_{r12} - w_{p,net2} = \alpha_{r2}(p_i - p_{r2}) - \alpha_{r12}(p_{r2} - p_{r1}) - w_{p,net2} = \kappa_{r2}\frac{dp_{r2}}{dt} \qquad (3.65)$$

Initial Conditions : $\Delta p_{r1} = \Delta p_{r2} = 0$ @ $t = 0$ (3.66)

The solutions describing the pressure behavior of the shallow and deep reservoirs can be obtained from Equations 3.64 - 3.66 by using Laplace transformation. Details of the solution procedure can be found in Appendix-G. The solutions for both reservoirs in terms of pressure changes, $\Delta p_{r1}(t)$ and $\Delta p_{r2}(t)$, are given as follows:

$$\Delta p_{r1}(t) = w_{p,net1}\left[\frac{a_1}{\mu_1\mu_2} - \frac{\mu_1 - \kappa_{r1}a_1}{\kappa_{r1}\mu_1(\mu_1-\mu_2)}exp(-\mu_1 t) + \frac{\mu_2 - \kappa_{r1}a_1}{\kappa_{r1}\mu_2(\mu_1-\mu_2)}exp(-\mu_2 t)\right] + w_{p,net2}\left[\frac{a_2}{\mu_1\mu_2} + \frac{a_2}{\mu_1(\mu_1-\mu_2)}exp(-\mu_1 t) - \frac{a_2}{\mu_2(\mu_1-\mu_2)}exp(-\mu_2 t)\right] \quad (3.67)$$

$$\Delta p_{r2}(t) = w_{p,net1}\left[\frac{a_2}{\mu_1\mu_2} + \frac{a_2}{\mu_1(\mu_1-\mu_2)}exp(-\mu_1 t) - \frac{a_2}{\mu_2(\mu_1-\mu_2)}exp(-\mu_2 t)\right] + w_{p,net2}\left[\frac{a_3}{\mu_1\mu_2} - \frac{\mu_1 - \kappa_{r2}a_3}{\kappa_{r2}\mu_1(\mu_1-\mu_2)}exp(-\mu_1 t) + \frac{\mu_2 - \kappa_{r2}a_3}{\kappa_{r2}\mu_2(\mu_1-\mu_2)}exp(-\mu_2 t)\right] \quad (3.68)$$

where μ_1 and μ_2 are the roots of $s^2 + a_4 s + a_5$ given in Appendix-G.

$$\mu_1 = \frac{a_4 + \sqrt{a_4^2 - 4a_5}}{2} \quad , \quad \mu_2 = \frac{a_4 - \sqrt{a_4^2 - 4a_5}}{2} \quad (3.69)$$

$$\left.\begin{aligned} a_1 &= \frac{\alpha_{r2} + \alpha_{r12}}{\kappa_{r1}\kappa_{r2}} \\ a_2 &= \frac{\alpha_{r12}}{\kappa_{r1}\kappa_{r2}} \\ a_3 &= \frac{\alpha_{r1} + \alpha_{r12}}{\kappa_{r1}\kappa_{r2}} \\ a_4 &= \frac{\alpha_{r1} + \alpha_{r12}}{\kappa_{r1}} + \frac{\alpha_{r2} + \alpha_{r12}}{\kappa_{r2}} \\ a_5 &= \frac{\alpha_{r1}\alpha_{r2} + \alpha_{r12}(\alpha_{r1} + \alpha_{r2})}{\kappa_{r1}\kappa_{r2}} \end{aligned}\right\} \quad (3.70)$$

Since there is a flow connection between the shallow and deep reservoirs, their pressure behaviors are affected by the production rates of each other (Equations 3.67 and 3.68).

Sufficiently early and late time approximations of Equations 3.67 and 3.68 are obtained by using the exponential approximations.

For early-time : $exp(-\mu_1 t) \approx 1-\mu_1 t$ and $exp(-\mu_2 t) \approx 1-\mu_2 t$

- for shallow reservoir : $\Delta p_{r1}(t) = \frac{w_{p,net1}}{\kappa_{r1}} t$ (3.71)

- for deep reservoir : $\Delta p_{r2}(t) = \frac{w_{p,net2}}{\kappa_{r2}} t$ (3.72)

Equations 3.71 and 3.72 show that pressures of both shallow and deep reservoirs decline linearly with time as obtained for the models discussed before.

For late-time : $exp(-\mu_1 t) \cong 0$ and $exp(-\mu_2 t) \cong 0$

- for shallow reservoir : $\Delta p_{r1ss} = \frac{w_{p,net1}(\alpha_{r2}+\alpha_{r12}) + w_{p,net2}(\alpha_{r12})}{\alpha_{r1}\alpha_{r2} + \alpha_{r12}(\alpha_{r1}+\alpha_{r2})}$ (3.73)

- for deep reservoir : $\Delta p_{r2ss} = \frac{w_{p,net1}(\alpha_{r12}) + w_{p,net2}(\alpha_{r1}+\alpha_{r12})}{\alpha_{r1}\alpha_{r2} + \alpha_{r12}(\alpha_{r1}+\alpha_{r2})}$ (3.74)

Both shallow and deep reservoir pressures reach steady-state flow and they stabilize with a constant value function of production rates of both reservoirs. The stabilization times of shallow and deep reservoirs are the same, t_{ss}, and it is obtained by $\mu_2 t > 5$, since $|\mu_1| > |\mu_2|$.

$$t_{ss} = \frac{10\kappa_{r1}\kappa_{r2}}{\kappa_{r2}(\alpha_{r1}+\alpha_{r12}) + \kappa_{r1}(\alpha_{r2}+\alpha_{r12}) - SQRT} \tag{3.75}$$

$$SQRT = \sqrt{\begin{matrix}(\kappa_{r2}\alpha_{r1} - \kappa_{r1}\alpha_{r2})^2 + (\kappa_{r2}\alpha_{r12} + \kappa_{r1}\alpha_{r12})^2 \\ + (\kappa_{r2} - \kappa_{r1})(2\kappa_{r2}\alpha_{r1}\alpha_{r12} - 2\kappa_{r1}\alpha_{r2}\alpha_{r12})\end{matrix}} \tag{3.76}$$

3.4.2 2 reservoir tanks without aquifer model (without initial hydraulic equilibrium)

The case of the shallow and deep reservoirs and the recharge source without an initial hydraulic equilibrium is investigated in this part. To obtain the analytical

solution of this system, mass balances on both reservoirs (Equations 3.64 and 3.65) given in Chapter 3.4.1 can be applied. However, the initial conditions are altered as given below:

$$\text{Initial Conditions} \quad : \quad p_{r1} = p_{r1i} \ @\, t = 0 \quad , \quad p_{r2} = p_{r2i} \ @\, t = 0 \tag{3.77}$$

The solutions of system of Equations 3.64 and 3.65 with the initial condition of Equation 3.77 are obtained as below (Appendix-H):

$$\begin{aligned}\Delta p_{r1}(t) = {} & \frac{w_{p,net1}}{\kappa_{r1}}\left[\frac{a_4}{\mu_1\mu_2} - \frac{\mu_1 - a_4}{\mu_1(\mu_1-\mu_2)}exp(-\mu_1 t) + \frac{\mu_2 - a_4}{\mu_2(\mu_1-\mu_2)}exp(-\mu_2 t)\right] \\ & + \frac{w_{ii2}}{\kappa_{r2}}\left[\frac{a_5}{\mu_1\mu_2} + \frac{a_5}{\mu_1(\mu_1-\mu_2)}exp(-\mu_1 t) - \frac{a_5}{\mu_2(\mu_1-\mu_2)}exp(-\mu_2 t)\right] \\ & + \frac{exp(-\mu_1 t)}{\mu_1(\mu_1-\mu_2)}\left[\frac{a_{10}\mu_1}{\kappa_{r1}} - \frac{a_4 a_{10}}{\kappa_{r1}} + \frac{a_5 a_9}{\kappa_{r2}}\right] - \frac{exp(-\mu_2 t)}{\mu_2(\mu_1-\mu_2)}\left[\frac{a_{10}\mu_2}{\kappa_{r1}} - \frac{a_4 a_{10}}{\kappa_{r1}} + \frac{a_5 a_9}{\kappa_{r2}}\right] \\ & + \frac{1}{\mu_1\mu_2}\left[\frac{a_5 a_9}{\kappa_{r2}} - \frac{a_4 a_{10}}{\kappa_{r1}}\right]\end{aligned} \tag{3.78}$$

$$\begin{aligned}\Delta p_{r2}(t) = {} & \frac{w_{p,net1}}{\kappa_{r1}}\left[\frac{a_6}{\mu_1\mu_2} + \frac{a_6}{\mu_1(\mu_1-\mu_2)}exp(-\mu_1 t) - \frac{a_6}{\mu_2(\mu_1-\mu_2)}exp(-\mu_2 t)\right] \\ & + \frac{w_{p,net2}}{\kappa_{r2}}\left[\frac{a_3}{\mu_1\mu_2} - \frac{\mu_1 - a_3}{\mu_1(\mu_1-\mu_2)}exp(-\mu_1 t) + \frac{\mu_2 - a_3}{\mu_2(\mu_1-\mu_2)}exp(-\mu_2 t)\right] \\ & + \frac{exp(-\mu_1 t)}{\mu_1(\mu_1-\mu_2)}\left[-\frac{a_9\mu_1}{\kappa_{r2}} + \frac{a_3 a_9}{\kappa_{r2}} - \frac{a_6 a_{10}}{\kappa_{r1}}\right] - \frac{exp(-\mu_2 t)}{\mu_2(\mu_1-\mu_2)}\left[-\frac{a_9\mu_2}{\kappa_{r2}} + \frac{a_3 a_9}{\kappa_{r2}} - \frac{a_6 a_{10}}{\kappa_{r1}}\right] \\ & + \frac{1}{\mu_1\mu_2}\left[\frac{a_3 a_9}{\kappa_{r2}} - \frac{a_6 a_{10}}{\kappa_{r1}}\right]\end{aligned} \tag{3.79}$$

where μ_1 and μ_2 are the roots of $s^2 + a_7 s + a_8$ given in Appendix-H.

$$\mu_1 = \frac{a_7 + \sqrt{a_7^2 - 4a_8}}{2} \quad , \quad \mu_2 = \frac{a_7 - \sqrt{a_7^2 - 4a_8}}{2} \tag{3.80}$$

$$\left.\begin{aligned} & a_3 = \frac{\alpha_{r1} + \alpha_{r12}}{\kappa_{r1}} \ , \ a_4 = \frac{\alpha_{r2} + \alpha_{r12}}{\kappa_{r2}} \ , \ a_5 = \frac{\alpha_{r12}}{\kappa_{r1}} \quad , \quad a_6 = \frac{\alpha_{r12}}{\kappa_{r2}} \\ & a_7 = \frac{\alpha_{r1} + \alpha_{r12}}{\kappa_{r1}} + \frac{\alpha_{r2} + \alpha_{r12}}{\kappa_{r2}} \quad , \quad a_8 = \frac{\alpha_{r1}\alpha_{r2} + \alpha_{r12}(\alpha_{r1} + \alpha_{r2})}{\kappa_{r1}\kappa_{r2}} \\ & a_9 = -\alpha_{r2}(p_i - p_{r2i}) + \alpha_{r12}(p_{r2i} - p_{r1i}) \\ & a_{10} = \alpha_{r1}(p_i - p_{r1i}) + \alpha_{r12}(p_{r2i} - p_{r1i}) \end{aligned}\right\} \tag{3.81}$$

The early-time pressure drops in the shallow and deep reservoirs are dependent on the production rates, storage capacities, and the differences in initial pressure and are given by

- for shallow reservoir $: \Delta p_{r1}(t) = \frac{w_{p,net1}}{\kappa_{r1}} t - \frac{\alpha_{r12}(p_{r2i} - p_{r1i}) + \alpha_{r1}(p_i - p_{r1i})}{\kappa_{r1}} t$

(3.82)

- for deep reservoir $: \Delta p_{r2}(t) = \frac{w_{p,net2}}{\kappa_{r2}} t + \frac{\alpha_{r12}(p_{r2i} - p_{r1i}) - \alpha_{r2}(p_i - p_{r2i})}{\kappa_{r2}} t$

(3.83)

The late-time pressures in the shallow and deep reservoirs are given by Equations 3.84 and 3.85, respectively.

$$\Delta p_{r1ss} = \frac{w_{p,net1}(\alpha_{r2} + \alpha_{r12}) + w_{p,net2}(\alpha_{r12})}{\alpha_{r1}\alpha_{r2} + \alpha_{r12}(\alpha_{r1} + \alpha_{r2})} - (p_i - p_{r1i}) \tag{3.84}$$

$$\Delta p_{r2ss} = \frac{w_{p,net1}(\alpha_{r12}) + w_{p,net2}(\alpha_{r1} + \alpha_{r12})}{\alpha_{r1}\alpha_{r2} + \alpha_{r12}(\alpha_{r1} + \alpha_{r2})} - (p_i - p_{r2i}) \tag{3.85}$$

The stabilization time is,

$$t_{ss} = \frac{10\kappa_{r1}\kappa_{r2}}{\kappa_{r2}(\alpha_{r1} + \alpha_{r12}) + \kappa_{r1}(\alpha_{r2} + \alpha_{r12}) - SQRT} \tag{3.86}$$

$$SQRT = \sqrt{\begin{matrix}(\kappa_{r2}\alpha_{r1} - \kappa_{r1}\alpha_{r2})^2 + (\kappa_{r2}\alpha_{r12} + \kappa_{r1}\alpha_{r12})^2 \\ + (\kappa_{r2} - \kappa_{r1})(2\kappa_{r2}\alpha_{r1}\alpha_{r12} - 2\kappa_{r1}\alpha_{r2}\alpha_{r12})\end{matrix}} \tag{3.87}$$

3.5 1 Shallow Reservoir – 1 Deep Reservoir – 1 Aquifer With Recharge Source (2 Reservoir Tanks With Aquifer Model)

As different from the lumped model considered in Chapter 3.4, one aquifer is included in the geothermal system which consists of 1 shallow (upper) reservoir and 1 deep (lower) reservoir. Both reservoirs are interconnected and supplied by the aquifer which is connected to a constant pressure recharge source (Figure 3.8).

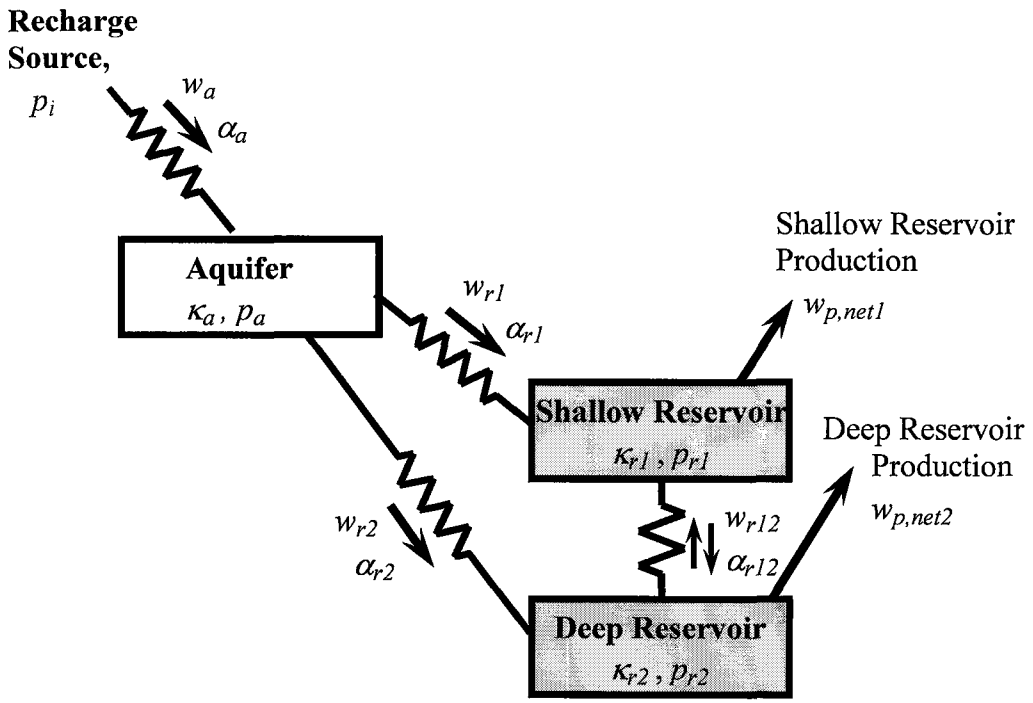

Figure 3.8 Schematic of a 2 reservoir tanks with aquifer model.

In the following sections, the cases of the system with and without the initial hydraulic equilibrium are investigated separately.

3.5.1 2 reservoir tanks with aquifer model (with initial hydraulic equilibrium)

Mass balances on both reservoirs and the initial conditions can be expressed as below:

For Aquifer :

$$w_a - w_{r1} - w_{r2} = \alpha_a(p_i - p_a) - \alpha_{r1}(p_a - p_{r1}) - \alpha_{r2}(p_a - p_{r2}) = \kappa_a \frac{dp_a}{dt} \qquad (3.88)$$

For Shallow Reservoir :

$$w_{r1} + w_{r12} - w_{p,net1} = \alpha_{r1}(p_a - p_{r1}) + \alpha_{r12}(p_{r2} - p_{r1}) - w_{p,net1} = \kappa_{r1} \frac{dp_{r1}}{dt} \qquad (3.89)$$

For Deep Reservoir :

$$w_{r2} - w_{r12} - w_{p,net2} = \alpha_{r2}(p_a - p_{r2}) - \alpha_{r12}(p_{r2} - p_{r1}) - w_{p,net2} = \kappa_{r2} \frac{dp_{r2}}{dt} \qquad (3.90)$$

Initial Conditions : $\Delta p_a = \Delta p_{r1} = \Delta p_{r2} = 0 \ @ \ t = 0$ (3.91)

The solutions describing the pressure behavior of the shallow and deep reservoirs can be obtained from Equations 3.88 - 3.91 by using Laplace transformation. Details of the solution procedure can be found in Appendix-I. The solutions for the both reservoirs in terms of pressure changes, $\Delta p_{r1}(t)$ and $\Delta p_{r2}(t)$, are given as follows:

$$\Delta p_{r1}(t) = \frac{w_{p,net1}}{\kappa_{r1}} \left\{ \begin{array}{l} \frac{a_1 a_9 - a_3 a_7}{\mu_1 \mu_2 \mu_3} - \frac{\mu_1^2 - (a_1 + a_9)\mu_1 + a_1 a_9 - a_3 a_7}{\mu_1 (\mu_2 - \mu_1)(\mu_3 - \mu_1)} exp(-\mu_1 t) \\ - \frac{\mu_2^2 - (a_1 + a_9)\mu_2 + a_1 a_9 - a_3 a_7}{\mu_2 (\mu_1 - \mu_2)(\mu_3 - \mu_2)} exp(-\mu_2 t) \\ - \frac{\mu_3^2 - (a_1 + a_9)\mu_3 + a_1 a_9 - a_3 a_7}{\mu_3 (\mu_1 - \mu_3)(\mu_2 - \mu_3)} exp(-\mu_3 t) \end{array} \right\} \quad (3.92)$$

$$+ \frac{w_{p,net2}}{\kappa_{r2}} \left\{ \begin{array}{l} \frac{a_1 a_6 + a_3 a_4}{\mu_1 \mu_2 \mu_3} - \frac{-a_6 \mu_1 + a_1 a_6 + a_3 a_4}{\mu_1 (\mu_2 - \mu_1)(\mu_3 - \mu_1)} exp(-\mu_1 t) \\ - \frac{-a_6 \mu_2 + a_1 a_6 + a_3 a_4}{\mu_2 (\mu_1 - \mu_2)(\mu_3 - \mu_2)} exp(-\mu_2 t) \\ - \frac{-a_6 \mu_3 + a_1 a_6 + a_3 a_4}{\mu_3 (\mu_1 - \mu_3)(\mu_2 - \mu_3)} exp(-\mu_3 t) \end{array} \right\}$$

$$\Delta p_{r2}(t) = \frac{w_{p,net1}}{\kappa_{r1}} \left\{ \begin{array}{l} \frac{a_1 a_8 + a_2 a_7}{\mu_1 \mu_2 \mu_3} - \frac{-a_8 \mu_1 + a_1 a_8 + a_2 a_7}{\mu_1 (\mu_2 - \mu_1)(\mu_3 - \mu_1)} exp(-\mu_1 t) \\ - \frac{-a_8 \mu_2 + a_1 a_8 + a_2 a_7}{\mu_2 (\mu_1 - \mu_2)(\mu_3 - \mu_2)} exp(-\mu_2 t) \\ - \frac{-a_8 \mu_3 + a_1 a_8 + a_2 a_7}{\mu_3 (\mu_1 - \mu_3)(\mu_2 - \mu_3)} exp(-\mu_3 t) \end{array} \right\}$$

$$+ \frac{w_{p,net2}}{\kappa_{r2}} \left\{ \begin{array}{l} \frac{a_1 a_5 - a_2 a_4}{\mu_1 \mu_2 \mu_3} - \frac{\mu_1^2 - (a_1 + a_5)\mu_1 + a_1 a_5 - a_2 a_4}{\mu_1 (\mu_2 - \mu_1)(\mu_3 - \mu_1)} exp(-\mu_1 t) \\ - \frac{\mu_2^2 - (a_1 + a_5)\mu_2 + a_1 a_5 - a_2 a_4}{\mu_2 (\mu_1 - \mu_2)(\mu_3 - \mu_2)} exp(-\mu_2 t) \\ - \frac{\mu_3^2 - (a_1 + a_5)\mu_3 + a_1 a_5 - a_2 a_4}{\mu_3 (\mu_1 - \mu_3)(\mu_2 - \mu_3)} exp(-\mu_3 t) \end{array} \right\} \quad (3.93)$$

where μ_1, μ_2, and μ_3 are the roots of cubic equation given in Appendix-I.

$$\left.\begin{aligned}\mu_1 &= 2\sqrt{Q}\cos\left(\frac{\theta}{3}\right)+\frac{(a_1+a_5+a_9)}{3}\\ \mu_2 &= 2\sqrt{Q}\cos\left(\frac{\theta+2\pi}{3}\right)+\frac{(a_1+a_5+a_9)}{3}\\ \mu_3 &= 2\sqrt{Q}\cos\left(\frac{\theta+4\pi}{3}\right)+\frac{(a_1+a_5+a_9)}{3}\end{aligned}\right\} \tag{3.94}$$

where

$$Q=\frac{(a_1+a_5+a_9)^2-3(a_5a_9-a_6a_8+a_1a_5+a_1a_9-a_2a_4-a_3a_7)}{9}$$

$$R=\frac{1}{54}\begin{bmatrix}2(a_1+a_5+a_9)^3\\ -9(a_1+a_5+a_9)(a_5a_9-a_6a_8+a_1a_5+a_1a_9-a_2a_4-a_3a_7)\\ +27(a_1a_5a_9-a_1a_6a_8-a_2a_4a_9-a_2a_6a_7-a_3a_4a_8-a_3a_5a_7)\end{bmatrix} \tag{3.95}$$

$$\theta=arc\cos\left(\frac{R}{\sqrt{Q^3}}\right)$$

$$\left.\begin{aligned}a_1&=\frac{\alpha_a+\alpha_{r1}+\alpha_{r2}}{\kappa_a}\ ,\ a_2=\frac{\alpha_{r1}}{\kappa_a}\ ,\ a_3=\frac{\alpha_{r2}}{\kappa_a}\\ a_4&=\frac{\alpha_{r1}}{\kappa_{r1}}\ ,\ a_5=\frac{\alpha_{r1}+\alpha_{r12}}{\kappa_{r1}}\ ,\ a_6=\frac{\alpha_{r12}}{\kappa_{r1}}\\ a_7&=\frac{\alpha_{r2}}{\kappa_{r2}}\ ,\ a_8=\frac{\alpha_{r12}}{\kappa_{r2}}\ ,\ a_9=\frac{\alpha_{r2}+\alpha_{r12}}{\kappa_{r2}}\end{aligned}\right\} \tag{3.96}$$

At early-time : $exp(-\mu_1 t)\approx 1-\mu_1 t$, $exp(-\mu_2 t)\approx 1-\mu_2 t$ and $exp(-\mu_3 t)\approx 1-\mu_3 t$

- for shallow reservoir : $\Delta p_{r1}(t)=\dfrac{w_{p,net1}}{\kappa_{r1}}t$ (3.97)

- for deep reservoir : $\Delta p_{r2}(t)=\dfrac{w_{p,net2}}{\kappa_{r2}}t$ (3.98)

At late-time : $exp(-\mu_1 t)\cong 0$, $exp(-\mu_2 t)\cong 0$, and $exp(-\mu_3 t)\cong 0$

- for shallow reservoir :

$$\Delta p_{r1ss} = \frac{w_{p,net1}\left[(\alpha_{r2}+\alpha_{r12})(\alpha_a+\alpha_{r1})+\alpha_{r2}\alpha_{r12}\right]}{\alpha_a\alpha_{r1}\alpha_{r2}+\alpha_a\alpha_{r12}(\alpha_{r1}+\alpha_{r2})} + \frac{w_{p,net2}\left[\alpha_{r12}(\alpha_a+\alpha_{r1}+\alpha_{r2})+\alpha_{r1}\alpha_{r2}\right]}{\alpha_a\alpha_{r1}\alpha_{r2}+\alpha_a\alpha_{r12}(\alpha_{r1}+\alpha_{r2})} \quad (3.99)$$

- for deep reservoir :

$$\Delta p_{r2ss} = \frac{w_{p,net1}\left[\alpha_{r12}(\alpha_a+\alpha_{r1}+\alpha_{r2})+\alpha_{r1}\alpha_{r2}\right]}{\alpha_a\alpha_{r1}\alpha_{r2}+\alpha_a\alpha_{r12}(\alpha_{r1}+\alpha_{r2})} + \frac{w_{p,net2}\left[(\alpha_{r1}+\alpha_{r12})(\alpha_a+\alpha_{r2})+\alpha_{r1}\alpha_{r12}\right]}{\alpha_a\alpha_{r1}\alpha_{r2}+\alpha_a\alpha_{r12}(\alpha_{r1}+\alpha_{r2})} \quad (3.100)$$

The stabilization time of shallow and deep reservoirs, t_{ss}, is obtained by $\mu_2 t > 5$, since $|\mu_1| > |\mu_3| > |\mu_2|$.

$$t_{ss} = \frac{5}{2\sqrt{Q}\cos\left(\frac{\theta+2\pi}{3}\right)+\frac{(a_1+a_5+a_9)}{3}} \quad (3.101)$$

3.5.2 2 reservoir tanks with aquifer model (without initial hydraulic equilibrium)

The analytical solution for the case of the shallow and deep reservoirs, aquifer and recharge source not in hydraulic equilibrium initially is obtained by mass balances on the both reservoirs and aquifer. In this case, Equations 3.88, 3.89 and 3.90 are applied and only the initial conditions are altered as given below:

$$\text{Initial Conditions} \quad : \quad \left.\begin{array}{l} p_a = p_{ai} \ @\, t = 0 \\ p_{r1} = p_{r1i} \ @\, t = 0 \\ p_{r2} = p_{r2i} \ @\, t = 0 \end{array}\right\} \quad (3.102)$$

The pressure drop solutions of the shallow and deep reservoirs are given below and the detailed formulations are described in Appendix-J.

$$\Delta p_{r1}(t)=\frac{w_{p,net1}}{\kappa_{r1}}\left[\begin{array}{l}\dfrac{a_1a_{11}-a_3a_9}{\mu_1\mu_2\mu_3}-\dfrac{\mu_1^2-(a_1+a_{11})\mu_1+a_1a_{11}-a_3a_9}{\mu_1(\mu_2-\mu_1)(\mu_3-\mu_1)}exp(-\mu_1 t)\\ -\dfrac{\mu_2^2-(a_1+a_{11})\mu_2+a_1a_{11}-a_3a_9}{\mu_2(\mu_1-\mu_2)(\mu_3-\mu_2)}exp(-\mu_2 t)\\ -\dfrac{\mu_3^2-(a_1+a_{11})\mu_3+a_1a_{11}-a_3a_9}{\mu_3(\mu_1-\mu_3)(\mu_2-\mu_3)}exp(-\mu_3 t)\end{array}\right]$$

$$+\frac{w_{p,net2}}{\kappa_{r2}}\left[\begin{array}{l}\dfrac{a_1a_7+a_3a_5}{\mu_1\mu_2\mu_3}+\dfrac{a_7\mu_1-a_1a_7-a_3a_5}{\mu_1(\mu_2-\mu_1)(\mu_3-\mu_1)}exp(-\mu_1 t)\\ +\dfrac{a_7\mu_2-a_1a_7-a_3a_5}{\mu_2(\mu_1-\mu_2)(\mu_3-\mu_2)}exp(-\mu_2 t)+\dfrac{a_7\mu_3-a_1a_7-a_3a_5}{\mu_3(\mu_1-\mu_3)(\mu_2-\mu_3)}exp(-\mu_3 t)\end{array}\right]$$

$$+exp(-\mu_1 t)\left[-\frac{a_8\mu_1^2-a_{14}\mu_1+a_{13}}{\mu_1(\mu_2-\mu_1)(\mu_3-\mu_1)}\right]+exp(-\mu_2 t)\left[-\frac{a_8\mu_2^2-a_{14}\mu_2+a_{13}}{\mu_2(\mu_1-\mu_2)(\mu_3-\mu_2)}\right]$$

$$+exp(-\mu_3 t)\left[-\frac{a_8\mu_3^2-a_{14}\mu_3+a_{13}}{\mu_3(\mu_1-\mu_3)(\mu_2-\mu_3)}\right]+\frac{a_{13}}{\mu_1\mu_2\mu_3} \tag{3.103}$$

$$\Delta p_{r2}(t)=\frac{w_{p,net1}}{\kappa_{r1}}\left[\begin{array}{l}\dfrac{a_1a_{10}+a_2a_9}{\mu_1\mu_2\mu_3}+\dfrac{a_{10}\mu_1-a_1a_{10}-a_2a_9}{\mu_1(\mu_2-\mu_1)(\mu_3-\mu_1)}exp(-\mu_1 t)\\ +\dfrac{a_{10}\mu_2-a_1a_{10}-a_2a_9}{\mu_2(\mu_1-\mu_2)(\mu_3-\mu_2)}exp(-\mu_2 t)\\ +\dfrac{a_{10}\mu_3-a_1a_{10}-a_2a_9}{\mu_3(\mu_1-\mu_3)(\mu_2-\mu_3)}exp(-\mu_3 t)\end{array}\right]$$

$$+\frac{w_{p,net2}}{\kappa_{r2}}\left[\begin{array}{l}\dfrac{a_1a_6-a_2a_5}{\mu_1\mu_2\mu_3}-\dfrac{\mu_1^2-(a_1+a_6)\mu_1+a_1a_6-a_2a_5}{\mu_1(\mu_2-\mu_1)(\mu_3-\mu_1)}exp(-\mu_1 t)\\ -\dfrac{\mu_2^2-(a_1+a_6)\mu_2+a_1a_6-a_2a_5}{\mu_2(\mu_1-\mu_2)(\mu_3-\mu_2)}exp(-\mu_2 t)\\ -\dfrac{\mu_3^2-(a_1+a_6)\mu_3+a_1a_6-a_2a_5}{\mu_3(\mu_1-\mu_3)(\mu_2-\mu_3)}exp(-\mu_3 t)\end{array}\right]$$

$$+exp(-\mu_1 t)\left[-\frac{a_{12}\mu_1^2-a_{16}\mu_1+a_{15}}{\mu_1(\mu_2-\mu_1)(\mu_3-\mu_1)}\right]+exp(-\mu_2 t)\left[-\frac{a_{12}\mu_2^2-a_{16}\mu_2+a_{15}}{\mu_2(\mu_1-\mu_2)(\mu_3-\mu_2)}\right]$$

$$+exp(-\mu_3 t)\left[-\frac{a_{12}\mu_3^2-a_{16}\mu_3+a_{15}}{\mu_3(\mu_1-\mu_3)(\mu_2-\mu_3)}\right]+\frac{a_{15}}{\mu_1\mu_2\mu_3} \tag{3.104}$$

where μ_1, μ_2, and μ_3 are the roots of cubic equation given in Appendix-J.

$$\left.\begin{aligned}
\mu_1 &= 2\sqrt{Q}\cos\left(\frac{\theta}{3}\right)+\frac{(a_1+a_6+a_{11})}{3}\\
\mu_2 &= 2\sqrt{Q}\cos\left(\frac{\theta+2\pi}{3}\right)+\frac{(a_1+a_6+a_{11})}{3}\\
\mu_3 &= 2\sqrt{Q}\cos\left(\frac{\theta+4\pi}{3}\right)+\frac{(a_1+a_6+a_{11})}{3}
\end{aligned}\right\} \qquad (3.105)$$

where

$$Q=\frac{(a_1+a_6+a_{11})^2-3(a_6a_{11}-a_7a_{10}+a_1a_6+a_1a_{11}-a_2a_5-a_3a_9)}{9}$$

$$R=\frac{1}{54}\begin{bmatrix}2(a_1+a_6+a_{11})^3\\-9(a_1+a_6+a_{11})(a_6a_{11}-a_7a_{10}+a_1a_6+a_1a_{11}-a_2a_5-a_3a_9)\\+27(a_1a_6a_{11}-a_1a_7a_{10}-a_2a_5a_{11}-a_2a_7a_9-a_3a_5a_{10}-a_3a_6a_9)\end{bmatrix} \qquad (3.106)$$

$$\theta=arc\cos\left(\frac{R}{\sqrt{Q^3}}\right)$$

$$a_1=\frac{\alpha_a+\alpha_{r1}+\alpha_{r2}}{\kappa_a},\ a_2=\frac{\alpha_{r1}}{\kappa_a},\ a_3=\frac{\alpha_{r2}}{\kappa_a}$$

$$a_4=\frac{-\alpha_a\Delta p_{ac}+\alpha_{r1}\Delta p_{r1c}+\alpha_{r2}\Delta p_{r2c}}{\kappa_a}$$

$$a_5=\frac{\alpha_{r1}}{\kappa_{r1}},\ a_6=\frac{\alpha_{r1}+\alpha_{r12}}{\kappa_{r1}},\ a_7=\frac{\alpha_{r12}}{\kappa_{r1}}$$

$$a_8=\frac{-\alpha_{r1}\Delta p_{r1c}-\alpha_{r12}\Delta p_{rc}}{\kappa_{r1}},\ a_9=\frac{\alpha_{r2}}{\kappa_{r2}},\ a_{10}=\frac{\alpha_{r12}}{\kappa_{r2}}$$

$$a_{11}=\frac{\alpha_{r2}+\alpha_{r12}}{\kappa_{r2}},\ a_{12}=\frac{-\alpha_{r2}\Delta p_{r2c}+\alpha_{r12}\Delta p_{rc}}{\kappa_{r2}} \qquad (3.107)$$

$$a_{13}=a_1a_8a_{11}+a_1a_7a_{12}+a_4a_5a_{11}+a_4a_7a_9+a_3a_5a_{12}-a_3a_8a_9$$

$$a_{14}=a_8a_{11}+a_7a_{12}+a_1a_8+a_4a_5$$

$$a_{15}=a_1a_6a_{12}+a_1a_8a_{10}+a_2a_8a_9+a_4a_5a_{10}+a_4a_6a_9-a_2a_5a_{12}$$

$$a_{16}=a_6a_{12}+a_8a_{10}+a_1a_{12}+a_4a_9$$

The early- and the late-time solutions of both reservoirs contain the terms of initial pressure differences as different from the solutions obtained in Chapter 3.5.1. The solutions are given below.

For early-time :

- for shallow reservoir : $\Delta p_{r1}(t) = \frac{w_{p,net1}}{\kappa_{r1}} t - \frac{\alpha_{r12}(p_{r2i} - p_{r1i}) + \alpha_{r1}(p_{ai} - p_{r1i})}{\kappa_{r1}} t$

(3.108)

- for deep reservoir : $\Delta p_{r2}(t) = \frac{w_{p,net2}}{\kappa_{r2}} t + \frac{\alpha_{r12}(p_{r2i} - p_{r1i}) - \alpha_{r2}(p_{ai} - p_{r2i})}{\kappa_{r2}} t$

(3.109)

For late-time :

- for shallow reservoir :

$$\Delta p_{r1ss} = w_{p,net1} \frac{[\alpha_{r2}(\alpha_a + \alpha_{r1}) + \alpha_{r12}(\alpha_a + \alpha_{r1} + \alpha_{r2})]}{\alpha_a(\alpha_{r1}\alpha_{r2} + \alpha_{r1}\alpha_{r12} + \alpha_{r2}\alpha_{r12})} + w_{p,net2} \frac{[\alpha_{r1}\alpha_{r2} + \alpha_{r12}(\alpha_a + \alpha_{r1} + \alpha_{r2})]}{\alpha_a(\alpha_{r1}\alpha_{r2} + \alpha_{r1}\alpha_{r12} + \alpha_{r2}\alpha_{r12})} - (p_i - p_{r1i})$$

(3.110)

- for deep reservoir :

$$\Delta p_{r2ss} = w_{p,net1} \frac{[\alpha_{r1}\alpha_{r2} + \alpha_{r12}(\alpha_a + \alpha_{r1} + \alpha_{r2})]}{\alpha_a(\alpha_{r1}\alpha_{r2} + \alpha_{r1}\alpha_{r12} + \alpha_{r2}\alpha_{r12})} + w_{p,net2} \frac{[\alpha_{r1}(\alpha_a + \alpha_{r2}) + \alpha_{r12}(\alpha_a + \alpha_{r1} + \alpha_{r2})]}{\alpha_a(\alpha_{r1}\alpha_{r2} + \alpha_{r1}\alpha_{r12} + \alpha_{r2}\alpha_{r12})} - (p_i - p_{r2i})$$

(3.111)

$$t_{ss} = \frac{5}{2\sqrt{Q}\cos\left(\frac{\theta + 2\pi}{3}\right) + \frac{(a_1 + a_5 + a_9)}{3}} \tag{3.112}$$

3.6 Modeling Variable Mass Flow Rate

The Duhamel's principle is applied to obtain the solutions for the variable mass flow rate. From the Duhamel's principle (Thompson and Reynolds, 1986; Kuchuk and Ayestaran, 1985), the pressure drop in the reservoir is given by

$$\Delta p(t) = \int_0^t w_{p,net}(\tau) \Delta p_u'(t - \tau) d\tau \tag{3.113}$$

or in terms of pressure,

$$p(t) = p_i - \int_0^t w_{p,net}(\tau)\Delta p_u'(t-\tau)d\tau \tag{3.114}$$

where Δp_u is the pressure drop that would be obtained if the system were produced with the unit constant mass rate of $w_{p,net}$ and $\Delta p_u'$ is the time rate of change (or simply time derivative) of Δp_u. For example, Equation 3.11 is the general solution for 1-tank model for the constant mass withdrawal $w_{p,net}$, then if $w_{p,net} = 1$ kg/s is set in Equation 3.11, then the unit-rate pressure change, $\Delta p_u(t)$, and its time derivative, $\Delta p_u'(t)$, could be obtained, respectively, as

$$\Delta p_u(t) = \frac{1}{\alpha_r}\left[1 - exp\left(-\frac{\alpha_r t}{\kappa_r}\right)\right] \quad \text{and} \quad \Delta p_u'(t) = \frac{1}{\kappa_r} exp\left(-\frac{\alpha_r t}{\kappa_r}\right) \tag{3.115}$$

For the other lumped models discussed previously, one can similarly derive the unit-rate pressure change and its time derivative and apply Equation 3.113 or 3.114 to generate the pressure response for a given variable mass flow rate history. In cases where mass flow rate history can be represented with step changes, a partition of the time interval (0,t) is considered as $0 = t_0 < t_1 < t_2 < \cdots < t_n < t_{n+1} = t$ and Equation 3.113 can be written as

$$\Delta p(t) = p_i - p(t) = \sum_{j=0}^{n} \int_{t_j}^{t_{j+1}} w_{p,net}(\tau)\Delta p_u'(t-\tau)d\tau \tag{3.116}$$

Following Thompson and Reynolds (1986), and Kuchuk and Ayestaran (1985), Equation 3.116 can be approximated as:

$$\Delta p(t) = \sum_{j=0}^{n} \Delta w_{p,net}(t_{j+1})\,\Delta p_u(t - t_j) \tag{3.117}$$

where $\Delta w_{p,net}(t_{j+1}) = w_{p,net}(t_{j+1}) - w_{p,net}(t_j)$ represents mass flow rate steps. Note that in deriving Equation 3.117, $t_0 = 0$, $w_{p,net}(0) = 0$, and $\Delta p_u(0) = 0$ are used.

3.7 Optimization Procedure

After a geothermal reservoir is produced for a period of time, a lumped parameter model can be matched to observed pressure (or water level) data with the available production/reinjection rate history to obtain optimum parameters of a particular lumped model. As more data become available, more information can be obtained about the reservoir and the system. With time there are data available which may be used to improve the understanding the behavior of the reservoir. Therefore, in modeling, data must be collected as the reservoir is produced. The model is limited to the data used, so all the pressure (or water level) responses must be included for honoring all the data available. In matching observed production data, in general, more and accurate production data are desired. This is quite important in reducing the uncertainty in performance predictions as well as in further development of the system under consideration.

Fitting model parameters to the observed data requires accurate and fast approaches. The method of least squares fitting is a convenient one to apply. As is well known (Bard, 1974), traditional (unweighted) least squares estimation is often unsatisfactory when some observations are less reliable than others and/or various measurements having disparate orders of magnitude are simultaneously used in estimation. In the former case, we want to make sure that our parameter estimates will be more influenced by the more reliable observations than by the less reliable ones. In the latter case, we wish to make sure that any information contained in the data with small magnitudes is not lost because of summing together squares of numbers of such disparate orders of magnitude. Therefore, in this study, weighted least-squares fitting is considered so that the above mentioned disadvantages associated with the standard least squares fitting can be overcome.

The inverse problem of estimating unknown parameters from various lumped models derived in Chapter 3 can be formulated as a nonlinear optimization problem. A nonlinear parameter estimation is performed by minimizing a weighted least-squares (LS) objective function (J) for which the weights (inverse of the variances of measurement errors assumed to be normal and independent) are assumed to be known. In general, a weighted least-squares objective function is minimized (Onur and Kuchuk, 2000):

$$J(\vec{\chi}) = \sum_{j=1}^{M} \sum_{i=1}^{n} w_{j,i} \left[f_j(t_i, \vec{\chi}) - y_j(t_i) \right]^2 \tag{3.118}$$

where M represents the total number of model function f and, $(t_i, y_j(t_i))$, i=1,…,n is a set of n observations of the model function f_j, j=1,…,M. $\vec{\chi}$ is an l-dimensional column vector whose elements are unknown parameters for a chosen lumped model. In Equation 3.118, the positive weights $w_{j,i}$ are the inverse of variance of measurement errors corresponding to measured value y_j at time t_i. In our applications, y_j could represent pressure (or water level) data measured as a function of time from wells in reservoirs or aquifers.

One can construct weighted LS objective functions based on Equation 3.118, depending on the pressure (or water level) data available and the lumped model chosen for regression, and consider matching of a single pressure data set (M=1 in Equation 3.118, e.g. 1-, 2- and 3-tank models) as well as simultaneous matching of different pressure data sets (M=2 in Equation 3.118, e.g. 2-reservoir tanks with/without aquifer model) to optimize $\vec{\chi}$. Suppose a 2-reservoir tanks without aquifer model is considered, where the system is assumed to be consisted of one deep reservoir and shallow reservoir and assume that we have a set of n measured pressure data from a well in the deep reservoir and a set of n measured pressure data from a well in the shallow reservoir. Then, M = 2 in Equation 3.118, and one can choose y_1 and f_1 to represent the measured and model pressure data for the deep reservoir, whereas y_2 and f_2 to represent measured and model pressure data for the shallow reservoir, respectively. In this case, the positive weights $w_{1,i}$, i=1,…,n, will represent the inverse of variance of the measurement error for the ith measured pressure for the deep reservoir, whereas, $w_{2,i}$, i=1,…,n, will represent the inverse of variance of the measurement error for the ith measured pressure for the shallow reservoir. It means that for this case, a weighted-LS objective function is constructed based on two different sets of pressure data and simultaneously match both sets to optimize $\vec{\chi}$, where, for this lumped model, in general, $\vec{\chi}$ can be represented as

$$\vec{\chi} = \left[\kappa_{r1}, \kappa_{r2}, \alpha_{a1}, \alpha_{a2}, \alpha_r \right]^T \tag{3.119}$$

where T denotes the transpose.

In our applications, we minimize the objective function given by Equation 3.118 by using the Levenberg-Marquardt method with a restricted step procedure as described by Fletcher (1987) and constrain the unknown parameters in nonlinear regression by using the so-called imaging method of Carvalho et al. (1996). In addition, we compute 95% confidence intervals and correlation coefficients by using the standard definitions (Dogru et al., 1977). As is well known, computing and inspecting such statistics in regression analysis is very useful for identifying which parameters can be reliably determined from available data. Lower the confidence interval, higher the certainty of the estimated model parameter.

As is well known, in nonlinear regression, parameter estimation from lumped models starts with a set of initial guess for the parameters, and then the parameters are updated by the method discussed above until a successful match of data with the model response can be obtained. The standard terminating criteria given by Gill et al. (1993) are used. At termination, for each data set matched, the standard deviation of errors as well as the root mean square errors (RMS) are also computed. Here, we use the standard definition of RMS given by

$$RMS_j = \sqrt{\frac{1}{n}\sum_{i=1}^{n}\left[f_j(t_i,\vec{\chi}_o) - y_j(t_i)\right]^2} \tag{3.120}$$

where $\vec{\chi}_o$ represents the optimized parameter vector. The value of RMS shows the matching quality as quantitatively. Lower the RMS value, better the matching between field and model data.

Before closing this chapter, we should note that choosing good initial guesses and constraints for parameters plays an important role in nonlinear regression analysis because nonlinear regression algorithms could often become trapped at unacceptable local minima. Particularly, this would be valid in cases where the models with a large number of unknown parameters are chosen for the data to be matched and/or the observed data contain large measurement errors. The data obtained from such as geological, hydrogeological and geophysical surveys can be useful to obtain a good set of initial guesses for the parameters prior to performing nonlinear regression analysis.

4. FIELD APPLICATIONS

This chapter deals with the applications of the new lumped parameter models to field cases. The models are used to match the long-term measured water level or pressure response to a given production history. For history matching purposes, an optimization algorithm described in Chapter 3, Section 3.7. In addition, the parameters are constrained during nonlinear minimization process to keep them physically meaningful and compute statistics (e.g., standard 95% confidence intervals) to assess uncertainty in the estimated parameters. Moreover, the root mean square errors (RMS) are calculated for each data set to show the matching quality as quantitatively. Four field examples (three fields are located in Iceland and one in Turkey) are studied to validate the use of the models and optimization algorithm.

For the field applications discussed below, all observed data were given in terms of water levels. All the measured water level data first converted to pressure equivalence by $p_r(t)=\rho g h(t)$ and then used in regression algorithm. Thus, all parameter estimates are given in pressure units. However, all graphical results are presented in terms of water levels to be consistent with the field data.

4.1 Laugarnes Field

The Laugarnes field in SW-Iceland is a considerably large field. The major feed zones are between depths of 700 and 1300 m and the water temperature is between 115 and 135°C. A continuous water level record was available from one well. The Laugarnes field is discussed in Axelsson and Gunnlaugsson (2000), and Axelsson (1989). Axelsson (1989) used the water level data to simulate the pressure response of the field and to estimate its production capacity.

Prior to exploitation the hydrostatic pressure at the surface in the geothermal field was 6-7 bars corresponding to a free water level 60-70 m above the land surface. Therefore, the initial water level is assumed to be 65 m and the water level data is modified before performing nonlinear regression analysis. Exploitation caused

pressure drop in the field and water level fell. Figure 4.1 shows the water level changes and production history of the Laugarnes system.

Axelsson (1989) used a closed three capacitor lumped model (a 3-tank with closed outer boundary model) for simulation. He treated the modeling as an inverse problem. He obtained quite a satisfactory match between the measured and calculated data (Figure 4.2). Results of our 3-tank closed model assuming the values of parameters given by Axelsson are also plotted for comparison. Axelsson's match and our match look almost identical.

Next, nonlinear regression analysis based on our 1- , 2-, and 3-tank models are performed to estimate the parameters. The best fit was obtained with the parameters given in Table 4.1 (Sarak et al, 2003b).

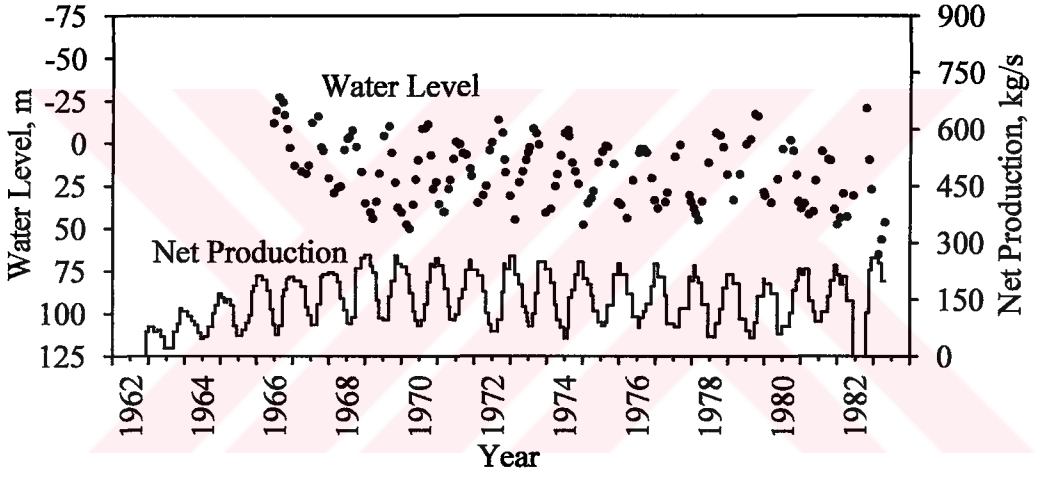

Figure 4.1 Water level changes and production history of Laugarnes field (Axelsson, 1989; Axelsson and Gunnlaugsson, 2000).

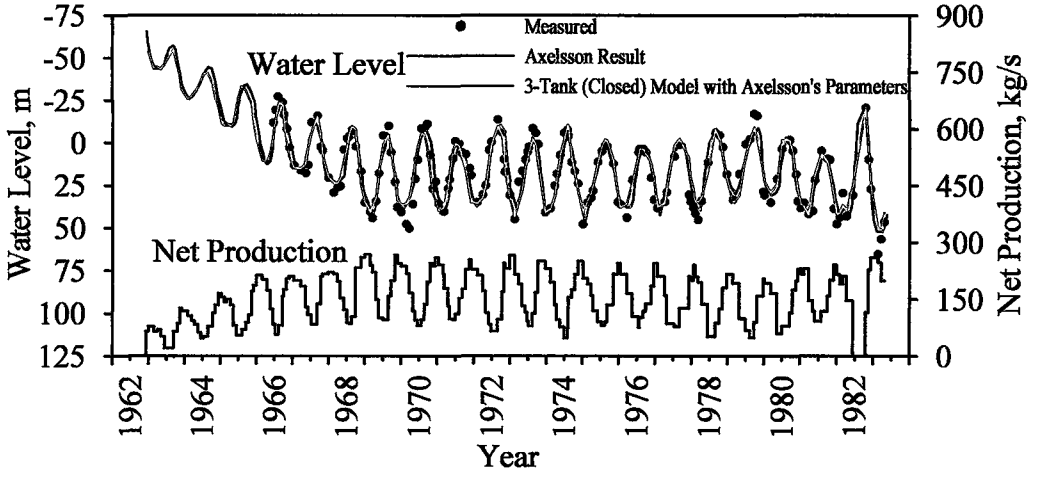

Figure 4.2 Comparison of measured and calculated water level changes in Laugarnes field.

Here and throughout, the numbers given in parentheses represent the 95% absolute confidence interval for the relevant parameters. The Axelsson's parameters are also given for comparison purposes but Axelsson did not compute the confidence intervals for the parameters.

The RMS value for 1-tank model is the highest one of RMS values of the models tried. Higher RMS value is a result of larger deviation between the model and measured water levels. Figure 4.3 presents the 1-tank model result.

The comparison of 2-tank open and closed models (Table 4.1 and Figure 4.4) indicates that both models are almost identical. However since its RMS value is lower, 2-tank open model seems to be more appropriate than 2-tank closed model to simulate the Laugarnes field.

Although the RMS values of 3-tank open and closed models are same, the confidence interval for the parameter α_{oa} is quite high (±8.4), indicating that this parameter is not well determined compared to the other parameters from the data. Consequently, the 3-tank closed model looks more appropriate than 3-tank open model. The results of 3-tank open and closed models are presented in Figure 4.5.

Table 4.1 Parameters of the best fitting lumped parameters (1-, 2-, and 3-tank models) for Laugarnes field.

	Axelsson (3-Tank Closed)	**1-Tank**	**2-Tank Closed**	**2-Tank Open**	**3-Tank Closed**	**3-Tank Open**
α_{oa}, kg/bar-s	--	--	--	--	--	0.006 (±8.4)
κ_{oa}, kg/bar	$3.64\text{x}10^{10}$	--	--	--	$2.99\text{x}10^{10}$ ($\pm 4.3\text{x}10^{9}$)	$3.0\text{x}10^{10}$ ($\pm 5.0\text{x}10^{9}$)
α_{ia} (α_a for 2-T), kg/bar-s	61.8	--	--	36.81 (±4.56)	78.8 (±19.70)	77.78 (±35.78)
κ_{ia} (κ_a for 2-T), kg/bar	$2.09\text{x}10^{9}$	--	$2.63\text{x}10^{10}$ ($\pm 2.8\text{x}10^{9}$)	$1.05\text{x}10^{10}$ ($\pm 2.7\text{x}10^{9}$)	$2.6\text{x}10^{9}$ ($\pm 2.8\text{x}10^{9}$)	$2.59\text{x}10^{9}$ ($\pm 2.9\text{x}10^{9}$)
α_r, kg/bar-s	36.8	20.47 (±0.55)	26.64 (±0.93)	30.46 (±1.83)	33.87 (±3.08)	33.97 (±4.28)
κ_r, kg/bar	$7.73\text{x}10^{7}$	$1.0\text{x}10^{8}$ ($\pm 1.5\text{x}10^{7}$)	$9.99\text{x}10^{7}$ ($\pm 1.1\text{x}10^{7}$)	$8.94\text{x}10^{7}$ ($\pm 1.2\text{x}10^{7}$)	$8.25\text{x}10^{7}$ ($\pm 1.7\text{x}10^{7}$)	$8.23\text{x}10^{7}$ ($\pm 1.8\text{x}10^{7}$)
RMS, bar	--	1.140	0.616	0.566	0.525	0.525

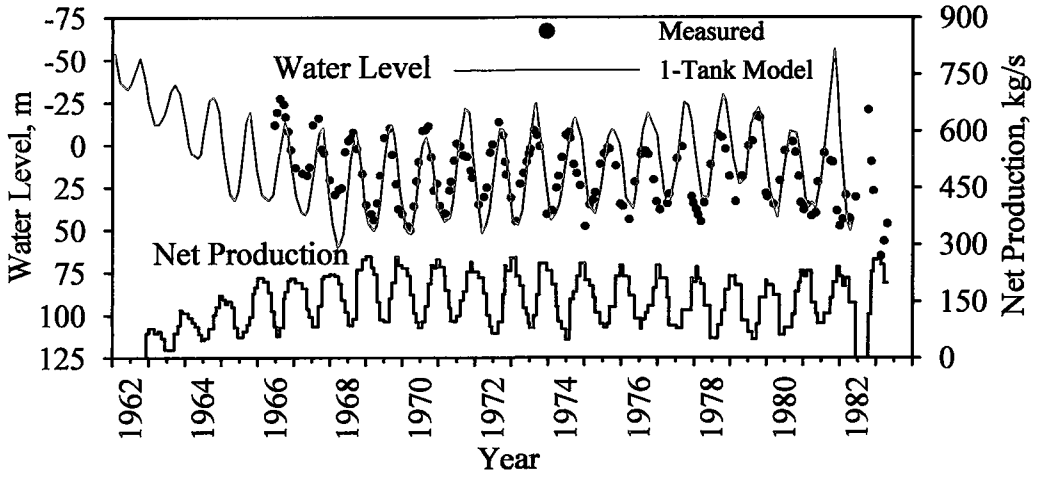

Figure 4.3 Simulation results of 1-tank model.

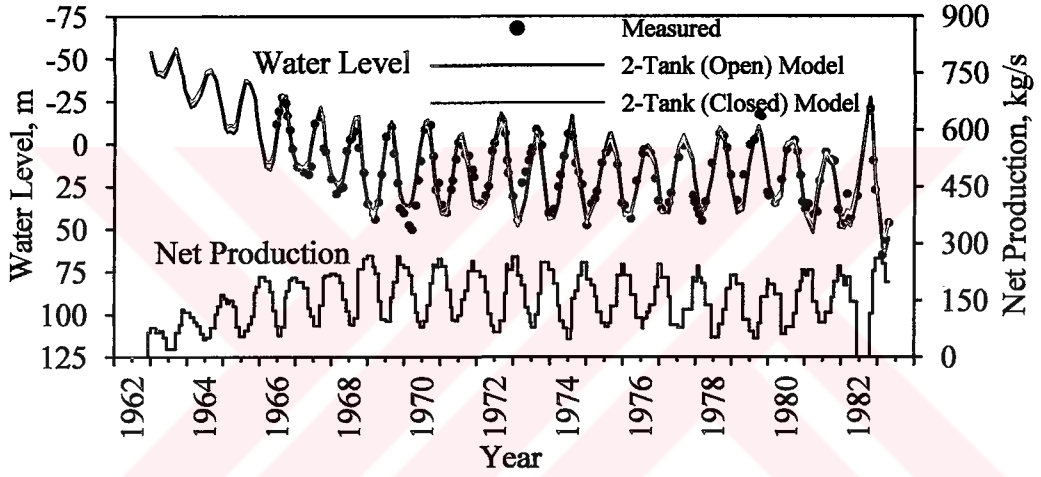

Figure 4.4 Simulation results of 2-tank open and closed models.

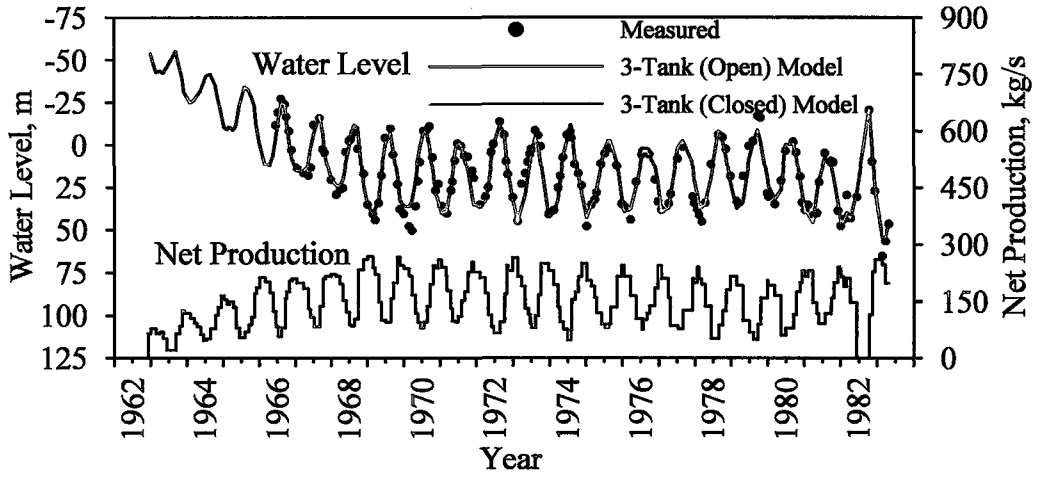

Figure 4.5 Simulation results of 3-tank open and closed models.

The 1-tank model does not give an acceptable match. Although the 3-tank models gave good matches with lower RMS values, however, the 2-tank open model also gave a reasonable match as well as it yields lower confidence intervals for the parameters. Regarding to the 3-tank closed model, we note that the confidence interval for the parameter κ_{ia} is determined as $\pm 2.8 \times 10^9$ which means the value of κ_{ia} can be in between 0 and $5.4\ 10^9$. This emphasizes that κ_{ia} from this data can not be determined well. When the confidence intervals for the parameters relating to 2-tank open model and the RMS values are considered, it would be appropriate to state that 2-tank open model is the best one representing the measured data.

Figure 4.6 shows the comparison of Axelsson's result and our 3-tank closed model results. Notice that, Figure 4.2 and 4.6 look almost identical. However they reflect the modeling results based on different sets of data. Figure 4.2 gives the results of our 3-tank closed model using Axelsson's parameters whereas Figure 4.6 shows the results of our 3-tank closed model using the parameters obtained from our regression analysis (Table 4.1).

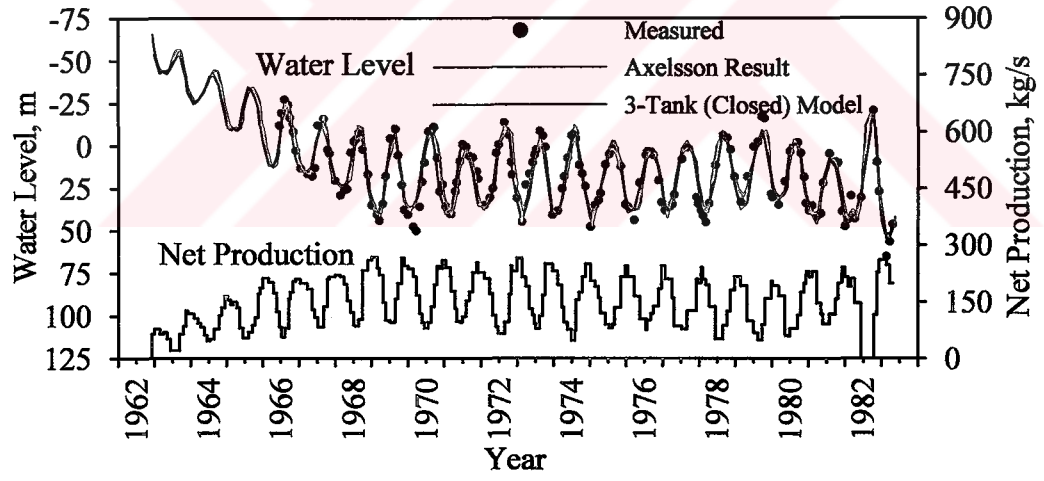

Figure 4.6 Comparison of Axelsson's match with 3-tank closed model.

4.2 Glerardalur Field

The water level and the production rate data in the Glerardalur low-temperature geothermal field in N-Iceland are presented in Figure 4.7 (Axelsson, 1989). This field has been utilized since 1982. The reservoir temperature at Glerardalur is about 61°C. The main feed zone is at 450 m depth. Most of the wells drilled are shallow (100-300 m) exploration wells.

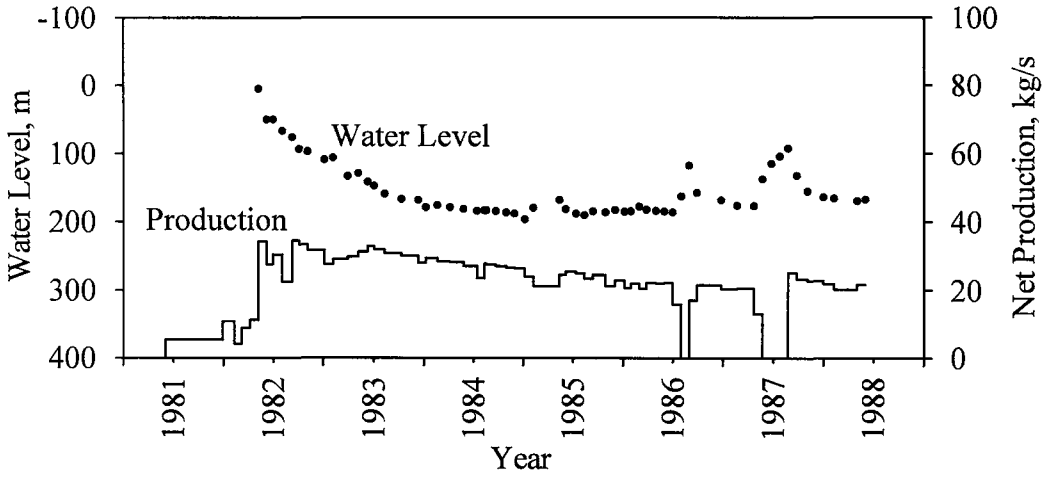

Figure 4.7 Water level data and data on the production in Glerardalur field (Axelsson, 1989).

One problem involved in simulating the Glerardalur field was the absence of the initial reservoir pressure or the initial water level data. Lumped parameter modeling requires the initial water level to be known a priori. Hence, the simulations were carried out to determine the reservoir and aquifer parameters and as well as the initial water level. Our optimization study of the field data yielded an initial water level of -53.5 m (corresponding to a free water level 53.5 m above the land surface).

The measured water level behavior shown in Fig. 4.7 for the Glerardalur field resembles the behavior of a system with constant pressure outer boundary. For a constant production rate, the reservoir pressure of a constant pressure outer boundary system declines sharply at early times and then reaches to a constant value at late times. Equations 3.17, and 3.27 given in Chapter 3 describe the late time behaviors of the 1- and 2-tank systems with constant pressure source. The late time steady-state reservoir pressure drop is a function of the harmonic average of reservoir and aquifer recharge constants, $(\overline{\alpha}_a = 1/\alpha_a + 1/\alpha_r)$, and the net production rate. Figure 4.7 exhibits a relatively constant production rate and a stabilized steady-state pressure drop. An equilibrium between production and recharge is eventually reached during long-term production, causing the reservoir pressure (or water level) drawdown to stabilize. Such a behavior is valid for systems with constant pressure outer boundary. Therefore, 2-tank model with constant pressure outer boundary is considered besides the 3-tank closed model as suggested by Axelsson (1989) for simulating the response of the Glerardalur field. Performing graphical analysis on the data by using the asymptotic equations given in Chapter 3, $\overline{\alpha}_a$ is estimated to be 1.13 kg/(bar-s) by

using the net production rate, $w_{p,net} = 27.5$ kg/s, and the stabilized steady-state pressure drop, $\Delta p_r = 24$ bar in Equation 3.27.

1- , 2- , and 3-tank simulation results of best fits yielded the parameters given in Table 4.2 (Sarak et al., 2003b). 1-tank model has the highest RMS value which means 1-tank model does not fit well the measured data. This concept is also supported by the plot of measured and simulated data obtained by 1-tank model (Figure 4.8). Addition to this, the initial water level (or pressure) is not well determined by 1-tank model (see the confidence intervals of p_i in Table 4.2).

Table 4.2 Parameters of the best fitting lumped parameters (1-, 2-, and 3-tank models) for Glerardalur field.

	Axelsson (3-Tank Closed)	**1-Tank**	**2-Tank Closed**	**2-Tank Open**	**3-Tank Closed**	**3-Tank Open**
α_{oa}, kg/bar-s	--	--	--	--	--	0.003 (±7.23)
κ_{oa}, kg/bar	$6.08\text{x}10^{8}$	--	--	--	$9.88\text{x}10^{8}$ ($\pm 6.8\text{x}10^{8}$)	$1.22\text{x}10^{9}$ ($\pm 1.4\text{x}10^{9}$)
α_{ia} (α_a for 2-T), kg/bar-s	1.89	--	--	1.42 (±0.077)	1.58 (±0.156)	1.54 (±0.166)
κ_{ia} (κ_a for 2-T), kg/bar	$6.66\text{x}10^{7}$	--	$5.55\text{x}10^{8}$ ($\pm 1.5\text{x}10^{8}$)	$8.75\text{x}10^{7}$ ($\pm 9.9\text{x}10^{6}$)	$7.05\text{x}10^{7}$ ($\pm 1.5\text{x}10^{7}$)	$7.32\text{x}10^{7}$ ($\pm 1.6\text{x}10^{7}$)
α_r, kg/bar-s	3.37	1.38 (±0.13)	1.47 (±0.12)	2.97 (±0.44)	3.29 (±0.608)	3.31 (±0.645)
κ_r, kg/bar	$5.9\text{x}10^{6}$	$5.48\text{x}10^{7}$ ($\pm 7.7\text{x}10^{6}$)	$2.99\text{x}10^{7}$ ($\pm 7.2\text{x}10^{6}$)	$8.15\text{x}10^{6}$ ($\pm 1.8\text{x}10^{6}$)	$7.41\text{x}10^{6}$ ($\pm 2.0\text{x}10^{6}$)	$7.37\text{x}10^{6}$ ($\pm 2.0\text{x}10^{6}$)
p_i, bar	--	-0.0058 (±1.45)	3.42 (±1.88)	5.15 (±0.95)	5.3 (±0.927)	5.14 (±0.930)
h_i, m*	--	0.006	-35.6	-53.5	-54.7	-53.5
RMS, bar	--	1.268	1.080	0.546	0.522	0.524

A comparison of 2-tank open and closed models indicates that the RMS value of 2-tank closed model is higher and the confidence intervals of the model parameters are slightly wider than the confidence intervals of the parameters for 2-tank open model (Table 4.2).

* *positive sign indicates the water level below the land surface and negative sign indicates the water level above the land surface.*

Therefore, it can be stated that 2-tank open model represents the data more satisfactorily than the 2-tank closed model does (Figure 4.9).

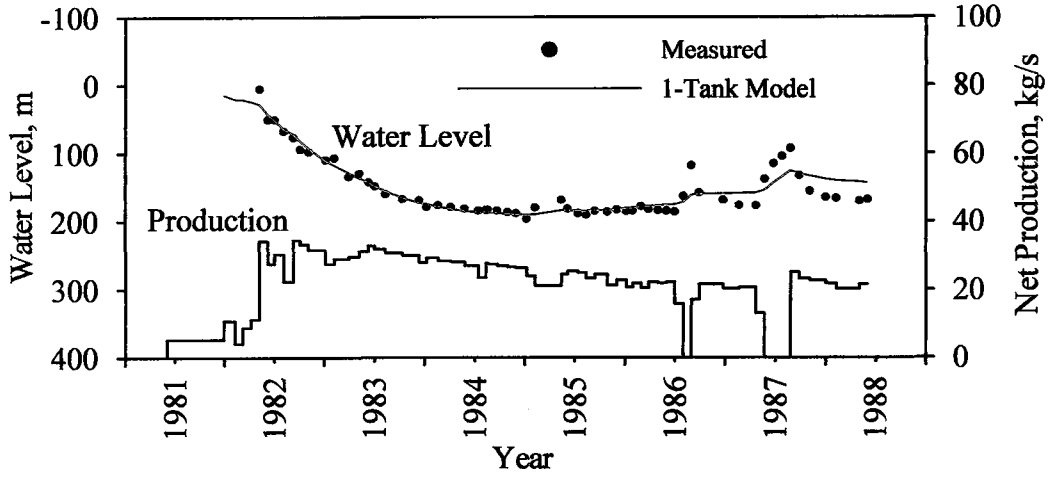

Figure 4.8 Simulation results of 1-tank model.

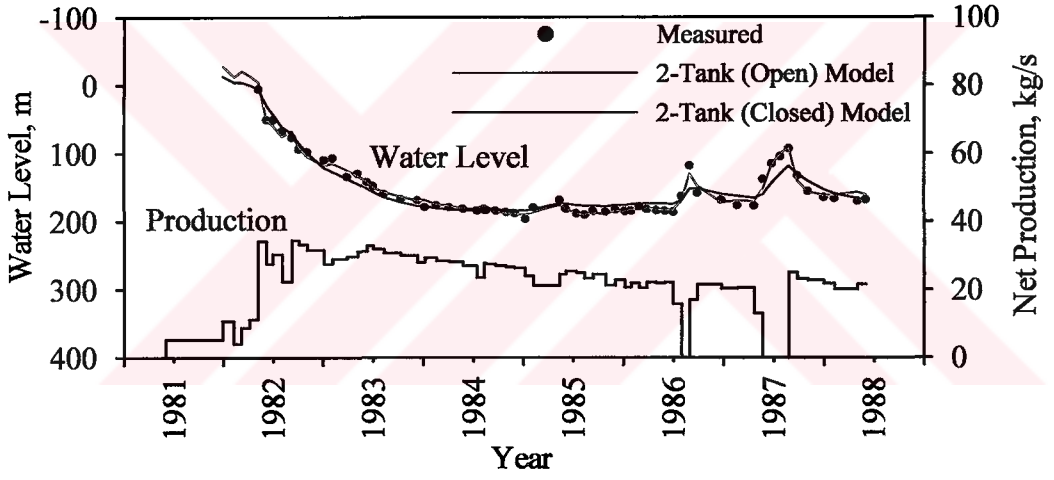

Figure 4.9 Simulation Results of 2-tank open and closed models.

Regression results for the 3-tank open and closed models yielded the parameters given in the sixth and the seventh columns of Table 4.2. A comparison of confidence intervals for model parameters and RMS values indicates that 3-tank closed model matches the field data better. The results of the simulations are presented in Figure 4.10.

As an overall result of the comparison of all models, due to its simplicity the 2-tank open model seems to be a preferable model to represent the geothermal system in Glerardalur field.

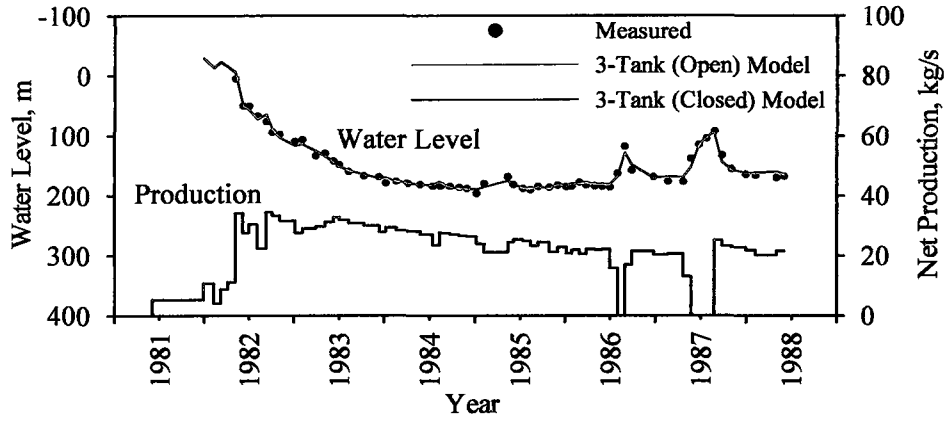

Figure 4.10 Simulation Results of 3-tank open and closed models.

As a next step, Axelsson's match is compared with our 3-tank closed model results employing Axelsson's parameters (Figure 4.11) and with our 3-tank closed model regression results (Figure 4.12). Since the model parameters Axelsson used and the parameters obtained by our regression analysis are almost identical, Figure 4.11 and Figure 4.12 give the similar results.

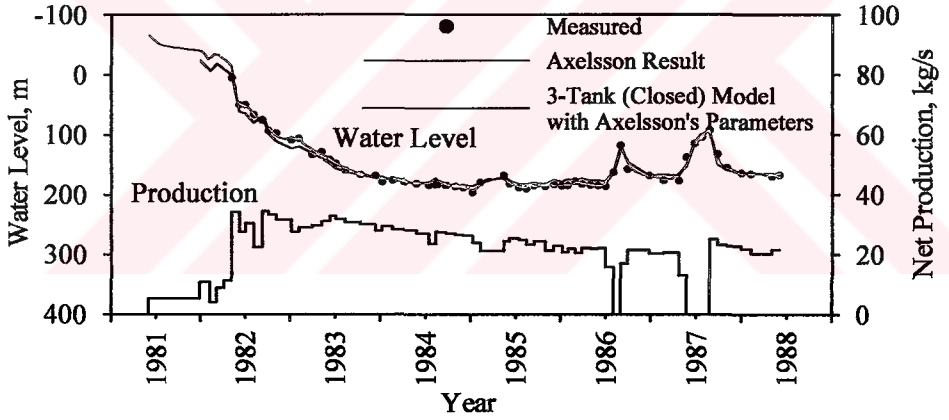

Figure 4.11 Comparison of measured and calculated water level changes.

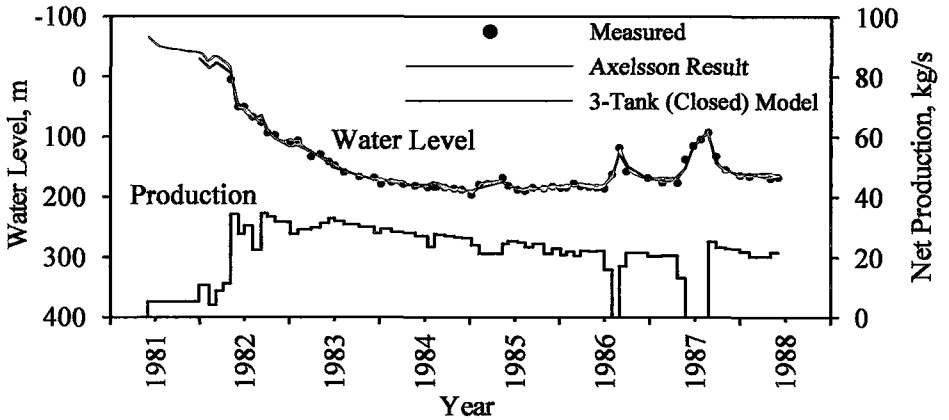

Figure 4.12 Comparison of Axelsson's match with 3-tank closed model.

4.3 Svartsengi Field

The Svartsengi field in Iceland is a liquid-dominated reservoir with fluids of nearly constant temperature at 235°C. Olsen (1984) reports that although the reservoir temperature is higher than the expected temperature of a low-temperature reservoir, the reservoir shows a liquid dominated reservoir rather than a two-phase reservoir behavior. Most of the wells are completed in the liquid zone and wells with varying depths show a uniform temperature and pressures of the wells are higher than the water saturation pressures at corresponding temperatures. Therefore, the reservoir is assumed to be a liquid dominated reservoir and our models are utilized to describe its behavior. The reservoir can be considered as a high temperature-high pressure reservoir with a liquid dominated reservoir behavior.

Fluid production from the reservoir started in 1976. The composition of the fluids produced is about two-thirds seawater and one-third rainwater. Fluid extraction and reservoir drawdown in Svartsengi were monitored. The drawdown was measured as water level in monitoring wells. The water level was measured in wells 4, 5 and 6.

The resistivity measurements indicated a reservoir surface area of 5 km^2 at 200 m depth, and 7 km^2 at 600 m below sea level.

Production response data of the Svartsengi geothermal reservoir consist of a seven-year continuous record from nearby observation wells in the field. These data are presented in Figure 4.13.

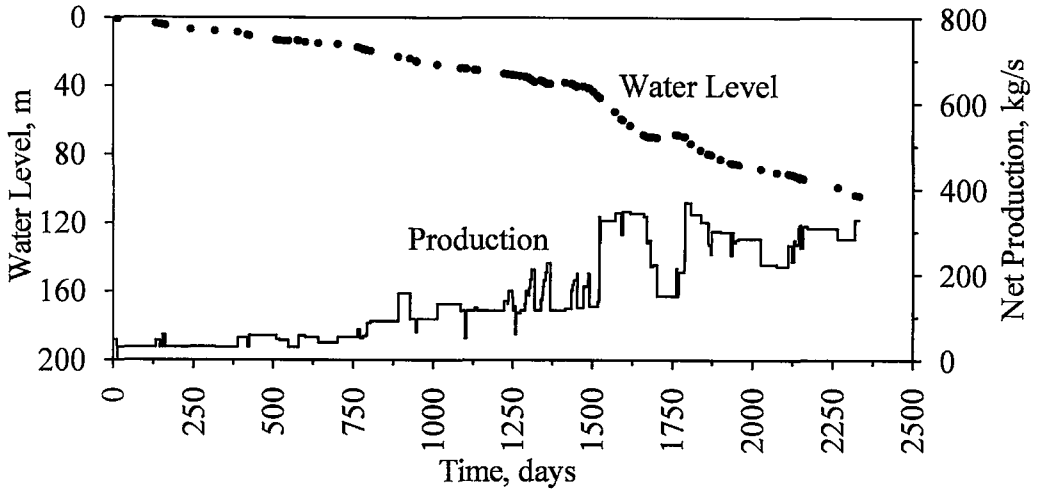

Figure 4.13 Production response data of the Svartsengi geothermal reservoir (Olsen, 1984).

Olsen (1984), and Gudmundsson and Olsen (1987) studied the production data of the Svartsengi field. Their objective was to study the use of water influx methods in geothermal reservoir evaluation. They derived depletion models for liquid dominated geothermal reservoirs and modeled water influx by using Schilthuis, Fetkovich and Hurst methods. They found that the steady state Schilthuis method (Schilthuis, 1936) gave a reasonable match and the Hurst simplified unsteady-state method (van Everdingen and Hurst, 1949) assuming an infinite radial aquifer gave the best match of the models they tried.

Figure 4.14 shows the Schilthuis steady-state match and the Hurst (simplified) unsteady-state match obtained by Olsen (1984). Olsen applied mass balance on the reservoir as in our 1-tank model. In Olsen's approach the water influx (W_a) is computed for each time step by using Schilthuis method according to $\sum_{j=1}^{n}(p_i - p_j)\Delta t_j$, and the mass balance is arranged as given in Equation 4.1. The plot of x_n vs y_n gives a straight line. The model parameters, κ_r and α_r, are estimated from the slope and the intercept of the straight line, respectively.

$$\frac{W_{pn}}{W_a/\alpha_r} = -\kappa_r \frac{\Delta p_n}{W_a/\alpha_r} + \alpha_r \quad or \quad y_n = -\kappa_r x_n + \alpha_r \tag{4.1}$$

where, W_{pn} is the cumulative mass production, and W_a is the water influx, Δp_n is the pressure drop at n'th time step.

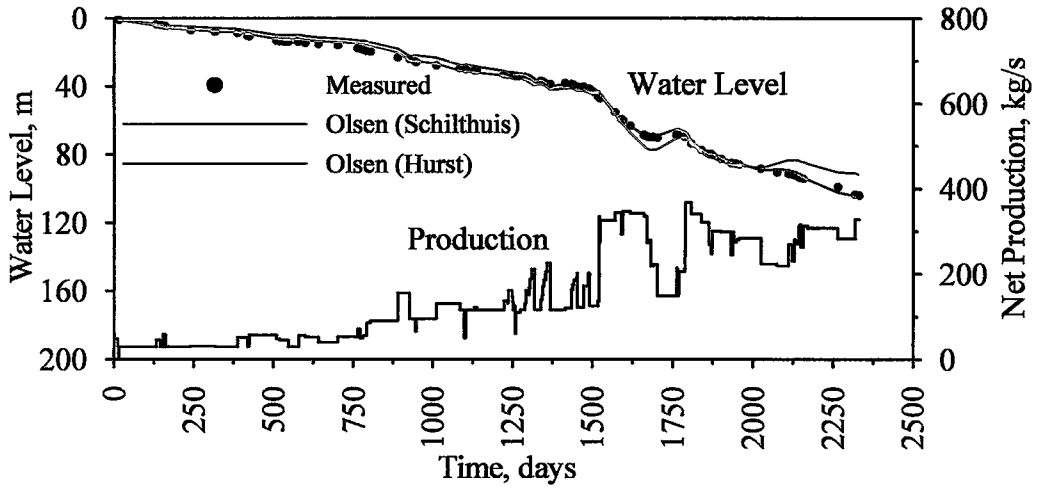

Figure 4.14 Schilthuis steady-state and Hurst (simplified) unsteady-state matches (Olsen, 1984).

The Schilthuis match is better for the early part of the data than for the later data. Olsen obtained the following values from the Schilthuis match: $\kappa_r = 6.68 \times 10^8$ kg/bar and $\alpha_r = 38.0$ kg/bar-s.

A nonlinear regression of the Svartsengi production data are employed by using 1-, 2- and 3-tank models given in this study. Figure 4.15 shows the results of 1-tank model.

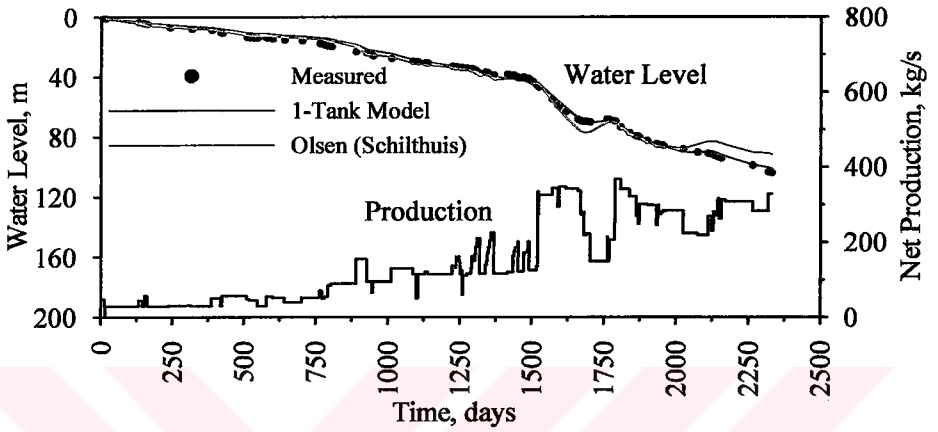

Figure 4.15 Comparison of observed and calculated water level changes.

The match obtained by Olsen using the Schilthuis steady-state model is also shown in Figure 4.15 for comparison purposes. Notice that the match based on our 1-tank model fits the measured water level data better than the Olsen's match based on the Schilthuis model.

Figures 4.16 and 4.17 present the results of 2- and 3-tank models, respectively. Table 4.3 summarizes the parameters of the best fitting lumped models.

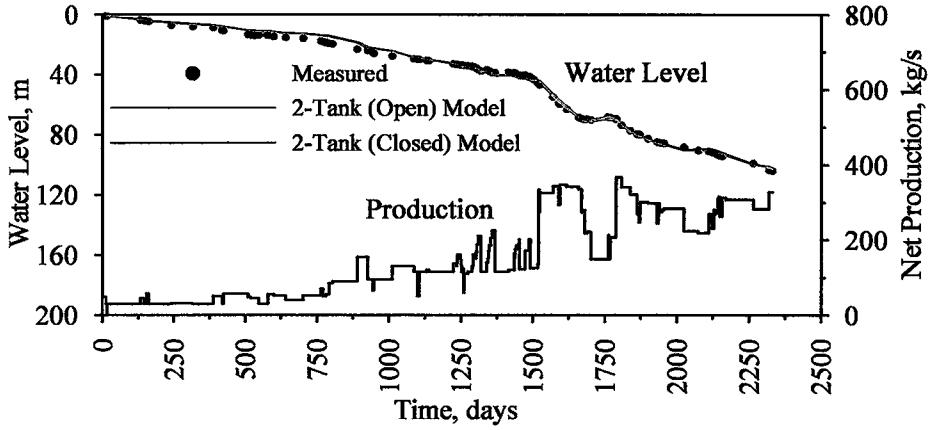

Figure 4.16 Simulation results of 2-tank models.

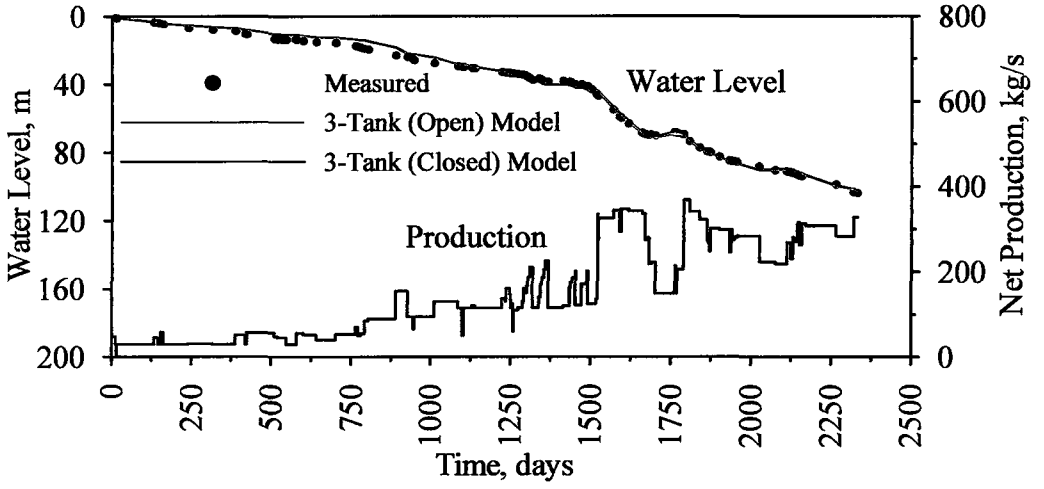

Figure 4.17 Simulation results of 3-tank models.

Table 4.3 Parameters of the best fitting lumped parameters (1-, 2-, and 3-tank models) for Svartsengi field.

	Olsen (Schilthuis)	**1-Tank**	**2-Tank Closed**	**2-Tank Open**	**3-Tank Closed**	**3-Tank Open**
α_{oa}, kg/bar-s	--	--	--	--	--	856.47 ($\pm 5.1 \times 10^{4}$)
κ_{oa}, kg/bar	--	--	--	--	1.84×10^{10} ($\pm 3.2 \times 10^{10}$)	3.06×10^{13} ($\pm 2.4 \times 10^{13}$)
α_{ia} (α_a for 2-T), kg/bar-s	--	--	--	35.36 ($\pm$9.370)	39.89 ($\pm$13.0)	0.002 ($\pm$0.077)
κ_{ia} (κ_a for 2-T), kg/bar	--	--	1.28×10^{10} ($\pm 8.8 \times 10^{9}$)	8.59×10^{8} ($\pm 3.3 \times 10^{8}$)	7.65×10^{8} ($\pm 4.1 \times 10^{8}$)	1.25×10^{10} ($\pm 8.7 \times 10^{9}$)
α_r, kg/bar-s	38.0	30.75 ($\pm$1.045)	37.7 ($\pm$6.183)	179.72 ($\pm$256.99)	220.3 ($\pm$449.41)	37.86 ($\pm$6.512)
κ_r, kg/bar	6.68×10^{8}	1.27×10^{9} ($\pm 7.4 \times 10^{7}$)	1.13×10^{9} ($\pm 1.3 \times 10^{8}$)	7.64×10^{8} ($\pm 4.8 \times 10^{8}$)	6.98×10^{8} ($\pm 6.4 \times 10^{8}$)	1.13×10^{9} ($\pm 1.6 \times 10^{8}$)
RMS, bar	--	0.403	0.403	0.406	0.405	0.403

Although the matches obtained by 2- and 3-tank models are quite same, the confidence intervals given in Table 4.3 computed for the parameters of the 2-tank open, and 3-tank open and closed models are quite high, (particularly see confidence intervals for α_{oa}, α_r and κ_{oa}). This indicates that the 3-tank open and closed, and 2-tank open models are inappropriate for the data. However, 1-tank and 2-tank closed models appear to be appropriate for the data as the fits between the measured and simulated data are quite satisfactory (see confidence intervals and RMS values in

Table 4.3) for both models. The $\pm 8.8 \times 10^9$ confidence interval for κ_{ia} in the 2-tank closed model shows that this parameter is not well determined compared to the other parameters of the model from the data available. Because results of our 1-tank and 2-tank closed model simulations did not exhibit any significant differences, further information on geology and geophysics as well as detailed analysis are required to identify the most appropriate model for the system. Due to its simplicity, however, 1-tank model could be chosen as an appropriate model to simulate Svartsengi field production data.

4.4 Balcova-Narlidere Field

4.4.1 About the field

Balcova-Narlidere geothermal field, which is known as the oldest geothermal system in Turkey, is situated 10 km away from the west of Izmir. The geothermal water with the temperature ranging from 80 to 140°C is produced from the wells with the depths ranging from 48.5 m to 1100 m. The first well was drilled by General Directorate of Mineral Research and Exploration (MTA) in 1963. There are about 50 wells drilled up to date and they are classified as gradient, shallow and deep wells. The field started to feed a district heating system with a capacity of approximately 5000 residences in 1996.

A total of 21 wells (9 deep and 12 shallow wells) are operated since 1996. The deepest well is BD-5 with a depth of 1100 m and the shallowest well is B-9 with a depth of 48.5 m. Six deep wells, BD-2, BD-3, BD-4, BD-5, BD-6 and BD-7, and four shallow wells, B-4, B-5, B-10 and B-11 are being continuously or periodically used for production. The deep wells were produced in winter and the shallow wells were produced in summer months in general. Until September 2002, three shallow wells, B-2, B-9 and B-12 were used for reinjection. However in 2002 the reinjection was switched to deep wells and a new well, BD-8, drilled in 2001 has been used for reinjection since then. The depths and the temperatures of the shallow and deep wells are presented in Table 4.4, and the locations of the wells are shown in Figure 4.18.

Table 4.4 The depths and the temperatures of the wells in Balcova-Narlidere field.

Well	Depth (m)	Temperature (°C)	Well	Depth (m)	Temperature (°C)
B-1	104	115	BD-1	564	140
B-2	150	113	BD-2	677	133
B-3	161	112	BD-3	750	140
B-4	125	112	BD-4	624	140
B-5	108.5	114	BD-5	1100	130
B-6	150	93	BD-6	605	140
B-7	120	115	BD-7	702	140
B-8	155	93	BD-8	625	133
B-9	48.5	122	BD-9	770	140
B-10	125	114			
B-11	125	109			
B-12	120	100			

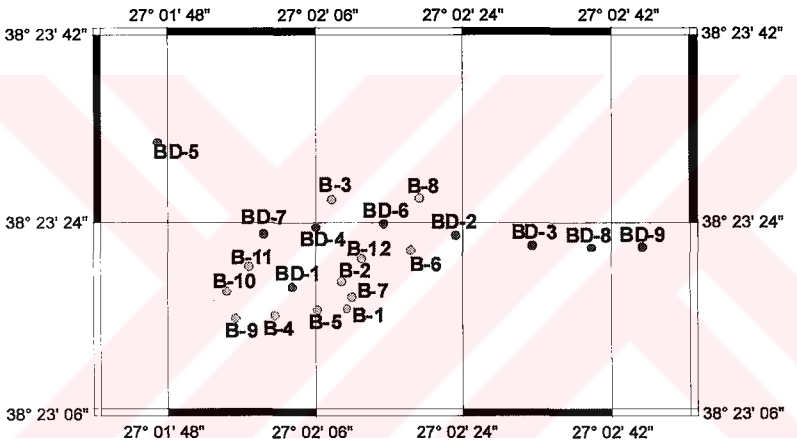

Figure 4.18 Locations of the wells in Balcova-Narlidere field.

The geological data, well logs, temperature profiles, well tests and geochemistry of the produced fluid are discussed in detail by Satman et al. (2002).

The production/reinjection and water level changes are measured in 8 shallow and 8 deep wells, some periodically and some intermittently. Figures 4.19, 4.20 and 4.21 show the net production (production-reinjection) data of shallow wells, deep wells and whole field, respectively. The shallow wells were used for reinjection and the deep wells for production until September 2002. However the reinjection into shallow wells was terminated in September 2002 (Figure 4.19 and Table 4.5). BD-8 is being used for reinjection since September 2002 (Figure 4.20).

Table 4.5 Summary of operations in the field.

Date	Comments
02.10.2000	Water level measurements of BD-1 started
02.10.2000-09.08.2002	Water level measurements of BD-5 are recorded
20.11.2002	BD-5 begun to produce
24.09.2002	Reinjection into B-9 stopped, BD-8 begun to be used for reinjection
04.01.2003	Water level measurements of BD-6 started

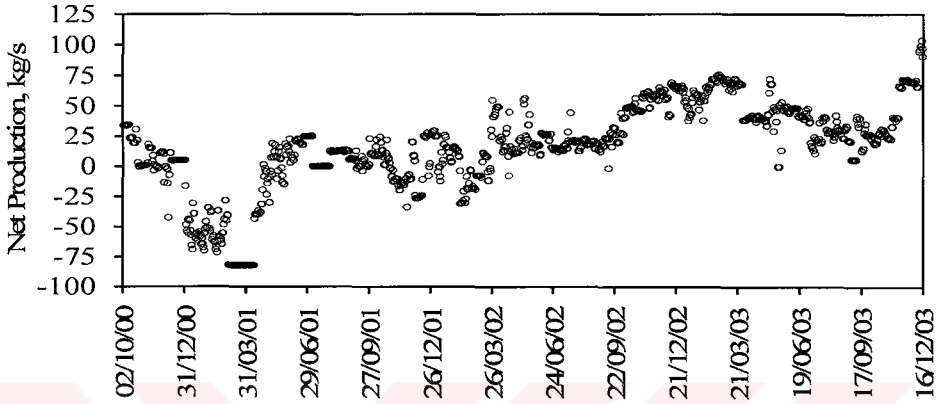

Figure 4.19 Net production history of shallow wells.

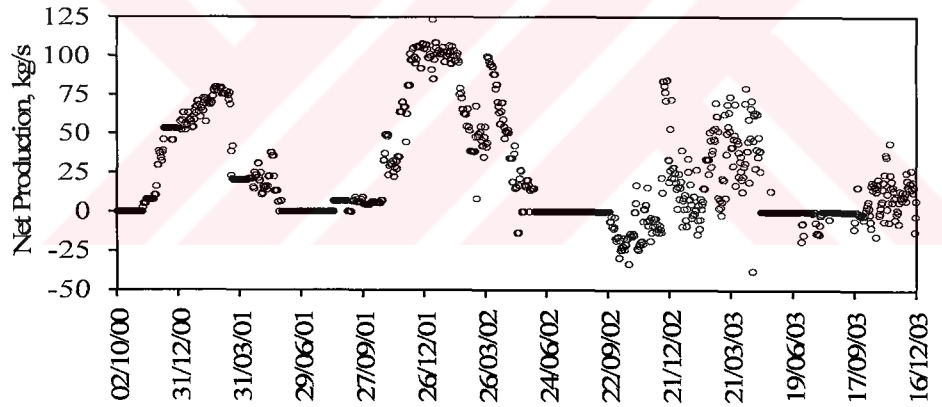

Figure 4.20 Net production history of deep wells.

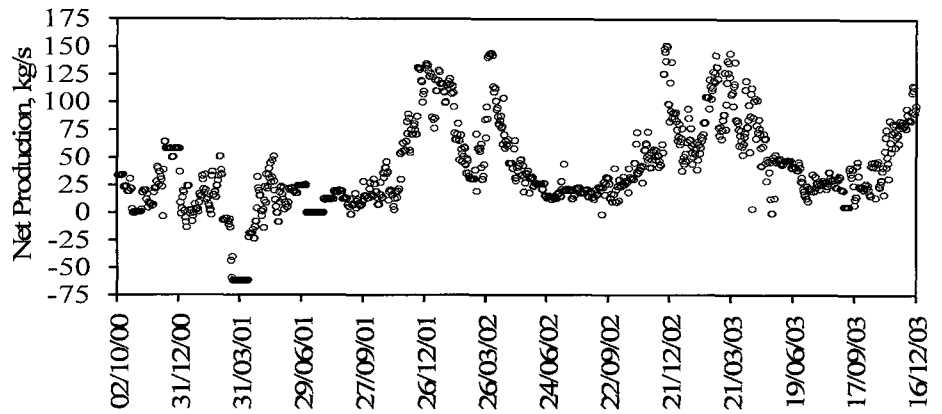

Figure 4.21 Net production history of the field.

The water level data of the deep wells (BD-1, BD-5 and BD-6), and the shallow wells (B-9 and B-12) are presented in Figures 4.22, 4.23, 4.24, 4.25 and 4.26, respectively. The data are taken from the top of the well.

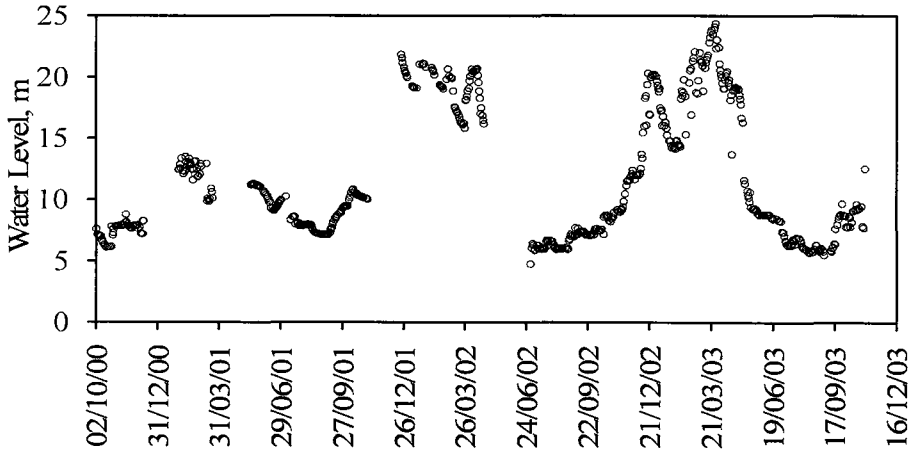

Figure 4.22 Water level data of BD-1.

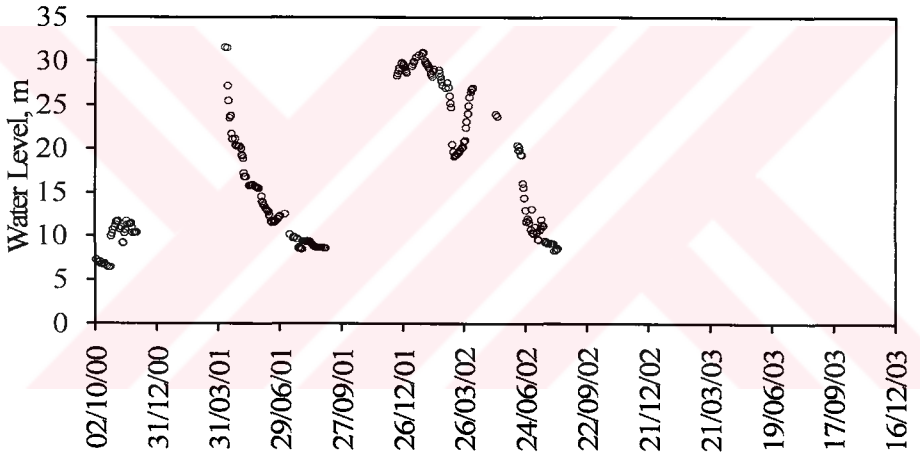

Figure 4.23 Water level data of BD-5.

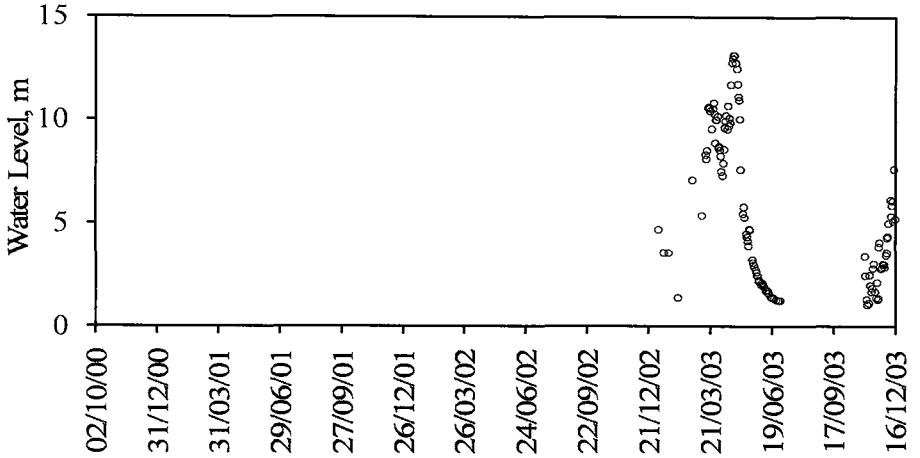

Figure 4.24 Water level data of BD-6.

BD-1 is a well with a moderate depth and is located near the center of the production area (Table 4.4 and Figure 4.18). It has been used as an observation well. Satman et al. (2002) states that the water level of BD-1 is strongly affected by the production from and the reinjection into the shallow wells and also affected by the production from the deep wells.

BD-5 is situated in northwestern of the field. The water level of BD-5 (see Figure 4.23) shows a similar behavior as BD-1 does. However, BD-5 exhibits greater water level changes than BD-1 does. The reasons for such difference in behavior are thought to be; (1) the direction of the natural recharge is from east to south-west in the field thus the natural recharge support is felt weaker at BD-5, (2) BD-5 is further away from the reinjection region so that the reinjection into the shallow wells causes a stronger support to BD-1.

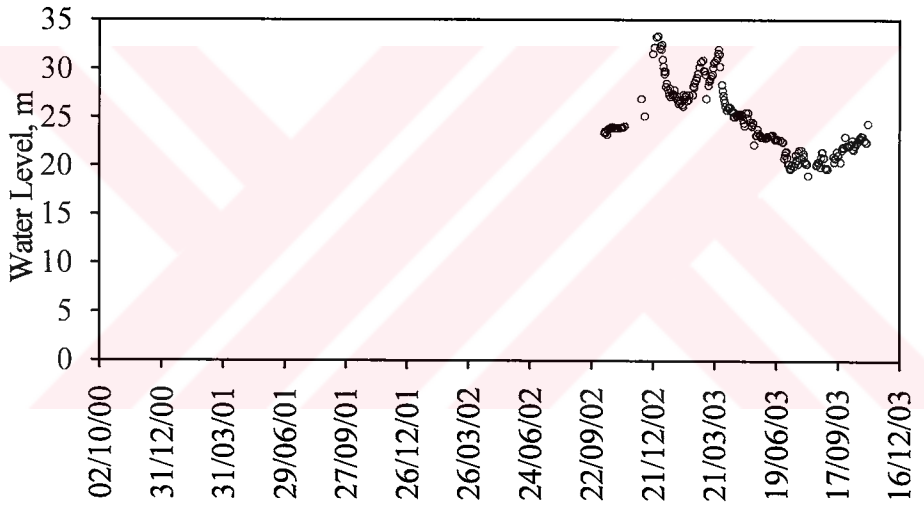

Figure 4.25 Water level data of B-9.

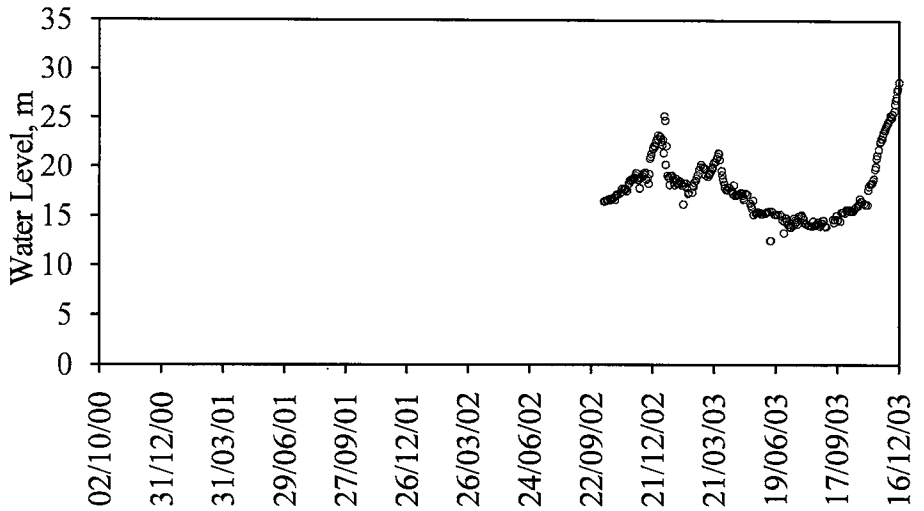

Figure 4.26 Water level data of B-12.

The third deep well, BD-6, used in modeling is also located near the center of the production area. It was used as a production well until 18.11.2002. Later it was used as an observation well and the water level measurements were recorded.

The deep well, BD-1 has the longest duration of water level recording whereas the water level recordings of the other wells (BD-5, BD-6, B-9 and B-12) are either of short duration or not recorded continuously (Figures 4.22, 4.23, 4.24, 4.25, and 4.26).

4.4.2 Applications of lumped models

The most important problem involved in modeling Balcova-Narlidere geothermal field is the lack of continuous measurements of water level (Figures 4.22, 4.23, 4.24, 4.25 and 4.26) and the short duration of available water level data.

First, 1-tank model is applied by using the net production (production-reinjection) data of the whole field (deep + shallow) and the measured water level values of the three deep wells, BD-1, BD-5 and BD-6.

The modeling results for BD-1, BD-5 and BD-6 are given for various time periods in Table 4.6 and Figures 4.27, 4.28, 4.29 and 4.30. BD-1 is modeled for the period of 02.10.00/30.10.03 (the first row of Table 4.6) which covers the whole production period of the field with water level recordings and then for the period of 24.09.02/30.10.03 (the second row of Table 4.6) which is the period of BD-8 used for reinjection purposes. The modeling studies are performed for BD-5 and BD-6 for time periods in which their water level measurements are available.

Table 4.6 Parameters of the 1-tank model for Balcova-Narlidere Field.

Period	Well	Model Parameters		RMS, bar
		α_r, kg/bar-s	κ_r, kg/bar	
02.10.2000-30.10.2003	BD-1	77.67 (±2.53)	8.25×10^7 ($\pm 9.18 \times 10^6$)	0.226
24.09.2002-30.10.2003	BD-1	58.78 (±1.74)	5.0×10^7 ($\pm 4.88 \times 10^6$)	0.307
02.10.2000-09.08.2002	BD-5	81.66 (±6.71)	2.96×10^7 ($\pm 1.22 \times 10^7$)	0.511
04.01.2003-15.12.2003	BD-6	74.38 (±4.94)	1.29×10^8 ($\pm 1.44 \times 10^7$)	0.173

Comparing the confidence intervals obtained from the modeling study (Table 4.6), the model for the period of 24.09.02/30.10.03 gives more reliable results than other periods. The early time water level data of BD-1 could not be matched properly. The main reason for that could be the changing the production/reinjection schedule of the field at 24.09.2002. The shallow wells, B-2, B-9 and B-12, were used for reinjection until 24.09.02, and BD-8 was used after.

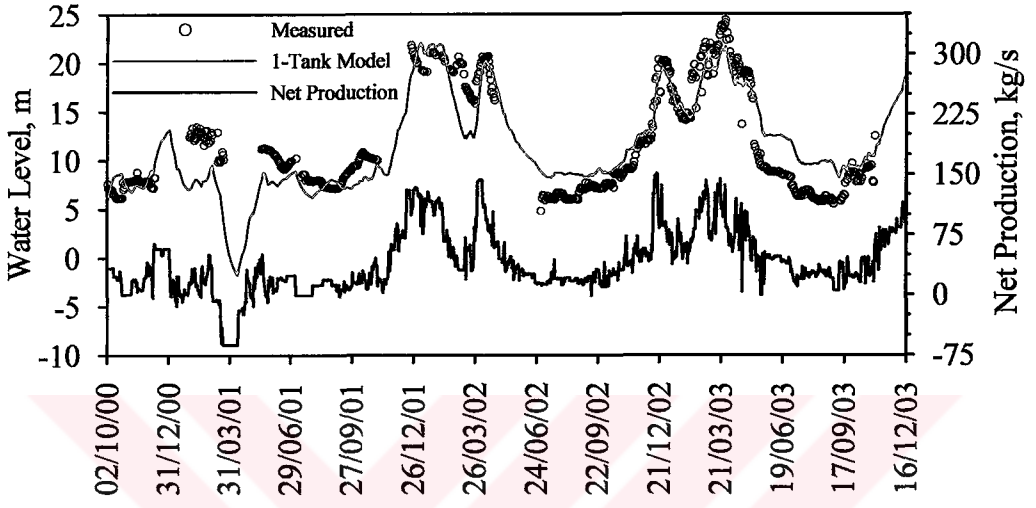

Figure 4.27 Simulation result of BD-1 (All data were matched)
(α_r =77.67 kg/bar-s, κ_r =8.25x10^7 kg/bar)

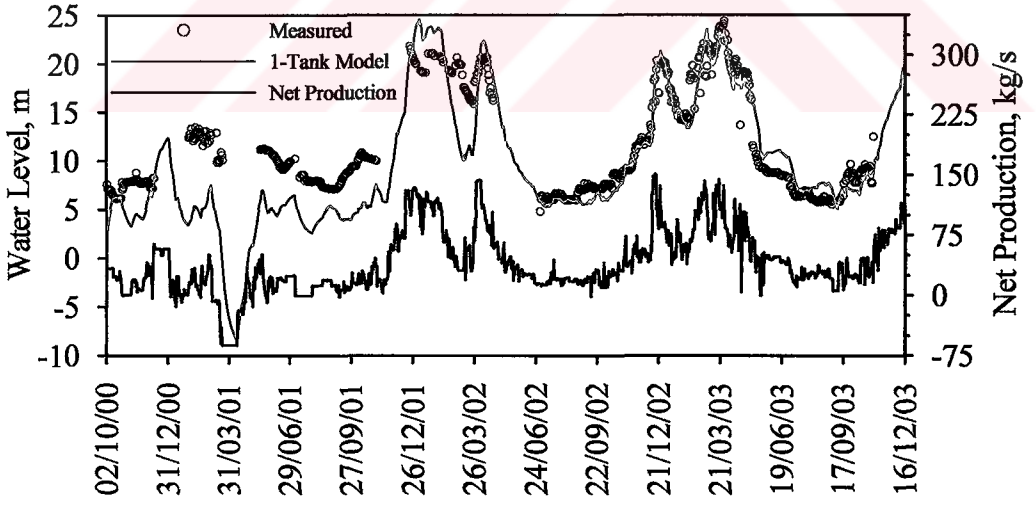

Figure 4.28 Simulation result of BD-1 (Data after 24.09.02 were matched)
(α_r =58.78 kg/bar-s, κ_r =5.0x10^7 kg/bar)

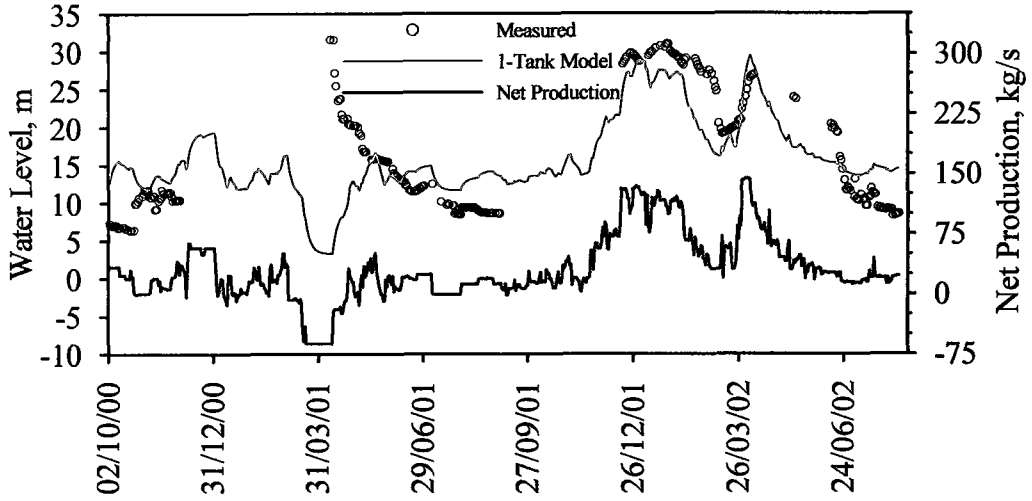

Figure 4.29 Simulation result of BD-5 (α_r =81.66 kg/bar-s, κ_r =2.96x10^7 kg/bar)

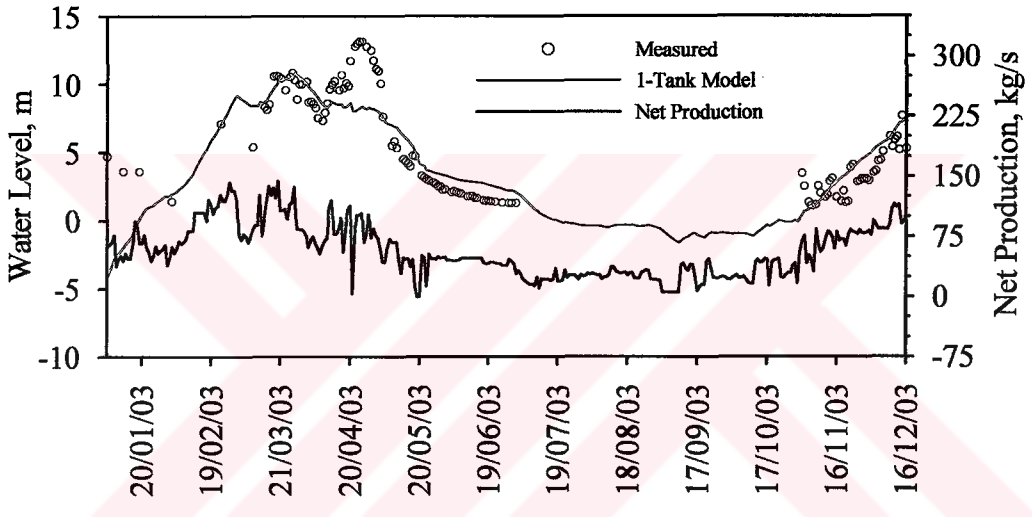

Figure 4.30 Simulation result of BD-6 (α_r =74.38 kg/bar-s, κ_r =1.29x10^8 kg/bar)

Since the confidence intervals of parameters obtained for BD-1 for a period of 24.09.02/30.10.03 are the lowest (see Table 4.6), α_r =58.78 kg/bar-s and κ_r =5.0x10^7 kg/bar could be chosen for 1-tank model parameters to model Balcova-Narlidere geothermal field.

2-tank open model (with constant pressure outer boundary) is applied for the deep wells and for the time intervals discussed above. The modeling results are presented in Table 4.7. As seen from Table 4.7, the confidence intervals computed for the reservoir and aquifer parameters are quite high indicating the inadequacy of the 2-tank open model. Probably a longer period of measured data is required to increase the reliability of the model.

Table 4.7 Parameters of the 2-tank (open) model for Balcova-Narlidere Field.

Period	Well	Model Parameters				RMS, bar
		α_a, kg/bar-s	κ_a, kg/bar	α_r, kg/bar-s	κ_r, kg/bar	
02.10.2000-30.10.2003	BD-1	707.27 (±12669)	$3.58\text{x}10^{8}$ ($\pm1.0\text{x}10^{10}$)	87.17 (±192.48)	$7.82\text{x}10^{7}$ ($\pm4.1\text{x}10^{7}$)	0.226
24.09.2002-30.10.2003	BD-1	248.9 (±3530.1)	$6.73\text{x}10^{7}$ ($\pm1.39\text{x}10^{9}$)	76.85 (±336.73)	$4.63\text{x}10^{7}$ ($\pm3.3\text{x}10^{7}$)	0.307
02.10.2000-09.08.2002	BD-5	999.93 (±6519.4)	$1.91\text{x}10^{10}$ ($\pm1.5\text{x}10^{11}$)	83.21 (±10.90)	$2.78\text{x}10^{7}$ ($\pm1.2\text{x}10^{7}$)	0.510
04.01.2003-15.12.2003	BD-6	336.32 (±328.08)	$2.99\text{x}10^{8}$ ($\pm4.57\text{x}10^{9}$)	93.47 (±257.56)	$1.14\text{x}10^{8}$ ($\pm8.3\text{x}10^{7}$)	0.173

2-tank (closed) and 3-tank (open/closed) models are also utilized for these three deep wells, however similar to 2-tank (open) model results, the reservoir and aquifer parameters can not be determined well as is clear from large confidence intervals for some of the parameters. Therefore the modeling results are not discussed here.

Based on the observations on the production and reinjection behavior of the field (Satman et al., 2002) among the models discussed in Chapter 3, the 2 reservoir tanks with/without aquifer model could also be an appropriate model to represent the production/reinjection-water level response behavior of the Balcova-Narlidere geothermal field.

2 reservoir tanks with aquifer and without aquifer models are applied by using the water level data of BD-1 and BD-6 representing the deep reservoir, and B-9 and B-12 representing the shallow reservoir. In each modeling water level responses of 1 deep well and 1 shallow well were modeled. The simulation results of 2-reservoir tanks without aquifer and with aquifer models are shown in Table 4.8 and Table 4.9, respectively.

The recharge constant between the shallow and the deep reservoirs, α_{r12}, could not be well determined by performing 2-reservoir tanks without aquifer model for BD-6&B-9 and BD-6&B-12 (see confidence interval of α_{r12} in Table 4.8). The ±1.82 confidence interval for α_{r12} (which means the value of α_{r12} can be in between 0.62 and 4.26) in the modeling of BD-1&B-9 indicates that this parameter is also not well determined compared to the other parameters of the model from the data available.

The modeling of BD-1&B-12 appears to be appropriate for the data with regard to the confidence intervals and RMS values in Table 4.8.

Table 4.8 Simulation results of 2-reservoir tanks without aquifer model.

	Wells	BD-1&B-12	BD-1&B-9	BD-6&B-12	BD-6&B-9
Model Parameters	α_{r1}, kg/bar-s	44.12 (±2.78)	31.08 (±2.25)	38.11 (±3.14)	24.65 (±2.69)
	κ_{r1}, kg/bar	1.67×10^{7} ($\pm4.7\times10^{6}$)	6.42×10^{7} ($\pm1.2\times10^{7}$)	2.49×10^{7} ($\pm4.1\times10^{6}$)	2.16×10^{8} ($\pm2.4\times10^{7}$)
	α_{r2}, kg/bar-s	39.09 (±2.35)	45.46 (±2.78)	84.92 (±11.71)	74.57 (±8.39)
	κ_{r2}, kg/bar	3.48×10^{7} ($\pm5.1\times10^{6}$)	3.37×10^{7} ($\pm5.1\times10^{6}$)	3.11×10^{7} ($\pm1.5\times10^{7}$)	3.11×10^{7} ($\pm1.0\times10^{7}$)
	α_{r12}, kg/bar-s	14.94 (±2.84)	2.44 (±1.82)	4.36×10^{-5} (±2.40)	6.0×10^{-6} (±0.75)
	$RMS_{shallow}$,bar	0.190	0.208	0.289	0.239
	RMS_{deep}, bar	0.224	0.264	0.206	0.154

Table 4.9 Simulation results of 2-reservoir tanks with aquifer model.

	Wells	BD-1&B-12	BD-1&B-9	BD-6&B-12	BD-6&B-9
Model Parameters	α_{r1}, kg/bar-s	45.98 (±3.22)	36.20 (±7.56)	39.72 (±9.60)	23.46 (±13.12)
	κ_{r1}, kg/bar	1.57×10^{7} ($\pm4.9\times10^{6}$)	1.97×10^{8} ($\pm2.9\times10^{7}$)	1.43×10^{7} ($\pm3.3\times10^{6}$)	1.69×10^{8} ($\pm3.1\times10^{7}$)
	α_{r2}, kg/bar-s	39.95 (±2.74)	48.16 (±5.82)	175.62 (±60.48)	75.93 (±23.5)
	κ_{r2}, kg/bar	3.51×10^{7} ($\pm5.5\times10^{6}$)	3.62×10^{7} ($\pm5.7\times10^{6}$)	2.79×10^{7} ($\pm3.4\times10^{7}$)	2.38×10^{7} ($\pm9.9\times10^{6}$)
	α_{r12}, kg/bar-s	13.52 (±2.97)	0.01 (±4.96)	0.01 (±7.99)	0.01 (±10.8)
	α_{a}, kg/bar-s	999.98 (±4816.5)	39.83 (±117.0)	32.66 (±136.87)	17.61 (±203.5)
	κ_{a}, kg/bar	2.99×10^{10} ($\pm2.2\times10^{11}$)	1.78×10^{9} ($\pm1.2\times10^{9}$)	1.62×10^{9} ($\pm4.9\times10^{8}$)	1.01×10^{9} ($\pm3.4\times10^{8}$)
	$RMS_{shallow}$,bar	0.199	0.244	0.285	0.268
	RMS_{deep}, bar	0.216	0.207	0.269	0.156

Simulation results of BD-1&B-9, BD-1&B-12, BD-6&B-9 and BD-6&B-12 are given in Figures 4.31, 4.32, 4.33 and 4.34, respectively.

Although the confidence intervals for the model parameters given in Table 4.8 seem acceptable, however, the matches in Figure 4.32 exhibits the discrepancy between the measured data and model for shallow and deep reservoirs. This might be due to following reasons: (1) 2-reservoir tank without aquifer model could not represent the field data successfully, (2) the production and/or the water level data have some errors, (3) the duration of the available data is not long enough to see unique feature of the 2-reservoir models.

On the other hand, 2-reservoir tanks with aquifer model could not give the satisfactory results (Table 4.9). The confidence intervals of the aquifer parameters are computed to be quite high and so not reliable.

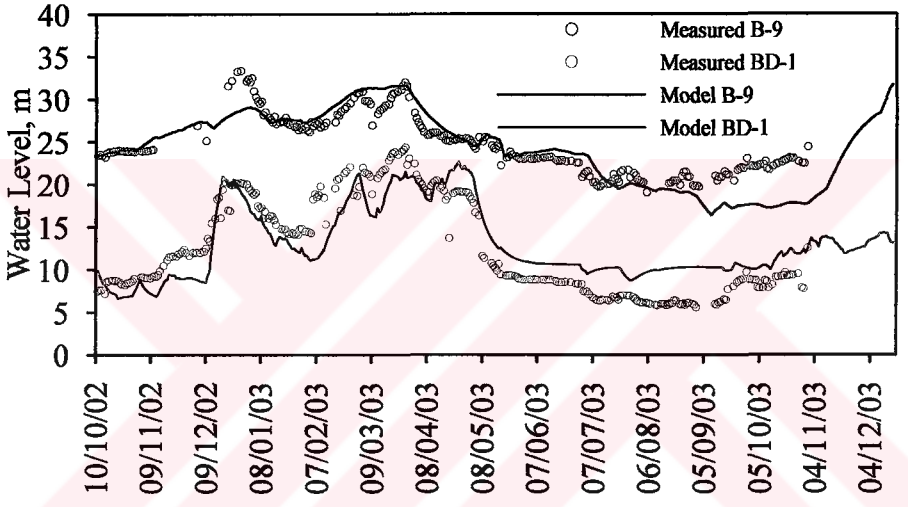

Figure 4.31 Modeling results of BD-1&B-9.

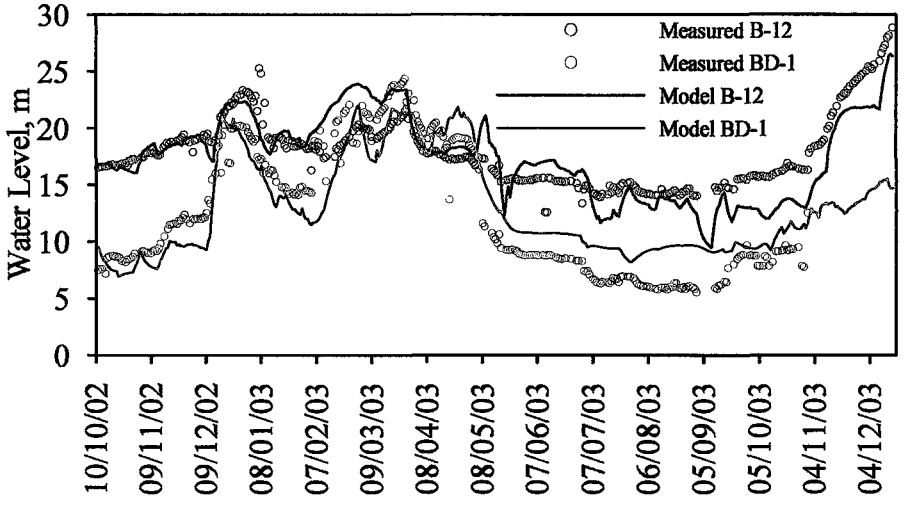

Figure 4.32 Modeling results of BD-1&B-12.

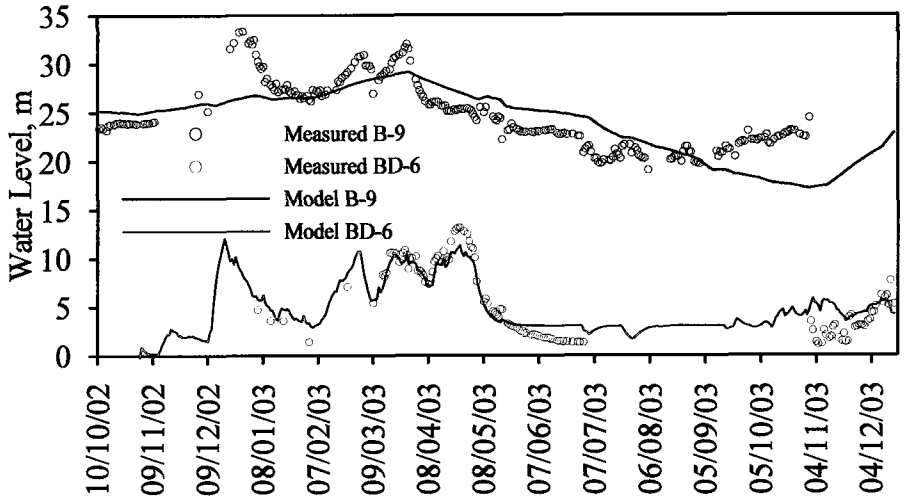

Figure 4.33 Modeling results of BD-6&B-9.

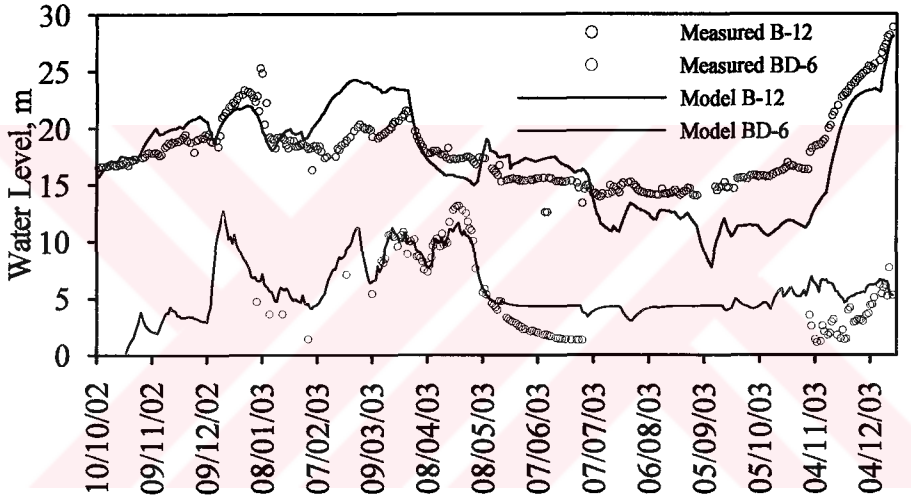

Figure 4.34 Modeling results of BD-6&B-12.

4.4.3 Future performance predictions

The main objective of modeling a geothermal reservoir is to assess its future production potential. How the lumped models are used to predict the water level changes in the reservoir for different production/reinjection scenarios are studied here.

4.4.3.1 Results based on 1-tank model

Future performance of Balcova-Narlidere geothermal field is predicted by 1-tank model for the next ten years. Since the BD-1 water level changes are best modeled with the lowest confidence intervals for the 1-tank model parameters of α_r=58.78

kg/bar-s and κ_r=5.0x10^7 kg/bar obtained for the period of 24.09.2002/30.10.2003, these model parameters are used to forecast the future field performance.

The water level predictions are made for three different production/reinjection scenarios: (I) the production/reinjection data valid for 15.12.2002/15.12.2003 period is maintained for the next ten years, (II) the 15.12.2002/15.12.2003 production/reinjection values are increased by 20% in each year for the next ten years, (III) the 15.12.2002/15.12.2003 production/reinjection values are increased by 100% and kept constant for the next five years and then increased again by another 100% and kept constant for the following five years.

The predictions for these three scenarios are presented in Figures 4.35, 4.36 and 4.37, respectively.

For Scenario-I, the water level changes in BD-1 are expected to remain constant for next ten years (Figure 4.35). The water level that occurs in winter is predicted to be about 23 m and the water level that occurs in summer when the production is lowest is predicted to be 5 m.

In the case of Scenario-II, the water level drops continuously for next ten years (Figure 4.36). The water level decreases to 65 m in winter 2013 and reaches to 10 m in summer 2013. Comparing with the existing water level changes in BD-1, increasing the net production from the field by 20% in each year for the next ten years or in other words increasing the net production by three times of the present value causes nearly 42 m additional drop in water level in winter and about 5 m additional drop in water level in summer.

In the case of Scenario-III (Figure 4.37), the water level changes between 45 m and 9 m in first five years (2003-2008) and between 65 m and 10 m in last five years (2009-2013). As far as water levels obtained at the end of 10 years are concerned, Scenarios II and III yield exactly the same results.

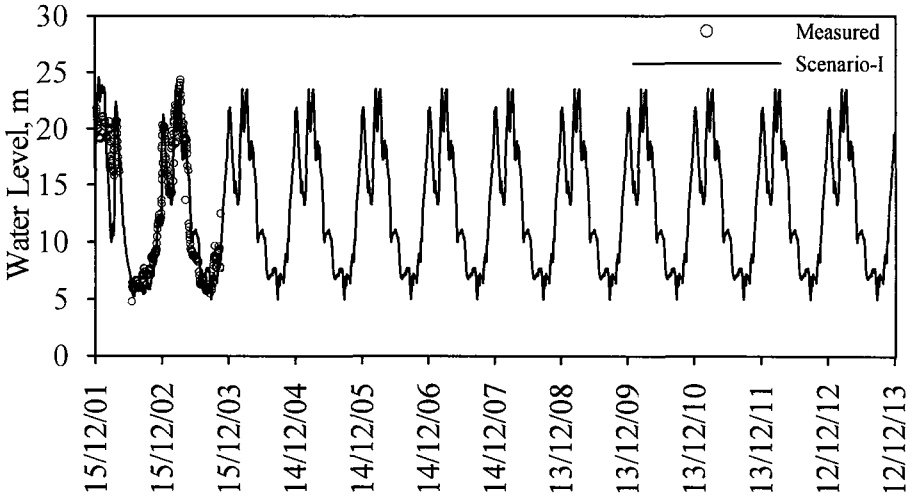

Figure 4.35 Water level changes in BD-1 for scenario-I.

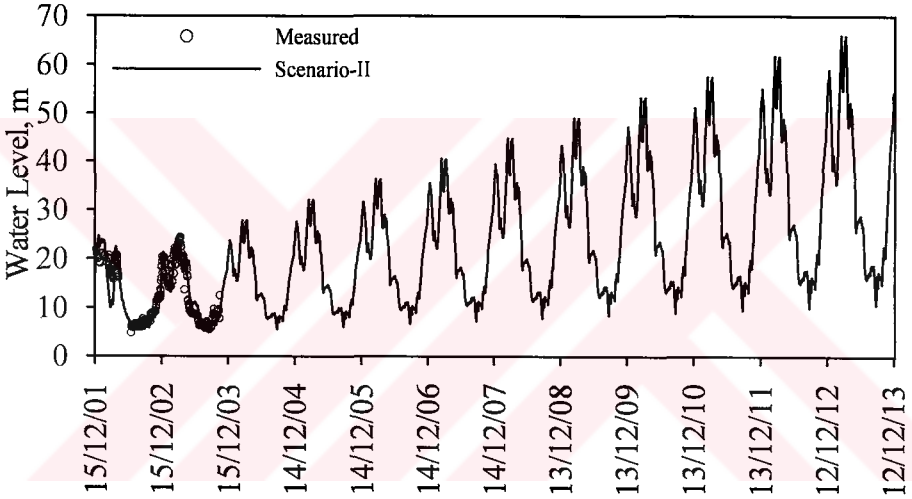

Figure 4.36 Water level changes in BD-1 for scenario-II.

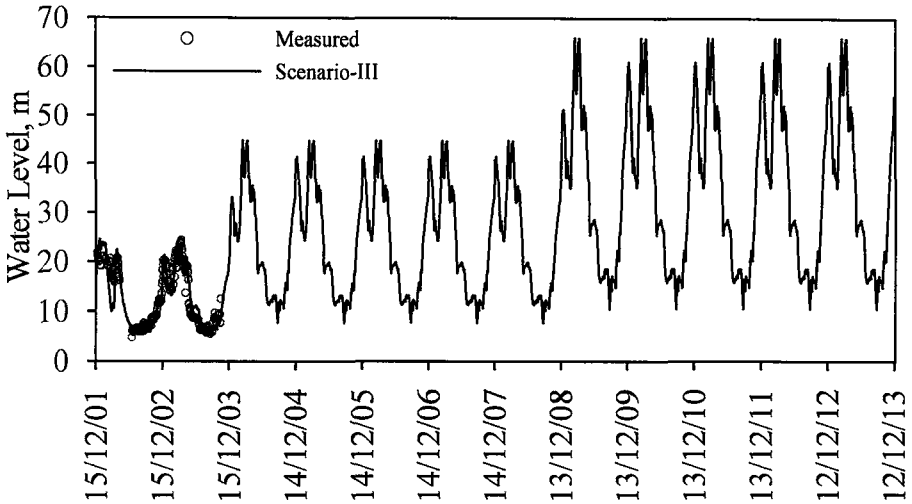

Figure 4.37 Water level changes in BD-1 for scenario-III.

4.4.3.2 Results based on 2-reservoir tanks without aquifer model

Future performances of the Balcova -Narlidere geothermal field modeled to be consisted of the deep and the shallow reservoirs are predicted by using 2-reservoir tanks without aquifer model again for the next ten years. Since the best fit is obtained for BD-1&B-12 water level data, the model parameters of α_{r1}=44.12 kg/bar-s, κ_{r1}=1.67x10^7 kg/bar, α_{r2}=39.09 kg/bar-s, κ_{r2}=3.48x10^7 kg/bar and α_{r12}=14.94 kg/bar-s, are used for prediction purposes.

Four different production/reinjection scenarios are generated to predict the future performance. (I) the 15.12.2002/15.12.2003 production/reinjection data of deep and shallow reservoirs are maintained for the next ten years, (II) the 15.12.2002/15.12.2003 production/reinjection values are increased by 20% each years, only the deep reservoir is used for production/reinjection purposes and the shallow reservoir is not utilized for production or reinjection at all, for the next ten years, (III) the 15.12.2002/15.12.2003 production/reinjection values are increased by 20% each year, only the shallow reservoir is used for production/reinjection purposes and the deep reservoir is not utilized for production or reinjection at all, for the next ten years, (IV) the 15.12.2002/15.12.2003 production/reinjection values of the both deep and shallow reservoirs are increased by 20% in each year for next ten years.

The water level predictions in wells BD-1 and B-12 for Scenarios I, II, III and IV are presented in Figures 4.38, 4.39, 4.40 and 4.41, respectively.

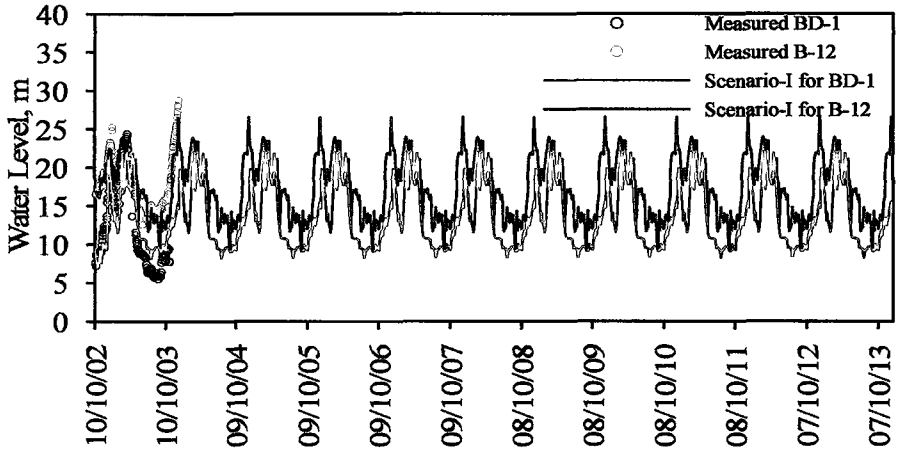

Figure 4.38 Water level changes in BD-1 and B-12 for scenario-I.

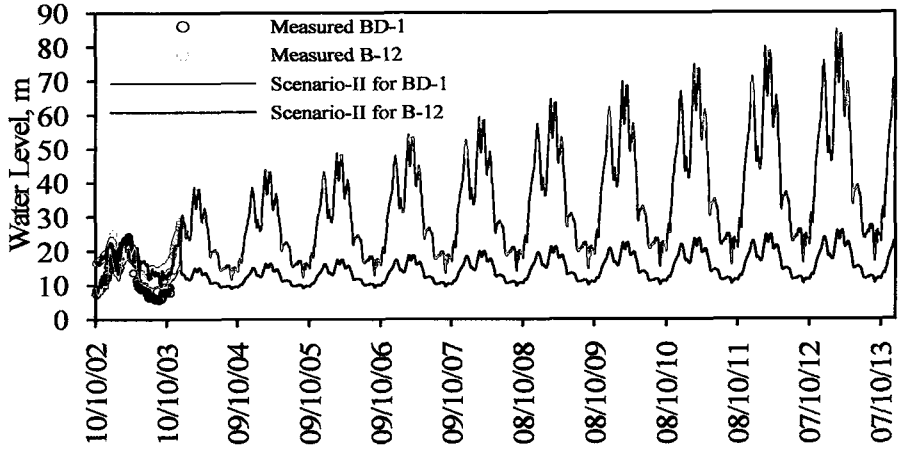

Figure 4.39 Water level changes in BD-1 and B-12 for scenario-II.

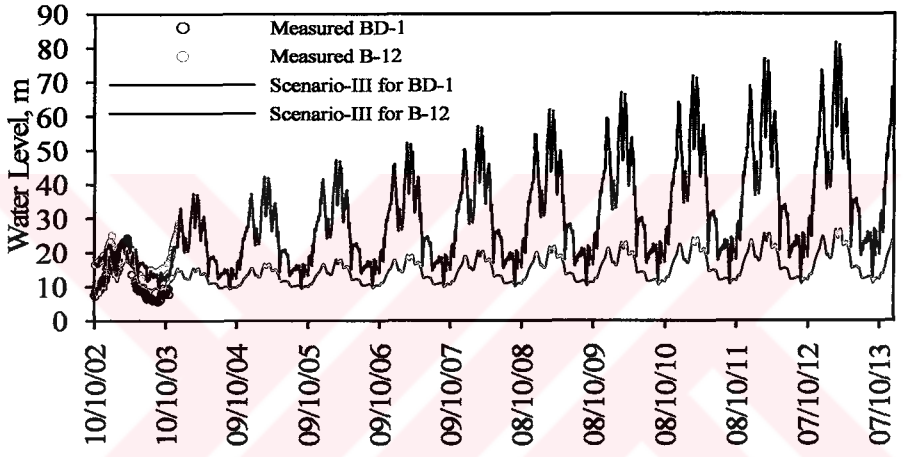

Figure 4.40 Water level changes in BD-1 and B-12 for scenario-III.

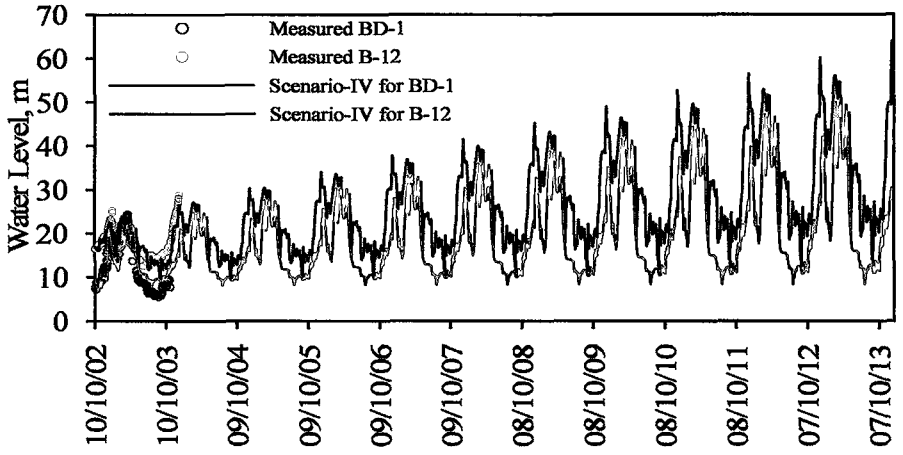

Figure 4.41 Water level changes in BD-1 and B-12 for scenario-IV.

For Scenario-I, water level changes in BD-1 and B-12 remain constant for next ten years (Figure 4.38). The water level drops to 27 m in shallow reservoir in winter and

levels at 9.5 m in summer. In deep reservoir the water level decreases to about 22 m in winter and levels at 9 m in summer.

In the case which the deep reservoir is used for all production/reinjection operations (Scenario-II), the water level of deep reservoir drops to 85 m in winter 2013 and levels at 16 m in summer 2013 (Figure 4.39). Although the shallow reservoir is not used for production/reinjection, the water level of shallow reservoir is affected from the deep reservoir and it drops to 24 m in winter and levels at 11 m in summer at the end of the next ten years. The hydraulic conductivity between the deep and the shallow reservoirs is the reason of decreasing water level in shallow reservoir.

For Scenario-III in which the shallow reservoir is used for all production/reinjection operations, the water level of shallow reservoir drops to 82 m in winter 2013 and levels at 12.5 m in summer 2013 (Figure 4.40). Although the deep reservoir is not used for production/reinjection, the water level of deep reservoir is affected from the shallow reservoir and it drops to 25 m in winter and levels at 12 m in summer at the end of the next ten years.

For Scenario-IV in which the production/reinjection values of both deep and shallow reservoirs are increased by 20%, the water level of shallow reservoir drops to 63 m in winter 2013 and levels at 12 m in summer 2013 (Figure 4.41). Moreover, the water level of deep reservoir drops to 50 m in winter and levels at 9 m in summer at the end of the next ten years.

All the production wells in Balcova-Narlidere field are operated by pumps set in the wellbores. The pumps in deep wells are installed at an average depth of 150 m from the surface whereas the pumps in shallow wells are installed at about 70 m. For safe and efficient operation of the wellbore pumps to avoid the possible cavitation a minimum liquid level above the pump must be maintained. This minimum liquid level is recommended to be 30 m in deep wells and 15 m in shallow wells above the pumps. Therefore, the water level is allowed to drop to 120 m in deep wells and 55 m in shallow wells unless the installation depths of the pumps are changed. Thus the pump depths are the limiting constraints in operation of the field. The water levels should not drop below 120 m in deep wells and 55 m in shallow wells. Otherwise the pumps at the present installation depths will be unoperational.

In the case of Scenario III when the shallow wells are utilized for whole production/reinjection operations, the water level of the shallow wells is predicted to drop to 82 m in 2013. Since 82 m water level is below the safe liquid level of 55 m, the pumps will not operate. In fact, the results indicate that the water level of 55 m in shallow wells is reached just after 5 years of operation according to Scenario III (Figure 4.40). Thus the pump depths in shallow wells become the limiting factor for the production from the field.

A similar comment is also valid for Scenario IV in which the production/reinjection values are increased by 20% in each of the next ten years. While the model results indicate no problem for the deep wells, however, the water level in shallow wells is expected to drop to 63 m at the end of 10 years of operation, which is lower than the safe liquid level of 55 m for the shallow wells.

Particularly the results of Scenarios III and IV indicate the danger involved in utilizing the shallow wells in production operations. Therefore the field management is recommended to limit the production from the shallow wells. If the production from the field is to be increased, a significant portion of the production should be obtained through the deep wells.

4.4.3.3 Discussion of prediction results

It should be reminded that all the modeling results given and discussed above for the Balcova-Narlidere geothermal field are based on limited production and water level history. Therefore the results and discussions should be taken cautiously. They are believed to be qualitatively correct however might be in error quantitatively. A longer history of production and water level data is definitely required. Application of our lumped models is recommended when more field data are available.

It should also be mentioned that the inaccuracy as well as the discontinuity of the input data such as the production/reinjection flow rates and the water level measurements greatly affects the confidence intervals and RMS values computed from the match.

Short history, discontinuity and possible inaccuracies in the input data are probable reasons why we obtain best matches with the simple models such as 1-tank model and 2-reservoir tanks without aquifer model.

4.4.4 About the fluid and heat recovery

As discussed in Chapter 2.1 (see Figures 2.3 and 2.4), the pressure-production behavior of the low-temperature geothermal system follows an isothermal behavior. Production from the reservoir causes decline in pressure without any change in temperature. In this section, we want to demonstrate this fact by using our 1-tank model. For simplicity, a constant net mass production rate, $w_{p,net}$ = 75 kg/s, was assumed and our 1-tank model with the model parameters obtained from the regression analysis of the Balcova-Narlidere field, α_r=58.78 kg/bar-s and κ_r=5x10^7 kg/bar, were used. We also assumed that the reservoir temperature is 140°C, the porosity is 0.05, the diameter of the reservoir is 2 km, and the thickness is 300 m. We run our 1-tank model up to 1000 days of production time. The pressure drop as a function of time is given in Figure 4.42. For comparison purposes, the pressure behavior for various values of α_r are also shown in the figure.

Notice that the case of α_r = 0.0 in Figure 4.42 corresponds to a closed geothermal reservoir with the pressure behavior given as Point C in Figure 2.3 and 1ϕ behavior in Figure 2.4. The path is essentially isothermal since no boiling takes place during the production.

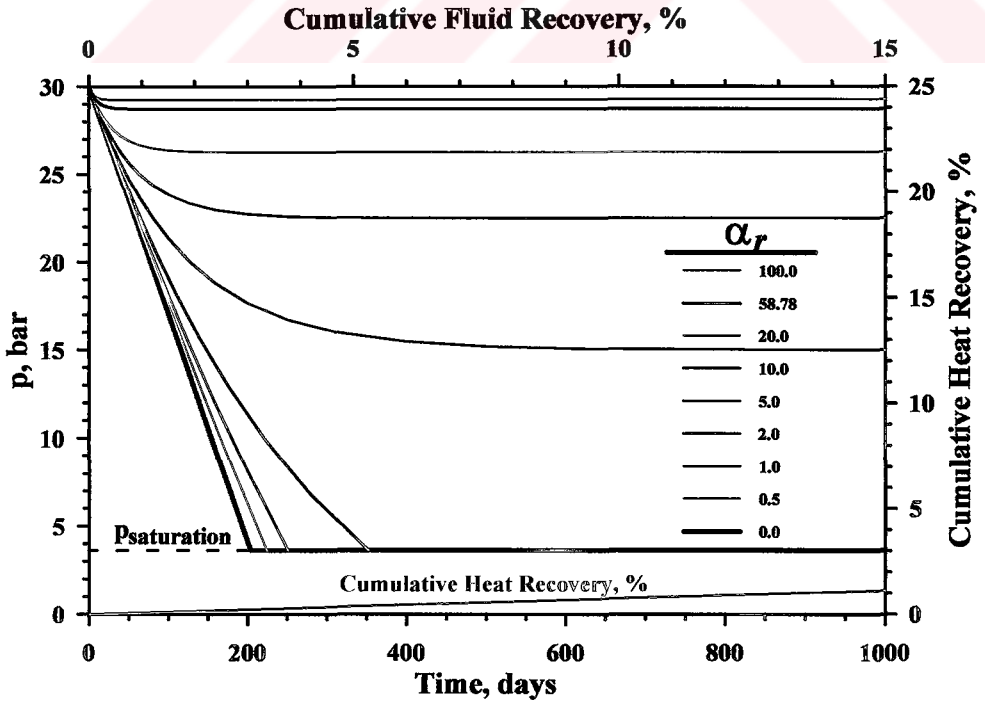

Figure 4.42 Cumulative fluid and heat recovery.

The following definitions are required for our discussion:

$$OWIP = V_r \phi_r \rho_w \tag{4.2}$$

$$\text{Cumulative Water Production, \%} = \frac{w_{p,net}\, t}{OWIP} \times 100 \tag{4.3}$$

where $OWIP$ is the original water in place, and cumulative water production is the amount of water produced at production time, t.

$$\text{Total Heat Content} = V_r \Delta T \left[\rho_w C_w \phi_r + \rho_r C_r (1-\phi_r)\right] \tag{4.4}$$

$$\text{Cumulative Heat Recovery, \%} = \frac{w_{p,net}\, t\, h_w}{Total\ Heat\ Content} \times 100 \tag{4.5}$$

where ΔT is the temperature difference above 0°C (140°C), C_w is the specific heat capacity of water (~1 kcal/kg-°C), C_r is the specific heat capacity of rock (~0.25 kcal/kg-°C), ρ_w is the water density at 140°C (~927 kg/m^3), ρ_r is the rock density (2455 kg/m^3) and h_w is the enthalpy of water at 140°C (140.6 kcal/kg).

If the numerical values of rock, fluid, and reservoir properties are substituted into Equation 4.2 and 4.4, we found $OWIP = 4.36 \times 10^{10}$ kg and total heat content = 8.306×10^{13} kcal, respectively.

In the case of $\alpha_r = 58.78$ kg/bar-s, a pressure drop of 1.28 bar occurs at the end of 1000 days production period. Only 15% $OWIP$ is produced as water and 1.097% of total heat content is recovered as heat with water. Especially the very low cumulative heat recovery resulted at the end of 1000 days of production supports the validity of the isothermal production path for this type of low-temperature geothermal reservoirs. The temperature change as a result of 1.097% cumulative heat recovery can easily be ignored.

Moreover, this kind of a field is not generally produced continuously for 1000 days. They are only produced during the cold winter season. The fluid recovery by recharge and heat recovery from the surrounding formations during the hot season when the field is produced at minimum level replenish the fluid and heat content of

the reservoir and thus, even a lesser amount of heat effect than calculated is expected to occur in the reservoir. This is probably the main explanation why the heat balance can be neglected.

4.5 Hypothetical Application of 2-Reservoir Tanks With Aquifer Model

Since the validity and applicability of our 2-reservoir tanks with aquifer model could not be tested for any actual field data, the applicability of the model is studied for a hypothetical field case. For this purpose, the pressure drop (Δp) data are generated for the deep and the shallow reservoirs for 10 years of production/reinjection. In constructing the production/reinjection history, the flow rate history for Balcova-Narlidere field for the period of 15.12.2002 and 15.12.2003 were taken for the first year and the same data were assumed to be valid for next 9 years. Thus, it represents the constant yearly production/reinjection case. However, a new set of model parameters were assumed for this hypothetical case. The flow rate history and the model parameters used to generate pressure drop data of the deep and the shallow reservoirs are presented in Figure 4.43 and in forward run column in Table 4.10, respectively. The pressure drop data generated by forward run are shown in Figure 4.44.

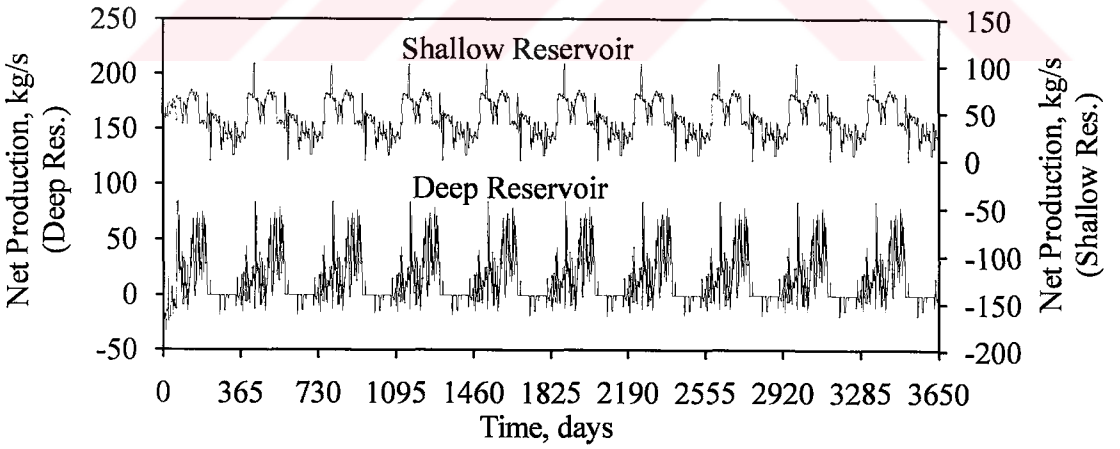

Figure 4.43 Production-reinjection history of both deep and shallow reservoirs.

Table 4.10 Model parameters of the 2-reservoir tanks with aquifer model.

Model Parameters	Forward Run (True Values)	Initial Guesses	Regression Results-I	Regression Results-II	Regression Results-III
α_{r1}, kg/bar-s	30.0	3.0	30.0 ($\pm 1.6 \times 10^{-8}$)	32.19 (± 4.91)	36.29 (± 4.85)
κ_{r1}, kg/bar	2.0×10^{7}	2.0×10^{6}	2.0×10^{7} (± 0.014)	1.74×10^{7} ($\pm 4.0 \times 10^{6}$)	1.28×10^{7} ($\pm 3.1 \times 10^{6}$)
α_{r2}, kg/bar-s	50.0	70.0	50.0 ($\pm 3.3 \times 10^{-8}$)	52.21 (± 10.10)	59.21 (± 10.20)
κ_{r2}, kg/bar	4.0×10^{7}	4.0×10^{8}	4.0×10^{7} (± 0.036)	3.23×10^{7} ($\pm 1.0 \times 10^{7}$)	2.39×10^{7} ($\pm 8.3 \times 10^{6}$)
α_{r12}, kg/bar-s	5.0	20.0	5.0 ($\pm 1.2 \times 10^{-8}$)	2.54 (± 3.60)	0.037 (± 3.42)
α_{a}, kg/bar-s	10.0	50.0	10.0 ($\pm 1.9 \times 10^{-9}$)	9.90 (± 0.62)	9.67 (± 0.57)
κ_{a}, kg/bar	2.0×10^{8}	2.0×10^{7}	2.0×10^{8} (± 0.046)	2.09×10^{8} ($\pm 1.4 \times 10^{7}$)	2.15×10^{8} ($\pm 1.3 \times 10^{7}$)
$RMS_{shallow}$, bar			2.91×10^{-9}	1.00	0.998
RMS_{deep}, bar			3.38×10^{-4}	0.99	0.988

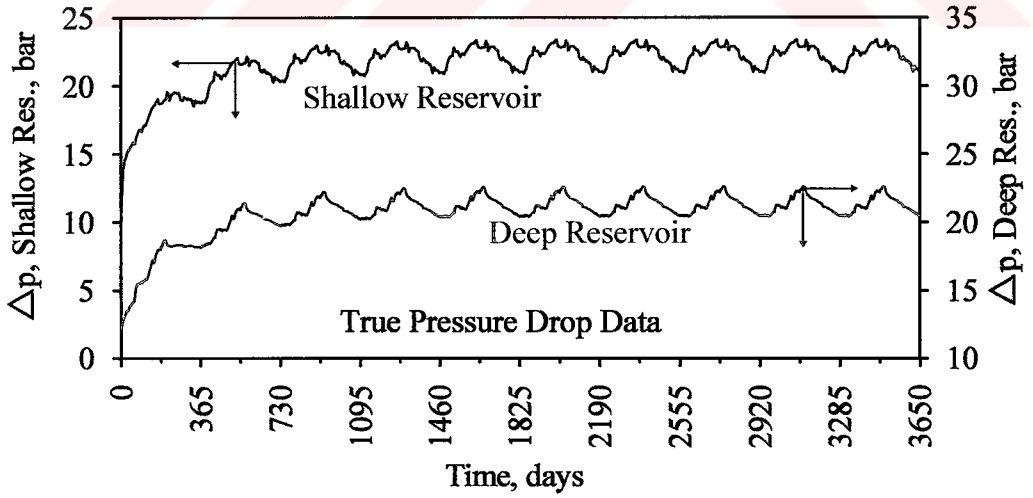

Figure 4.44 Forward run results.

As a next step, assuming that the true pressure drop data are data generated by forward run, i.e., pressure data do not contain any errors, the regression is applied (called regression-I) by the initial guesses given in Table 4.10. An excellent match

was obtained. The model parameters from regression have low confidence intervals and RMS values (the fourth column in Table 4.10). A comparison of forward run (true pressure drop data) and regression-I results is shown in Figure 4.45.

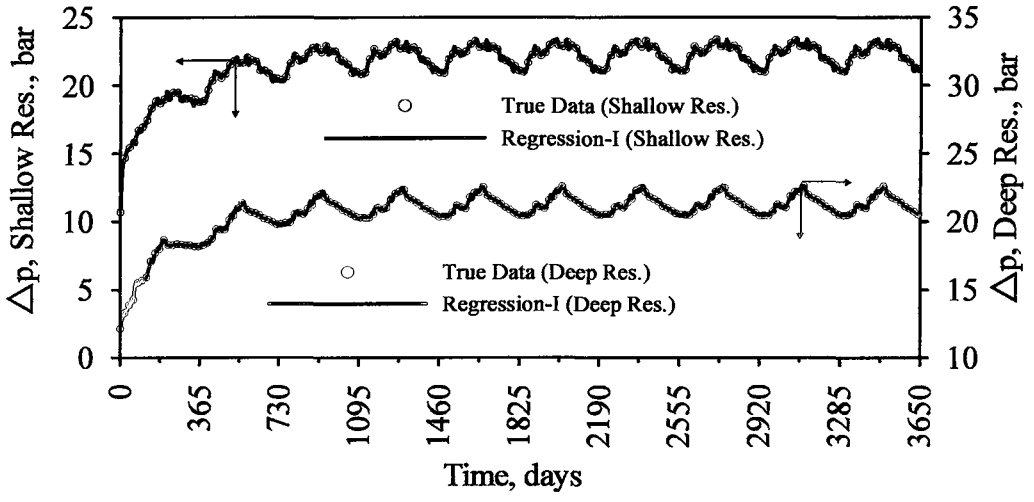

Figure 4.45 A Comparison of true pressure drop data and regression-I results.

To investigate the effects of data errors in regression, the true pressure drop data are corrupted by adding randomly normal distributed errors with mean zero and standard deviation of 1 bar. The pressure drop data with error and as well as the true pressure drop data without any error added are plotted in Figure 4.46. Then the regression (called regression-II) is performed on this pressure drop data by the same production/reinjection history used in regression-I. The regression-II results are presented in Table 4.10 and a comparison of pressure drop data with error and regression-II results are shown in Figure 4.47.

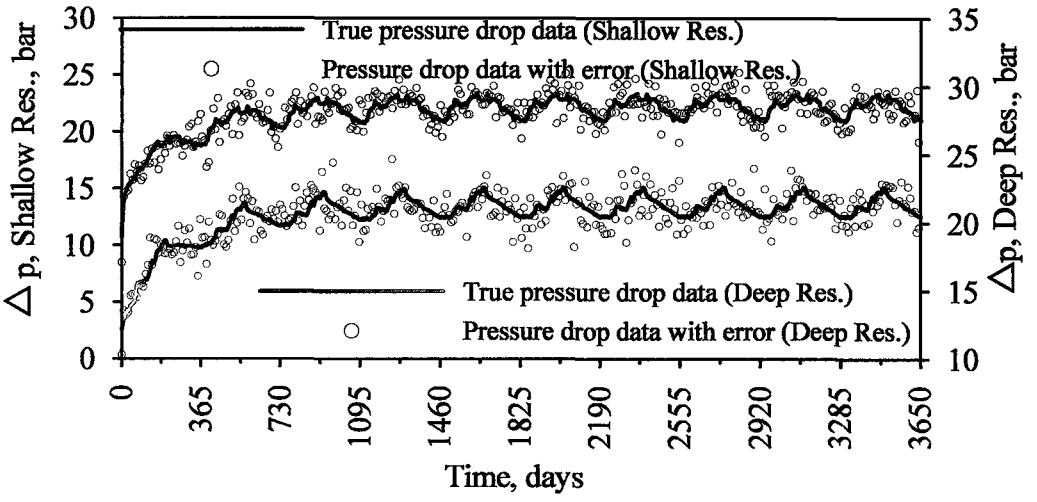

Figure 4.46 A Comparison of true pressure drop data and pressure drop data with error.

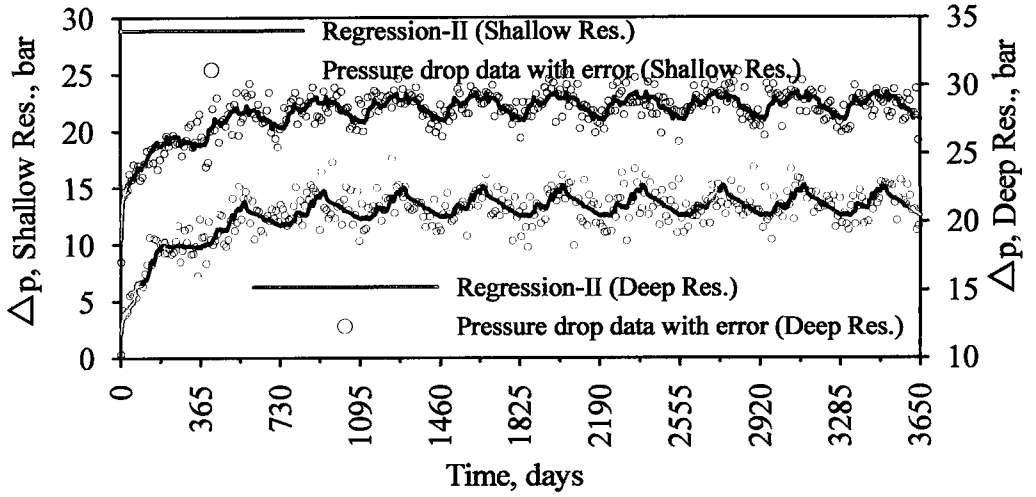

Figure 4.47 A Comparison of pressure drop data with data and regression-II results.

Finally, both true pressure drop data and true production/reinjection data are corrupted by adding randomly normal distributed errors with mean zero and standard deviation of 1 bar and 1 kg/s, respectively. Then the regression (called regression-III) is performed with these data sets. The regression-III results are presented in Table 4.10 and a comparison of pressure drop data with error and regression-III results are shown in Figure 4.48.

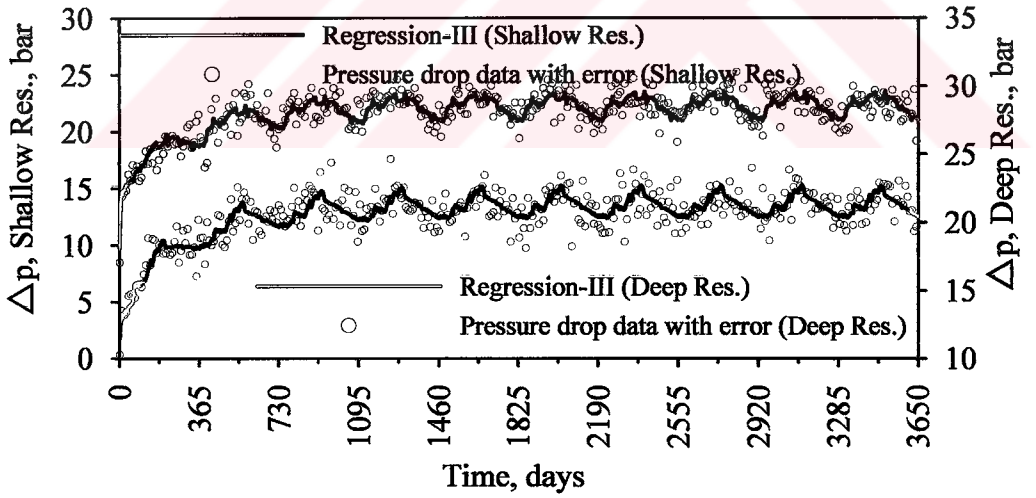

Figure 4.48 A Comparison of pressure drop data with error and regression-III results.

Results given in Table 4.10 indicate that the confidence intervals of the model parameters are higher in the case of pressure drop data including error (regression-II) as compared to the case of pressure drop data with no errors (regression-I). Similar comments are valid for regression-III case in which both the pressure drop and production/reinjection data contain errors. Although, reasonable matches are

obtained from regression-II and regression-III (Figures 4.47 and 4.48, respectively), the parameters estimated from both regressions clearly deviate from the true values.

Extremely low confidence intervals and RMS values obtained from the regression-I reflect the importance of accuracy of the field case pressure drop (or water level) data and production/reinjection history on modeling.

4.6 About Identifying The Right Model

As a next step, we investigated whether the true data obtained from the hypothetical 2-reservoir tanks with aquifer model could be matched with the other models studied in this thesis. The pressure drop data generated by forward run of 2-reservoir tanks with aquifer model (model parameters given in the first column in Table 4.11) were assumed to be the input data for regression analysis. Both shallow and deep reservoir pressure drop data were utilized in matching with 2-reservoir tanks with/without aquifer model whereas only the deep reservoir pressure drop data were assumed to represent the whole reservoir and used in matching with 1-, 2-, and 3-tank models. The production history of whole field (shallow+deep) were used for 1-, 2-, and 3-tank models. Then 1-tank, 2-tank (open/closed), 3-tank (open/closed), and 2-reservoir tanks without aquifer models were all tried separately to match the input data. Results of the model applications were evaluated and compared based on confidence intervals and RMS values obtained for each model. Except the 2-tank (closed) and 3-tank model (open/closed) models, others yielded matches with acceptable confidence intervals and RMS values. The highest RMS value was obtained for 2-tank (closed) model as shown in Table 4.11. The 3-tank (both open and closed) models yielded relatively high confidence intervals and RMS values. Hence we will not discuss them here any further. The regression results of the matches obtained with other models are given in Table 4.11 and Figure 4.49 for comparison purposes.

This part of study demonstrates one major problem in inverse modeling. No unique solution can exist if the type of model is not known as a priori. Except the 2-tank (closed) and 3-tank models, other models tried yielded almost excellent matches. For example the match with the 1-tank model is shown in Figure 4.50. The excellent match in Figure 4.50 and the results of regression in Table 4.11 indicate that the

different models may exhibit a very similar reservoir pressure response. Therefore one should be very careful in using the type of the models.

Table 4.11 Comparison of the 2-reservoir tanks with/without aquifer model and 1- and 2-tank model results.

Model Parameters	Forward Run (True Values)	2-Reservoir Tank With Aquifer	2-Reservoir Tank Without Aquifer	2-Tank Open	2-Tank Closed	1-Tank
α_{r1}, kg/bar-s	30.0	30.0 ($\pm 1.6 \times 10^{-8}$)	1.37 (± 0.082)	--	--	--
κ_{r1}, kg/bar	2.0×10^{7}	2.0×10^{7} (± 0.014)	1.59×10^{7} ($\pm 5.7 \times 10^{5}$)	--	--	--
α_{r2}, kg/bar-s	50.0	50.0 ($\pm 3.3 \times 10^{-8}$)	7.58 (± 0.109)	--	--	--
κ_{r2}, (or κ_r) kg/bar	4.0×10^{7}	4.0×10^{7} (± 0.036)	2.1×10^{8} ($\pm 1.4 \times 10^{6}$)	6.45×10^{7} ($\pm 7.8 \times 10^{6}$)	6.72×10^{8} ($\pm 1.6 \times 10^{8}$)	2.02×10^{8} ($\pm 1.6 \times 10^{6}$)
α_{r12}, kg/bar-s	5.0	5.0 ($\pm 1.2 \times 10^{-8}$)	35.91 (± 0.514)	117.27 (± 13.36)	28.87 (± 6.28)	7.51 (± 0.031)
α_a, kg/bar-s	10.0	10.0 ($\pm 1.9 \times 10^{-9}$)	--	7.86 (± 0.068)	--	--
κ_a, kg/bar	2.0×10^{8}	2.0×10^{8} (± 0.046)	--	1.53×10^{8} ($\pm 6.4 \times 10^{6}$)	2.24×10^{9} ($\pm 1.8 \times 10^{8}$)	--
$RMS_{shallow}$, bar		2.91×10^{-9}	0.048	--	--	--
RMS_{deep}, bar		3.38×10^{-4}	0.192	0.148	1.474	0.191

Additional data obtained from other sources such as geological, geophysical and hydrological studies should be coupled with the regression results for identifying the right model for the geothermal system. The additional data could be such as the reservoir area estimated from the geophysical resistivity measurements, the volumetric extent of the reservoir estimated from the wells drilled in the geothermal field, the directional movement of the recharge water obtained from the hydrological studies, the limiting boundaries of the field determined from the well tests and temperature surveys, the extension of the aquifer surrounding the reservoir determined from the basin geological analysis (see Axelsson and Dong, 1998; Olsen, 1984).

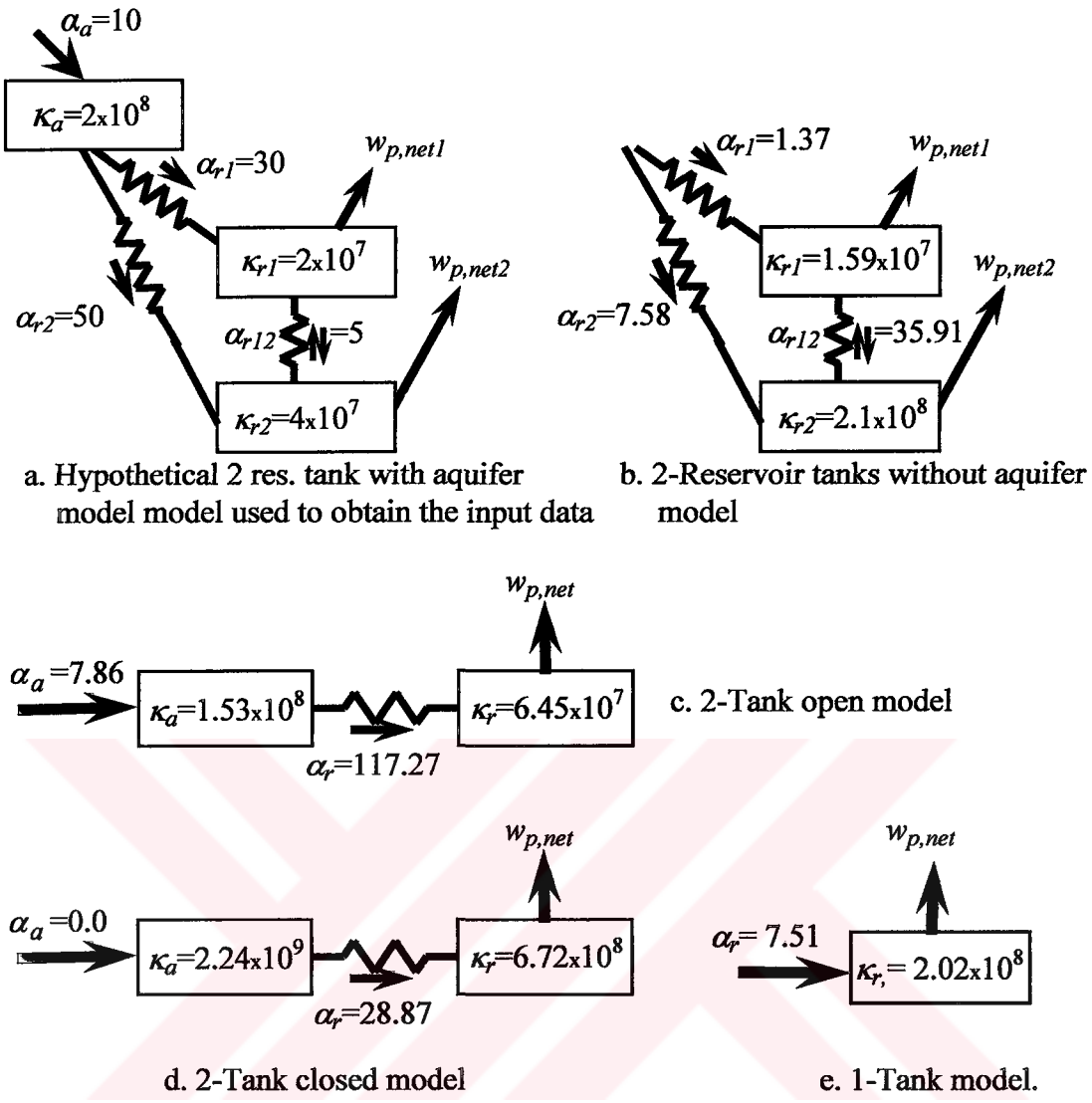

Figure 4.49 Regression results of the models.

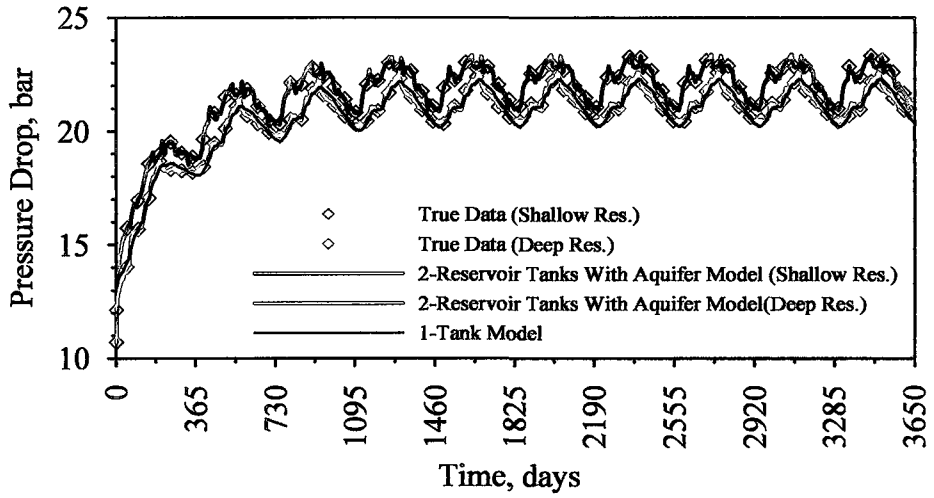

Figure 4.50 A Comparison of 2-reservoir tank with aquifer and 1-tank models.

5. CONCLUSIONS

The study covered in this dissertation has two main parts:

1) The pressure (or water level) behavior of the low-temperature geothermal systems has been investigated and analytical expressions for new lumped parameter models have been developed. In modeling, the geothermal system is considered with mainly three parts, reservoir, aquifer and recharge source.

2) The models have been used to match the measured pressure or water level response of some field cases. The measured production/reinjection and water level data of Laugarnes Field, Glerardalur Field, Svartsengi Field, and Balcova-Narlidere Field have been investigated and modeled. For history matching purposes, an optimization algorithm based on the Levenberg-Marquardt method have been utilized to minimize an objective function based on weighted least-squares for estimating relevant reservoir/aquifer parameters. 95% confidence intervals are computed to assess uncertainty in the estimated parameters and RMS values are computed to show the matching quality as quantitatively.

The following major conclusions from the study of the lumped parameter models (Chapter 3) are drawn:

- The pressure drop – time behavior of all models for constant net production rate exhibit three district regions, the early-time region, the transition region and the late-time region.

- The first region, the early-time region, reflects the pseudosteady-state behavior of the reservoir tank itself and yields a Δp versus t straight line with a slope of $w_{p,net} / \kappa_r$. In other words, the reservoir pressure declines linearly with production time as a function of net production term, $w_{p,net}$, and reservoir storage capacity, κ_r. This behavior occurs for all models.

- The last region, the late time-region, reflects the pseudosteady-state behavior of the total system (reservoir + aquifer) for the closed model whereas it exhibits the

steady-state behavior of the total system for the open model. The pseudosteady-state behavior of the closed model is characterized by a straight line on a Δp versus t plot and the slope of the straight line is a function of the aquifer and the reservoir storage capacities, κ_a, κ_r, and net production term, $w_{p,net}$. The steady-state behavior of the open model is identified when Δp reaches a constant value which is a function of the aquifer and the reservoir recharge constants, α_a, α_r, and net production term, $w_{p,net}$.

- The duration of the transition region between the early-time region and the late-time region is mainly dependent on the aquifer and the reservoir recharge constants and storage capacities, α_a, α_r, and κ_a, κ_r, respectively. Whenever $\kappa_a >> \kappa_r$ holds, the open and close models show the pseudosteady-state straight line relationship in the transition region and the duration of this relationship gets longer when κ_a is larger. In other words, before feeling the effects of the recharge source the open model exhibits the pseudosteady-state behavior similar to the closed model as long as $\kappa_a >> \kappa_r$.

Based on the field applications of the new lumped parameter models, the following conclusions summarize the second part (Chapter 4) of the study:

- The inaccuracy as well as the discontinuity of the input data such as the production/reinjection flow rates and the water level (or pressure) measurements greatly affect the confidence intervals and RMS values computed from the matching analysis of the model. In the case of short period of measured data and the large number of unknown model parameters are available, the model parameters are estimated with larger confidence intervals and the matches are obtained with higher RMS values. Therefore, continuous water level, production/reinjection data and as well as accurate measurements are definitely required to increase the reliability of the model parameters and to obtain the better matches.

- The modeling analysis on the field cases available in the literature (e.g. Axelsson's modeling study for Laugarnes and Glerardalur Fields and Olsen's study for Svartsengi Field) yields consistent results with the modeling approaches on those

field cases which shows the applicability and reliability of our models. These three field case study results support our models.

- All the modeling results discussed for the Balcova-Narlidere geothermal field are based on limited production and water level history. Therefore the results and discussions, particularly on the future predictions of the field pressure behavior, should be taken cautiously. They are believed to be qualitatively correct however might be in error quantitatively. A longer history of production/reinjection and water level data is preferred in order to reflect the long-term behavior of the geothermal system and the characteristics of the parts of the system. Application of our lumped models when more field data are available is recommended.
- One should be very careful in using the type of the models. The type of the best matching model obtained from the regression analysis should be supported and confirmed by the additional geological, geophysical and hydrological data.

REFERENCES

Alkan, H. and Satman, A., 1990. A new lumped parameter model for geothermal reservoirs in the presence of carbon dioxide, *Geothermics*, **19/5**, 469-479.

Allard, D. R. and Chen, S. M., 1988. Calculation of water influx for bottomwater drive reservoirs, *SPE Reservoir Engineering*, May, 369-379.

Axelsson, G., 1989. Simulation of pressure response data from geothermal reservoirs by lumped parameter models, *14th Workshop on Geothermal Reservoir Engineering*, Stanford University, Palo Alto, California, 257-263.

Axelsson, G. and Dong, Z., 1998. The Tanggu geothermal reservoir (Tianjin, China), *Geothermics*, **27/3**, 271-294.

Axelsson, G. and Gunnlaugsson, E., 2000. Long-term monitoring of high-and low-enthalpy fields under exploitation, International Geothermal Association, WGC2000 Short Courses, Kokonoe, Kyushu District, Japan, 28-30 May.

Bard, Y., 1974. *Nonlinear Parameter Estimation*, Academic Press, San Diego.

Bodvarsson, G. S., Benson, S. M. and Witherspoon, P. A., 1982. Theory of the development of geothermal systems charged by vertical faults, *Journal of Geophysical Research*, November, **87/B11**, 9317-9328.

Bodvarsson, G. S., Pruess, K. and Lippmann, M. J., 1986. Modeling of geothermal systems, *Journal of Petroleum Technology*, September, 1007-1021.

Brigham, W. E., 1998. Water influx and its effect on oil recovery: Part1. Aquifer flow, *Technical Report,* **SUPRI TR 103**, Stanford University, Palo Alto, California, December.

Brigham, W.E. and Ramey, H.J.Jr., 1981. Material and energy balance in geothermal reservoirs, *Reservoir Engineering Assessment of Geothermal Systems*, Ramey, H.J.Jr. (editor), Petroleum Engineering Department, Stanford University, Palo Alto, California.

Bullivant, D. P., O'Sullivan, M. J. and Zyvolosk, G. A., 1991. Enhancements of the MULKOM geothermal simulator, *13th New Zealand Geothermal Workshop*, Auckland, New Zealand, 175-182.

Carvalho, R. et al., 1996. Simple procedures for imposing constraints for nonlinear least squares optimization, *SPE Journal*, December, 395-402.

Castanier, L.M., Sanyal, S.K. and Brigham, W.E., 1980. A practical analytical model for geothermal reservoir simulation, *50th Annual California Regional Meeting of SPE*, Los Angeles, California, April 9-11, SPE 8887.

Castanier, L.M. and Brigham, W.E., 1983. Use of lumped parameter modeling for geothermal engineering, *SPE California Regional Meeting*, Ventura, California, March 23-25, SPE 11730.

Chatas, A. T. and Malekfam, H., 1970. The estimation of aquifer properties from reservoir performance in water-drive fields, *SPE 2970,* (Unsolicited Paper).

Craft, B.C. and Hawkins, M., 1959. *Applied Petroleum Reservoir Engineering*, Prentice-Hall, Inc., Englewood Cliffs, New Jersey.

Dogru, A.H., Dixon, T.N., and Edgar, T.F., 1977. Confidence limits on the parameters and predictions of slightly compressible, single phase reservoirs, *SPEJ*, February, 42-56.

Gill, P.E., Murray, W., Wright, M.H., 1993. *Practical Optimization*, Academic Press, Inc., San Diego, CA ,305.

Goyal, K. P. and Kassoy, D. R., 1981. A plausible two-dimensional vertical model of the East Mesa geothermal field, California, *Journal of Geophysical Research*, November, **86/B11**, 10719-10733.

Grant, A.M., Donaldson, I.G., Bixley, P.F., 1982. *Geothermal Reservoir Engineering*, pp. 55-57, Academic Press., Inc., New York.

Gudmundsson, J.S. and Olsen, G., 1987. Water-influx modeling of the Svartsengi geothermal field, Iceland, *SPE Reservoir Engineering*, February, 77-84.

Edwardson, M.J., Parkison, H.R., Williams, C.D. and Matthews, C.S., 1962. Calculation of formation temperature disturbances caused by mud circulation, *Journal of Petroleum Technology*, April, 416-426.

Erdélyi, A., 1954. *Tables of Integral Transforms*, McGraw-Hill Book Company, Inc., USA.

Fanchi, J. R., 1985. Analytical representation of the van Everdingen-Hurst aquifer influence functions for reservoir simulation, *Journal of Petroleum Technology*, June, 405-406.

Fetkovich, M. J., 1971. A simplified approach to water influx calculations-finite aquifer systems, *Journal of Petroleum Technology*, July, 814-828.

Fletcher, R., 1987. *Practical Methods of Optimization*, John Wiley & Sons, New York City 101.

Horne, R. N. and O'Sullivan, M. J., 1977. Numerical modeling of the Wairakei geothermal reservoir, *47th Annual California Regional Meeting of the SPE*, Bakersfield, California, April 13-15, SPE 6536.

Klins, M. A., Bouchard, A. J. and Cable, C. L., 1988. A polynomial approach to the van Everdingen-Hurst dimensionless variables for water encroachment, *SPE Reservoir Engineering*, February, 320-326.

Kohl, T. and Hopkirk, R. J., 1995. FRACTure – A simulation code for forced fluid flow and transport in fractured, porous rock, *Geothermics*, **24/3**, 333-343.

Kreyszig, E., 1999. *Advanced Engineering Mathematics*, John Wiley & Sons, Inc., Singapore.

Kuchuk, F.J., Ayestaran, L., 1985. Analysis of simultaneously measured pressure and sandface flow rate in transient testing, *Journal of Petroleum Technology*, February, 323-334.

Marcou, J. A. and Gudmundsson, J. S., 1986. Development model for geothermal reservoirs, *56th California Regional Meeting of SPE*, Oakland, California, April 2-4, SPE 15119.

Nishikiori, N. and Hayashida, Y., 1999. Investigation and modeling of complex water influx into the sandstone reservoir, Khafji oil field, Arabian Gulf, *SPE Annual Technical Conference and Exhibition*, Houston, Texas, October 3-6, SPE 56428.

Olsen, G., 1984. Depletion modeling of liquid dominated geothermal reservoirs, *Technical Report,* **SGP-TR-80**, Stanford Geothermal Program, Stanford University, Palo Alto, California.

Onur, M., 2001. A note on material balance with recharge, Petroleum and Natural Gas Engineering Department, Istanbul Technical University, (Unpublished Study).

Onur, M., Kuchuk, F.J., 2000. Nonlinear regression analysis of well-test pressure data with uncertain variance, *SPE Annual Technical Conference and Exhibition*, Dallas, October 1-4, SPE 62918.

Permadi, A. K., Mamora, D. D. and Lee, W. J., 1998. Modeling simultaneous oil and water flow in reservoirs with water influx or water injection using single-phase semi-analytical solutions, *SPE Asia Pacific Conference*, Kuala Lumpur, Malaysia, March 23-24, SPE 39755.

Pruess, K., 1990. Modeling of geothermal reservoirs: Fundamental processes, computer simulation and field applications, *Geothermics*, **19/1**, 3-15.

Richards, J. W. and Wallroth, T., 1995. Approaches to the modeling of HDR reservoirs: A review, *Geothermics*, **24/3**, 307-332.

Sanyal, S. K., Butler, S. J., Swenson, D. and Hardeman, B., 2000. Review of the state-of-the-art of numerical simulation of enhanced geothermal systems, *Geothermal Resources Council Transactions*, September 24-27, **24**, 181-186.

Sanyal, S. K., Sengul, M. and Mediav, H. T., 1976. A semi-analytical approach to geothermal reservoir performance prediction, *2nd Workshop on Geothermal Reservoir Engineering*, Stanford University, Palo Alto, California, December, 1-3.

Sarak, H., Onur, M., Satman, A., 2003. New lumped parameter models for simulation of low-temperature geothermal reservoirs, *28th Workshop on Geothermal Reservoir Engineering*, Stanford University, Stanford, CA.

Sarak, H., Onur, M., Satman, A., 2003. Applications of lumped parameter models for simulation of low-temperature geothermal reservoirs, *28th Workshop on Geothermal Reservoir Engineering*, Stanford University, Stanford, CA.

Satman, A., 2003. Jeotermal enerjinin doğası, *Jeotermal Enerji Doğrudan Isıtma Sistemleri; Temelleri ve Tasarımı Seminer Kitabı*, 3-17, **MMO/2001/270**, İzmir.

Satman, A., Serpen, U., Onur, M., 2002. Reservoir and production performance project for Izmir Balcova-Narlidere geothermal field, project report, Istanbul Technical University, Petroleum and Natural Gas Engineering Department.

Schilthuis, R. J., 1936. Active oil and reservoir energy, *Trans. AIME*, **118**, 33-52.

Slider, H.C., 1983. *Worldwide Practical Petroleum Reservoir Engineering Methods*, PeenWell Books, Tulsa.

Thompson, L.G., Reynolds, A.C., 1986. Analysis of variable rate well-test pressure data using Duhamel's principle, *SPE Formation Evaluation*, October, 453-469.

van Everdingen, A. F. and Hurst, W., 1949. The application of the laplace transformation to flow problems in reservoirs, *Trans. AIME*, **186**, 305-324.

Whiting, R.L. and Ramey, H.J.Jr., 1969. Application of material and energy balances to geothermal steam production, *Journal of Petroleum Technology*, July, 893-900.

Zyvoloski, G. A. and O'Sullivan, M. J., 1980. Simulation of a gas-dominated, two-phase geothermal reservoir, *Journal of Petroleum Technology*, February, 52-57.

APPENDIX-A

1 RESERVOIR WITH RECHARGE SOURCE (1-TANK MODEL)

The mass balance on the reservoir tank becomes,

$$W_c = W_i - W_p + W_a + W_{inj} \tag{A-1}$$

where the current mass, W_c, equals that initially in the reservoir, W_i, minus what has been produced, W_p, plus any water influx, W_a, and plus reinjected mass, W_{inj}.

For a reservoir of volume V_r, the liquid mass in place is given by

$$W_c = V_r \phi_r \rho_w \tag{A-2}$$

where ϕ_r is reservoir porosity, and ρ_w liquid density. Substituting Equation A-2 into A-1 gives

$$V_r \phi_r \rho_w = W_i - W_p + W_a + W_{inj} \tag{A-3}$$

Differentiating Equation A-3 with respect to time gives the following equation in terms of mass flow rates, w,

$$w_a - w_p + w_{inj} = V_r \frac{d(\phi_r \rho_w)}{dt} \tag{A-4}$$

The last term of Equation A-4 can be differentiated by using chain rule as follows:

$$\frac{d(\phi_r \rho_w)}{dt} = \phi_r \frac{d\rho_w}{dt} + \rho_w \frac{d\phi_r}{dt} \tag{A-5}$$

Dividing by $(\phi_r \rho_w)$ gives

$$\frac{1}{\phi_r \rho_w} \frac{d(\phi_r \rho_w)}{dt} = \frac{1}{\rho_w} \frac{d\rho_w}{dt} + \frac{1}{\phi_r} \frac{d\phi_r}{dt} \tag{A-6}$$

Applying chain rule and rewriting Equation (A-6) gives

$$\frac{1}{\phi_r \rho_w}\frac{d(\phi_r \rho_w)}{dt} = \frac{1}{\rho_w}\frac{d\rho_w}{dp_r}\frac{dp_r}{dt} + \frac{1}{\phi_r}\frac{d\phi_r}{dp_r}\frac{dp_r}{dt} \tag{A-7}$$

Here $\frac{1}{\rho_w}\frac{d\rho_w}{dp_r}$ is known as fluid compressibility, c_f, and $\frac{1}{\phi_r}\frac{d\phi_r}{dp_r}$ as formation compressibility, c_r. Using the definition of fluid and formation compressibilities, Equation A-7 reduces to

$$\frac{1}{\phi_r \rho_w}\frac{d(\phi_r \rho_w)}{dt} = (c_f + c_r)\frac{dp_r}{dt} \tag{A-8}$$

Applying the definition of total compressibility, $c_t = c_f + c_r$ in Equation A-8 gives

$$\frac{1}{\phi_r \rho_w}\frac{d(\phi_r \rho_w)}{dt} = c_t \frac{dp_r}{dt} \quad \text{or} \quad \frac{d(\phi_r \rho_w)}{dt} = \phi_r \rho_w c_t \frac{dp_r}{dt} \tag{A-9}$$

Substituting Equation A-9 into Equation A-4

$$w_a - w_p + w_{inj} = V_r \phi_r \rho_w c_t \frac{dp_r}{dt} \tag{A-10}$$

The production and injection terms could be defined as "*Net Production Term*" as given in Equation A-10.

$$w_{p,net} = w_p - w_{inj} \tag{A-11}$$

Therefore Equation A-10 becomes as follows.

$$w_a - w_{p,net} = V_r\, \phi_r\, \rho_w\, c_t \frac{dp_r}{dt} = \kappa_r \frac{dp_r}{dt} \tag{A-12}$$

where κ_r is the reservoir storage capacity and it can be defined as,

$$\kappa_r = V_r \phi_r \rho_w c_t \tag{A-13}$$

Water influx (or recharge) rate, w_a, in Equation A-12 can be expressed by Schilthuis steady-state model as follows;

$$w_a = \alpha_r [p_i - p_r(t)] \tag{A-14}$$

Here, α_r is the reservoir recharge constant and coressponds to α in Equation 2.7. Using Equation A-14 in Equation A-12 and rearranging the resulting equation gives,

$$w_{p,net} = \alpha_r [p_i - p_r(t)] - \kappa_r \frac{dp}{dt} \tag{A-15}$$

Because of the assumption of constant recharge pressure, Equation A-15 can be recast in terms of $\Delta p_r(t) = p_i - p_r(t)$ as;

$$\frac{d\Delta p_r}{dt} + \frac{\alpha_r}{\kappa_r} \Delta p_r = \frac{w_{p,net}}{\kappa_r} \tag{A-16}$$

Note that Equation A-16 is a first order ordinary differantial equation, and its solution is given by (assuming κ_r, α_r, and $w_{p,net}$ are constant)

$$\Delta p_r(t) = c\ exp(-\alpha_r t / \kappa_r) + \frac{w_{p,net}}{\alpha_r} \tag{A-17}$$

where c is an arbitrary constant. To determine c, an initial conditon on Δp is needed. Because at t=0, the system shown in Figure 3.1 is in hydraulic equilibrium, then initial condition can be written as,

$$p_r(t=0) = p_i \quad \text{or} \quad \Delta p_r(t=0) = 0 \tag{A-18}$$

Using Equation A-18 in Equation A-17, c is

$$c = -\frac{w_{p,net}}{\alpha_r} \tag{A-19}$$

Subsitituting Equation A-19 into Equation A-17 gives,

$$\Delta p_r(t) = \frac{w_{p,net}}{\alpha_r} [1 - exp(-\alpha_r t / \kappa_r)] \tag{A-20}$$

or

$$p_r(t) = p_i - \frac{w_{p,net}}{\alpha_r} [1 - exp(-\alpha_r t / \kappa_r)] \tag{A-21}$$

APPENDIX-B

1 RESERVOIR – 1 AQUIFER WITH RECHARGE SOURCE (2-TANK OPEN SYSTEM)

Mass balances on the reservoir and the aquifer, recharge of the reservoir and the aquifer, initial conditions are expressed as;

Mass Balance on the Aquifer :

$$w_a - w_r = \kappa_a \frac{dp_a}{dt} \tag{B-1}$$

Mass Balance on the Reservoir :

$$w_r - w_{p,net} = \kappa_r \frac{dp_r}{dt} \tag{B-2}$$

Recharge of the Aquifer : $w_a = \alpha_a (p_i - p_a)$ (B-3)

Recharge of the Reservoir : $w_r = \alpha_r (p_a - p_r)$ (B-4)

Initial Conditions : $p_a = p_r = p_i \ @ \ t = 0$ (B-5)

Substituting Equations B-3 and B-4 into Equations B-1 and B-2 gives

$$\alpha_a (p_i - p_a) - \alpha_r (p_a - p_r) = \kappa_a \frac{dp_a}{dt} \tag{B-6}$$

$$\alpha_r (p_a - p_r) - w_{p,net} = \kappa_r \frac{dp_r}{dt} \tag{B-7}$$

It is convenient to write Equations B-6 and B-7 in terms of the pressure changes. The relevant pressure changes and their derivatives with respect to time are given by

$$\left.\begin{aligned} \Delta p_a = p_i - p_a \;\Rightarrow\; p_a = p_i - \Delta p_a \;\Rightarrow\; \frac{d\,\Delta p_a}{dt} = -\frac{dp_a}{dt} \\ \Delta p_r = p_i - p_r \;\Rightarrow\; p_r = p_i - \Delta p_r \;\Rightarrow\; \frac{d\,\Delta p_r}{dt} = -\frac{dp_r}{dt} \end{aligned}\right\} \tag{B-8}$$

and initial conditions become

$$\left.\begin{aligned} \Delta p_a(t=0) = p_i - p_a(t=0) = p_i - p_i = 0 \\ \Delta p_r(t=0) = p_i - p_r(t=0) = p_i - p_i = 0 \end{aligned}\right\} \tag{B-9}$$

Using Equation B-8 in Equations B-6 and B-7 gives

$$\alpha_a\,\Delta p_a - \alpha_r\left(p_i - \Delta p_a - p_i + \Delta p_r\right) = -\kappa_a \frac{d\,\Delta p_a}{dt} \tag{B-10}$$

$$\alpha_r\left(p_i - \Delta p_a - p_i + \Delta p_r\right) - w_{p,net} = -\kappa_r \frac{d\,\Delta p_r}{dt} \tag{B-11}$$

Equations B-10 and B-11 can be simplified and rearranged as follows:

$$\alpha_a\,\Delta p_a - \alpha_r\left(\Delta p_r - \Delta p_a\right) = -\kappa_a \frac{d\,\Delta p_a}{dt} \tag{B-12}$$

$$\alpha_r\left(\Delta p_r - \Delta p_a\right) - w_{p,net} = -\kappa_r \frac{d\,\Delta p_r}{dt} \tag{B-13}$$

or

$$\kappa_a \frac{d\,\Delta p_a}{dt} + \left(\alpha_a + \alpha_r\right)\Delta p_a - \alpha_r\,\Delta p_r = 0 \tag{B-14}$$

$$\kappa_r \frac{d\,\Delta p_r}{dt} - \alpha_r\,\Delta p_a + \alpha_r\,\Delta p_r = w_{p,net} \tag{B-15}$$

Applying Laplace transformation (Erdélyi, 1954) to Equations B-14 and B-15 and using initial conditions (Equation B-9) gives

$$\kappa_a\, s\,\overline{\Delta p_a} + \left(\alpha_a + \alpha_r\right)\overline{\Delta p_a} - \alpha_r\,\overline{\Delta p_r} = 0 \tag{B-16}$$

$$\kappa_r\, s\, \overline{\Delta p_r} - \alpha_r\, \overline{\Delta p_a} + \alpha_r\, \overline{\Delta p_r} = \frac{w_{p,net}}{s} \tag{B-17}$$

where

$$\overline{\Delta p_a} = \int_0^\infty e^{-st} \Delta p_a\, d\tau \quad , \quad \overline{\Delta p_r} = \int_0^\infty e^{-st} \Delta p_r\, d\tau \tag{B-18}$$

Note that $\overline{\Delta p_a}$ and $\overline{\Delta p_r}$ are Δp_a and Δp_r in Laplace space, and s is the Laplace parameter. Rearranging Equations B-16 and B-17 gives

$$\left(\kappa_a\, s + \alpha_a + \alpha_r\right) \overline{\Delta p_a} - \alpha_r\, \overline{\Delta p_r} = 0 \tag{B-19}$$

$$-\alpha_r\, \overline{\Delta p_a} + \left(\kappa_r\, s + \alpha_r\right) \overline{\Delta p_r} = \frac{w_{p,net}}{s} \tag{B-20}$$

or

$$\left[s + \frac{\left(\alpha_a + \alpha_r\right)}{\kappa_a}\right] \overline{\Delta p_a} - \frac{\alpha_r}{\kappa_a}\, \overline{\Delta p_r} = 0 \tag{B-21}$$

$$-\frac{\alpha_r}{\kappa_r}\, \overline{\Delta p_a} + \left[s + \frac{\alpha_r}{\kappa_r}\right] \overline{\Delta p_r} = \frac{w_{p,net}}{\kappa_r\, s} \tag{B-22}$$

The solutions to two equations (Equations B-21 and B-22) with two unknowns ($\overline{\Delta p_a}, \overline{\Delta p_r}$) can be found by using Cramer's rule (Kreyszig, 1999) as below:

$$\overline{\Delta p_a} = \frac{D_a}{D} \; , \; \overline{\Delta p_r} = \frac{D_r}{D} \tag{B-23}$$

$$D_a = \begin{vmatrix} 0 & -\dfrac{\alpha_r}{\kappa_a} \\ \dfrac{w_{p,net}}{\kappa_r\, s} & s + \dfrac{\alpha_r}{\kappa_r} \end{vmatrix} = \frac{\alpha_r}{\kappa_a \kappa_r} \frac{w_{p,net}}{s} \tag{B-24}$$

$$D_r = \begin{vmatrix} s + \dfrac{(\alpha_a + \alpha_r)}{\kappa_a} & 0 \\ -\dfrac{\alpha_r}{\kappa_r} & \dfrac{w_{p,net}}{\kappa_r s} \end{vmatrix} = \frac{w_{p,net}}{\kappa_r s}\left[s + \frac{(\alpha_a + \alpha_r)}{\kappa_a} \right] \tag{B-25}$$

$$D = \begin{vmatrix} s + \dfrac{(\alpha_a + \alpha_r)}{\kappa_a} & -\dfrac{\alpha_r}{\kappa_a} \\ -\dfrac{\alpha_r}{\kappa_r} & s + \dfrac{\alpha_r}{\kappa_r} \end{vmatrix} = \left[s + \frac{(\alpha_a + \alpha_r)}{\kappa_a} \right]\left(s + \frac{\alpha_r}{\kappa_r} \right) - \frac{\alpha_r^2}{\kappa_a \kappa_r} \tag{B-26}$$

$$\overline{\Delta p_a} = \frac{D_a}{D} = \frac{\alpha_r}{\kappa_a \kappa_r} \frac{w_{p,net}}{s} \frac{1}{\left\{ \left[s + \dfrac{(\alpha_a + \alpha_r)}{\kappa_a} \right]\left(s + \dfrac{\alpha_r}{\kappa_r} \right) - \dfrac{\alpha_r^2}{\kappa_a \kappa_r} \right\}} \tag{B-27}$$

$$\overline{\Delta p_r} = \frac{D_r}{D} = \frac{w_{p,net}}{\kappa_r s} \frac{\left[s + \dfrac{(\alpha_a + \alpha_r)}{\kappa_a} \right]}{\left\{ \left[s + \dfrac{(\alpha_a + \alpha_r)}{\kappa_a} \right]\left(s + \dfrac{\alpha_r}{\kappa_r} \right) - \dfrac{\alpha_r^2}{\kappa_a \kappa_r} \right\}} \tag{B-28}$$

Rearranging the denominator in Equations B-27 and B-28 gives

$$\left\{ \left[s + \frac{(\alpha_a + \alpha_r)}{\kappa_a} \right]\left(s + \frac{\alpha_r}{\kappa_r} \right) - \frac{\alpha_r^2}{\kappa_a \kappa_r} \right\} = s^2 + \left[\frac{\alpha_a + \alpha_r}{\kappa_a} + \frac{\alpha_r}{\kappa_r} \right] s + \frac{\alpha_a \alpha_r}{\kappa_a \kappa_r} \tag{B-29}$$

and the roots of Equation B-29 (μ_1, μ_2) are found as follows;

$$\left.\begin{aligned} \mu_1 &= \frac{\left[\dfrac{(\alpha_a + \alpha_r)}{\kappa_a} + \dfrac{\alpha_r}{\kappa_r} \right] + \sqrt{\left[\dfrac{(\alpha_a + \alpha_r)}{\kappa_a} + \dfrac{\alpha_r}{\kappa_r} \right]^2 - 4\dfrac{\alpha_a \alpha_r}{\kappa_a \kappa_r}}}{2} \\ \mu_2 &= \frac{\left[\dfrac{(\alpha_a + \alpha_r)}{\kappa_a} + \dfrac{\alpha_r}{\kappa_r} \right] - \sqrt{\left[\dfrac{(\alpha_a + \alpha_r)}{\kappa_a} + \dfrac{\alpha_r}{\kappa_r} \right]^2 - 4\dfrac{\alpha_a \alpha_r}{\kappa_a \kappa_r}}}{2} \end{aligned}\right\} \tag{B-30}$$

and Equation B-29 can be written as

$$s^2 + \left[\frac{\alpha_a + \alpha_r}{\kappa_a} + \frac{\alpha_r}{\kappa_r}\right]s + \frac{\alpha_a \alpha_r}{\kappa_a \kappa_r} = (s+\mu_1)(s+\mu_2) \tag{B-31}$$

Using Equation B-31 in Equations B-27 and B-28, and rearranging give

$$\overline{\Delta p_a} = \frac{\alpha_r}{\kappa_a \kappa_r} w_{p,net} \frac{1}{(s+0)(s+\mu_1)(s+\mu_2)} \tag{B-32}$$

$$\overline{\Delta p_r} = \frac{w_{p,net}}{\kappa_r} \frac{(s+d)}{(s+0)(s+\mu_1)(s+\mu_2)} \quad \text{and} \quad d = \frac{(\alpha_a + \alpha_r)}{\kappa_a} \tag{B-33}$$

In order to find the values of $\overline{\Delta p_a}$ and $\overline{\Delta p_r}$ in real space, inverse Laplace transforms of Equations B-32 and B-33 are obtained as follows:

$$\Delta p_a(t) = L^{-1}\left\{\overline{\Delta p_a}\right\} = \frac{\alpha_r}{\kappa_a \kappa_r} w_{p,net} L^{-1}\left\{\frac{1}{(s+0)(s+\mu_1)(s+\mu_2)}\right\} \tag{B-34}$$

$$\Delta p_r(t) = L^{-1}\left\{\overline{\Delta p_r}\right\} = \frac{w_{p,net}}{\kappa_r} L^{-1}\left\{\frac{(s+d)}{(s+0)(s+\mu_1)(s+\mu_2)}\right\} \tag{B-35}$$

Inverse Laplace transforms of the terms of $\frac{1}{(s+0)(s+\mu_1)(s+\mu_2)}$ and $\frac{(s+d)}{(s+0)(s+\mu_1)(s+\mu_2)}$ in Equations B-34 and B-35 are obtained by using the formula (Equation B-36) given below (Erdélyi, 1954):

$$\begin{aligned} L^{-1}\left\{\frac{\lambda^2 s + \mu s + \nu}{(s+\alpha)(s+\beta)(s+\gamma)}\right\} &= \frac{\lambda\alpha^2 + \mu\alpha + \nu}{(\alpha-\beta)(\alpha-\gamma)} exp(-\alpha t) \\ &+ \frac{\lambda\beta^2 - \mu\beta + \nu}{(\beta-\alpha)(\beta-\gamma)} exp(-\beta t) \\ &+ \frac{\lambda\gamma^2 - \mu\gamma + \nu}{(\gamma-\alpha)(\gamma-\beta)} exp(-\gamma t) \end{aligned} \tag{B-36}$$

Applying Equation B-36 in Equation B-34 gives

$$\lambda = 0 \;,\; \mu = 0 \;,\; \nu = 1$$
$$\alpha = 0 \;,\; \beta = \mu_1 \;,\; \gamma = \mu_2 \tag{B-37}$$

and

$$L^{-1}\left\{\frac{1}{(s+0)(s+\mu_1)(s+\mu_2)}\right\} = \frac{1}{\mu_1\mu_2} + \frac{1}{\mu_1(\mu_1-\mu_2)}exp(-\mu_1 t) + \frac{1}{\mu_2(\mu_2-\mu_1)}exp(-\mu_2 t) \tag{B-38}$$

is obtained. Similarly, applying Equation B-36 in Equation B-35 gives

$$\lambda = 0 \;,\; \mu = 1 \;,\; \nu = d$$
$$\alpha = 0 \;,\; \beta = \mu_1 \;,\; \gamma = \mu_2 \tag{B-39}$$

and

$$L^{-1}\left\{\frac{(s+d)}{(s+0)(s+\mu_1)(s+\mu_2)}\right\} = \frac{d}{\mu_1\mu_2} + \frac{(\mu_1-d)}{\mu_1(\mu_2-\mu_1)}exp(-\mu_1 t) + \frac{(\mu_2-d)}{\mu_2(\mu_1-\mu_2)}exp(-\mu_2 t) \tag{B-40}$$

is obtained. By substituting Equation B-38 into Equation B-34, pressure changes in the aquifer tank as a function of time is obtained as follows:

$$\Delta p_a(t) = \frac{\alpha_r}{\kappa_a\kappa_r} w_{p,net}\left\{\frac{1}{\mu_1\mu_2} + \frac{1}{\mu_1(\mu_1-\mu_2)}exp(-\mu_1 t) + \frac{1}{\mu_2(\mu_2-\mu_1)}exp(-\mu_2 t)\right\}$$

or

$$\Delta p_a(t) = \frac{\alpha_r}{\kappa_a\kappa_r} w_{p,net}\left[\frac{(\mu_1-\mu_2)+\mu_2\, exp(-\mu_1 t)-\mu_1\, exp(-\mu_2 t)}{\mu_1\mu_2(\mu_1-\mu_2)}\right] \tag{B-41}$$

Similarly, by using Equation B-40 in Equation B-35, pressure changes in the reservoir tank as a function of time is obtained as follows:

$$\Delta p_r(t) = \frac{w_{p,net}}{\kappa_r}\left[\frac{d}{\mu_1\mu_2} + \frac{(\mu_1-d)}{\mu_1(\mu_2-\mu_1)}exp(-\mu_1 t) + \frac{(\mu_2-d)}{\mu_2(\mu_1-\mu_2)}exp(-\mu_2 t)\right] \tag{B-42}$$

The pressures of the reservoir and the aquifer tanks as a function of time are obtained by using Equations B-41 and B-42 as below.

$$p_a(t) = p_i - \frac{\alpha_r}{\kappa_a \kappa_r} w_{p,net} \left[\frac{(\mu_1 - \mu_2) + \mu_2 \, exp(-\mu_1 t) - \mu_1 \, exp(-\mu_2 t)}{\mu_1 \mu_2 (\mu_1 - \mu_2)} \right] \tag{B-43}$$

$$p_r(t) = p_i - \frac{w_{p,net}}{\kappa_r} \left[\frac{d}{\mu_1 \mu_2} + \frac{(\mu_1 - d)}{\mu_1 (\mu_2 - \mu_1)} exp(-\mu_1 t) + \frac{(\mu_2 - d)}{\mu_2 (\mu_1 - \mu_2)} exp(-\mu_2 t) \right] \tag{B-44}$$

APPENDIX-C

1 RESERVOIR – 1 AQUIFER WITHOUT RECHARGE SOURCE (2-TANK CLOSED SYSTEM)

Mass balances on the reservoir and the aquifer, recharge of the reservoir, initial conditions are expressed as;

Mass Balance on the Aquifer :

$$-w_r = \kappa_a \frac{dp_a}{dt} \tag{C-1}$$

Mass Balance on the Reservoir :

$$w_r - w_{p,net} = \kappa_r \frac{dp_r}{dt} \tag{C-2}$$

Recharge of the Reservoir : $w_r = \alpha_r (p_a - p_r)$ (C-3)

Initial Conditions : $p_a = p_r = p_i \ @ \ t = 0$ (C-4)

Substituting Equation C-3 into Equations C-1 and C-2 gives

$$-\alpha_r (p_a - p_r) = \kappa_a \frac{dp_a}{dt} \tag{C-5}$$

$$\alpha_r (p_a - p_r) - w_{p,net} = \kappa_r \frac{dp_r}{dt} \tag{C-6}$$

Equations C-5 and C-6 can be expressed in terms of pressure changes. The pressure changes and their derivatives with respect to time are given by

$$\left.\begin{aligned} \Delta p_a = p_i - p_a \;\Rightarrow\; p_a = p_i - \Delta p_a \;\Rightarrow\; \frac{d\,\Delta p_a}{dt} = -\frac{dp_a}{dt} \\ \Delta p_r = p_i - p_r \;\Rightarrow\; p_r = p_i - \Delta p_r \;\Rightarrow\; \frac{d\,\Delta p_r}{dt} = -\frac{dp_r}{dt} \end{aligned}\right\} \quad \text{(C-7)}$$

and initial conditons in terms of pressure changes are written as below:

$$\left.\begin{aligned} \Delta p_a(t=0) = p_i - p_a(t=0) = p_i - p_i = 0 \\ \Delta p_r(t=0) = p_i - p_r(t=0) = p_i - p_i = 0 \end{aligned}\right\} \quad \text{(C-8)}$$

Substituting Equation C-7 into Equations C-5 and C-6 gives

$$-\alpha_r(p_i - \Delta p_a - p_i + \Delta p_r) = -\kappa_a \frac{d\,\Delta p_a}{dt} \quad \text{(C-9)}$$

$$\alpha_r(p_i - \Delta p_a - p_i + \Delta p_r) - w_{p,net} = -\kappa_r \frac{d\,\Delta p_r}{dt} \quad \text{(C-10)}$$

Equations C-9 and C-10 can be simplified and rearranged as follows:

$$-\alpha_r(\Delta p_r - \Delta p_a) = -\kappa_a \frac{d\,\Delta p_a}{dt} \quad \text{(C-11)}$$

$$\alpha_r(\Delta p_r - \Delta p_a) - w_{p,net} = -\kappa_r \frac{d\,\Delta p_r}{dt} \quad \text{(C-12)}$$

or

$$\kappa_a \frac{d\,\Delta p_a}{dt} + \alpha_r\,\Delta p_a - \alpha_r\,\Delta p_r = 0 \quad \text{(C-13)}$$

$$\kappa_r \frac{d\,\Delta p_r}{dt} - \alpha_r\,\Delta p_a + \alpha_r\,\Delta p_r = w_{p,net} \quad \text{(C-14)}$$

Applying Laplace transformation (Erdélyi, 1954) to Equations C-13 and C-14 and using initial conditions (Equation C-8) gives

$$\kappa_a\, s\,\overline{\Delta p_a} + \alpha_r\,\overline{\Delta p_a} - \alpha_r\,\overline{\Delta p_r} = 0 \quad \text{(C-15)}$$

$$\kappa_r\, s\, \overline{\Delta p_r} - \alpha_r\, \overline{\Delta p_a} + \alpha_r\, \overline{\Delta p_r} = \frac{w_{p,net}}{s} \tag{C-16}$$

where

$$\overline{\Delta p_a} = \int_0^\infty e^{-st} \Delta p_a\, d\tau \quad , \quad \overline{\Delta p_r} = \int_0^\infty e^{-st} \Delta p_r\, d\tau \tag{C-17}$$

Rearranging Equations C-15 and C-16 gives

$$(\kappa_a s + \alpha_r)\, \overline{\Delta p_a} - \alpha_r\, \overline{\Delta p_r} = 0 \tag{C-18}$$

$$-\alpha_r\, \overline{\Delta p_a} + (\kappa_r s + \alpha_r) \overline{\Delta p_r} = \frac{w_{p,net}}{s} \tag{C-19}$$

or

$$\left[s + \frac{\alpha_r}{\kappa_a} \right] \overline{\Delta p_a} - \frac{\alpha_r}{\kappa_a}\, \overline{\Delta p_r} = 0 \tag{C-20}$$

$$-\frac{\alpha_r}{\kappa_r}\, \overline{\Delta p_a} + \left[s + \frac{\alpha_r}{\kappa_r} \right] \overline{\Delta p_r} = \frac{w_{p,net}}{\kappa_r\, s} \tag{C-21}$$

Equations C-20 and C-21 represent a system of two equations with two unknowns ($\overline{\Delta p_a}, \overline{\Delta p_r}$) and can be solved using Cramer's rule (Kreyszig, 1999) as below:

$$\overline{\Delta p_a} = \frac{D_a}{D} \ , \ \overline{\Delta p_r} = \frac{D_r}{D} \tag{C-22}$$

$$D_a = \begin{vmatrix} 0 & -\dfrac{\alpha_r}{\kappa_a} \\ \dfrac{w_{p,net}}{\kappa_r\, s} & s + \dfrac{\alpha_r}{\kappa_r} \end{vmatrix} = \frac{\alpha_r}{\kappa_a \kappa_r} \frac{w_{p,net}}{s} \tag{C-23}$$

$$D_r = \begin{vmatrix} s + \frac{\alpha_r}{\kappa_a} & 0 \\ -\frac{\alpha_r}{\kappa_r} & \frac{w_{p,net}}{\kappa_r s} \end{vmatrix} = \frac{w_{p,net}}{\kappa_r s}\left[s + \frac{\alpha_r}{\kappa_a} \right] \tag{C-24}$$

$$D = \begin{vmatrix} s + \frac{\alpha_r}{\kappa_a} & -\frac{\alpha_r}{\kappa_a} \\ -\frac{\alpha_r}{\kappa_r} & s + \frac{\alpha_r}{\kappa_r} \end{vmatrix} = \left(s + \frac{\alpha_r}{\kappa_a} \right)\left(s + \frac{\alpha_r}{\kappa_r} \right) - \frac{\alpha_r^2}{\kappa_a \kappa_r} = s\left[s + \alpha_r \left(\frac{\kappa_a + \kappa_r}{\kappa_a \kappa_r} \right) \right] \tag{C-25}$$

$$\overline{\Delta p_a} = \frac{D_a}{D} = \frac{\alpha_r}{\kappa_a \kappa_r} \frac{w_{p,net}}{s} \frac{1}{s\left[s + \alpha_r \left(\frac{\kappa_a + \kappa_r}{\kappa_a \kappa_r} \right) \right]} \tag{C-26}$$

$$\overline{\Delta p_r} = \frac{D_r}{D} = \frac{w_{p,net}}{\kappa_r s} \frac{\left[s + \frac{\alpha_r}{\kappa_a} \right]}{s\left[s + \alpha_r \left(\frac{\kappa_a + \kappa_r}{\kappa_a \kappa_r} \right) \right]} \tag{C-27}$$

Rearranging Equations C-26 and C-27 gives

$$\overline{\Delta p_a} = \frac{\alpha_r}{\kappa_a \kappa_r} w_{p,net} \frac{1}{s^2\left[s + \alpha_r \left(\frac{\kappa_a + \kappa_r}{\kappa_a \kappa_r} \right) \right]} = \frac{\alpha_r}{\kappa_a \kappa_r} w_{p,net} \frac{1}{s^2[s + C]} \tag{C-28}$$

$$\begin{aligned} \overline{\Delta p_r} &= \frac{w_{p,net}}{\kappa_r} \frac{1}{s\left[s + \alpha_r \left(\frac{\kappa_a + \kappa_r}{\kappa_a \kappa_r} \right) \right]} + \frac{\alpha_r}{\kappa_a \kappa_r} w_{p,net} \frac{1}{s^2\left[s + \alpha_r \left(\frac{\kappa_a + \kappa_r}{\kappa_a \kappa_r} \right) \right]} \\ &= \frac{w_{p,net}}{\kappa_r} \frac{1}{s[s + C]} + \frac{\alpha_r}{\kappa_a \kappa_r} w_{p,net} \frac{1}{s^2[s + C]} \end{aligned} \tag{C-29}$$

where

$$C = \alpha_r \left(\frac{\kappa_a + \kappa_r}{\kappa_a \kappa_r} \right) \tag{C-30}$$

In order to find the values of $\overline{\Delta p_a}$ and $\overline{\Delta p_r}$ in real space, inverse Laplace transforms of Equations C-28 and C-29 are obtained as follows:

$$\Delta p_a(t) = L^{-1}\left\{\overline{\Delta p_a}\right\} = L^{-1}\left\{\frac{\alpha_r}{\kappa_a \kappa_r} w_{p,net} \frac{1}{s^2[s+C]}\right\} = \frac{\alpha_r}{\kappa_a \kappa_r} w_{p,net} L^{-1}\left\{\frac{1}{s^2[s+C]}\right\} \tag{C-31}$$

$$\Delta p_r(t) = L^{-1}\left\{\overline{\Delta p_r}\right\} = L^{-1}\left\{\frac{w_{p,net}}{\kappa_r} \frac{1}{s[s+C]}\right\} + L^{-1}\left\{\frac{\alpha_r}{\kappa_a \kappa_r} w_{p,net} \frac{1}{s^2[s+C]}\right\} \tag{C-32}$$

$$= \frac{w_{p,net}}{\kappa_r} L^{-1}\left\{\frac{1}{s[s+C]}\right\} + \frac{\alpha_r}{\kappa_a \kappa_r} w_{p,net} L^{-1}\left\{\frac{1}{s^2[s+C]}\right\}$$

Inverse Laplace transform of the term of $\frac{1}{s^2[s+C]}$ in Equations C-31 and C-32 is obtained by using the formula (Equation C-33) given below (Erdélyi, 1954):

$$L^{-1}\{f(s)g(s)\} = \int_0^t F(\tau)G(t-\tau)d\tau \tag{C-33}$$

Applying Equation C-33 in Equations C-31 and C-32 gives

$$f(s) = 1/s^2, \quad g(s) = 1/(s+C) \tag{C-34}$$

and

$$F(\tau) = L^{-1}\left\{\frac{1}{s^2}\right\} = \tau, \quad G(t-\tau) = L^{-1}\left\{\frac{1}{s+C}\right\} = exp[-C(t-\tau)] \tag{C-35}$$

$$L^{-1}\left\{\frac{1}{s^2[s+C]}\right\} = \int_0^t \tau \; exp[-C(t-\tau)]\, d\tau = \frac{t}{C} + \frac{1}{C^2}[exp(-Ct) - 1] \tag{C-36}$$

is obtained.

Substituting Equation C-36 into Equation C-31 gives

$$\Delta p_a(t) = \frac{\alpha_r}{\kappa_a \kappa_r} w_{p,net} L^{-1}\left\{\frac{1}{s^2[s+C]}\right\} = \frac{\alpha_r}{\kappa_a \kappa_r} w_{p,net}\left\{\frac{t}{C} + \frac{1}{C^2}[exp(-Ct)-1]\right\}$$

(C-37)

and using Equation C-30 in Equation C-37, the pressure change of the aquifer tank is obtained as follows:

$$\Delta p_a(t) = \frac{\alpha_r}{\kappa_a \kappa_r} w_{p,net}\left\{\frac{\kappa_a \kappa_r}{\alpha_r(\kappa_a+\kappa_r)}t + \left(\frac{\kappa_a \kappa_r}{\alpha_r(\kappa_a+\kappa_r)}\right)^2\left[exp\left(-\frac{\alpha_r(\kappa_a+\kappa_r)}{\kappa_a \kappa_r}t\right)-1\right]\right\}$$

$$\Delta p_a(t) = \frac{w_{p,net}}{(\kappa_a+\kappa_r)}t + \left(w_{p,net}\frac{\kappa_a \kappa_r}{\alpha_r(\kappa_a+\kappa_r)^2}\right)\left[exp\left(-\frac{\alpha_r(\kappa_a+\kappa_r)}{\kappa_a \kappa_r}t\right)-1\right] \quad \text{(C-38)}$$

Inverse Laplace transform of the term of $\frac{1}{s[s+C]}$ in Equation C-32 is obtained by using the formula (Equation C-39) given below (Erdélyi, 1954):

$$L^{-1}\left\{\frac{1}{(s-a)(s-b)}\right\} = \frac{1}{a-b}[exp(at)-exp(bt)] \quad \text{(C-39)}$$

Applying Equation C-39 in Equation C-32 gives

$$a=0,\ b=-C \quad \text{(C-40)}$$

and

$$L^{-1}\left\{\frac{1}{s[s+C]}\right\} = \frac{1}{0+C}[exp(0t)-exp(-Ct)] = \frac{1-exp[-Ct]}{C} \quad \text{(C-41)}$$

is obtained. Using Equations C-36 and C-41 in Equation C-32 gives the pressure changes of the reservoir tank as a function of time as follows:

$$\Delta p_r(t) = \frac{w_{p,net}}{\kappa_r} L^{-1}\left\{\frac{1}{s[s+C]}\right\} + \frac{\alpha_r}{\kappa_a \kappa_r} w_{p,net} L^{-1}\left\{\frac{1}{s^2[s+C]}\right\}$$

$$= \frac{w_{p,net}}{\kappa_r}\left[\frac{1-exp[-Ct]}{C}\right] + \frac{\alpha_r}{\kappa_a \kappa_r} w_{p,net}\left[\frac{t}{C} + \frac{1}{C^2}[exp(-Ct)-1]\right] \quad \text{(C-42)}$$

and substituting Equation C-30 into Equation C-42 and rearranging gives

$$\Delta p_r(t) = \frac{w_{p,net}}{(\kappa_a + \kappa_r)} t + \frac{w_{p,net}}{\alpha_r} \left(\frac{\kappa_a}{\kappa_a + \kappa_r} \right)^2 \left[1 - exp\left(-\alpha_r \frac{\kappa_a + \kappa_r}{\kappa_a \kappa_r} t \right) \right] \quad \text{(C-43)}$$

Thus, The pressures of the reservoir and the aquifer tanks as a function of time are obtained by using Equations C-38 and C-43 as below.

$$p_a(t) = p_i - \frac{w_{p,net}}{(\kappa_a + \kappa_r)} t - \left(w_{p,net} \frac{\kappa_a \kappa_r}{\alpha_r (\kappa_a + \kappa_r)^2} \right) \left[exp\left(-\frac{\alpha_r (\kappa_a + \kappa_r)}{\kappa_a \kappa_r} t \right) - 1 \right] \quad \text{(C-44)}$$

$$p_r(t) = p_i - \frac{w_{p,net}}{(\kappa_a + \kappa_r)} t - \frac{w_{p,net}}{\alpha_r} \left(\frac{\kappa_a}{\kappa_a + \kappa_r} \right)^2 \left[1 - exp\left(-\alpha_r \frac{\kappa_a + \kappa_r}{\kappa_a \kappa_r} t \right) \right] \quad \text{(C-45)}$$

APPENDIX-D

1 RESERVOIR – 1 AQUIFER WITH RECHARGE SOURCE (WITHOUT INITIAL HYDRAULIC EQUILIBRIUM)

Mass balances on the reservoir and the aquifer, recharge of the reservoir and the aquifer, initial condition are expressed as;

Mass Balance on the Aquifer :

$$w_a - w_r = \kappa_a \frac{dp_a}{dt} \tag{D-1}$$

Mass Balance on the Reservoir :

$$w_r - w_{p,net} = \kappa_r \frac{dp_r}{dt} \tag{D-2}$$

Recharge of the Aquifer : $w_a = \alpha_a (p_i - p_a)$ (D-3)

Recharge of the Reservoir : $w_r = \alpha_r (p_a - p_r)$ (D-4)

Initial Conditions : $p_a = p_r = p_o \ @ \ t = 0$ (D-5)

Substituting Equations D-3 and D-4 into Equations D-1 and D-2 gives

$$\alpha_a (p_i - p_a) - \alpha_r (p_a - p_r) = \kappa_a \frac{dp_a}{dt} \tag{D-6}$$

$$\alpha_r (p_a - p_r) - w_{p,net} = \kappa_r \frac{dp_r}{dt} \tag{D-7}$$

The pressure changes and their derivatives with respect to time as given by

$$\left.\begin{aligned} \Delta p_a = p_o - p_a \;\Rightarrow\; p_a = p_o - \Delta p_a \;\Rightarrow\; \frac{d\,\Delta p_a}{dt} = -\frac{dp_a}{dt} \\ \Delta p_r = p_o - p_r \;\Rightarrow\; p_r = p_o - \Delta p_r \;\Rightarrow\; \frac{d\,\Delta p_r}{dt} = -\frac{dp_r}{dt} \end{aligned}\right\} \quad \text{(D-8)}$$

Initial conditons are obtained by applying Equation D-8 in Equation D-5 as follows:

$$\left.\begin{aligned} \Delta p_a(t=0) = p_o - p_a(t=0) = p_o - p_o = 0 \\ \Delta p_r(t=0) = p_o - p_r(t=0) = p_o - p_o = 0 \end{aligned}\right\} \quad \text{(D-9)}$$

Using Equation D-8 in Equations D-6 and D-7 gives

$$\alpha_a\left(p_i - p_o + \Delta p_a\right) - \alpha_r\left(p_o - \Delta p_a - p_o + \Delta p_r\right) = -\kappa_a \frac{d\,\Delta p_a}{dt} \quad \text{(D-10)}$$

$$\alpha_r\left(p_o - \Delta p_a - p_o + \Delta p_r\right) - w_{p,net} = -\kappa_r \frac{d\,\Delta p_r}{dt} \quad \text{(D-11)}$$

Initial pressure difference between the recharge source and the reservoir or the aquifer tank, $p_i - p_o$, can be defined as below.

$$\Delta p_c = p_i - p_o = constant \quad \text{(D-12)}$$

Substituting Equation D-12 into Equations D-10 and D-11 and rearranging gives

$$\alpha_a\left(\Delta p_c + \Delta p_a\right) - \alpha_r\left(\Delta p_r - \Delta p_a\right) = -\kappa_a \frac{d\,\Delta p_a}{dt} \quad \text{(D-13)}$$

$$\alpha_r\left(\Delta p_r - \Delta p_a\right) - w_{p,net} = -\kappa_r \frac{d\,\Delta p_r}{dt} \quad \text{(D-14)}$$

or

$$\kappa_a \frac{d\,\Delta p_a}{dt} + \left(\alpha_a + \alpha_r\right)\Delta p_a - \alpha_r\,\Delta p_r = -\alpha_a \Delta p_c \quad \text{(D-15)}$$

$$\kappa_r \frac{d\,\Delta p_r}{dt} - \alpha_r\,\Delta p_a + \alpha_r\,\Delta p_r = w_{p,net} \quad \text{(D-16)}$$

Applying Laplace transformation (Erdélyi, 1954) to Equations D-15 and D-16 and using initial conditions (Equation D-9) gives

$$\kappa_a\, s\, \overline{\Delta p_a} + (\alpha_a + \alpha_r)\, \overline{\Delta p_a} - \alpha_r\, \overline{\Delta p_r} = -\alpha_a \frac{\Delta p_c}{s} \tag{D-17}$$

$$\kappa_r\, s\, \overline{\Delta p_r} - \alpha_r\, \overline{\Delta p_a} + \alpha_r\, \overline{\Delta p_r} = \frac{w_{p,net}}{s} \tag{D-18}$$

where

$$\overline{\Delta p_a} = \int_0^\infty e^{-st} \Delta p_a\, d\tau \quad , \quad \overline{\Delta p_r} = \int_0^\infty e^{-st} \Delta p_r\, d\tau \tag{D-19}$$

Rearranging Equations D-17 and D-18 gives

$$(\kappa_a\, s + \alpha_a + \alpha_r)\, \overline{\Delta p_a} - \alpha_r\, \overline{\Delta p_r} = -\alpha_a \frac{\Delta p_c}{s} \tag{D-20}$$

$$-\alpha_r\, \overline{\Delta p_a} + (\kappa_r\, s + \alpha_r) \overline{\Delta p_r} = \frac{w_{p,net}}{s} \tag{D-21}$$

or

$$\left[s + \frac{(\alpha_a + \alpha_r)}{\kappa_a} \right] \overline{\Delta p_a} - \frac{\alpha_r}{\kappa_a}\, \overline{\Delta p_r} = -\frac{\alpha_a}{\kappa_a} \frac{\Delta p_c}{s} \tag{D-22}$$

$$-\frac{\alpha_r}{\kappa_r}\, \overline{\Delta p_a} + \left[s + \frac{\alpha_r}{\kappa_r} \right] \overline{\Delta p_r} = \frac{w_{p,net}}{\kappa_r\, s} \tag{D-23}$$

By using Cramer's rule (Kreyszig, 1999), the solutions for two equations (Equations D-22 and D-23) with two unknowns ($\overline{\Delta p_a}, \overline{\Delta p_r}$) can be found as below:

$$\overline{\Delta p_a} = \frac{D_a}{D} \ , \ \overline{\Delta p_r} = \frac{D_r}{D} \tag{D-24}$$

$$D_a = \begin{vmatrix} -\frac{\alpha_a}{\kappa_a}\frac{\Delta p_c}{s} & -\frac{\alpha_r}{\kappa_a} \\ \frac{w_{p,net}}{\kappa_r s} & s+\frac{\alpha_r}{\kappa_r} \end{vmatrix} = -\left(\frac{\alpha_a}{\kappa_a}\Delta p_c\right) - \left(\frac{\alpha_a\alpha_r}{\kappa_a\kappa_r}\frac{\Delta p_c}{s}\right) + \left(\frac{\alpha_r}{\kappa_a\kappa_r s}w_{p,net}\right) \quad \text{(D-25)}$$

$$D_r = \begin{vmatrix} s+\frac{(\alpha_a+\alpha_r)}{\kappa_a} & -\frac{\alpha_a}{\kappa_a}\frac{\Delta p_c}{s} \\ -\frac{\alpha_r}{\kappa_r} & \frac{w_{p,net}}{\kappa_r s} \end{vmatrix} = \frac{w_{p,net}}{\kappa_r s}\left[s+\frac{(\alpha_a+\alpha_r)}{\kappa_a}\right] - \frac{\alpha_a\alpha_r}{\kappa_a\kappa_r}\frac{\Delta p_c}{s} \quad \text{(D-26)}$$

$$D = \begin{vmatrix} s+\frac{(\alpha_a+\alpha_r)}{\kappa_a} & -\frac{\alpha_r}{\kappa_a} \\ -\frac{\alpha_r}{\kappa_r} & s+\frac{\alpha_r}{\kappa_r} \end{vmatrix} = \left[s+\frac{(\alpha_a+\alpha_r)}{\kappa_a}\right]\left(s+\frac{\alpha_r}{\kappa_r}\right) - \frac{\alpha_r^2}{\kappa_a\kappa_r} \quad \text{(D-27)}$$

$$\overline{\Delta p_a} = \frac{D_a}{D} = \frac{-\left(\frac{\alpha_a}{\kappa_a}\Delta p_c\right) - \left(\frac{\alpha_a\alpha_r}{\kappa_a\kappa_r}\frac{\Delta p_c}{s}\right) + \left(\frac{\alpha_r}{\kappa_a\kappa_r s}w_{p,net}\right)}{\left\{\left[s+\frac{(\alpha_a+\alpha_r)}{\kappa_a}\right]\left(s+\frac{\alpha_r}{\kappa_r}\right) - \frac{\alpha_r^2}{\kappa_a\kappa_r}\right\}} \quad \text{(D-28)}$$

$$\overline{\Delta p_r} = \frac{D_r}{D} = \frac{\frac{w_{p,net}}{\kappa_r s}\left[s+\frac{(\alpha_a+\alpha_r)}{\kappa_a}\right] - \frac{\alpha_a\alpha_r}{\kappa_a\kappa_r}\frac{\Delta p_c}{s}}{\left\{\left[s+\frac{(\alpha_a+\alpha_r)}{\kappa_a}\right]\left(s+\frac{\alpha_r}{\kappa_r}\right) - \frac{\alpha_r^2}{\kappa_a\kappa_r}\right\}} \quad \text{(D-29)}$$

Rearranging the denominator in Equations D-28 and D-29 gives

$$\left\{\left[s+\frac{(\alpha_a+\alpha_r)}{\kappa_a}\right]\left(s+\frac{\alpha_r}{\kappa_r}\right) - \frac{\alpha_r^2}{\kappa_a\kappa_r}\right\} = s^2 + \left[\frac{\alpha_a+\alpha_r}{\kappa_a}+\frac{\alpha_r}{\kappa_r}\right]s + \frac{\alpha_a\alpha_r}{\kappa_a\kappa_r} \quad \text{(D-30)}$$

and the roots of Equation D-30 (μ_1, μ_2) are found as follows;

$$\left.\begin{aligned}\mu_1 &= \frac{\left[\frac{(\alpha_a+\alpha_r)}{\kappa_a}+\frac{\alpha_r}{\kappa_r}\right]+\sqrt{\left[\frac{(\alpha_a+\alpha_r)}{\kappa_a}+\frac{\alpha_r}{\kappa_r}\right]^2-4\frac{\alpha_a\alpha_r}{\kappa_a\kappa_r}}}{2}\\ \mu_2 &= \frac{\left[\frac{(\alpha_a+\alpha_r)}{\kappa_a}+\frac{\alpha_r}{\kappa_r}\right]-\sqrt{\left[\frac{(\alpha_a+\alpha_r)}{\kappa_a}+\frac{\alpha_r}{\kappa_r}\right]^2-4\frac{\alpha_a\alpha_r}{\kappa_a\kappa_r}}}{2}\end{aligned}\right\} \quad \text{(D-31)}$$

and Equation D-30 can be rearranged as

$$s^2+\left[\frac{\alpha_a+\alpha_r}{\kappa_a}+\frac{\alpha_r}{\kappa_r}\right]s+\frac{\alpha_a\alpha_r}{\kappa_a\kappa_r}=(s+\mu_1)(s+\mu_2) \quad \text{(D-32)}$$

Using Equation D-32 in Equations D-28 and D-29, and rearranging give

$$\overline{\Delta p_a}=-\frac{\left(\frac{\alpha_a}{\kappa_a}\Delta p_c\right)}{(s+\mu_1)(s+\mu_2)}-\frac{\left(\frac{\alpha_a\alpha_r}{\kappa_a\kappa_r}\frac{\Delta p_c}{s}\right)}{(s+\mu_1)(s+\mu_2)}+\frac{\left(\frac{\alpha_r}{\kappa_a\kappa_r s}w_{p,net}\right)}{(s+\mu_1)(s+\mu_2)} \quad \text{(D-33)}$$

$$\overline{\Delta p_r}=\frac{\frac{w_{p,net}}{\kappa_r s}(s+d)}{(s+\mu_1)(s+\mu_2)}-\frac{\frac{\alpha_a\alpha_r}{\kappa_a\kappa_r}\frac{\Delta p_c}{s}}{(s+\mu_1)(s+\mu_2)} \text{ and } d=\frac{(\alpha_a+\alpha_r)}{\kappa_a} \quad \text{(D-34)}$$

or

$$\overline{\Delta p_a}=-\frac{\left(\frac{\alpha_a}{\kappa_a}\Delta p_c\right)}{(s+\mu_1)(s+\mu_2)}-\frac{\left(\frac{\alpha_a\alpha_r}{\kappa_a\kappa_r}\Delta p_c\right)}{(s+0)(s+\mu_1)(s+\mu_2)}+\frac{\left(\frac{\alpha_r}{\kappa_a\kappa_r}w_{p,net}\right)}{(s+0)(s+\mu_1)(s+\mu_2)} \quad \text{(D-35)}$$

$$\overline{\Delta p_r}=\frac{\frac{w_{p,net}}{\kappa_r}(s+d)}{(s+0)(s+\mu_1)(s+\mu_2)}-\frac{\frac{\alpha_a\alpha_r}{\kappa_a\kappa_r}\Delta p_c}{(s+0)(s+\mu_1)(s+\mu_2)} \quad \text{(D-36)}$$

where $d=\frac{\alpha_a+\alpha_r}{\kappa_a}$

In order to find the values of $\overline{\Delta p_a}$ and $\overline{\Delta p_r}$ in real space, inverse Laplace transforms of Equations D-35 and D-36 are obtained as follows:

$$\Delta p_a(t) = L^{-1}\left(\overline{\Delta p_a}\right) = -\frac{\alpha_a}{\kappa_a}\Delta p_c\, L^{-1}\left\{\frac{1}{(s+\mu_1)(s+\mu_2)}\right\} - \frac{\alpha_a\alpha_r}{\kappa_a\kappa_r}\Delta p_c\, L^{-1}\left\{\frac{1}{(s+0)(s+\mu_1)(s+\mu_2)}\right\} + \frac{\alpha_r}{\kappa_a\kappa_r} w_{p,net}\, L^{-1}\left\{\frac{1}{(s+0)(s+\mu_1)(s+\mu_2)}\right\} \quad \text{(D-37)}$$

$$\Delta p_r(t) = L^{-1}\left\{\overline{\Delta p_r}\right\} = \frac{w_{p,net}}{\kappa_r} L^{-1}\left\{\frac{(s+d)}{(s+0)(s+\mu_1)(s+\mu_2)}\right\} - \frac{\alpha_a\alpha_r}{\kappa_a\kappa_r}\Delta p_c\, L^{-1}\left\{\frac{1}{(s+0)(s+\mu_1)(s+\mu_2)}\right\} \quad \text{(D-38)}$$

Inverse Laplace transform of the term of $\frac{1}{(s+\mu_1)(s+\mu_2)}$ in Equation D-37 is obtained by using the formula given in Equation C-39. Applying Equation C-39 in Equation D-37 gives

$$a = -\mu_1, \quad b = -\mu_2 \quad \text{(D-39)}$$

and

$$L^{-1}\left\{\frac{1}{(s+\mu_1)(s+\mu_2)}\right\} = \frac{1}{\mu_2-\mu_1}\left[exp(-\mu_1 t) - exp(-\mu_2 t)\right] \quad \text{(D-40)}$$

is obtained.

Inverse Laplace transforms of the terms of $\frac{1}{(s+0)(s+\mu_1)(s+\mu_2)}$ and $\frac{(s+d)}{(s+0)(s+\mu_1)(s+\mu_2)}$ in Equations D-37 and D-38 are obtained by using the formula given in Equation B-36. Using Equation B-36 in Equations D-37 and D-38 gives

$$\lambda = 0 \;,\; \mu = 0 \;,\; \nu = 1$$
$$\alpha = 0 \;,\; \beta = \mu_1 \;,\; \gamma = \mu_2 \quad \text{(D-41)}$$

and

$$L^{-1}\left\{\frac{1}{(s+0)(s+\mu_1)(s+\mu_2)}\right\}=\frac{1}{\mu_1\mu_2}+\frac{1}{\mu_1(\mu_1-\mu_2)}exp(-\mu_1 t)+\frac{1}{\mu_2(\mu_2-\mu_1)}exp(-\mu_2 t) \tag{D-42}$$

is obtained. Using Equation B-36 in Equation D-38 gives

$$\lambda=0\ ,\ \mu=1\ ,\ \nu=d$$
$$\alpha=0\ ,\ \beta=\mu_1\ ,\ \gamma=\mu_2 \tag{D-43}$$

and

$$L^{-1}\left\{\frac{(s+d)}{(s+0)(s+\mu_1)(s+\mu_2)}\right\}=\frac{d}{\mu_1\mu_2}+\frac{(\mu_1-d)}{\mu_1(\mu_2-\mu_1)}exp(-\mu_1 t)+\frac{(\mu_2-d)}{\mu_2(\mu_1-\mu_2)}exp(-\mu_2 t) \tag{D-44}$$

is obtained. Substituting Equations D-40 and D-42 into Equation D-37 gives the pressure changes of the aquifer tank as below:

$$\Delta p_a(t)=-\frac{\alpha_a}{\kappa_a}\Delta p_c\left\{\frac{1}{\mu_2-\mu_1}[exp(-\mu_1 t)-exp(-\mu_2 t)]\right\}$$
$$-\frac{\alpha_a\alpha_r}{\kappa_a\kappa_r}\Delta p_c\left\{\frac{1}{\mu_1\mu_2}+\frac{1}{\mu_1(\mu_1-\mu_2)}exp(-\mu_1 t)+\frac{1}{\mu_2(\mu_2-\mu_1)}exp(-\mu_2 t)\right\}$$
$$+\frac{\alpha_r}{\kappa_a\kappa_r}w_{p,net}\left\{\frac{1}{\mu_1\mu_2}+\frac{1}{\mu_1(\mu_1-\mu_2)}exp(-\mu_1 t)+\frac{1}{\mu_2(\mu_2-\mu_1)}exp(-\mu_2 t)\right\}$$

or

$$\Delta p_a(t)=-\frac{\alpha_a}{\kappa_a}(p_i-p_o)\left\{\frac{1}{\mu_2-\mu_1}[exp(-\mu_1 t)-exp(-\mu_2 t)]\right\}$$
$$+\left[\frac{\alpha_r}{\kappa_a\kappa_r}w_{p,net}-\frac{\alpha_a\alpha_r}{\kappa_a\kappa_r}(p_i-p_o)\right]\left\{\frac{(\mu_1-\mu_2)+\mu_2\,exp(-\mu_1 t)-\mu_1\,exp(-\mu_2 t)}{\mu_1\mu_2(\mu_1-\mu_2)}\right\} \tag{D-45}$$

Similarly, using Equations D-42 and D-44 in Equation D-38 gives the pressure changes of reservoir as below:

$$\Delta p_r(t) = \frac{w_{p,net}}{\kappa_r}\left\{\frac{d}{\mu_1\mu_2} + \frac{(\mu_1 - d)}{\mu_1(\mu_2 - \mu_1)}exp(-\mu_1 t) + \frac{(\mu_2 - d)}{\mu_2(\mu_1 - \mu_2)}exp(-\mu_2 t)\right\}$$
$$-\frac{\alpha_a\alpha_r}{\kappa_a\kappa_r}\Delta p_c\left\{\frac{1}{\mu_1\mu_2} + \frac{1}{\mu_1(\mu_1 - \mu_2)}exp(-\mu_1 t) + \frac{1}{\mu_2(\mu_2 - \mu_1)}exp(-\mu_2 t)\right\}$$

or

$$\Delta p_r(t) = \frac{w_{p,net}}{\kappa_r}\left\{\frac{d}{\mu_1\mu_2} + \frac{(\mu_1 - d)}{\mu_1(\mu_2 - \mu_1)}exp(-\mu_1 t) + \frac{(\mu_2 - d)}{\mu_2(\mu_1 - \mu_2)}exp(-\mu_2 t)\right\}$$
$$+\frac{\alpha_a\alpha_r}{\kappa_a\kappa_r}(p_i - p_o)\left\{\frac{(\mu_2 - \mu_1) - \mu_2\, exp(-\mu_1 t) + \mu_1\, exp(-\mu_2 t)}{\mu_1\mu_2(\mu_1 - \mu_2)}\right\}$$

(D-46)

Thus, pressure behavior of the reservoir and the aquifer as a function of time is obtained as follows.

$$p_a(t) = p_i + \frac{\alpha_a}{\kappa_a}(p_i - p_o)\left\{\frac{1}{\mu_2 - \mu_1}[exp(-\mu_1 t) - exp(-\mu_2 t)]\right\}$$
$$-\left[\frac{\alpha_r}{\kappa_a\kappa_r}w_{p,net} - \frac{\alpha_a\alpha_r}{\kappa_a\kappa_r}(p_i - p_o)\right]\left\{\frac{(\mu_1 - \mu_2) + \mu_2\, exp(-\mu_1 t) - \mu_1\, exp(-\mu_2 t)}{\mu_1\mu_2(\mu_1 - \mu_2)}\right\}$$

(D-47)

$$p_r(t) = p_i - \frac{w_{p,net}}{\kappa_r}\left\{\frac{d}{\mu_1\mu_2} + \frac{(\mu_1 - d)}{\mu_1(\mu_2 - \mu_1)}exp(-\mu_1 t) + \frac{(\mu_2 - d)}{\mu_2(\mu_1 - \mu_2)}exp(-\mu_2 t)\right\}$$
$$-\frac{\alpha_a\alpha_r}{\kappa_a\kappa_r}(p_i - p_o)\left\{\frac{(\mu_2 - \mu_1) - \mu_2\, exp(-\mu_1 t) + \mu_1\, exp(-\mu_2 t)}{\mu_1\mu_2(\mu_1 - \mu_2)}\right\}$$

(D-48)

APPENDIX-E

1 RESERVOIR – 2 AQUIFERS WITH RECHARGE SOURCE (3-TANK OPEN SYSTEM)

Mass balances on the reservoir and the aquifers, recharge of the reservoir and the aquifers, initial conditions are expressed as;

Mass Balance on the Outer Aquifer :

$$w_{oa} - w_{ia} = \kappa_{oa} \frac{dp_{oa}}{dt} \tag{E-1}$$

Mass Balance on the Inner Aquifer :

$$w_{ia} - w_r = \kappa_{ia} \frac{dp_{ia}}{dt} \tag{E-2}$$

Mass Balance on the Reservoir :

$$w_r - w_{p,net} = \kappa_r \frac{dp_r}{dt} \tag{E-3}$$

Recharge of the Outer Aquifer : $w_{oa} = \alpha_{oa}(p_i - p_{oa})$ (E-4)

Recharge of the Inner Aquifer : $w_{ia} = \alpha_{ia}(p_{oa} - p_{ia})$ (E-5)

Recharge of the Reservoir : $w_r = \alpha_r(p_{ia} - p_r)$ (E-6)

Initial Conditions : $p_{ia} = p_{oa} = p_r = p_i \ @ \ t = 0$ (E-7)

Substituting Equations E-4, E-5, and E-6 into Equations E-1, E-2, and E-3 gives

$$\alpha_{oa}(p_i - p_{oa}) - \alpha_{ia}(p_{oa} - p_{ia}) = \kappa_{oa} \frac{dp_{oa}}{dt} \tag{E-8}$$

$$\alpha_{ia}(p_{oa}-p_{ia})-\alpha_r(p_{ia}-p_r)=\kappa_{ia}\frac{dp_{ia}}{dt} \tag{E-9}$$

$$\alpha_r(p_{ia}-p_r)-w_{p,net}=\kappa_r\frac{dp_r}{dt} \tag{E-10}$$

Equations E-8, E-9, and E-10 can be writen in terms of pressure changes. The pressure changes and their derivatives with respect to time are given by

$$\left.\begin{aligned}
&\Delta p_{ia}=p_i-p_{ia}\ \Rightarrow\ p_{ia}=p_i-\Delta p_{ia1}\ \Rightarrow\ \frac{d\,\Delta p_{ia}}{dt}=-\frac{dp_{ia}}{dt}\\
&\Delta p_{oa}=p_i-p_{oa}\ \Rightarrow\ p_{oa}=p_i-\Delta p_{oa}\ \Rightarrow\ \frac{d\,\Delta p_{oa}}{dt}=-\frac{dp_{oa}}{dt}\\
&\Delta p_r=p_i-p_r\ \Rightarrow\ p_r=p_i-\Delta p_r\ \Rightarrow\ \frac{d\,\Delta p_r}{dt}=-\frac{dp_r}{dt}
\end{aligned}\right\} \tag{E-11}$$

and initial conditions become

$$\left.\begin{aligned}
&\Delta p_{ia}(t=0)=p_i-p_{ia}(t=0)=p_i-p_i=0\\
&\Delta p_{oa}(t=0)=p_i-p_{oa}(t=0)=p_i-p_i=0\\
&\Delta p_r(t=0)=p_i-p_r(t=0)=p_i-p_i=0
\end{aligned}\right\} \tag{E-12}$$

Using Equation E-11 in Equations E-8, E-9, and E-10 gives

$$\alpha_{oa}(p_i-p_i+\Delta p_{oa})-\alpha_{ia}(p_i-\Delta p_{oa}-p_i+\Delta p_{ia})=-\kappa_{oa}\frac{d\Delta p_{oa}}{dt} \tag{E-13}$$

$$\alpha_{ia}(p_i-\Delta p_{oa}-p_i+\Delta p_{ia})-\alpha_r(p_i-\Delta p_{ia}-p_i+\Delta p_r)=-\kappa_{ia}\frac{d\Delta p_{ia}}{dt} \tag{E-14}$$

$$\alpha_r(p_i-\Delta p_{ia}-p_i+\Delta p_r)-w_{p,net}=-\kappa_r\frac{d\Delta p_r}{dt} \tag{E-15}$$

Equations E-13, E-14, and E-15 can be simplified and rearranged as follows:

$$\alpha_{oa}\,\Delta p_{oa}-\alpha_{ia}(\Delta p_{ia}-\Delta p_{oa})=-\kappa_{oa}\frac{d\Delta p_{oa}}{dt} \tag{E-16}$$

$$\alpha_{ia}(\Delta p_{ia}-\Delta p_{oa})-\alpha_r(\Delta p_r-\Delta p_{ia})=-\kappa_{ia}\frac{d\Delta p_{ia}}{dt} \tag{E-17}$$

$$\alpha_r(\Delta p_r - \Delta p_{ia}) - w_{p,net} = -\kappa_r \frac{d\Delta p_r}{dt} \tag{E-18}$$

or

$$\kappa_{oa} \frac{d\Delta p_{oa}}{dt} + (\alpha_{oa} + \alpha_{ia})\Delta p_{oa} - \alpha_{ia}\Delta p_{ia} = 0 \tag{E-19}$$

$$\kappa_{ia} \frac{d\Delta p_{ia}}{dt} - \alpha_{ia}\Delta p_{oa} + (\alpha_{ia} + \alpha_r)\Delta p_{ia} - \alpha_r \Delta p_r = 0 \tag{E-20}$$

$$\kappa_r \frac{d\Delta p_r}{dt} - \alpha_r \Delta p_{ia} + \alpha_r \Delta p_r = w_{p,net} \tag{E-21}$$

Applying Laplace transformation (Erdélyi, 1954) to Equations E-19, E-20, and E-21 and using initial conditions (Equation E-12) gives

$$\kappa_{oa}\, s\, \overline{\Delta p_{oa}} + (\alpha_{oa} + \alpha_{ia})\overline{\Delta p_{oa}} - \alpha_{ia}\, \overline{\Delta p_{ia}} = 0 \tag{E-22}$$

$$\kappa_{ia}\, s\, \overline{\Delta p_{ia}} - \alpha_{ia}\, \overline{\Delta p_{oa}} + (\alpha_{ia} + \alpha_r)\overline{\Delta p_{ia}} - \alpha_r\, \overline{\Delta p_r} = 0 \tag{E-23}$$

$$\kappa_r\, s\, \overline{\Delta p_r} - \alpha_r\, \overline{\Delta p_{ia}} + \alpha_r\, \overline{\Delta p_r} = \frac{w_{p,net}}{s} \tag{E-24}$$

where

$$\overline{\Delta p_{ia}} = \int_0^\infty e^{-st} \Delta p_{ia}\, d\tau \quad , \quad \overline{\Delta p_{oa}} = \int_0^\infty e^{-st} \Delta p_{oa}\, d\tau \quad , \quad \overline{\Delta p_r} = \int_0^\infty e^{-st} \Delta p_r\, d\tau \tag{E-25}$$

Rearranging Equations E-22, E-23, and E-24 gives

$$(\kappa_{oa}\, s + \alpha_{oa} + \alpha_{ia})\overline{\Delta p_{oa}} - \alpha_{ia}\, \overline{\Delta p_{ia}} = 0 \tag{E-26}$$

$$-\alpha_{ia}\, \overline{\Delta p_{oa}} + (\kappa_{ia}\, s + \alpha_{ia} + \alpha_r)\overline{\Delta p_{ia}} - \alpha_r\, \overline{\Delta p_r} = 0 \tag{E-27}$$

$$-\alpha_r\, \overline{\Delta p_{ia}} + (\kappa_r\, s + \alpha_r)\overline{\Delta p_r} = \frac{w_{p,net}}{s} \tag{E-28}$$

or

$$\left(s+\frac{\alpha_{oa}+\alpha_{ia}}{\kappa_{oa}}\right)\overline{\Delta p_{oa}}-\frac{\alpha_{ia}}{\kappa_{oa}}\overline{\Delta p_{ia}}=0 \tag{E-29}$$

$$-\frac{\alpha_{ia}}{\kappa_{ia}}\overline{\Delta p_{oa}}+\left(s+\frac{\alpha_{ia}+\alpha_{r}}{\kappa_{ia}}\right)\overline{\Delta p_{ia}}-\frac{\alpha_{r}}{\kappa_{ia}}\overline{\Delta p_{r}}=0 \tag{E-30}$$

$$-\frac{\alpha_{r}}{\kappa_{r}}\overline{\Delta p_{ia}}+\left(s+\frac{\alpha_{r}}{\kappa_{r}}\right)\overline{\Delta p_{r}}=\frac{w_{p,net}}{\kappa_{r}}\frac{1}{s} \tag{E-31}$$

The solutions to three equations (Equations E-29, E-30, and E-31) with three unknowns ($\overline{\Delta p_{oa}}$, $\overline{\Delta p_{ia}}$, $\overline{\Delta p_{r}}$) can be obtained by using Cramer's rule (Kreyszig, 1999) as follows:

$$\overline{\Delta p_{ia}}=\frac{D_{ia}}{D}\ ,\ \overline{\Delta p_{oa}}=\frac{D_{oa}}{D}\ ,\ \overline{\Delta p_{r}}=\frac{D_{r}}{D} \tag{E-32}$$

$$D_{ia}=\begin{vmatrix} s+\dfrac{\alpha_{oa}+\alpha_{ia}}{\kappa_{oa}} & 0 & 0 \\ -\dfrac{\alpha_{ia}}{\kappa_{ia}} & 0 & -\dfrac{\alpha_{r}}{\kappa_{ia}} \\ 0 & \dfrac{w_{p,net}}{\kappa_{r}}\dfrac{1}{s} & s+\dfrac{\alpha_{r}}{\kappa_{r}} \end{vmatrix} \tag{E-33}$$

$$D_{oa}=\begin{vmatrix} 0 & -\dfrac{\alpha_{ia}}{\kappa_{oa}} & 0 \\ 0 & s+\dfrac{\alpha_{ia}+\alpha_{r}}{\kappa_{ia}} & -\dfrac{\alpha_{r}}{\kappa_{ia}} \\ \dfrac{w_{p,net}}{\kappa_{r}}\dfrac{1}{s} & -\dfrac{\alpha_{r}}{\kappa_{r}} & s+\dfrac{\alpha_{r}}{\kappa_{r}} \end{vmatrix} \tag{E-34}$$

$$D_r = \begin{vmatrix} s + \dfrac{\alpha_{oa} + \alpha_{ia}}{\kappa_{oa}} & -\dfrac{\alpha_{ia}}{\kappa_{oa}} & 0 \\ -\dfrac{\alpha_{ia}}{\kappa_{ia}} & s + \dfrac{\alpha_{ia} + \alpha_r}{\kappa_{ia}} & 0 \\ 0 & -\dfrac{\alpha_r}{\kappa_r} & \dfrac{w_{p,net}}{\kappa_r}\dfrac{1}{s} \end{vmatrix} \tag{E-35}$$

$$= \frac{w_{p,net}}{\kappa_r s}\left\{ \begin{array}{l} s^2 + \left[\dfrac{\kappa_{ia}(\alpha_{ia} + \alpha_{oa}) + \kappa_{oa}(\alpha_{ia} + \alpha_r)}{\kappa_{ia}\kappa_{oa}}\right] s \\ + \dfrac{\alpha_{ia}\alpha_r + \alpha_{oa}\alpha_r + \alpha_{ia}\alpha_{oa}}{\kappa_{ia}\kappa_{oa}} \end{array} \right\}$$

$$D = \begin{vmatrix} s + \dfrac{\alpha_{oa} + \alpha_{ia}}{\kappa_{oa}} & -\dfrac{\alpha_{ia}}{\kappa_{oa}} & 0 \\ -\dfrac{\alpha_{ia}}{\kappa_{ia}} & s + \dfrac{\alpha_{ia} + \alpha_r}{\kappa_{ia}} & -\dfrac{\alpha_r}{\kappa_{ia}} \\ 0 & -\dfrac{\alpha_r}{\kappa_r} & s + \dfrac{\alpha_r}{\kappa_r} \end{vmatrix}$$

$$= s^3 + \left[\frac{\kappa_{oa}\kappa_r(\alpha_{ia} + \alpha_r) + \kappa_{ia}\kappa_r(\alpha_{ia} + \alpha_{oa}) + \kappa_{ia}\kappa_{oa}\alpha_r}{\kappa_{ia}\kappa_{oa}\kappa_r}\right] s^2 \tag{E-36}$$

$$+ \left[\frac{\kappa_r(\alpha_{ia}\alpha_{oa} + \alpha_{ia}\alpha_r + \alpha_{oa}\alpha_r) + \kappa_{ia}(\alpha_{ia}\alpha_r + \alpha_{oa}\alpha_r) + \kappa_{oa}(\alpha_{ia}\alpha_r)}{\kappa_{ia}\kappa_{oa}\kappa_r}\right] s$$

$$+ \frac{\alpha_{ia}\alpha_{oa}\alpha_r}{\kappa_{ia}\kappa_{oa}\kappa_r}$$

Equations E-35 and E-36 can be rewritten as follows:

$$D_r = \frac{w_{p,net}}{\kappa_r s}\left(s^2 + a_1 s + a_2\right) \tag{E-37}$$

$$D = s^3 + a_3 s^2 + a_4 s + a_5 \tag{E-38}$$

where

$$a_1 = \frac{\kappa_{ia}(\alpha_{ia}+\alpha_{oa})+\kappa_{oa}(\alpha_{ia}+\alpha_r)}{\kappa_{ia}\kappa_{oa}}$$

$$a_2 = \frac{\alpha_{ia}\alpha_r+\alpha_{oa}\alpha_r+\alpha_{ia}\alpha_{oa}}{\kappa_{ia}\kappa_{oa}}$$

$$a_3 = \frac{\kappa_{oa}\kappa_r(\alpha_{ia}+\alpha_r)+\kappa_{ia}\kappa_r(\alpha_{ia}+\alpha_{oa})+\kappa_{ia}\kappa_{oa}\alpha_r}{\kappa_{ia}\kappa_{oa}\kappa_r} \qquad \text{(E-39)}$$

$$a_4 = \frac{\kappa_r(\alpha_{ia}\alpha_{oa}+\alpha_{ia}\alpha_r+\alpha_{oa}\alpha_r)+\kappa_{ia}(\alpha_{ia}\alpha_r+\alpha_{oa}\alpha_r)+\kappa_{oa}(\alpha_{ia}\alpha_r)}{\kappa_{ia}\kappa_{oa}\kappa_r}$$

$$a_5 = \frac{\alpha_{ia}\alpha_{oa}\alpha_r}{\kappa_{ia}\kappa_{oa}\kappa_r}$$

Substituting Equations E-37 and E-38 in Equation E-32 gives

$$\overline{\Delta p_r} = \frac{D_r}{D} = \frac{w_{p,net}}{\kappa_r s}\frac{s^2+a_1 s+a_2}{s^3+a_3 s^2+a_4 s+a_5} \qquad \text{(E-40)}$$

The roots of the $(s^3+a_3 s^2+a_4 s+a_5)$ are found as follows:

$$Q = \frac{a_3^2-3a_4}{9}\ ,\quad R = \frac{2a_3^3-9a_3a_4+27a_5}{54}\ ,\quad \theta = arc\,cos\left(\frac{R}{\sqrt{Q^3}}\right) \qquad \text{(E-41)}$$

$$\mu_1 = 2\sqrt{Q}\ cos\left(\frac{\theta}{3}\right)+\frac{a_3}{3}$$

$$\mu_2 = 2\sqrt{Q}\ cos\left(\frac{\theta+2\pi}{3}\right)+\frac{a_3}{3} \qquad \text{(E-42)}$$

$$\mu_3 = 2\sqrt{Q}\ cos\left(\frac{\theta+4\pi}{3}\right)+\frac{a_3}{3}$$

Using Equation E-42, the following expression can be written

$$s^3+a_3 s^2+a_4 s+a_5 = (s+\mu_1)(s+\mu_2)(s+\mu_3) \qquad \text{(E-43)}$$

Substituting Equation E-43 into Equation E-40 gives

$$\overline{\Delta p_r} = \frac{w_{p,net}}{\kappa_r s}\frac{s^2+a_1 s+a_2}{(s+\mu_1)(s+\mu_2)(s+\mu_3)} \qquad \text{(E-44)}$$

In order to find the value of $\overline{\Delta p_r}$ in real space, inverse Laplace transform of Equation E-44 is obtained as follows:

$$\Delta p_r(t) = L^{-1}\left\{\overline{\Delta p_r}\right\} = \frac{w_{p,net}}{\kappa_r} L^{-1}\left\{\frac{s^2 + a_1 s + a_2}{(s+0)(s+\mu_1)(s+\mu_2)(s+\mu_3)}\right\} \tag{E-45}$$

Inverse Laplace transforms of the term $\frac{s^2 + a_1 s + a_2}{(s+0)(s+\mu_1)(s+\mu_2)(s+\mu_3)}$ in Equation E-45 is obtained by separation of the terms as follows:

$$\frac{s^2 + a_1 s + a_2}{(s+0)(s+\mu_1)(s+\mu_2)(s+\mu_3)} = \frac{A}{(s+0)} + \frac{B}{(s+\mu_1)} + \frac{C}{(s+\mu_2)} + \frac{D}{(s+\mu_3)} \tag{E-46}$$

$$A = lim_{s\to 0}\,(s+0)\frac{s^2 + a_1 s + a_2}{(s+0)(s+\mu_1)(s+\mu_2)(s+\mu_3)} = \frac{a_2}{\mu_1\mu_2\mu_3} \tag{E-47}$$

$$B = lim_{s\to -\mu_1}\,(s+\mu_1)\frac{s^2 + a_1 s + a_2}{(s+0)(s+\mu_1)(s+\mu_2)(s+\mu_3)} = -\frac{\mu_1^2 - a_1\mu_1 + a_2}{\mu_1(\mu_2 - \mu_1)(\mu_3 - \mu_1)} \tag{E-48}$$

$$C = lim_{s\to -\mu_2}\,(s+\mu_2)\frac{s^2 + a_1 s + a_2}{(s+0)(s+\mu_1)(s+\mu_2)(s+\mu_3)} = -\frac{\mu_2^2 - a_1\mu_2 + a_2}{\mu_2(\mu_1 - \mu_2)(\mu_3 - \mu_2)} \tag{E-49}$$

$$D = lim_{s\to -\mu_3}\,(s+\mu_3)\frac{s^2 + a_1 s + a_2}{(s+0)(s+\mu_1)(s+\mu_2)(s+\mu_3)} = -\frac{\mu_3^2 - a_1\mu_3 + a_2}{\mu_3(\mu_1 - \mu_3)(\mu_2 - \mu_3)} \tag{E-50}$$

$$\begin{aligned} &L^{-1}\left\{\frac{s^2 + a_1 s + a_2}{(s+0)(s+\mu_1)(s+\mu_2)(s+\mu_3)}\right\} \\ &= L^{-1}\left\{\frac{A}{(s+0)} + \frac{B}{(s+\mu_1)} + \frac{C}{(s+\mu_2)} + \frac{D}{(s+\mu_3)}\right\} \\ &= A\,L^{-1}\left\{\frac{1}{(s+0)}\right\} + B\,L^{-1}\left\{\frac{1}{(s+\mu_1)}\right\} + C\,L^{-1}\left\{\frac{1}{(s+\mu_2)}\right\} + D\,L^{-1}\left\{\frac{1}{(s+\mu_3)}\right\} \end{aligned} \tag{E-51}$$

$$L^{-1}\left\{\frac{1}{(s+0)}\right\}=1\ ,\ \ L^{-1}\left\{\frac{1}{(s+\mu_1)}\right\}=exp(-\mu_1 t)$$
$$L^{-1}\left\{\frac{1}{(s+\mu_2)}\right\}=exp(-\mu_2 t)\ ,\ \ L^{-1}\left\{\frac{1}{(s+\mu_3)}\right\}=exp(-\mu_3 t) \qquad \text{(E-52)}$$

Using Equation E-52 in Equation E-51 gives

$$L^{-1}\left\{\frac{s^2+a_1 s+a_2}{(s+0)(s+\mu_1)(s+\mu_2)(s+\mu_3)}\right\} \qquad \text{(E-53)}$$
$$= A+B\,exp(-\mu_1 t)+C\,exp(-\mu_2 t)+D\,exp(-\mu_3 t)$$

Substituting Equation E-53 into Equation E-45 gives

$$\Delta p_r(t)=\frac{w_{p,net}}{\kappa_r}[A+B\,exp(-\mu_1 t)+C\,exp(-\mu_2 t)+D\,exp(-\mu_3 t)] \qquad \text{(E-54)}$$

The reservoir pressure as a function of time is obtained by using Equation E-54 as below.

$$p_r(t)=p_i-\frac{w_{p,net}}{\kappa_r}[A+B\,exp(-\mu_1 t)+C\,exp(-\mu_2 t)+D\,exp(-\mu_3 t)] \qquad \text{(E-55)}$$

APPENDIX-F

1 RESERVOIR – 2 AQUIFERS WITHOUT RECHARGE SOURCE (3-TANK CLOSED SYSTEM)

Mass Balances on the reservoir and the aquifers, recharge of the reservoir and the aquifers, initial conditions are expressed as;

Mass Balance on the Outer Aquifer :

$$-w_{ia} = \kappa_{oa}\frac{dp_{oa}}{dt} \tag{F-1}$$

Mass Balance on the Inner Aquifer :

$$w_{ia} - w_r = \kappa_{ia}\frac{dp_{ia}}{dt} \tag{F-2}$$

Mass Balance on the Reservoir :

$$w_r - w_{p,net} = \kappa_r\frac{dp_r}{dt} \tag{F-3}$$

Recharge of the Inner Aquifer : $w_{ia} = \alpha_{ia}(p_{oa} - p_{ia})$ (F-4)

Recharge of the Reservoir : $w_r = \alpha_r(p_{ia} - p_r)$ (F-5)

Initial Conditions : $p_{ia} = p_{oa} = p_r = p_i \ @\ t = 0$ (F-6)

Substituting Equations F-4 and F-5 into Equations F-1, F-2, and F-3 gives

$$-\alpha_{ia}(p_{oa} - p_{ia}) = \kappa_{oa}\frac{dp_{oa}}{dt} \tag{F-7}$$

$$\alpha_{ia}(p_{oa} - p_{ia}) - \alpha_r(p_{ia} - p_r) = \kappa_{ia}\frac{dp_{ia}}{dt} \tag{F-8}$$

$$\alpha_r(p_{ia} - p_r) - w_{p,net} = \kappa_r \frac{dp_r}{dt} \tag{F-9}$$

Equations F-7, F-8, and F-9 can be written in terms of pressure changes. The pressure changes and their derivatives with respect to time are given by

$$\left.\begin{aligned}
\Delta p_{ia} = p_i - p_{ia} \;\Rightarrow\; p_{ia} = p_i - \Delta p_{ia} \;\Rightarrow\; \frac{d\,\Delta p_{ia}}{dt} = -\frac{dp_{ia}}{dt} \\
\Delta p_{oa} = p_i - p_{oa} \;\Rightarrow\; p_{oa} = p_i - \Delta p_{oa} \;\Rightarrow\; \frac{d\,\Delta p_{oa}}{dt} = -\frac{dp_{oa}}{dt} \\
\Delta p_r = p_i - p_r \;\Rightarrow\; p_r = p_i - \Delta p_r \;\Rightarrow\; \frac{d\,\Delta p_r}{dt} = -\frac{dp_r}{dt}
\end{aligned}\right\} \tag{F-10}$$

and initial conditions become

$$\left.\begin{aligned}
\Delta p_{ia}(t=0) = p_i - p_{ia}(t=0) = p_i - p_i = 0 \\
\Delta p_{oa}(t=0) = p_i - p_{oa}(t=0) = p_i - p_i = 0 \\
\Delta p_r(t=0) = p_i - p_r(t=0) = p_i - p_i = 0
\end{aligned}\right\} \tag{F-11}$$

Using Equation F-10 in Equations F-7, F-8, and F-9 gives

$$-\alpha_{ia}(p_i - \Delta p_{oa} - p_i + \Delta p_{ia}) = -\kappa_{oa} \frac{d\Delta p_{oa}}{dt} \tag{F-12}$$

$$\alpha_{ia}(p_i - \Delta p_{oa} - p_i + \Delta p_{ia}) - \alpha_r(p_i - \Delta p_{ia} - p_i + \Delta p_r) = -\kappa_{ia} \frac{d\Delta p_{ia}}{dt} \tag{F-13}$$

$$\alpha_r(p_i - \Delta p_{ia} - p_i + \Delta p_r) - w_{p,net} = -\kappa_r \frac{d\Delta p_r}{dt} \tag{F-14}$$

Equations F-12, F-13, and F-14 can be simplified and rearranged as follows:

$$-\alpha_{ia}(\Delta p_{ia} - \Delta p_{oa}) = -\kappa_{oa} \frac{d\Delta p_{oa}}{dt} \tag{F-15}$$

$$\alpha_{ia}(\Delta p_{ia} - \Delta p_{oa}) - \alpha_r(\Delta p_r - \Delta p_{ia}) = -\kappa_{ia} \frac{d\Delta p_{ia}}{dt} \tag{F-16}$$

$$\alpha_r(\Delta p_r - \Delta p_{ia}) - w_{p,net} = -\kappa_r \frac{d\Delta p_r}{dt} \tag{F-17}$$

or

$$\kappa_{oa}\frac{d\Delta p_{oa}}{dt}+\alpha_{ia}\,\Delta p_{oa}-\alpha_{ia}\Delta p_{ia}=0 \tag{F-18}$$

$$\kappa_{ia}\frac{d\Delta p_{ia}}{dt}-\alpha_{ia}\Delta p_{oa}+(\alpha_{ia}+\alpha_r)\Delta p_{ia}-\alpha_r\Delta p_r=0 \tag{F-19}$$

$$\kappa_r\frac{d\Delta p_r}{dt}-\alpha_r\Delta p_{ia}+\alpha_r\Delta p_r=w_{p,net} \tag{F-20}$$

Applying Laplace transformation (Erdélyi, 1954) to Equation F-18, F-19, and F-20 and using initial conditions (Equation F-11) gives

$$\kappa_{oa}\,s\,\overline{\Delta p_{oa}}+\alpha_{ia}\,\overline{\Delta p_{oa}}-\alpha_{ia}\,\overline{\Delta p_{ia}}=0 \tag{F-21}$$

$$\kappa_{ia}\,s\,\overline{\Delta p_{ia}}-\alpha_{ia}\,\overline{\Delta p_{oa}}+(\alpha_{ia}+\alpha_r)\overline{\Delta p_{ia}}-\alpha_r\,\overline{\Delta p_r}=0 \tag{F-22}$$

$$\kappa_r\,s\,\overline{\Delta p_r}-\alpha_r\,\overline{\Delta p_{ia}}+\alpha_r\,\overline{\Delta p_r}=\frac{w_{p,net}}{s} \tag{F-23}$$

where

$$\overline{\Delta p_{ia}}=\int_0^\infty e^{-st}\Delta p_{ia}\,d\tau\quad,\quad\overline{\Delta p_{oa}}=\int_0^\infty e^{-st}\Delta p_{oa}\,d\tau\quad,\quad\overline{\Delta p_r}=\int_0^\infty e^{-st}\Delta p_r\,d\tau \tag{F-24}$$

Rearranging Equations F-21, F-22, and F-23 gives

$$(\kappa_{oa}\,s+\alpha_{ia})\overline{\Delta p_{oa}}-\alpha_{ia}\,\overline{\Delta p_{ia}}=0 \tag{F-25}$$

$$-\alpha_{ia}\,\overline{\Delta p_{oa}}+(\kappa_{ia}\,s+\alpha_{ia}+\alpha_r)\overline{\Delta p_{ia}}-\alpha_r\,\overline{\Delta p_r}=0 \tag{F-26}$$

$$-\alpha_r\,\overline{\Delta p_{ia}}+(\kappa_r\,s+\alpha_r)\overline{\Delta p_r}=\frac{w_{p,net}}{s} \tag{F-27}$$

or

$$\left(s+\frac{\alpha_{ia}}{\kappa_{oa}}\right)\overline{\Delta p_{oa}}-\frac{\alpha_{ia}}{\kappa_{oa}}\overline{\Delta p_{ia}}=0 \tag{F-28}$$

$$-\frac{\alpha_{ia}}{\kappa_{ia}}\overline{\Delta p_{oa}}+\left(s+\frac{\alpha_{ia}+\alpha_r}{\kappa_{ia1}}\right)\overline{\Delta p_{ia}}-\frac{\alpha_r}{\kappa_{ia}}\overline{\Delta p_r}=0 \tag{F-29}$$

$$-\frac{\alpha_r}{\kappa_r}\overline{\Delta p_{ia}}+\left(s+\frac{\alpha_r}{\kappa_r}\right)\overline{\Delta p_r}=\frac{w_{p,net}}{\kappa_r}\frac{1}{s} \tag{F-30}$$

The solutions to three equations (Equation F-28, F-29, and F-30) with three unknows ($\overline{\Delta p_{ia}}$, $\overline{\Delta p_{oa}}$, $\overline{\Delta p_r}$) can be obtained by using Cramer's rule (Kreyszig, 1999) as follows:

$$\overline{\Delta p_{ia}}=\frac{D_{ia}}{D}\ ,\ \overline{\Delta p_{oa}}=\frac{D_{oa}}{D}\ ,\ \overline{\Delta p_r}=\frac{D_r}{D} \tag{F-31}$$

$$D_{ia}=\begin{vmatrix} s+\frac{\alpha_{ia}}{\kappa_{oa}} & 0 & 0 \\ -\frac{\alpha_{ia}}{\kappa_{ia}} & 0 & -\frac{\alpha_r}{\kappa_{ia}} \\ 0 & \frac{w_{p,net}}{\kappa_r}\frac{1}{s} & s+\frac{\alpha_r}{\kappa_r} \end{vmatrix} \tag{F-32}$$

$$D_{oa}=\begin{vmatrix} 0 & -\frac{\alpha_{ia}}{\kappa_{oa}} & 0 \\ 0 & s+\frac{\alpha_{ia}+\alpha_r}{\kappa_{ia}} & -\frac{\alpha_r}{\kappa_{ia}} \\ \frac{w_{p,net}}{\kappa_r}\frac{1}{s} & -\frac{\alpha_r}{\kappa_r} & s+\frac{\alpha_r}{\kappa_r} \end{vmatrix} \tag{F-33}$$

$$D_r = \begin{vmatrix} s + \frac{\alpha_{ia}}{\kappa_{oa}} & -\frac{\alpha_{ia}}{\kappa_{oa}} & 0 \\ -\frac{\alpha_{ia}}{\kappa_{ia}} & s + \frac{\alpha_{ia} + \alpha_r}{\kappa_{ia}} & 0 \\ 0 & -\frac{\alpha_r}{\kappa_r} & \frac{w_{p,net}}{\kappa_r}\frac{1}{s} \end{vmatrix}$$

$$= \frac{w_{p,net}}{\kappa_r s}\left\{ s^2 + \left[\frac{\kappa_{oa}(\alpha_{ia} + \alpha_r) + \kappa_{ia}\alpha_{ia}}{\kappa_{ia}\kappa_{oa}} \right] s + \frac{\alpha_{ia}\alpha_r}{\kappa_{ia}\kappa_{oa}} \right\} \tag{F-34}$$

$$D = \begin{vmatrix} s + \frac{\alpha_{ia}}{\kappa_{oa}} & -\frac{\alpha_{ia}}{\kappa_{oa}} & 0 \\ -\frac{\alpha_{ia}}{\kappa_{ia}} & s + \frac{\alpha_{ia} + \alpha_r}{\kappa_{ia}} & -\frac{\alpha_r}{\kappa_{ia}} \\ 0 & -\frac{\alpha_r}{\kappa_r} & s + \frac{\alpha_r}{\kappa_r} \end{vmatrix}$$

$$= s^3 + \left[\frac{\kappa_{oa}\kappa_r(\alpha_{ia} + \alpha_r) + \kappa_{ia}\kappa_r\alpha_{ia} + \kappa_{ia}\kappa_{oa}\alpha_r}{\kappa_{ia}\kappa_{oa}\kappa_r} \right] s^2 + \left[\frac{(\kappa_{ia} + \kappa_{oa} + \kappa_r)\alpha_{ia}\alpha_r}{\kappa_{ia}\kappa_{oa}\kappa_r} \right] s \tag{F-35}$$

Equations F-34 and F-35 can be rewritten as follows:

$$D_r = \frac{w_{p,net}}{\kappa_r s}\left(s^2 + a_1 s + a_2 \right) \tag{F-36}$$

$$D = s^3 + a_3 s^2 + a_4 s = s\left(s^2 + a_3 s + a_4 \right) \tag{F-37}$$

where

$$\begin{aligned} a_1 &= \frac{\kappa_{oa}(\alpha_{ia} + \alpha_r) + \kappa_{ia}\alpha_{ia}}{\kappa_{ia}\kappa_{oa}} \\ a_2 &= \frac{\alpha_{ia}\alpha_r}{\kappa_{ia}\kappa_{oa}} \\ a_3 &= \frac{\kappa_{oa}\kappa_r(\alpha_{ia} + \alpha_r) + \kappa_{ia}\kappa_r\alpha_{ia} + \kappa_{ia}\kappa_{oa}\alpha_r}{\kappa_{ia}\kappa_{oa}\kappa_r} \\ a_4 &= \frac{(\kappa_{ia} + \kappa_{oa} + \kappa_r)\alpha_{ia}\alpha_r}{\kappa_{ia}\kappa_{oa}\kappa_r} \end{aligned} \tag{F-38}$$

Substituting Equations F-36 and F-37 into Equation F-31 gives

$$\overline{\Delta p_r} = \frac{D_r}{D} = \frac{w_{p,net}}{\kappa_r s} \frac{s^2 + a_1 s + a_2}{s\left(s^2 + a_3 s + a_4\right)} \tag{F-39}$$

or

$$\begin{aligned} \overline{\Delta p_r} &= \frac{w_{p,net}}{\kappa_r} \frac{s^2 + a_1 s + a_2}{s^2\left(s^2 + a_3 s + a_4\right)} \\ &= \frac{w_{p,net}}{\kappa_r} \left\{ \frac{1}{\left(s^2 + a_3 s + a_4\right)} + \frac{a_1}{s\left(s^2 + a_3 s + a_4\right)} + \frac{a_2}{s^2\left(s^2 + a_3 s + a_4\right)} \right\} \end{aligned} \tag{F-40}$$

In order to find the value of $\overline{\Delta p_r}$ in real space, inverse Laplace transform of Equation F-40 is obtained as follows:

$$\begin{aligned} \Delta p_r(t) = L^{-1}\left\{ \overline{\Delta p_r} \right\} &= \frac{w_{p,net}}{\kappa_r} L^{-1}\left\{ \frac{1}{\left(s^2 + a_3 s + a_4\right)} \right\} + \frac{w_{p,net}}{\kappa_r} a_1 L^{-1}\left\{ \frac{1}{s\left(s^2 + a_3 s + a_4\right)} \right\} \\ &+ \frac{w_{p,net}}{\kappa_r} a_2 L^{-1}\left\{ \frac{1}{s^2\left(s^2 + a_3 s + a_4\right)} \right\} \end{aligned} \tag{F-41}$$

The roots of the $\left(s^2 + a_3 s + a_4\right)$ are obtained as follows:

$$\begin{aligned} \mu_1 &= \frac{a_3 + \sqrt{a_3^2 - 4a_4}}{2} \\ \mu_2 &= \frac{a_3 - \sqrt{a_3^2 - 4a_4}}{2} \end{aligned} \tag{F-42}$$

Using Equation F-42, the following expression can be written

$$s^2 + a_3 s + a_4 = (s + \mu_1)(s + \mu_2) \tag{F-43}$$

Substituting Equation F-43 into Equation F-41 gives

$$\Delta p_r(t) = \frac{w_{p,net}}{\kappa_r} L^{-1}\left\{\frac{1}{(s+\mu_1)(s+\mu_2)}\right\} + \frac{w_{p,net}}{\kappa_r} a_1 L^{-1}\left\{\frac{1}{s(s+\mu_1)(s+\mu_2)}\right\} + \frac{w_{p,net}}{\kappa_r} a_2 L^{-1}\left\{\frac{1}{s^2(s+\mu_1)(s+\mu_2)}\right\} \quad \text{(F-44)}$$

Inverse Laplace transform of the term of $\frac{1}{(s+\mu_1)(s+\mu_2)}$ in Equation F-44 is obtained by using the formula given in Equation C-39. Applying C-39 in Equation F-44 gives

$$a = -\mu_1, \quad b = -\mu_2 \quad \text{(F-45)}$$

and

$$L^{-1}\left\{\frac{1}{(s+\mu_1)(s+\mu_2)}\right\} = \frac{1}{\mu_2 - \mu_1}[exp(-\mu_1 t) - exp(-\mu_2 t)] \quad \text{(F-46)}$$

Inverse Laplace transform of the term of $\frac{1}{s(s+\mu_1)(s+\mu_2)}$ in Equation F-44 is obtained by using the formula given in Equation C-33. Applying C-33 in Equation F-44 gives

$$f(s) = \frac{1}{s}, \quad g(s) = \frac{1}{(s+\mu_1)(s+\mu_2)} \quad \text{(F-47)}$$

and

$$F(\tau) = L^{-1}\left\{\frac{1}{s}\right\} = 1$$

$$G(t-\tau) = L^{-1}\left\{\frac{1}{(s+\mu_1)(s+\mu_2)}\right\} = \frac{1}{\mu_2 - \mu_1}\{exp[-\mu_1(t-\tau)] - exp[-\mu_2(t-\tau)]\} \quad \text{(F-48)}$$

Substituting Equation F-48 into Equation C-33 gives

$$L^{-1}\left\{\frac{1}{s(s+\mu_1)(s+\mu_2)}\right\} = \int_0^t \frac{1}{\mu_2-\mu_1}\{exp[-\mu_1(t-\tau)] - exp[-\mu_2(t-\tau)]\}\, d\tau$$

$$= \frac{1}{\mu_2-\mu_1}\left\{\frac{1-exp(-\mu_1 t)}{\mu_1} - \frac{1-exp(-\mu_2 t)}{\mu_2}\right\} \tag{F-49}$$

Inverse Laplace transform of the term of $\frac{1}{s^2(s+\mu_1)(s+\mu_2)}$ in Equation F-44 is obtained by using the formula given in Equation C-33. Applying C-33 in Equation F-44 gives

$$f(s) = \frac{1}{s^2},\quad g(s) = \frac{1}{(s+\mu_1)(s+\mu_2)} \tag{F-50}$$

and

$$F(\tau) = L^{-1}\left\{\frac{1}{s^2}\right\} = \tau$$

$$G(t-\tau) = L^{-1}\left\{\frac{1}{(s+\mu_1)(s+\mu_2)}\right\} \tag{F-51}$$

$$= \frac{1}{\mu_2-\mu_1}\{exp[-\mu_1(t-\tau)] - exp[-\mu_2(t-\tau)]\}$$

Substituting Equation F-51 into Equation C-33 gives

$$L^{-1}\left\{\frac{1}{s^2(s+\mu_1)(s+\mu_2)}\right\}$$

$$= \int_0^t \tau \frac{1}{\mu_2-\mu_1}\{exp[-\mu_1(t-\tau)] - exp[-\mu_2(t-\tau)]\}\, d\tau \tag{F-52}$$

$$= \frac{t}{\mu_1\mu_2} + \frac{1}{\mu_2-\mu_1}\left\{\frac{exp(-\mu_1 t)-1}{\mu_1^2} - \frac{exp(-\mu_2 t)-1}{\mu_2^2}\right\}$$

Substituting Equations F-46, F-49, and F-52 into Equation F-44 gives the reservoir pressure change as a function of time as follows:

$$\Delta p_r(t) = \frac{w_{p,net}}{\kappa_r}\left\{\frac{1}{\mu_2-\mu_1}\left[exp(-\mu_1 t)-exp(-\mu_2 t)\right]\right\}$$
$$+\frac{w_{p,net}}{\kappa_r}a_1\left\{\frac{1}{\mu_2-\mu_1}\left[\frac{1-exp(-\mu_1 t)}{\mu_1}-\frac{1-exp(-\mu_2 t)}{\mu_2}\right]\right\} \quad \text{(F-53)}$$
$$+\frac{w_{p,net}}{\kappa_r}a_2\left\{\frac{t}{\mu_1\mu_2}+\frac{1}{\mu_2-\mu_1}\left[\frac{exp(-\mu_1 t)-1}{\mu_1^2}-\frac{exp(-\mu_2 t)-1}{\mu_2^2}\right]\right\}$$

or

$$\Delta p_r(t) = \frac{w_{p,net}}{\kappa_r}a_2\left\{\frac{t}{\mu_1\mu_2}+\frac{1}{\mu_2-\mu_1}\left[\frac{exp(-\mu_1 t)-1}{\mu_1^2}-\frac{exp(-\mu_2 t)-1}{\mu_2^2}\right]\right\}$$
$$+\frac{w_{p,net}}{\kappa_r}a_1\left\{\frac{1}{\mu_2-\mu_1}\left[\frac{1-exp(-\mu_1 t)}{\mu_1}-\frac{1-exp(-\mu_2 t)}{\mu_2}\right]\right\} \quad \text{(F-54)}$$
$$+\frac{w_{p,net}}{\kappa_r}\left\{\frac{1}{\mu_2-\mu_1}\left[exp(-\mu_1 t)-exp(-\mu_2 t)\right]\right\}$$

The reservoir pressure as a function of time is obtained by using Equation F-54 as below.

$$p_r(t) = p_{i-}\frac{w_{p,net}}{\kappa_r}a_2\left\{\frac{t}{\mu_1\mu_2}+\frac{1}{\mu_2-\mu_1}\left[\frac{exp(-\mu_1 t)-1}{\mu_1^2}-\frac{exp(-\mu_2 t)-1}{\mu_2^2}\right]\right\}$$
$$-\frac{w_{p,net}}{\kappa_r}a_1\left\{\frac{1}{\mu_2-\mu_1}\left[\frac{1-exp(-\mu_1 t)}{\mu_1}-\frac{1-exp(-\mu_2 t)}{\mu_2}\right]\right\} \quad \text{(F-55)}$$
$$-\frac{w_{p,net}}{\kappa_r}\left\{\frac{1}{\mu_2-\mu_1}\left[exp(-\mu_1 t)-exp(-\mu_2 t)\right]\right\}$$

APPENDIX-G

2 RESERVOIR TANK MODEL WITHOUT AQUIFER (WITH INITIAL HYDRAULIC EQUILIBRIUM)

Mass balances on the shallow and deep reservoirs, recharges of the reservoirs, initial conditions are expresser as;

Mass Balance on the Shallow Reservoir :

$$w_{r1} + w_{r12} - w_{p,net1} = \kappa_{r1} \frac{dp_{r1}}{dt} \qquad \text{(G-1)}$$

Mass Balance on the Deep Reservoir :

$$w_{r2} - w_{r12} - w_{p,net2} = \kappa_{r2} \frac{dp_{r2}}{dt} \qquad \text{(G-2)}$$

Recharge of the Shallow Reservoir : $w_{r1} = \alpha_{r1}(p_i - p_{r1})$ (G-3)

Recharge of the Deep Reservoir : $w_{r2} = \alpha_{r2}(p_i - p_{r2})$ (G-4)

Recharge between the Shallow and Deep Reservoirs :

$$w_{r12} = \alpha_{r12}(p_{r2} - p_{r1}) \qquad \text{(G-5)}$$

Initial Conditions : $p_{r1} = p_{r2} = p_i \ @\ t = 0$ (G-6)

Substituting Equations G-3, G-4, and G-5 into Equations G-1 and G-2 gives

$$\alpha_{r1}(p_i - p_{r1}) + \alpha_{r12}(p_{r2} - p_{r1}) - w_{p,net1} = \kappa_{r1} \frac{dp_{r1}}{dt} \qquad \text{(G-7)}$$

$$\alpha_{r2}(p_i - p_{r2}) - \alpha_{r12}(p_{r2} - p_{r1}) - w_{p,net2} = \kappa_{r2} \frac{dp_{r2}}{dt} \qquad \text{(G-8)}$$

Equations G-7 and G-8 can be written in terms of pressure changes. The pressure changes and their derivatives with respect to time are given by

$$\left.\begin{aligned} \Delta p_{r1} = p_i - p_{r1} \Rightarrow p_{r1} = p_i - \Delta p_{r1} \Rightarrow \frac{d\,\Delta p_{r1}}{dt} = -\frac{dp_{r1}}{dt} \\ \Delta p_{r2} = p_i - p_{r2} \Rightarrow p_{r2} = p_i - \Delta p_{r2} \Rightarrow \frac{d\,\Delta p_{r2}}{dt} = -\frac{dp_{r2}}{dt} \end{aligned}\right\} \quad \text{(G-9)}$$

and initial conditions become

$$\left.\begin{aligned} \Delta p_{r1}(t=0) = p_i - p_{r1}(t=0) = p_i - p_i = 0 \\ \Delta p_{r2}(t=0) = p_i - p_{r2}(t=0) = p_i - p_i = 0 \end{aligned}\right\} \quad \text{(G-10)}$$

Using Equation G-9 in Equations G-7 and G-8 gives

$$\alpha_{r1}(p_i - p_i + \Delta p_{r1}) + \alpha_{r12}(p_i - \Delta p_{r2} - p_i + \Delta p_{r1}) - w_{p,net1} = -\kappa_{r1}\frac{d\Delta p_{r1}}{dt} \quad \text{(G-11)}$$

$$\alpha_{r2}(p_i - p_i + \Delta p_{r2}) - \alpha_{r12}(p_i - \Delta p_{r2} - p_i + \Delta p_{r1}) - w_{p,net2} = -\kappa_{r2}\frac{d\Delta p_{r2}}{dt} \quad \text{(G-12)}$$

Equations G-11 and G-12 can be simplified and rearranged as follows:

$$\alpha_{r1}\Delta p_{r1} + \alpha_{r12}(\Delta p_{r1} - \Delta p_{r2}) - w_{p,net1} = -\kappa_{r1}\frac{d\Delta p_{r1}}{dt} \quad \text{(G-13)}$$

$$\alpha_{r2}\Delta p_{r2} - \alpha_{r12}(\Delta p_{r1} - \Delta p_{r2}) - w_{p,net2} = -\kappa_{r2}\frac{d\Delta p_{r2}}{dt} \quad \text{(G-14)}$$

or

$$\kappa_{r1}\frac{d\Delta p_{r1}}{dt} + (\alpha_{r1} + \alpha_{r12})\Delta p_{r1} - \alpha_{r12}\Delta p_{r2} = w_{p,net1} \quad \text{(G-15)}$$

$$\kappa_{r2}\frac{d\Delta p_{r2}}{dt} - \alpha_{r12}\Delta p_{r1} + (\alpha_{r2} + \alpha_{r12})\Delta p_{r2} = w_{p,net2} \quad \text{(G-16)}$$

Applying Laplace transformation (Erdélyi, 1954) to Equations G-15 and G-16 and using initial conditions (Equation G-10) gives

$$\kappa_{r1}\, s\, \overline{\Delta p_{r1}} + (\alpha_{r1} + \alpha_{r12})\, \overline{\Delta p_{r1}} - \alpha_{r12}\, \overline{\Delta p_{r2}} = \frac{w_{p,net1}}{s} \tag{G-17}$$

$$\kappa_{r2}\, s\, \overline{\Delta p_{r2}} - \alpha_{r12}\, \overline{\Delta p_{r1}} + (\alpha_{r2} + \alpha_{r12})\, \overline{\Delta p_{r2}} = \frac{w_{p,net2}}{s} \tag{G-18}$$

where

$$\overline{\Delta p_{r1}} = \int_0^\infty e^{-st} \Delta p_{r1}\, d\tau \quad , \quad \overline{\Delta p_{r2}} = \int_0^\infty e^{-st} \Delta p_{r2}\, d\tau \tag{G-19}$$

Rearranging Equations G-17 and G-18 gives

$$(\kappa_{r1}\, s + \alpha_{r1} + \alpha_{r12})\, \overline{\Delta p_{r1}} - \alpha_{r12}\, \overline{\Delta p_{r2}} = \frac{w_{p,net1}}{s} \tag{G-20}$$

$$-\alpha_{r12}\, \overline{\Delta p_{r1}} + (\kappa_{r2}\, s + \alpha_{r2} + \alpha_{r12})\, \overline{\Delta p_{r2}} = \frac{w_{p,net2}}{s} \tag{G-21}$$

or

$$\left(s + \frac{\alpha_{r1} + \alpha_{r12}}{\kappa_{r1}} \right) \overline{\Delta p_{r1}} - \frac{\alpha_{r12}}{\kappa_{r1}}\, \overline{\Delta p_{r2}} = \frac{w_{p,net1}}{\kappa_{r1}} \frac{1}{s} \tag{G-22}$$

$$-\frac{\alpha_{r12}}{\kappa_{r2}}\, \overline{\Delta p_{r1}} + \left(s + \frac{\alpha_{r2} + \alpha_{r12}}{\kappa_{r2}} \right) \overline{\Delta p_{r2}} = \frac{w_{p,net2}}{\kappa_{r2}} \frac{1}{s} \tag{G-23}$$

The solutions to two equations (Equations G-22 and G-23) with two unknowns ($\overline{\Delta p_{r1}}, \overline{\Delta p_{r2}}$) can be obtained by using Cramer's rule (Kreyszig, 1999) as follows:

$$\overline{\Delta p_{r1}} = \frac{D_{r1}}{D} \ , \ \overline{\Delta p_{r2}} = \frac{D_{r2}}{D} \tag{G-24}$$

$$D_{r1} = \begin{vmatrix} \dfrac{w_{p,net1}}{\kappa_{r1}} \dfrac{1}{s} & -\dfrac{\alpha_{r12}}{\kappa_{r1}} \\ \dfrac{w_{p,net2}}{\kappa_{r2}} \dfrac{1}{s} & s + \dfrac{\alpha_{r2} + \alpha_{r12}}{\kappa_{r2}} \end{vmatrix} = \frac{w_{p,net1}}{\kappa_{r1}} + \left[\frac{w_{p,net1}(\alpha_{r2} + \alpha_{r12}) + w_{p,net2}\alpha_{r12}}{\kappa_{r1}\kappa_{r2}} \right] \frac{1}{s} \tag{G-25}$$

$$D_{r2}=\begin{vmatrix} s+\dfrac{\alpha_{r1}+\alpha_{r12}}{\kappa_{r1}} & \dfrac{w_{p,net1}}{\kappa_{r1}}\dfrac{1}{s} \\ -\dfrac{\alpha_{r12}}{\kappa_{r2}} & \dfrac{w_{p,net2}}{\kappa_{r2}}\dfrac{1}{s} \end{vmatrix}=\frac{w_{p,net2}}{\kappa_{r2}}+\left[\frac{w_{p,net2}(\alpha_{r1}+\alpha_{r12})+w_{p,net1}\alpha_{r12}}{\kappa_{r1}\kappa_{r2}}\right]\frac{1}{s} \tag{G-26}$$

$$\begin{aligned} D&=\begin{vmatrix} s+\dfrac{\alpha_{r1}+\alpha_{r12}}{\kappa_{r1}} & -\dfrac{\alpha_{r12}}{\kappa_{r1}} \\ -\dfrac{\alpha_{r12}}{\kappa_{r2}} & s+\dfrac{\alpha_{r2}+\alpha_{r12}}{\kappa_{r2}} \end{vmatrix} \\ &=s^2+\left(\frac{\alpha_{r1}+\alpha_{r12}}{\kappa_{r1}}+\frac{\alpha_{r2}+\alpha_{r12}}{\kappa_{r2}}\right)s+\frac{\alpha_{r1}\alpha_{r2}+\alpha_{r12}(\alpha_{r1}+\alpha_{r2})}{\kappa_{r1}\kappa_{r2}} \end{aligned} \tag{G-27}$$

Equations G-25-, G-26, and G-27 can be written as follows:

$$D_{r1}=\frac{w_{p,net1}}{\kappa_{r1}}+\left[w_{p,net1}a_1+w_{p,net2}a_2\right]\frac{1}{s} \tag{G-28}$$

$$D_{r2}=\frac{w_{p,net2}}{\kappa_{r2}}+\left[w_{p,net2}a_3+w_{p,net1}a_2\right]\frac{1}{s} \tag{G-29}$$

$$D=s^2+a_4s+a_5 \tag{G-30}$$

where

$$\begin{aligned} a_1&=\frac{\alpha_{r2}+\alpha_{r12}}{\kappa_{r1}\kappa_{r2}}\quad,\quad a_2=\frac{\alpha_{r12}}{\kappa_{r1}\kappa_{r2}}\quad,\quad a_3=\frac{\alpha_{r1}+\alpha_{r12}}{\kappa_{r1}\kappa_{r2}} \\ a_4&=\frac{\alpha_{r1}+\alpha_{r12}}{\kappa_{r1}}+\frac{\alpha_{r2}+\alpha_{r12}}{\kappa_{r2}}\quad,\quad a_5=\frac{\alpha_{r1}\alpha_{r2}+\alpha_{r12}(\alpha_{r1}+\alpha_{r2})}{\kappa_{r1}\kappa_{r2}} \end{aligned} \tag{G-31}$$

Substituting Equations G-28, G-29, and G-30 into G-24 gives

$$\overline{\Delta p_{r1}}=\frac{D_{r1}}{D}=\frac{\dfrac{w_{p,net1}}{\kappa_{r1}}+\left[w_{p,net1}a_1+w_{p,net2}a_2\right]\dfrac{1}{s}}{s^2+a_4s+a_5} \tag{G-32}$$

$$\overline{\Delta p_{r2}}=\frac{D_{r2}}{D}=\frac{\dfrac{w_{p,net2}}{\kappa_{r2}}+\left[w_{p,net2}a_3+w_{p,net1}a_2\right]\dfrac{1}{s}}{s^2+a_4s+a_5} \tag{G-33}$$

The roots of the $(s^2 + a_4 s + a_5)$ are found as follows:

$$\left.\begin{aligned} \mu_1 &= \frac{a_4 + \sqrt{a_4^2 - 4a_5}}{2} \\ \mu_2 &= \frac{a_4 - \sqrt{a_4^2 - 4a_5}}{2} \end{aligned}\right\} \tag{G-34}$$

Using Equation G-34, the following expression can be written

$$s^2 + a_4 s + a_5 = (s + \mu_1)(s + \mu_2) \tag{G-35}$$

Substituing Equation G-35 into Equations G-32 and G-33 gives

$$\overline{\Delta p_{r1}} = \frac{\frac{w_{p,net1}}{\kappa_{r1}} s + w_{p,net1} a_1 + w_{p,net2} a_2}{(s+0)(s+\mu_1)(s+\mu_2)} \tag{G-36}$$

$$\overline{\Delta p_{r2}} = \frac{\frac{w_{p,net2}}{\kappa_{r2}} s + w_{p,net2} a_3 + w_{p,net1} a_2}{(s+0)(s+\mu_1)(s+\mu_2)} \tag{G-37}$$

In order to find the values of Δp_{r1} and Δp_{r2} in real space, inverse Laplace transform of Equations G-36 and G-37 are obtained as follows:

$$\Delta p_{r1} = L^{-1}\left\{\overline{\Delta p_{r1}}\right\} = L^{-1}\left\{\frac{\frac{w_{p,net1}}{\kappa_{r1}} s + w_{p,net1} a_1 + w_{p,net2} a_2}{(s+0)(s+\mu_1)(s+\mu_2)}\right\} \tag{G-38}$$

$$\Delta p_{r2} = L^{-1}\left\{\overline{\Delta p_{r2}}\right\} = L^{-1}\left\{\frac{\frac{w_{p,net2}}{\kappa_{r2}} s + w_{p,net2} a_3 + w_{p,net1} a_2}{(s+0)(s+\mu_1)(s+\mu_2)}\right\} \tag{G-39}$$

Inverse Laplace transform of the term of $\dfrac{\dfrac{w_{p,net1}}{\kappa_{r1}}s + w_{p,net1}a_1 + w_{p,net2}a_2}{(s+0)(s+\mu_1)(s+\mu_2)}$ in Equation G-38 is obtained by using the formula given in Equation B-36. Applying B-36 in Equation G-38 gives

$$\begin{aligned} &\lambda = 0 \;,\; \mu = w_{p,net1}/\kappa_{r1} \;,\; \nu = w_{p,net1}a_1 + w_{p,net2}a_2 \\ &\alpha = 0 \;,\; \beta = \mu_1 \;,\; \gamma = \mu_2 \end{aligned} \tag{G-40}$$

and

$$\begin{aligned} L^{-1}\left\{\frac{\dfrac{w_{p,net1}}{\kappa_{r1}}s + w_{p,net1}a_1 + w_{p,net2}a_2}{(s+0)(s+\mu_1)(s+\mu_2)}\right\} &= \frac{w_{p,net1}a_1 + w_{p,net2}a_2}{\mu_1\mu_2} \\ &- \frac{(w_{p,net1}/\kappa_{r1})\mu_1 - w_{p,net1}a_1 - w_{p,net2}a_2}{\mu_1(\mu_1-\mu_2)}exp(-\mu_1 t) \\ &- \frac{(w_{p,net1}/\kappa_{r1})\mu_2 - w_{p,net1}a_1 - w_{p,net2}a_2}{\mu_2(\mu_2-\mu_1)}exp(-\mu_2 t) \end{aligned} \tag{G-41}$$

Substituting Equation G-41 into Equation G-38 and rearranging gives

$$\begin{aligned} \Delta p_{r1}(t) = {} & w_{p,net1}\left[\frac{a_1}{\mu_1\mu_2} - \frac{\mu_1 - \kappa_{r1}a_1}{\kappa_{r1}\mu_1(\mu_1-\mu_2)}exp(-\mu_1 t) + \frac{\mu_2 - \kappa_{r1}a_1}{\kappa_{r1}\mu_2(\mu_1-\mu_2)}exp(-\mu_2 t)\right] \\ & + w_{p,net2}\left[\frac{a_2}{\mu_1\mu_2} + \frac{a_2}{\mu_1(\mu_1-\mu_2)}exp(-\mu_1 t) - \frac{a_2}{\mu_2(\mu_1-\mu_2)}exp(-\mu_2 t)\right] \end{aligned} \tag{G-42}$$

Similiarly, inverse Laplace transform of the term of $\dfrac{\dfrac{w_{p,net2}}{\kappa_{r2}}s + w_{p,net2}a_3 + w_{p,net1}a_2}{(s+0)(s+\mu_1)(s+\mu_2)}$ in Equation G-39 is obtained by using the formula given in Equation B-36. Applying B-36 in Equation G-39 gives

$$\begin{aligned} &\lambda = 0 \;,\; \mu = w_{p,net2}/\kappa_{r2} \;,\; \nu = w_{p,net2}a_3 + w_{p,net1}a_2 \\ &\alpha = 0 \;,\; \beta = \mu_1 \;,\; \gamma = \mu_2 \end{aligned} \tag{G-43}$$

and

$$L^{-1}\left\{\frac{\frac{w_{p,net2}}{\kappa_{r2}}s + w_{p,net2}a_3 + w_{p,net1}a_2}{(s+0)(s+\mu_1)(s+\mu_2)}\right\} = \frac{w_{p,net2}a_3 + w_{p,net1}a_2}{\mu_1\mu_2}$$
$$-\frac{(w_{p,net2}/\kappa_{r2})\mu_1 - w_{p,net2}a_3 - w_{p,net1}a_2}{\mu_1(\mu_1-\mu_2)}exp(-\mu_1 t)$$
$$-\frac{(w_{p,net2}/\kappa_{r2})\mu_2 - w_{p,net2}a_3 - w_{p,net1}a_2}{\mu_2(\mu_2-\mu_1)}exp(-\mu_2 t) \quad \text{(G-44)}$$

Substituting Equation G-44 into Equation G-39 and rearranging gives

$$\Delta p_{r2}(t) = w_{p,net1}\left[\frac{a_2}{\mu_1\mu_2} + \frac{a_2}{\mu_1(\mu_1-\mu_2)}exp(-\mu_1 t) - \frac{a_2}{\mu_2(\mu_1-\mu_2)}exp(-\mu_2 t)\right]$$
$$+ w_{p,net2}\left[\frac{a_3}{\mu_1\mu_2} - \frac{\mu_1-\kappa_{r2}a_3}{\kappa_{r2}\mu_1(\mu_1-\mu_2)}exp(-\mu_1 t) + \frac{\mu_2-\kappa_{r2}a_3}{\kappa_{r2}\mu_2(\mu_1-\mu_2)}exp(-\mu_2 t)\right] \quad \text{(G-45)}$$

The shallow and deep reservoirs pressures as a function of time are obtained by using Equations G-42 and G-45 as below.

$$p_{r1}(t) = p_i - \left\{\begin{array}{l} w_{p,net1}\left[\begin{array}{l}\frac{a_1}{\mu_1\mu_2} - \frac{\mu_1-\kappa_{r1}a_1}{\kappa_{r1}\mu_1(\mu_1-\mu_2)}exp(-\mu_1 t) \\ + \frac{\mu_2-\kappa_{r1}a_1}{\kappa_{r1}\mu_2(\mu_1-\mu_2)}exp(-\mu_2 t)\end{array}\right] \\ + w_{p,net2}\left[\begin{array}{l}\frac{a_2}{\mu_1\mu_2} + \frac{a_2}{\mu_1(\mu_1-\mu_2)}exp(-\mu_1 t) \\ - \frac{a_2}{\mu_2(\mu_1-\mu_2)}exp(-\mu_2 t)\end{array}\right]\end{array}\right\} \quad \text{(G-46)}$$

$$p_{r2}(t) = p_i - \left\{\begin{array}{l} w_{p,net1}\left[\begin{array}{l}\frac{a_2}{\mu_1\mu_2} + \frac{a_2}{\mu_1(\mu_1-\mu_2)}exp(-\mu_1 t) \\ - \frac{a_2}{\mu_2(\mu_1-\mu_2)}exp(-\mu_2 t)\end{array}\right] \\ + w_{p,net2}\left[\begin{array}{l}\frac{a_3}{\mu_1\mu_2} - \frac{\mu_1-\kappa_{r2}a_3}{\kappa_{r2}\mu_1(\mu_1-\mu_2)}exp(-\mu_1 t) \\ + \frac{\mu_2-\kappa_{r2}a_3}{\kappa_{r2}\mu_2(\mu_1-\mu_2)}exp(-\mu_2 t)\end{array}\right]\end{array}\right\} \quad \text{(G-47)}$$

APPENDIX-H

2 RESERVOIR TANK MODEL WITHOUT AQUIFER (WITHOUT INITIAL HYDRAULIC EQUILIBRIUM)

Mass balances on the shallow and deep reservoirs, recharges of the reservoirs, initial conditions are expressed as;

Mass Balance on the Shallow Reservoir :

$$w_{r1} + w_{r12} - w_{p,net1} = \kappa_{r1} \frac{dp_{r1}}{dt} \tag{H-1}$$

Mass Balance on the Deep Reservoir :

$$w_{r2} - w_{r12} - w_{p,net2} = \kappa_{r2} \frac{dp_{r2}}{dt} \tag{H-2}$$

Recharge of the Shallow Reservoir : $w_{r1} = \alpha_{r1}(p_i - p_{r1})$ (H-3)

Recharge of the Deep Reservoir : $w_{r2} = \alpha_{r2}(p_i - p_{r2})$ (H-4)

Recharge between the Shallow and Deep Reservoirs :

$$w_{r12} = \alpha_{r12}(p_{r2} - p_{r1}) \tag{H-5}$$

Initial Conditions :

$$\left.\begin{aligned} p_{r1} &= p_{r1i} \ @\, t = 0 \\ p_{r2} &= p_{r2i} \ @\, t = 0 \end{aligned}\right\} \tag{H-6}$$

Substituting Equations H-3, H-4, and H-5 into Equations H-1 and H-2 gives

$$\alpha_{r1}(p_i - p_{r1}) + \alpha_{r12}(p_{r2} - p_{r1}) - w_{p,net1} = \kappa_{r1} \frac{dp_{r1}}{dt} \tag{H-7}$$

$$\alpha_{r2}(p_i - p_{r2}) - \alpha_{r12}(p_{r2} - p_{r1}) - w_{p,net2} = \kappa_{r2} \frac{dp_{r2}}{dt} \tag{H-8}$$

Equations H-7 and H-8 can be written in terms of pressure changes. The pressure changes and their derivatives with respect to time are given by

$$\left.\begin{aligned} \Delta p_{r1} = p_{r1i} - p_{r1} \;\Rightarrow\; p_{r1} = p_{r1i} - \Delta p_{r1} \;\Rightarrow\; \frac{d\,\Delta p_{r1}}{dt} = -\frac{dp_{r1}}{dt} \\ \Delta p_{r2} = p_{r2i} - p_{r2} \;\Rightarrow\; p_{r2} = p_{r2i} - \Delta p_{r2} \;\Rightarrow\; \frac{d\,\Delta p_{r2}}{dt} = -\frac{dp_{r2}}{dt} \end{aligned}\right\} \quad \text{(H-9)}$$

and initial conditions

$$\left.\begin{aligned} \Delta p_{r1}(t=0) = p_{r1i} - p_{r1}(t=0) = p_{r1i} - p_{r1i} = 0 \\ \Delta p_{r2}(t=0) = p_{r2i} - p_{r2}(t=0) = p_{r2i} - p_{r2i} = 0 \end{aligned}\right\} \quad \text{(H-10)}$$

Using Equation H-9 in Equations H-7 and H-8 gives

$$\alpha_{r1}(p_i - p_{r1i} + \Delta p_{r1}) + \alpha_{r12}(p_{r2i} - \Delta p_{r2} - p_{r1i} + \Delta p_{r1}) - w_{p,net1} = -\kappa_{r1}\frac{d\Delta p_{r1}}{dt} \quad \text{(H-11)}$$

$$\alpha_{r2}(p_i - p_{r2i} + \Delta p_{r2}) - \alpha_{r12}(p_{r2i} - \Delta p_{r2} - p_{r1i} + \Delta p_{r1}) - w_{p,net2} = -\kappa_{r2}\frac{d\Delta p_{r2}}{dt} \quad \text{(H-12)}$$

The following definitions can be made to simplify the equations.

$$\left.\begin{aligned} \Delta p_{r1i} = p_i - p_{r1i} \\ \Delta p_{r2i} = p_i - p_{r2i} \\ \Delta p_i = p_{r2i} - p_{r1i} \end{aligned}\right\} \quad \text{(H-13)}$$

Substituting Equation H-13 into Equations H-11 and H-12 gives

$$\alpha_{r1}(\Delta p_{r1i} + \Delta p_{r1}) + \alpha_{r12}(\Delta p_i + \Delta p_{r1} - \Delta p_{r2}) - w_{p,net1} = -\kappa_{r1}\frac{d\Delta p_{r1}}{dt} \quad \text{(H-14)}$$

$$\alpha_{r2}(\Delta p_{r2i} + \Delta p_{r2}) - \alpha_{r12}(\Delta p_i + \Delta p_{r1} - \Delta p_{r2}) - w_{p,net2} = -\kappa_{r2}\frac{d\Delta p_{r2}}{dt} \quad \text{(H-15)}$$

Equations H-14 and H-15 can be simplified and rearranged as follows:

$$\kappa_{r1}\frac{d\Delta p_{r1}}{dt} + (\alpha_{r1} + \alpha_{r12})\Delta p_{r1} - \alpha_{r12}\Delta p_{r2} = w_{p,net1} - \alpha_{r1}\Delta p_{r1i} - \alpha_{r12}\Delta p_i \quad \text{(H-16)}$$

$$\kappa_{r2}\frac{d\Delta p_{r2}}{dt} - \alpha_{r12}\Delta p_{r1} + (\alpha_{r2} + \alpha_{r12})\Delta p_{r2} = w_{p,net2} - \alpha_{r2}\Delta p_{r2i} + \alpha_{r12}\Delta p_i \quad \text{(H-17)}$$

Applying Laplace transformation (Erdélyi, 1954) to Equations H-16 and H-17 and using initial conditions (Equation H-10) gives

$$\kappa_{r1}\, s\, \overline{\Delta p_{r1}} + (\alpha_{r1} + \alpha_{r12})\, \overline{\Delta p_{r1}} - \alpha_{r12}\, \overline{\Delta p_{r2}} = \frac{w_{p,net1} - \alpha_{r1}\Delta p_{r1i} - \alpha_{r12}\Delta p_i}{s} \quad \text{(H-18)}$$

$$\kappa_{r2}\, s\, \overline{\Delta p_{r2}} - \alpha_{r12}\, \overline{\Delta p_{r1}} + (\alpha_{r2} + \alpha_{r12})\overline{\Delta p_{r2}} = \frac{w_{p,net2} - \alpha_{r2}\Delta p_{r2i} + \alpha_{r12}\Delta p_i}{s} \quad \text{(H-19)}$$

where

$$\overline{\Delta p_{r1}} = \int_0^\infty e^{-st}\Delta p_{r1}\, d\tau \quad , \quad \overline{\Delta p_{r2}} = \int_0^\infty e^{-st}\Delta p_{r2}\, d\tau \quad \text{(H-20)}$$

Rearranging Equations H-18 and H-19 gives

$$(\kappa_{r1}\, s + \alpha_{r1} + \alpha_{r12})\, \overline{\Delta p_{r1}} - \alpha_{r12}\, \overline{\Delta p_{r2}} = \frac{w_{p,net1} - \alpha_{r1}\Delta p_{r1i} - \alpha_{r12}\Delta p_i}{s} \quad \text{(H-21)}$$

$$-\alpha_{r12}\, \overline{\Delta p_{r1}} + (\kappa_{r2}\, s + \alpha_{r2} + \alpha_{r12})\overline{\Delta p_{r2}} = \frac{w_{p,net2} - \alpha_{r2}\Delta p_{r2i} + \alpha_{r12}\Delta p_i}{s} \quad \text{(H-22)}$$

or

$$\left(s + \frac{\alpha_{r1} + \alpha_{r12}}{\kappa_{r1}}\right)\overline{\Delta p_{r1}} - \frac{\alpha_{r12}}{\kappa_{r1}}\, \overline{\Delta p_{r2}} = \frac{w_{p,net1} - \alpha_{r1}\Delta p_{r1i} - \alpha_{r12}\Delta p_i}{\kappa_{r1}}\frac{1}{s} \quad \text{(H-23)}$$

$$-\frac{\alpha_{r12}}{\kappa_{r2}}\, \overline{\Delta p_{r1}} + \left(s + \frac{\alpha_{r2} + \alpha_{r12}}{\kappa_{r2}}\right)\overline{\Delta p_{r2}} = \frac{w_{p,net2} - \alpha_{r2}\Delta p_{r2i} + \alpha_{r12}\Delta p_i}{\kappa_{r2}}\frac{1}{s} \quad \text{(H-24)}$$

The solutions to two equations (Equations H-23 and H-24) with two unknowns ($\overline{\Delta p_{r1}}, \overline{\Delta p_{r2}}$) can be obtained by using Cramer's rule (Kreyszig, 1999) as follows:

$$\overline{\Delta p_{r1}} = \frac{D_{r1}}{D} \quad , \quad \overline{\Delta p_{r2}} = \frac{D_{r2}}{D} \quad \text{(H-25)}$$

$$D_{r1} = \begin{vmatrix} \dfrac{w_{p,net1} - \alpha_{r1}\Delta p_{r1i} - \alpha_{r12}\Delta p_i}{\kappa_{r1}}\dfrac{1}{s} & -\dfrac{\alpha_{r12}}{\kappa_{r1}} \\ \dfrac{w_{p,net2} - \alpha_{r2}\Delta p_{r2i} + \alpha_{r12}\Delta p_i}{\kappa_{r2}}\dfrac{1}{s} & s + \dfrac{\alpha_{r2} + \alpha_{r12}}{\kappa_{r2}} \end{vmatrix}$$

$$= \frac{w_{p,net1} - \alpha_{r1}\Delta p_{r1i} - \alpha_{r12}\Delta p_i}{\kappa_{r1}} + \frac{\left(w_{p,net1} - \alpha_{r1}\Delta p_{r1i} - \alpha_{r12}\Delta p_i\right)\left(\alpha_{r2} + \alpha_{r12}\right)}{\kappa_{r1}\kappa_{r2}}\frac{1}{s} + \frac{\left(w_{p,net2} - \alpha_{r2}\Delta p_{r2i} + \alpha_{r12}\Delta p_i\right)\alpha_{r12}}{\kappa_{r1}\kappa_{r2}}\frac{1}{s} \tag{H-26}$$

$$D_{r2} = \begin{vmatrix} s + \dfrac{\alpha_{r1} + \alpha_{r12}}{\kappa_{r1}} & \dfrac{w_{p,net1} - \alpha_{r1}\Delta p_{r1i} - \alpha_{r12}\Delta p_i}{\kappa_{r1}}\dfrac{1}{s} \\ -\dfrac{\alpha_{r12}}{\kappa_{r2}} & \dfrac{w_{p,net2} - \alpha_{r2}\Delta p_{r2i} + \alpha_{r12}\Delta p_i}{\kappa_{r2}}\dfrac{1}{s} \end{vmatrix}$$

$$= \frac{w_{p,net2} - \alpha_{r2}\Delta p_{r2i} + \alpha_{r12}\Delta p_i}{\kappa_{r2}} + \frac{\left(w_{p,net2} - \alpha_{r2}\Delta p_{r2i} + \alpha_{r12}\Delta p_i\right)\left(\alpha_{r1} + \alpha_{r12}\right)}{\kappa_{r1}\kappa_{r2}}\frac{1}{s} + \frac{\left(w_{p,net1} - \alpha_{r1}\Delta p_{r1i} - \alpha_{r12}\Delta p_i\right)\alpha_{r12}}{\kappa_{r1}\kappa_{r2}}\frac{1}{s} \tag{H-27}$$

$$D = \begin{vmatrix} s + \dfrac{\alpha_{r1} + \alpha_{r12}}{\kappa_{r1}} & -\dfrac{\alpha_{r12}}{\kappa_{r1}} \\ -\dfrac{\alpha_{r12}}{\kappa_{r2}} & s + \dfrac{\alpha_{r2} + \alpha_{r12}}{\kappa_{r2}} \end{vmatrix} \tag{H-28}$$

$$= s^2 + \left(\frac{\alpha_{r1} + \alpha_{r12}}{\kappa_{r1}} + \frac{\alpha_{r2} + \alpha_{r12}}{\kappa_{r2}}\right)s + \frac{\alpha_{r1}\alpha_{r2} + \alpha_{r12}\left(\alpha_{r1} + \alpha_{r2}\right)}{\kappa_{r1}\kappa_{r2}}$$

Equations H-26, H-27, and H-28 can be written as follows:

$$D_{r1} = a_1 + \frac{a_1 a_4}{s} + \frac{a_2 a_5}{s} \tag{H-29}$$

$$D_{r2} = a_2 + \frac{a_2 a_3}{s} + \frac{a_1 a_6}{s} \tag{H-30}$$

$$D = s^2 + a_7 s + a_8 \tag{H-31}$$

where

$$\begin{aligned} a_1 &= \frac{w_{p,net1} - \alpha_{r1}\Delta p_{r1i} - \alpha_{r12}\Delta p_i}{\kappa_{r1}} \quad , \quad a_2 = \frac{w_{p,net2} - \alpha_{r2}\Delta p_{r2i} + \alpha_{r12}\Delta p_i}{\kappa_{r2}} \\ a_3 &= \frac{\alpha_{r1} + \alpha_{r12}}{\kappa_{r1}} \quad , \quad a_4 = \frac{\alpha_{r2} + \alpha_{r12}}{\kappa_{r2}} \quad , \quad a_5 = \frac{\alpha_{r12}}{\kappa_{r1}} \quad , \quad a_6 = \frac{\alpha_{r12}}{\kappa_{r2}} \\ a_7 &= \frac{\alpha_{r1} + \alpha_{r12}}{\kappa_{r1}} + \frac{\alpha_{r2} + \alpha_{r12}}{\kappa_{r2}} \quad , a_8 = \frac{\alpha_{r1}\alpha_{r2} + \alpha_{r12}(\alpha_{r1} + \alpha_{r2})}{\kappa_{r1}\kappa_{r2}} \end{aligned} \tag{H-32}$$

Substituting Equations H-29, H-30 and H-31 into Equation H-25 gives

$$\overline{\Delta p_{r1}} = \frac{D_{r1}}{D} = \frac{a_1 + \frac{a_1 a_4}{s} + \frac{a_2 a_5}{s}}{s^2 + a_7 s + a_8} = \frac{a_1 s + a_1 a_4 + a_2 a_5}{s(s^2 + a_7 s + a_8)} \tag{H-33}$$

$$\overline{\Delta p_{r2}} = \frac{D_{r2}}{D} = \frac{a_2 + \frac{a_2 a_3}{s} + \frac{a_1 a_6}{s}}{s^2 + a_7 s + a_8} = \frac{a_2 s + a_2 a_3 + a_1 a_6}{s(s^2 + a_7 s + a_8)} \tag{H-34}$$

The roots of the $(s^2 + a_7 s + a_8)$ are found as follows:

$$\left.\begin{aligned} \mu_1 &= \frac{a_7 + \sqrt{a_7^2 - 4a_8}}{2} \\ \mu_2 &= \frac{a_7 - \sqrt{a_7^2 - 4a_8}}{2} \end{aligned}\right\} \tag{H-35}$$

Using Equation H-35, the following expression can be written

$$s^2 + a_7 s + a_8 = (s + \mu_1)(s + \mu_2) \tag{H-36}$$

Substituting Equation H-36 into Equations H-33 and H-34 gives

$$\overline{\Delta p_{r1}} = \frac{a_1 s + a_1 a_4 + a_2 a_5}{(s + 0)(s + \mu_1)(s + \mu_2)} \tag{H-37}$$

$$\overline{\Delta p_{r2}} = \frac{a_2 s + a_2 a_3 + a_1 a_6}{(s+0)(s+\mu_1)(s+\mu_2)} \tag{H-38}$$

In order to find the values of Δp_{r1} and Δp_{r2} in real space, inverse Laplace transform of Equations H-37 and H-38 are obtained as follows:

$$\Delta p_{r1} = L^{-1}\left\{\overline{\Delta p_{r1}}\right\} = L^{-1}\left\{\frac{a_1 s + a_1 a_4 + a_2 a_5}{(s+0)(s+\mu_1)(s+\mu_2)}\right\} \tag{H-39}$$

$$\Delta p_{r2} = L^{-1}\left\{\overline{\Delta p_{r2}}\right\} = L^{-1}\left\{\frac{a_2 s + a_2 a_3 + a_1 a_6}{(s+0)(s+\mu_1)(s+\mu_2)}\right\} \tag{H-40}$$

Inverse Laplace transform of the term of $\frac{a_1 s + a_1 a_4 + a_2 a_5}{(s+0)(s+\mu_1)(s+\mu_2)}$ in Equation H-39 and the term of $\frac{a_2 s + a_2 a_3 + a_1 a_6}{(s+0)(s+\mu_1)(s+\mu_2)}$ in Equation H-40 are obtained by using the formula given in Equation B-36. Applying Equation B-36 in Equation H-39 gives

$$\begin{aligned} &\lambda = 0 \;,\; \mu = a_1 \;,\; \nu = a_1 a_4 + a_2 a_5 \\ &\alpha = 0 \;,\; \beta = \mu_1 \;,\; \gamma = \mu_2 \end{aligned} \tag{H-41}$$

and

$$\begin{aligned} L^{-1}\left\{\frac{a_1 s + a_1 a_4 + a_2 a_5}{(s+0)(s+\mu_1)(s+\mu_2)}\right\} = {} & \frac{a_1 a_4 + a_2 a_5}{\mu_1 \mu_2} \\ & - \frac{a_1 \mu_1 - a_1 a_4 - a_2 a_5}{\mu_1 (\mu_1 - \mu_2)} exp(-\mu_1 t) \\ & - \frac{a_1 \mu_2 - a_1 a_4 - a_2 a_5}{\mu_2 (\mu_2 - \mu_1)} exp(-\mu_2 t) \end{aligned} \tag{H-42}$$

Substituting Equation H-42 into Equation H-39 gives

$$\Delta p_{r1}(t) = \frac{w_{p,net1}}{\kappa_{r1}}\left[\frac{a_4}{\mu_1\mu_2} - \frac{\mu_1 - a_4}{\mu_1(\mu_1-\mu_2)}exp(-\mu_1 t) + \frac{\mu_2 - a_4}{\mu_2(\mu_1-\mu_2)}exp(-\mu_2 t)\right]$$
$$+ \frac{w_{p,net2}}{\kappa_{r2}}\left[\frac{a_5}{\mu_1\mu_2} + \frac{a_5}{\mu_1(\mu_1-\mu_2)}exp(-\mu_1 t) - \frac{a_5}{\mu_2(\mu_1-\mu_2)}exp(-\mu_2 t)\right]$$
$$+ \frac{exp(-\mu_1 t)}{\mu_1(\mu_1-\mu_2)}\left[\frac{a_{10}\mu_1}{\kappa_{r1}} - \frac{a_4 a_{10}}{\kappa_{r1}} + \frac{a_5 a_9}{\kappa_{r2}}\right]$$
$$- \frac{exp(-\mu_2 t)}{\mu_2(\mu_1-\mu_2)}\left[\frac{a_{10}\mu_2}{\kappa_{r1}} - \frac{a_4 a_{10}}{\kappa_{r1}} + \frac{a_5 a_9}{\kappa_{r2}}\right] + \frac{1}{\mu_1\mu_2}\left[\frac{a_5 a_9}{\kappa_{r2}} - \frac{a_4 a_{10}}{\kappa_{r1}}\right] \quad \text{(H-43)}$$

where

$$a_9 = -\alpha_{r2}(p_i - p_{r2i}) + \alpha_{r12}(p_{r2i} - p_{r1i})$$
$$a_{10} = \alpha_{r1}(p_i - p_{r1i}) + \alpha_{r12}(p_{r2i} - p_{r1i}) \quad \text{(H-44)}$$

Similarly, Applying Equation B-36 in Equation H-40 gives

$$\lambda = 0 \ , \ \mu = a_2 \ , \ \nu = a_2 a_3 + a_1 a_6$$
$$\alpha = 0 \ , \ \beta = \mu_1 \ , \ \gamma = \mu_2 \quad \text{(H-45)}$$

and

$$L^{-1}\left\{\frac{a_2 s + a_2 a_3 + a_1 a_6}{(s+0)(s+\mu_1)(s+\mu_2)}\right\} = \frac{a_2 a_3 + a_1 a_6}{\mu_1\mu_2}$$
$$- \frac{a_2\mu_1 - a_2 a_3 - a_1 a_6}{\mu_1(\mu_1-\mu_2)}exp(-\mu_1 t) \quad \text{(H-46)}$$
$$- \frac{a_2\mu_2 - a_2 a_3 - a_1 a_6}{\mu_2(\mu_2-\mu_1)}exp(-\mu_2 t)$$

Substituting Equation H-46 into Equation H-40 gives

$$\Delta p_{r2}(t) = \frac{w_{p,net1}}{\kappa_{r1}}\left[\frac{a_6}{\mu_1\mu_2} + \frac{a_6}{\mu_1(\mu_1-\mu_2)}exp(-\mu_1 t) - \frac{a_6}{\mu_2(\mu_1-\mu_2)}exp(-\mu_2 t)\right]$$
$$+ \frac{w_{p,net2}}{\kappa_{r2}}\left[\frac{a_3}{\mu_1\mu_2} - \frac{\mu_1 - a_3}{\mu_1(\mu_1-\mu_2)}exp(-\mu_1 t) + \frac{\mu_2 - a_3}{\mu_2(\mu_1-\mu_2)}exp(-\mu_2 t)\right]$$
$$+ \frac{exp(-\mu_1 t)}{\mu_1(\mu_1-\mu_2)}\left[-\frac{a_9\mu_1}{\kappa_{r2}} + \frac{a_3 a_9}{\kappa_{r2}} - \frac{a_6 a_{10}}{\kappa_{r1}}\right]$$
$$- \frac{exp(-\mu_2 t)}{\mu_2(\mu_1-\mu_2)}\left[-\frac{a_9\mu_2}{\kappa_{r2}} + \frac{a_3 a_9}{\kappa_{r2}} - \frac{a_6 a_{10}}{\kappa_{r1}}\right] + \frac{1}{\mu_1\mu_2}\left[\frac{a_3 a_9}{\kappa_{r2}} - \frac{a_6 a_{10}}{\kappa_{r1}}\right] \quad \text{(H-47)}$$

The shallow and deep reservoirs pressures as a function of time are obtained by using Equations H-43 and H-47, respectively, as below.

$$p_{r1}(t) = p_{r1i} - \left\{ \begin{aligned} &\frac{w_{p,net1}}{\kappa_{r1}}\left[\frac{a_4}{\mu_1\mu_2} - \frac{\mu_1 - a_4}{\mu_1(\mu_1-\mu_2)}exp(-\mu_1 t) + \frac{\mu_2 - a_4}{\mu_2(\mu_1-\mu_2)}exp(-\mu_2 t)\right] \\ &+\frac{w_{p,net2}}{\kappa_{r2}}\left[\frac{a_5}{\mu_1\mu_2} + \frac{a_5}{\mu_1(\mu_1-\mu_2)}exp(-\mu_1 t) - \frac{a_5}{\mu_2(\mu_1-\mu_2)}exp(-\mu_2 t)\right] \\ &+\frac{exp(-\mu_1 t)}{\mu_1(\mu_1-\mu_2)}\left[\frac{a_{10}\mu_1}{\kappa_{r1}} - \frac{a_4 a_{10}}{\kappa_{r1}} + \frac{a_5 a_9}{\kappa_{r2}}\right] \\ &-\frac{exp(-\mu_2 t)}{\mu_2(\mu_1-\mu_2)}\left[\frac{a_{10}\mu_2}{\kappa_{r1}} - \frac{a_4 a_{10}}{\kappa_{r1}} + \frac{a_5 a_9}{\kappa_{r2}}\right] \\ &+\frac{1}{\mu_1\mu_2}\left[\frac{a_5 a_9}{\kappa_{r2}} - \frac{a_4 a_{10}}{\kappa_{r1}}\right] \end{aligned} \right\} \tag{H-48}$$

$$p_{r2}(t) = p_{r2i} - \left\{ \begin{aligned} &\frac{w_{p,net1}}{\kappa_{r1}}\left[\frac{a_6}{\mu_1\mu_2} + \frac{a_6}{\mu_1(\mu_1-\mu_2)}exp(-\mu_1 t) - \frac{a_6}{\mu_2(\mu_1-\mu_2)}exp(-\mu_2 t)\right] \\ &+\frac{w_{p,net2}}{\kappa_{r2}}\left[\frac{a_3}{\mu_1\mu_2} - \frac{\mu_1 - a_3}{\mu_1(\mu_1-\mu_2)}exp(-\mu_1 t) + \frac{\mu_2 - a_3}{\mu_2(\mu_1-\mu_2)}exp(-\mu_2 t)\right] \\ &+\frac{exp(-\mu_1 t)}{\mu_1(\mu_1-\mu_2)}\left[-\frac{a_9\mu_1}{\kappa_{r2}} + \frac{a_3 a_9}{\kappa_{r2}} - \frac{a_6 a_{10}}{\kappa_{r1}}\right] \\ &-\frac{exp(-\mu_2 t)}{\mu_2(\mu_1-\mu_2)}\left[-\frac{a_9\mu_2}{\kappa_{r2}} + \frac{a_3 a_9}{\kappa_{r2}} - \frac{a_6 a_{10}}{\kappa_{r1}}\right] \\ &+\frac{1}{\mu_1\mu_2}\left[\frac{a_3 a_9}{\kappa_{r2}} - \frac{a_6 a_{10}}{\kappa_{r1}}\right] \end{aligned} \right\} \tag{H-49}$$

APPENDIX-I

2 RESERVOIR TANK MODEL WITH AQUIFER (WITH INITIAL HYDRAULIC EQUILIBRIUM)

Mass balances on the shallow and deep reservoirs and the aquifer, recharges of the reservoirs and the aquifer, initial conditions are expressed as;

Mass Balance on the Aquifer :

$$w_a - w_{r1} - w_{r2} = \kappa_a \frac{dp_a}{dt} \tag{I-1}$$

Mass Balance on the Shallow Reservoir :

$$w_{r1} + w_{r12} - w_{p,net1} = \kappa_{r1} \frac{dp_{r1}}{dt} \tag{I-2}$$

Mass Balance on the Deep Reservoir :

$$w_{r2} - w_{r12} - w_{p,net2} = \kappa_{r2} \frac{dp_{r2}}{dt} \tag{I-3}$$

Recharge of the Aquifer : $w_a = \alpha_a (p_i - p_a)$ (I-4)

Recharge of the Shallow Reservoir : $w_{r1} = \alpha_{r1} (p_a - p_{r1})$ (I-5)

Recharge of the Deep Reservoir : $w_{r2} = \alpha_{r2} (p_a - p_{r2})$ (I-6)

Recharge between the Shallow and Deep Reservoirs :

$$w_{r12} = \alpha_{r12} (p_{r2} - p_{r1}) \tag{I-7}$$

Initial Conditions : $p_a = p_{r1} = p_{r2} = p_i \ @ \ t = 0$ (I-8)

Substituting Equations I-4, I-5, I-6, and I-7 into Equations I-1, I-2, and I-3 gives

$$\alpha_a(p_i - p_a) - \alpha_{r1}(p_a - p_{r1}) - \alpha_{r2}(p_a - p_{r2}) = \kappa_a \frac{dp_a}{dt} \tag{I-9}$$

$$\alpha_{r1}(p_a - p_{r1}) + \alpha_{r12}(p_{r2} - p_{r1}) - w_{p,net1} = \kappa_{r1} \frac{dp_{r1}}{dt} \tag{I-10}$$

$$\alpha_{r2}(p_a - p_{r2}) - \alpha_{r12}(p_{r2} - p_{r1}) - w_{p,net2} = \kappa_{r2} \frac{dp_{r2}}{dt} \tag{I-11}$$

Equations I-9, I-10, and I-11 can be written in terms of pressure changes. The pressure changes and their derivatives with respect to time are given by

$$\left.\begin{aligned} \Delta p_a = p_i - p_a \;&\Rightarrow\; p_a = p_i - \Delta p_a \;\Rightarrow\; \frac{d\,\Delta p_a}{dt} = -\frac{dp_a}{dt} \\ \Delta p_{r1} = p_i - p_{r1} \;&\Rightarrow\; p_{r1} = p_i - \Delta p_{r1} \;\Rightarrow\; \frac{d\,\Delta p_{r1}}{dt} = -\frac{dp_{r1}}{dt} \\ \Delta p_{r2} = p_i - p_{r2} \;&\Rightarrow\; p_{r2} = p_i - \Delta p_{r2} \;\Rightarrow\; \frac{d\,\Delta p_{r2}}{dt} = -\frac{dp_{r2}}{dt} \end{aligned}\right\} \tag{I-12}$$

and initial conditions become

$$\left.\begin{aligned} \Delta p_a(t=0) &= p_i - p_a(t=0) = p_i - p_i = 0 \\ \Delta p_{r1}(t=0) &= p_i - p_{r1}(t=0) = p_i - p_i = 0 \\ \Delta p_{r2}(t=0) &= p_i - p_{r2}(t=0) = p_i - p_i = 0 \end{aligned}\right\} \tag{I-13}$$

Using Equation I-12 in Equations I-9, I-10, and I-11 gives

$$\begin{aligned} \alpha_a(p_i - p_i + \Delta p_a) - \alpha_{r1}(p_i - \Delta p_a - p_i + \Delta p_{r1}) \\ - \alpha_{r2}(p_i - \Delta p_a - p_i + \Delta p_{r2}) = -\kappa_a \frac{d\Delta p_a}{dt} \end{aligned} \tag{I-14}$$

$$\alpha_{r1}(p_i - \Delta p_a - p_i + \Delta p_{r1}) + \alpha_{r12}(p_i - \Delta p_{r2} - p_i + \Delta p_{r1}) - w_{p,net1} = -\kappa_{r1} \frac{d\Delta p_{r1}}{dt} \tag{I-15}$$

$$\alpha_{r2}(p_i - \Delta p_a - p_i + \Delta p_{r2}) - \alpha_{r12}(p_i - \Delta p_{r2} - p_i + \Delta p_{r1}) - w_{p,net2} = -\kappa_{r2} \frac{d\Delta p_{r2}}{dt} \tag{I-16}$$

Equations I-14, I-15, and I-16 can be simplified and rearranged as follows:

$$\alpha_a \Delta p_a - \alpha_{r1}(\Delta p_{r1} - \Delta p_a) - \alpha_{r2}(\Delta p_{r2} - \Delta p_a) = -\kappa_a \frac{d\Delta p_a}{dt} \tag{I-17}$$

$$\alpha_{r1}(\Delta p_{r1} - \Delta p_a) + \alpha_{r12}(\Delta p_{r1} - \Delta p_{r2}) - w_{p,net1} = -\kappa_{r1} \frac{d\Delta p_{r1}}{dt} \tag{I-18}$$

$$\alpha_{r2}(\Delta p_{r2} - \Delta p_a) - \alpha_{r12}(\Delta p_{r1} - \Delta p_{r2}) - w_{p,net2} = -\kappa_{r2} \frac{d\Delta p_{r2}}{dt} \tag{I-19}$$

or

$$\kappa_a \frac{d\Delta p_a}{dt} + (\alpha_a + \alpha_{r1} + \alpha_{r2})\Delta p_a - \alpha_{r1}\Delta p_{r1} - \alpha_{r2}\Delta p_{r2} = 0 \tag{I-20}$$

$$\kappa_{r1} \frac{d\Delta p_{r1}}{dt} - \alpha_{r1}\Delta p_a + (\alpha_{r1} + \alpha_{r12})\Delta p_{r1} - \alpha_{r12}\Delta p_{r2} = w_{p,net1} \tag{I-21}$$

$$\kappa_{r2} \frac{d\Delta p_{r2}}{dt} - \alpha_{r2}\Delta p_a - \alpha_{r12}\Delta p_{r1} + (\alpha_{r2} + \alpha_{r12})\Delta p_{r2} = w_{p,net2} \tag{I-22}$$

Applying Laplace transformation (Erdélyi, 1954) to Equations I-20, I-21, and I-22 and using the initial conditions (Equation I-13) gives

$$\kappa_a s\,\overline{\Delta p_a} + (\alpha_a + \alpha_{r1} + \alpha_{r2})\,\overline{\Delta p_a} - \alpha_{r1}\,\overline{\Delta p_{r1}} - \alpha_{r2}\,\overline{\Delta p_{r2}} = 0 \tag{I-23}$$

$$\kappa_{r1} s\,\overline{\Delta p_{r1}} - \alpha_{r1}\,\overline{\Delta p_a} + (\alpha_{r1} + \alpha_{r12})\,\overline{\Delta p_{r1}} - \alpha_{r12}\,\overline{\Delta p_{r2}} = \frac{w_{p,net1}}{s} \tag{I-24}$$

$$\kappa_{r2} s\,\overline{\Delta p_{r2}} - \alpha_{r2}\,\overline{\Delta p_a} - \alpha_{r12}\,\overline{\Delta p_{r1}} + (\alpha_{r2} + \alpha_{r12})\,\overline{\Delta p_{r2}} = \frac{w_{p,net2}}{s} \tag{I-25}$$

where

$$\overline{\Delta p_a} = \int_0^\infty e^{-st}\Delta p_a\, d\tau \quad , \quad \overline{\Delta p_{r1}} = \int_0^\infty e^{-st}\Delta p_{r1}\, d\tau \quad , \quad \overline{\Delta p_{r2}} = \int_0^\infty e^{-st}\Delta p_{r2}\, d\tau \tag{I-26}$$

Rearranging Equations I-23, I-24, and I-25 gives

$$(\kappa_a s + \alpha_a + \alpha_{r1} + \alpha_{r2})\,\overline{\Delta p_a} - \alpha_{r1}\,\overline{\Delta p_{r1}} - \alpha_{r2}\,\overline{\Delta p_{r2}} = 0 \tag{I-27}$$

$$-\alpha_{r1}\,\overline{\Delta p_a}+\left(\kappa_{r1}s+\alpha_{r1}+\alpha_{r12}\right)\overline{\Delta p_{r1}}-\alpha_{r12}\,\overline{\Delta p_{r2}}=\frac{w_{p,net1}}{s} \tag{I-28}$$

$$-\alpha_{r2}\,\overline{\Delta p_a}-\alpha_{r12}\,\overline{\Delta p_{r1}}+\left(\kappa_{r2}s+\alpha_{r2}+\alpha_{r12}\right)\overline{\Delta p_{r2}}=\frac{w_{p,net2}}{s} \tag{I-29}$$

or

$$\left(s+\frac{\alpha_a+\alpha_{r1}+\alpha_{r2}}{\kappa_a}\right)\overline{\Delta p_a}-\frac{\alpha_{r1}}{\kappa_a}\overline{\Delta p_{r1}}-\frac{\alpha_{r2}}{\kappa_a}\overline{\Delta p_{r2}}=0 \tag{I-30}$$

$$-\frac{\alpha_{r1}}{\kappa_{r1}}\overline{\Delta p_a}+\left(s+\frac{\alpha_{r1}+\alpha_{r12}}{\kappa_{r1}}\right)\overline{\Delta p_{r1}}-\frac{\alpha_{r12}}{\kappa_{r1}}\overline{\Delta p_{r2}}=\frac{w_{p,net1}}{\kappa_{r1}}\frac{1}{s} \tag{I-31}$$

$$-\frac{\alpha_{r2}}{\kappa_{r2}}\overline{\Delta p_a}-\frac{\alpha_{r12}}{\kappa_{r2}}\overline{\Delta p_{r1}}+\left(s+\frac{\alpha_{r2}+\alpha_{r12}}{\kappa_{r2}}\right)\overline{\Delta p_{r2}}=\frac{w_{p,net2}}{\kappa_{r2}}\frac{1}{s} \tag{I-32}$$

The solutions to three equations (Equations I-30, I-31, and I-32) with three unknowns ($\overline{\Delta p_a}, \overline{\Delta p_{r1}}, \overline{\Delta p_{r2}}$) can be obtained by using Cramer's rule (Kreyszig, 1999) as follows:

$$\overline{\Delta p_a}=\frac{D_a}{D}\ ,\ \overline{\Delta p_{r1}}=\frac{D_{r1}}{D}\ ,\ \overline{\Delta p_{r2}}=\frac{D_{r2}}{D} \tag{I-33}$$

$$\begin{aligned} D_a &= \begin{vmatrix} 0 & -\frac{\alpha_{r1}}{\kappa_a} & -\frac{\alpha_{r2}}{\kappa_a} \\ \frac{w_{p,net1}}{\kappa_{r1}}\frac{1}{s} & \left(s+\frac{\alpha_{r1}+\alpha_{r12}}{\kappa_{r1}}\right) & -\frac{\alpha_{r12}}{\kappa_{r1}} \\ \frac{w_{p,net2}}{\kappa_{r2}}\frac{1}{s} & -\frac{\alpha_{r12}}{\kappa_{r2}} & \left(s+\frac{\alpha_{r2}+\alpha_{r12}}{\kappa_{r2}}\right) \end{vmatrix} \\ &= \begin{vmatrix} 0 & -a_2 & -a_3 \\ \frac{w_{p,net1}}{\kappa_{r1}}\frac{1}{s} & (s+a_5) & -a_6 \\ \frac{w_{p,net2}}{\kappa_{r2}}\frac{1}{s} & -a_8 & (s+a_9) \end{vmatrix} \end{aligned} \tag{I-34}$$

$$D_{r1}=\begin{vmatrix} \left(s+\dfrac{\alpha_a+\alpha_{r1}+\alpha_{r2}}{\kappa_a}\right) & 0 & -\dfrac{\alpha_{r2}}{\kappa_a} \\ -\dfrac{\alpha_{r1}}{\kappa_{r1}} & \dfrac{w_{p,net1}}{\kappa_{r1}}\dfrac{1}{s} & -\dfrac{\alpha_{r12}}{\kappa_{r1}} \\ -\dfrac{\alpha_{r2}}{\kappa_{r2}} & \dfrac{w_{p,net2}}{\kappa_{r2}}\dfrac{1}{s} & \left(s+\dfrac{\alpha_{r2}+\alpha_{r12}}{\kappa_{r2}}\right) \end{vmatrix}$$

$$=\begin{vmatrix} (s+a_1) & 0 & -a_3 \\ -a_4 & \dfrac{w_{p,net1}}{\kappa_{r1}}\dfrac{1}{s} & -a_6 \\ -a_7 & \dfrac{w_{p,net2}}{\kappa_{r2}}\dfrac{1}{s} & (s+a_9) \end{vmatrix}$$

$$=\frac{w_{p,net1}}{\kappa_{r1}}\frac{1}{s}\left[s^2+(a_1+a_9)s+a_1a_9-a_3a_7\right]+\frac{w_{p,net2}}{\kappa_{r2}}\frac{1}{s}\left[a_6s+a_1a_6+a_3a_4\right]$$

(I-35)

$$D_{r2}=\begin{vmatrix} \left(s+\dfrac{\alpha_a+\alpha_{r1}+\alpha_{r2}}{\kappa_a}\right) & -\dfrac{\alpha_{r1}}{\kappa_a} & 0 \\ -\dfrac{\alpha_{r1}}{\kappa_{r1}} & \left(s+\dfrac{\alpha_{r1}+\alpha_{r12}}{\kappa_{r1}}\right) & \dfrac{w_{p,net1}}{\kappa_{r1}}\dfrac{1}{s} \\ -\dfrac{\alpha_{r2}}{\kappa_{r2}} & -\dfrac{\alpha_{r12}}{\kappa_{r2}} & \dfrac{w_{p,net2}}{\kappa_{r2}}\dfrac{1}{s} \end{vmatrix}$$

$$=\begin{vmatrix} (s+a_1) & -a_2 & 0 \\ -a_4 & (s+a_5) & \dfrac{w_{p,net1}}{\kappa_{r1}}\dfrac{1}{s} \\ -a_7 & -a_8 & \dfrac{w_{p,net2}}{\kappa_{r2}}\dfrac{1}{s} \end{vmatrix}$$

$$=\frac{w_{p,net1}}{\kappa_{r1}}\frac{1}{s}\left[a_8s+a_1a_8+a_2a_7\right]+\frac{w_{p,net2}}{\kappa_{r2}}\frac{1}{s}\left[s^2+(a_1+a_5)s+a_1a_5-a_2a_4\right]$$

(I-36)

$$D = \begin{vmatrix} \left(s + \dfrac{\alpha_a + \alpha_{r1} + \alpha_{r2}}{\kappa_a}\right) & -\dfrac{\alpha_{r1}}{\kappa_a} & -\dfrac{\alpha_{r2}}{\kappa_a} \\ -\dfrac{\alpha_{r1}}{\kappa_{r1}} & \left(s + \dfrac{\alpha_{r1} + \alpha_{r12}}{\kappa_{r1}}\right) & -\dfrac{\alpha_{r12}}{\kappa_{r1}} \\ -\dfrac{\alpha_{r2}}{\kappa_{r2}} & -\dfrac{\alpha_{r12}}{\kappa_{r2}} & \left(s + \dfrac{\alpha_{r2} + \alpha_{r12}}{\kappa_{r2}}\right) \end{vmatrix}$$

$$= \begin{vmatrix} (s + a_1) & -a_2 & -a_3 \\ -a_4 & (s + a_5) & -a_6 \\ -a_7 & -a_8 & (s + a_9) \end{vmatrix}$$

$$= s^3 + (a_1 + a_5 + a_9)s^2 + (a_5 a_9 - a_6 a_8 + a_1 a_5 + a_1 a_9 - a_2 a_4 - a_3 a_7)s$$
$$+ a_1 a_5 a_9 - a_1 a_6 a_8 - a_2 a_4 a_9 - a_2 a_6 a_7 - a_3 a_4 a_8 - a_3 a_5 a_7$$

(I-37)

where

$$\left.\begin{aligned} a_1 &= \frac{\alpha_a + \alpha_{r1} + \alpha_{r2}}{\kappa_a}\ ,\ a_2 = \frac{\alpha_{r1}}{\kappa_a}\ ,\ a_3 = \frac{\alpha_{r2}}{\kappa_a} \\ a_4 &= \frac{\alpha_{r1}}{\kappa_{r1}}\ ,\ a_5 = \frac{\alpha_{r1} + \alpha_{r12}}{\kappa_{r1}}\ ,\ a_6 = \frac{\alpha_{r12}}{\kappa_{r1}} \\ a_7 &= \frac{\alpha_{r2}}{\kappa_{r2}}\ ,\ a_8 = \frac{\alpha_{r12}}{\kappa_{r2}}\ ,\ a_9 = \frac{\alpha_{r2} + \alpha_{r12}}{\kappa_{r2}} \end{aligned}\right\} \quad \text{(I-38)}$$

Substituting Equations I-35, I-36 and I-37 into Equation I-33 gives

$$\overline{\Delta p_{r1}} = \frac{\dfrac{w_{p,net1}}{\kappa_{r1}}\dfrac{1}{s}\left[s^2 + (a_1 + a_9)s + a_1 a_9 - a_3 a_7\right] + \dfrac{w_{p,net2}}{\kappa_{r2}}\dfrac{1}{s}\left[a_6 s + a_1 a_6 + a_3 a_4\right]}{\left[\begin{array}{l} s^3 + (a_1 + a_5 + a_9)s^2 + (a_5 a_9 - a_6 a_8 + a_1 a_5 + a_1 a_9 - a_2 a_4 - a_3 a_7)s \\ + a_1 a_5 a_9 - a_1 a_6 a_8 - a_2 a_4 a_9 - a_2 a_6 a_7 - a_3 a_4 a_8 - a_3 a_5 a_7 \end{array}\right]}$$

(I-39)

$$\overline{\Delta p_{r2}} = \frac{\dfrac{w_{p,net1}}{\kappa_{r1}}\dfrac{1}{s}\left[a_8 s + a_1 a_8 + a_2 a_7\right] + \dfrac{w_{p,net2}}{\kappa_{r2}}\dfrac{1}{s}\left[s^2 + (a_1 + a_5)s + a_1 a_5 - a_2 a_4\right]}{\left[\begin{array}{l} s^3 + (a_1 + a_5 + a_9)s^2 + (a_5 a_9 - a_6 a_8 + a_1 a_5 + a_1 a_9 - a_2 a_4 - a_3 a_7)s \\ + a_1 a_5 a_9 - a_1 a_6 a_8 - a_2 a_4 a_9 - a_2 a_6 a_7 - a_3 a_4 a_8 - a_3 a_5 a_7 \end{array}\right]}$$

(I-40)

The roots of the cubic equation in Equations I-39 and I-40 are found as follows:

$$Q = \frac{(a_1 + a_5 + a_9)^2 - 3(a_5a_9 - a_6a_8 + a_1a_5 + a_1a_9 - a_2a_4 - a_3a_7)}{9}$$

$$R = \frac{1}{54}\begin{bmatrix} 2(a_1 + a_5 + a_9)^3 - 9(a_1 + a_5 + a_9)(a_5a_9 - a_6a_8 + a_1a_5 + a_1a_9 - a_2a_4 - a_3a_7) \\ + 27(a_1a_5a_9 - a_1a_6a_8 - a_2a_4a_9 - a_2a_6a_7 - a_3a_4a_8 - a_3a_5a_7) \end{bmatrix}$$

$$\theta = arc\cos\left(\frac{R}{\sqrt{Q^3}}\right) \tag{I-41}$$

$$\mu_1 = 2\sqrt{Q}\cos\left(\frac{\theta}{3}\right) + \frac{a_1 + a_5 + a_9}{3}$$

$$\mu_2 = 2\sqrt{Q}\cos\left(\frac{\theta + 2\pi}{3}\right) + \frac{a_1 + a_5 + a_9}{3} \tag{I-42}$$

$$\mu_3 = 2\sqrt{Q}\cos\left(\frac{\theta + 4\pi}{3}\right) + \frac{a_1 + a_5 + a_9}{3}$$

Using Equation I-42, the following expression can be written

$$\begin{bmatrix} s^3 + (a_1 + a_5 + a_9)s^2 + \\ (a_5a_9 - a_6a_8 + a_1a_5 + a_1a_9 - a_2a_4 - a_3a_7)s + \\ a_1a_5a_9 - a_1a_6a_8 - a_2a_4a_9 - a_2a_6a_7 - a_3a_4a_8 - a_3a_5a_7 \end{bmatrix} = (s + \mu_1)(s + \mu_2)(s + \mu_3) \tag{I-43}$$

Substituting Equation I-43 into Equations I-39 and I-40 gives

$$\overline{\Delta p_{r1}} = \frac{\frac{w_{p,net1}}{\kappa_{r1}}\frac{1}{s}\left[s^2 + (a_1 + a_9)s + a_1a_9 - a_3a_7\right] + \frac{w_{p,net2}}{\kappa_{r2}}\frac{1}{s}\left[a_6s + a_1a_6 + a_3a_4\right]}{(s + \mu_1)(s + \mu_2)(s + \mu_3)} \tag{I-44}$$

$$\overline{\Delta p_{r2}} = \frac{\frac{w_{p,net1}}{\kappa_{r1}}\frac{1}{s}\left[a_8s + a_1a_8 + a_2a_7\right] + \frac{w_{p,net2}}{\kappa_{r2}}\frac{1}{s}\left[s^2 + (a_1 + a_5)s + a_1a_5 - a_2a_4\right]}{(s + \mu_1)(s + \mu_2)(s + \mu_3)} \tag{I-45}$$

In order to find the values of $\Delta\overline{p_{r1}}$ and $\Delta\overline{p_{r2}}$ in real space, inverse Laplace transform of Equations I-44 and I-45 are obtained as follows:

$$\Delta p_{r1} = L^{-1}\left\{\overline{\Delta p_{r1}}\right\} = \frac{w_{p,net1}}{\kappa_{r1}} L^{-1}\left\{\frac{s^2 + (a_1 + a_9)s + a_1a_9 - a_3a_7}{(s+0)(s+\mu_1)(s+\mu_2)(s+\mu_3)}\right\} + \frac{w_{p,net2}}{\kappa_{r2}} L^{-1}\left\{\frac{a_6 s + a_1a_6 + a_3a_4}{(s+0)(s+\mu_1)(s+\mu_2)(s+\mu_3)}\right\} \tag{I-46}$$

$$\Delta p_{r2} = L^{-1}\left\{\overline{\Delta p_{r2}}\right\} = \frac{w_{p,net1}}{\kappa_{r1}} L^{-1}\left\{\frac{a_8 s + a_1a_8 + a_2a_7}{(s+0)(s+\mu_1)(s+\mu_2)(s+\mu_3)}\right\} + \frac{w_{p,net2}}{\kappa_{r2}} L^{-1}\left\{\frac{s^2 + (a_1 + a_5)s + a_1a_5 - a_2a_4}{(s+0)(s+\mu_1)(s+\mu_2)(s+\mu_3)}\right\} \tag{I-47}$$

Inverse Laplace transform of the term of $\frac{s^2 + (a_1 + a_9)s + a_1a_9 - a_3a_7}{(s+0)(s+\mu_1)(s+\mu_2)(s+\mu_3)}$ in Equation I-46 is obtained by separation of the terms as follows:

$$\frac{s^2 + (a_1 + a_9)s + a_1a_9 - a_3a_7}{(s+0)(s+\mu_1)(s+\mu_2)(s+\mu_3)} = \frac{A_1}{(s+0)} + \frac{A_2}{(s+\mu_1)} + \frac{A_3}{(s+\mu_2)} + \frac{A_4}{(s+\mu_3)} \tag{I-48}$$

$$A_1 = lim_{s\to 0}\,(s+0)\frac{s^2 + (a_1 + a_9)s + a_1a_9 - a_3a_7}{(s+0)(s+\mu_1)(s+\mu_2)(s+\mu_3)} = \frac{a_1a_9 - a_3a_7}{\mu_1\mu_2\mu_3} \tag{I-49}$$

$$A_2 = lim_{s\to -\mu_1}\,(s+\mu_1)\frac{s^2 + (a_1 + a_9)s + a_1a_9 - a_3a_7}{(s+0)(s+\mu_1)(s+\mu_2)(s+\mu_3)} = -\frac{\mu_1^2 - (a_1 + a_9)\mu_1 + a_1a_9 - a_3a_7}{\mu_1(\mu_2 - \mu_1)(\mu_3 - \mu_1)} \tag{I-50}$$

$$A_3 = lim_{s\to -\mu_2}\,(s+\mu_2)\frac{s^2 + (a_1 + a_9)s + a_1a_9 - a_3a_7}{(s+0)(s+\mu_1)(s+\mu_2)(s+\mu_3)} = -\frac{\mu_2^2 - (a_1 + a_9)\mu_2 + a_1a_9 - a_3a_7}{\mu_2(\mu_1 - \mu_2)(\mu_3 - \mu_2)} \tag{I-51}$$

$$A_4 = lim_{s\to -\mu_3}\,(s+\mu_3)\frac{s^2+(a_1+a_9)s+a_1a_9-a_3a_7}{(s+0)(s+\mu_1)(s+\mu_2)(s+\mu_3)}$$
$$= -\frac{\mu_3^2-(a_1+a_9)\mu_3+a_1a_9-a_3a_7}{\mu_3(\mu_1-\mu_3)(\mu_2-\mu_3)} \qquad \text{(I-52)}$$

$$L^{-1}\left\{\frac{s^2+(a_1+a_9)s+a_1a_9-a_3a_7}{(s+0)(s+\mu_1)(s+\mu_2)(s+\mu_3)}\right\} = L^{-1}\left\{\frac{A_1}{(s+0)}+\frac{A_2}{(s+\mu_1)}+\frac{A_3}{(s+\mu_2)}+\frac{A_4}{(s+\mu_3)}\right\}$$
$$= A_1\,L^{-1}\left\{\frac{1}{(s+0)}\right\}+A_2\,L^{-1}\left\{\frac{1}{(s+\mu_1)}\right\}+A_3\,L^{-1}\left\{\frac{1}{(s+\mu_2)}\right\}+A_4L^{-1}\left\{\frac{1}{(s+\mu_3)}\right\} \qquad \text{(I-53)}$$

$$L^{-1}\left\{\frac{1}{(s+0)}\right\}=1\ ,\ L^{-1}\left\{\frac{1}{(s+\mu_1)}\right\}=exp(-\mu_1 t)$$
$$L^{-1}\left\{\frac{1}{(s+\mu_2)}\right\}=exp(-\mu_2 t)\ ,\ L^{-1}\left\{\frac{1}{(s+\mu_3)}\right\}=exp(-\mu_3 t) \qquad \text{(I-54)}$$

Using Equation I-54 in Equation I-53 gives

$$L^{-1}\left\{\frac{s^2+(a_1+a_9)s+a_1a_9-a_3a_7}{(s+0)(s+\mu_1)(s+\mu_2)(s+\mu_3)}\right\} = A_1+A_2\,exp(-\mu_1 t)$$
$$+A_3\,exp(-\mu_2 t)+A_4\,exp(-\mu_3 t) \qquad \text{(I-55)}$$

Inverse Laplace transform of the term of $\frac{a_6s+a_1a_6+a_3a_4}{(s+0)(s+\mu_1)(s+\mu_2)(s+\mu_3)}$ in Equation I-46 is obtained by separation of the terms as follows:

$$\frac{a_6s+a_1a_6+a_3a_4}{(s+0)(s+\mu_1)(s+\mu_2)(s+\mu_3)}=\frac{B_1}{(s+0)}+\frac{B_2}{(s+\mu_1)}+\frac{B_3}{(s+\mu_2)}+\frac{B_4}{(s+\mu_3)} \qquad \text{(I-56)}$$

$$B_1 = lim_{s\to 0}\,(s+0)\frac{a_6s+a_1a_6+a_3a_4}{(s+0)(s+\mu_1)(s+\mu_2)(s+\mu_3)}=\frac{a_1a_6+a_3a_4}{\mu_1\mu_2\mu_3} \qquad \text{(I-57)}$$

$$B_2 = lim_{s\to -\mu_1}\,(s+\mu_1)\frac{a_6s+a_1a_6+a_3a_4}{(s+0)(s+\mu_1)(s+\mu_2)(s+\mu_3)}$$
$$= -\frac{-a_6\mu_1+a_1a_6+a_3a_4}{\mu_1(\mu_2-\mu_1)(\mu_3-\mu_1)} \qquad \text{(I-58)}$$

$$B_3 = lim_{s\to -\mu_2}(s+\mu_2)\frac{a_6 s + a_1 a_6 + a_3 a_4}{(s+0)(s+\mu_1)(s+\mu_2)(s+\mu_3)}$$
$$= -\frac{-a_6\mu_2 + a_1 a_6 + a_3 a_4}{\mu_2(\mu_1-\mu_2)(\mu_3-\mu_2)} \quad \text{(I-59)}$$

$$B_4 = lim_{s\to -\mu_3}(s+\mu_3)\frac{a_6 s + a_1 a_6 + a_3 a_4}{(s+0)(s+\mu_1)(s+\mu_2)(s+\mu_3)}$$
$$= -\frac{-a_6\mu_3 + a_1 a_6 + a_3 a_4}{\mu_3(\mu_1-\mu_3)(\mu_2-\mu_3)} \quad \text{(I-60)}$$

$$L^{-1}\left\{\frac{a_6 s + a_1 a_6 + a_3 a_4}{(s+0)(s+\mu_1)(s+\mu_2)(s+\mu_3)}\right\} = L^{-1}\left\{\frac{B_1}{(s+0)} + \frac{B_2}{(s+\mu_1)} + \frac{B_3}{(s+\mu_2)} + \frac{B_4}{(s+\mu_3)}\right\}$$
$$= B_1 L^{-1}\left\{\frac{1}{(s+0)}\right\} + B_2 L^{-1}\left\{\frac{1}{(s+\mu_1)}\right\} + B_3 L^{-1}\left\{\frac{1}{(s+\mu_2)}\right\} + B_4 L^{-1}\left\{\frac{1}{(s+\mu_3)}\right\} \quad \text{(I-61)}$$

Using Equation I-54 in Equation I-61 gives

$$L^{-1}\left\{\frac{a_6 s + a_1 a_6 + a_3 a_4}{(s+0)(s+\mu_1)(s+\mu_2)(s+\mu_3)}\right\} = B_1 + B_2\, exp(-\mu_1 t) + B_3\, exp(-\mu_2 t) + B_4\, exp(-\mu_3 t) \quad \text{(I-62)}$$

Inverse Laplace transform of the term of $\frac{a_8 s + a_1 a_8 + a_2 a_7}{(s+0)(s+\mu_1)(s+\mu_2)(s+\mu_3)}$ in Equation I-47 is obtained by separation of the terms as follows:

$$\frac{a_8 s + a_1 a_8 + a_2 a_7}{(s+0)(s+\mu_1)(s+\mu_2)(s+\mu_3)} = \frac{C_1}{(s+0)} + \frac{C_2}{(s+\mu_1)} + \frac{C_3}{(s+\mu_2)} + \frac{C_4}{(s+\mu_3)} \quad \text{(I-63)}$$

$$C_1 = lim_{s\to 0}(s+0)\frac{a_8 s + a_1 a_8 + a_2 a_7}{(s+0)(s+\mu_1)(s+\mu_2)(s+\mu_3)} = \frac{a_1 a_8 + a_2 a_7}{\mu_1\mu_2\mu_3} \quad \text{(I-64)}$$

$$C_2 = lim_{s\to -\mu_1}(s+\mu_1)\frac{a_8 s + a_1 a_8 + a_2 a_7}{(s+0)(s+\mu_1)(s+\mu_2)(s+\mu_3)}$$
$$= -\frac{-a_8\mu_1 + a_1 a_8 + a_2 a_7}{\mu_1(\mu_2-\mu_1)(\mu_3-\mu_1)} \quad \text{(I-65)}$$

$$C_3 = lim_{s\to-\mu_2}(s+\mu_2)\frac{a_8 s + a_1 a_8 + a_2 a_7}{(s+0)(s+\mu_1)(s+\mu_2)(s+\mu_3)}$$
$$= -\frac{-a_8\mu_2 + a_1 a_8 + a_2 a_7}{\mu_2(\mu_1-\mu_2)(\mu_3-\mu_2)} \quad \text{(I-66)}$$

$$C_4 = lim_{s\to-\mu_3}(s+\mu_3)\frac{a_8 s + a_1 a_8 + a_2 a_7}{(s+0)(s+\mu_1)(s+\mu_2)(s+\mu_3)}$$
$$= -\frac{-a_8\mu_3 + a_1 a_8 + a_2 a_7}{\mu_3(\mu_1-\mu_3)(\mu_2-\mu_3)} \quad \text{(I-67)}$$

$$L^{-1}\left\{\frac{a_8 s + a_1 a_8 + a_2 a_7}{(s+0)(s+\mu_1)(s+\mu_2)(s+\mu_3)}\right\} = L^{-1}\left\{\frac{C_1}{(s+0)} + \frac{C_2}{(s+\mu_1)} + \frac{C_3}{(s+\mu_2)} + \frac{C_4}{(s+\mu_3)}\right\}$$
$$= C_1 L^{-1}\left\{\frac{1}{(s+0)}\right\} + C_2 L^{-1}\left\{\frac{1}{(s+\mu_1)}\right\} + C_3 L^{-1}\left\{\frac{1}{(s+\mu_2)}\right\} + C_4 L^{-1}\left\{\frac{1}{(s+\mu_3)}\right\} \quad \text{(I-68)}$$

Using Equation I-54 in Equation I-68 gives

$$L^{-1}\left\{\frac{a_8 s + a_1 a_8 + a_2 a_7}{(s+0)(s+\mu_1)(s+\mu_2)(s+\mu_3)}\right\} = C_1 + C_2\, exp(-\mu_1 t) + C_3\, exp(-\mu_2 t) + C_4\, exp(-\mu_3 t) \quad \text{(I-69)}$$

Inverse Laplace transform of the term of $\frac{s^2 + (a_1+a_5)s + a_1 a_5 - a_2 a_4}{(s+0)(s+\mu_1)(s+\mu_2)(s+\mu_3)}$ in Equation I-47 is obtained by separation of the terms as follows:

$$\frac{s^2 + (a_1+a_5)s + a_1 a_5 - a_2 a_4}{(s+0)(s+\mu_1)(s+\mu_2)(s+\mu_3)} = \frac{D_1}{(s+0)} + \frac{D_2}{(s+\mu_1)} + \frac{D_3}{(s+\mu_2)} + \frac{D_4}{(s+\mu_3)} \quad \text{(I-70)}$$

$$D_1 = lim_{s\to0}(s+0)\frac{s^2 + (a_1+a_5)s + a_1 a_5 - a_2 a_4}{(s+0)(s+\mu_1)(s+\mu_2)(s+\mu_3)} = \frac{a_1 a_5 - a_2 a_4}{\mu_1\mu_2\mu_3} \quad \text{(I-71)}$$

$$D_2 = lim_{s\to-\mu_1}(s+\mu_1)\frac{s^2 + (a_1+a_5)s + a_1 a_5 - a_2 a_4}{(s+0)(s+\mu_1)(s+\mu_2)(s+\mu_3)}$$
$$= -\frac{\mu_1^2 - (a_1+a_5)\mu_1 + a_1 a_5 - a_2 a_4}{\mu_1(\mu_2-\mu_1)(\mu_3-\mu_1)} \quad \text{(I-72)}$$

$$D_3 = lim_{s\to-\mu_2}(s+\mu_2)\frac{s^2+(a_1+a_5)s+a_1a_5-a_2a_4}{(s+0)(s+\mu_1)(s+\mu_2)(s+\mu_3)}$$
$$= -\frac{\mu_2^2-(a_1+a_5)\mu_2+a_1a_5-a_2a_4}{\mu_2(\mu_1-\mu_2)(\mu_3-\mu_2)} \quad \text{(I-73)}$$

$$D_4 = lim_{s\to-\mu_3}(s+\mu_3)\frac{s^2+(a_1+a_5)s+a_1a_5-a_2a_4}{(s+0)(s+\mu_1)(s+\mu_2)(s+\mu_3)}$$
$$= -\frac{\mu_3^2-(a_1+a_5)\mu_3+a_1a_5-a_2a_4}{\mu_3(\mu_1-\mu_3)(\mu_2-\mu_3)} \quad \text{(I-74)}$$

$$L^{-1}\left\{\frac{s^2+(a_1+a_5)s+a_1a_5-a_2a_4}{(s+0)(s+\mu_1)(s+\mu_2)(s+\mu_3)}\right\} = L^{-1}\left\{\frac{D_1}{(s+0)}+\frac{D_2}{(s+\mu_1)}+\frac{D_3}{(s+\mu_2)}+\frac{D_4}{(s+\mu_3)}\right\}$$
$$= D_1\,L^{-1}\left\{\frac{1}{(s+0)}\right\}+D_2\,L^{-1}\left\{\frac{1}{(s+\mu_1)}\right\}+D_3\,L^{-1}\left\{\frac{1}{(s+\mu_2)}\right\}+D_4L^{-1}\left\{\frac{1}{(s+\mu_3)}\right\} \quad \text{(I-75)}$$

Using Equation I-54 in Equation I-75 gives

$$L^{-1}\left\{\frac{s^2+(a_1+a_5)s+a_1a_5-a_2a_4}{(s+0)(s+\mu_1)(s+\mu_2)(s+\mu_3)}\right\} = D_1+D_2\,exp(-\mu_1 t) + D_3\,exp(-\mu_2 t)+D_4\,exp(-\mu_3 t) \quad \text{(I-76)}$$

Substituting Equations I-55 and I-62 into Equation I-46, and substituting Equations I-69 and I-76 into Equation I-47 gives

$$\Delta p_{r1}(t) = \frac{w_{p,net1}}{\kappa_{r1}}\{A_1+A_2\,exp(-\mu_1 t)+A_3\,exp(-\mu_2 t)+A_4\,exp(-\mu_3 t)\} + \frac{w_{p,net2}}{\kappa_{r2}}\{B_1+B_2\,exp(-\mu_1 t)+B_3\,exp(-\mu_2 t)+B_4\,exp(-\mu_3 t)\} \quad \text{(I-77)}$$

$$\Delta p_{r2}(t) = \frac{w_{p,net1}}{\kappa_{r1}}\{C_1+C_2\,exp(-\mu_1 t)+C_3\,exp(-\mu_2 t)+C_4\,exp(-\mu_3 t)\} + \frac{w_{p,net2}}{\kappa_{r2}}\{D_1+D_2\,exp(-\mu_1 t)+D_3\,exp(-\mu_2 t)+D_4\,exp(-\mu_3 t)\} \quad \text{(I-78)}$$

or

$$\Delta p_{r1}(t)=\frac{w_{p,net1}}{\kappa_{r1}}\left\{\begin{array}{l}\dfrac{a_1a_9-a_3a_7}{\mu_1\mu_2\mu_3}-\dfrac{\mu_1^2-(a_1+a_9)\mu_1+a_1a_9-a_3a_7}{\mu_1(\mu_2-\mu_1)(\mu_3-\mu_1)}exp(-\mu_1 t)\\ -\dfrac{\mu_2^2-(a_1+a_9)\mu_2+a_1a_9-a_3a_7}{\mu_2(\mu_1-\mu_2)(\mu_3-\mu_2)}exp(-\mu_2 t)\\ -\dfrac{\mu_3^2-(a_1+a_9)\mu_3+a_1a_9-a_3a_7}{\mu_3(\mu_1-\mu_3)(\mu_2-\mu_3)}exp(-\mu_3 t)\end{array}\right\}$$

$$+\frac{w_{p,net2}}{\kappa_{r2}}\left\{\begin{array}{l}\dfrac{a_1a_6+a_3a_4}{\mu_1\mu_2\mu_3}-\dfrac{-a_6\mu_1+a_1a_6+a_3a_4}{\mu_1(\mu_2-\mu_1)(\mu_3-\mu_1)}exp(-\mu_1 t)\\ -\dfrac{-a_6\mu_2+a_1a_6+a_3a_4}{\mu_2(\mu_1-\mu_2)(\mu_3-\mu_2)}exp(-\mu_2 t)\\ -\dfrac{-a_6\mu_3+a_1a_6+a_3a_4}{\mu_3(\mu_1-\mu_3)(\mu_2-\mu_3)}exp(-\mu_3 t)\end{array}\right\}$$

(I-79)

$$\Delta p_{r2}(t)=\frac{w_{p,net1}}{\kappa_{r1}}\left\{\begin{array}{l}\dfrac{a_1a_8+a_2a_7}{\mu_1\mu_2\mu_3}-\dfrac{-a_8\mu_1+a_1a_8+a_2a_7}{\mu_1(\mu_2-\mu_1)(\mu_3-\mu_1)}exp(-\mu_1 t)\\ -\dfrac{-a_8\mu_2+a_1a_8+a_2a_7}{\mu_2(\mu_1-\mu_2)(\mu_3-\mu_2)}exp(-\mu_2 t)\\ -\dfrac{-a_8\mu_3+a_1a_8+a_2a_7}{\mu_3(\mu_1-\mu_3)(\mu_2-\mu_3)}exp(-\mu_3 t)\end{array}\right\}$$

$$+\frac{w_{p,net2}}{\kappa_{r2}}\left\{\begin{array}{l}\dfrac{a_1a_5-a_2a_4}{\mu_1\mu_2\mu_3}-\dfrac{\mu_1^2-(a_1+a_5)\mu_1+a_1a_5-a_2a_4}{\mu_1(\mu_2-\mu_1)(\mu_3-\mu_1)}exp(-\mu_1 t)\\ -\dfrac{\mu_2^2-(a_1+a_5)\mu_2+a_1a_5-a_2a_4}{\mu_2(\mu_1-\mu_2)(\mu_3-\mu_2)}exp(-\mu_2 t)\\ -\dfrac{\mu_3^2-(a_1+a_5)\mu_3+a_1a_5-a_2a_4}{\mu_3(\mu_1-\mu_3)(\mu_2-\mu_3)}exp(-\mu_3 t)\end{array}\right\}$$

(I-80)

The shallow and deep reservoirs pressures as a function of production time are obtained by using Equations I-79 and I-80 as below.

$$p_{r1}(t) = p_i - \left\{ \begin{array}{l} \dfrac{w_{p,net1}}{\kappa_{r1}} \left[\begin{array}{l} \dfrac{a_1 a_9 - a_3 a_7}{\mu_1 \mu_2 \mu_3} - \dfrac{\mu_1^2 - (a_1 + a_9)\mu_1 + a_1 a_9 - a_3 a_7}{\mu_1 (\mu_2 - \mu_1)(\mu_3 - \mu_1)} exp(-\mu_1 t) \\ - \dfrac{\mu_2^2 - (a_1 + a_9)\mu_2 + a_1 a_9 - a_3 a_7}{\mu_2 (\mu_1 - \mu_2)(\mu_3 - \mu_2)} exp(-\mu_2 t) \\ - \dfrac{\mu_3^2 - (a_1 + a_9)\mu_3 + a_1 a_9 - a_3 a_7}{\mu_3 (\mu_1 - \mu_3)(\mu_2 - \mu_3)} exp(-\mu_3 t) \end{array} \right] \\ + \dfrac{w_{p,net2}}{\kappa_{r2}} \left[\begin{array}{l} \dfrac{a_1 a_6 + a_3 a_4}{\mu_1 \mu_2 \mu_3} - \dfrac{-a_6 \mu_1 + a_1 a_6 + a_3 a_4}{\mu_1 (\mu_2 - \mu_1)(\mu_3 - \mu_1)} exp(-\mu_1 t) \\ - \dfrac{-a_6 \mu_2 + a_1 a_6 + a_3 a_4}{\mu_2 (\mu_1 - \mu_2)(\mu_3 - \mu_2)} exp(-\mu_2 t) \\ - \dfrac{-a_6 \mu_3 + a_1 a_6 + a_3 a_4}{\mu_3 (\mu_1 - \mu_3)(\mu_2 - \mu_3)} exp(-\mu_3 t) \end{array} \right] \end{array} \right\} \quad \text{(I-81)}$$

$$p_{r2}(t) = p_i - \left\{ \begin{array}{l} \dfrac{w_{p,net1}}{\kappa_{r1}} \left[\begin{array}{l} \dfrac{a_1 a_8 + a_2 a_7}{\mu_1 \mu_2 \mu_3} - \dfrac{-a_8 \mu_1 + a_1 a_8 + a_2 a_7}{\mu_1 (\mu_2 - \mu_1)(\mu_3 - \mu_1)} exp(-\mu_1 t) \\ - \dfrac{-a_8 \mu_2 + a_1 a_8 + a_2 a_7}{\mu_2 (\mu_1 - \mu_2)(\mu_3 - \mu_2)} exp(-\mu_2 t) \\ - \dfrac{-a_8 \mu_3 + a_1 a_8 + a_2 a_7}{\mu_3 (\mu_1 - \mu_3)(\mu_2 - \mu_3)} exp(-\mu_3 t) \end{array} \right] \\ + \dfrac{w_{p,net2}}{\kappa_{r2}} \left[\begin{array}{l} \dfrac{a_1 a_5 - a_2 a_4}{\mu_1 \mu_2 \mu_3} - \dfrac{\mu_1^2 - (a_1 + a_5)\mu_1 + a_1 a_5 - a_2 a_4}{\mu_1 (\mu_2 - \mu_1)(\mu_3 - \mu_1)} exp(-\mu_1 t) \\ - \dfrac{\mu_2^2 - (a_1 + a_5)\mu_2 + a_1 a_5 - a_2 a_4}{\mu_2 (\mu_1 - \mu_2)(\mu_3 - \mu_2)} exp(-\mu_2 t) \\ - \dfrac{\mu_3^2 - (a_1 + a_5)\mu_3 + a_1 a_5 - a_2 a_4}{\mu_3 (\mu_1 - \mu_3)(\mu_2 - \mu_3)} exp(-\mu_3 t) \end{array} \right] \end{array} \right\} \quad \text{(I-82)}$$

APPENDIX-J

2 RESERVOIR TANK MODEL WITH AQUIFER (WITHOUT INITIAL HYDRAULIC EQUILIBRIUM)

Mass balances on the shallow and deep reservoirs and the aquifer, recharges of the reservoirs and the aquifer, initial conditions are expressed as;

Mass Balance on the Aquifer :

$$w_a - w_{r1} - w_{r2} = \kappa_a \frac{dp_a}{dt} \tag{J-1}$$

Mass Balance on the Shallow Reservoir :

$$w_{r1} + w_{r12} - w_{p,net1} = \kappa_{r1} \frac{dp_{r1}}{dt} \tag{J-2}$$

Mass Balance on the Deep Reservoir :

$$w_{r2} - w_{r12} - w_{p,net2} = \kappa_{r2} \frac{dp_{r2}}{dt} \tag{J-3}$$

Recharge of the Aquifer : $w_a = \alpha_a (p_i - p_a)$ (J-4)

Recharge of the Shallow Reservoir : $w_{r1} = \alpha_{r1} (p_a - p_{r1})$ (J-5)

Recharge of the Deep Reservoir : $w_{r2} = \alpha_{r2} (p_a - p_{r2})$ (J-6)

Recharge between the Shallow and Deep Reservoirs :

$$w_{r12} = \alpha_{r12} (p_{r2} - p_{r1}) \tag{J-7}$$

Initial Conditions :

$$\begin{aligned} p_a &= p_{ai} \quad @\ t = 0 \\ p_{r1} &= p_{r1i} \quad @\ t = 0 \\ p_{r2} &= p_{r2i} \quad @\ t = 0 \end{aligned} \tag{J-8}$$

Substituting Equations J-4, J-5, J-6, and J-7 into Equations J-1, J-2, and J-3 gives

$$\alpha_a(p_i - p_a) - \alpha_{r1}(p_a - p_{r1}) - \alpha_{r2}(p_a - p_{r2}) = \kappa_a \frac{dp_a}{dt} \tag{J-9}$$

$$\alpha_{r1}(p_a - p_{r1}) + \alpha_{r12}(p_{r2} - p_{r1}) - w_{p,net1} = \kappa_{r1} \frac{dp_{r1}}{dt} \tag{J-10}$$

$$\alpha_{r2}(p_a - p_{r2}) - \alpha_{r12}(p_{r2} - p_{r1}) - w_{p,net2} = \kappa_{r2} \frac{dp_{r2}}{dt} \tag{J-11}$$

Equations J-9, J-10, and J-11 can be written in terms of pressure changes. The pressure changes and their derivatives with respect to time are given by

$$\left.\begin{aligned}
&\Delta p_a = p_{ai} - p_a \;\Rightarrow\; p_a = p_{ai} - \Delta p_a \;\Rightarrow\; \frac{d\,\Delta p_a}{dt} = -\frac{dp_a}{dt} \\
&\Delta p_{r1} = p_{r1i} - p_{r1} \;\Rightarrow\; p_{r1} = p_{r1i} - \Delta p_{r1} \;\Rightarrow\; \frac{d\,\Delta p_{r1}}{dt} = -\frac{dp_{r1}}{dt} \\
&\Delta p_{r2} = p_{r2i} - p_{r2} \;\Rightarrow\; p_{r2} = p_{r2i} - \Delta p_{r2} \;\Rightarrow\; \frac{d\,\Delta p_{r2}}{dt} = -\frac{dp_{r2}}{dt}
\end{aligned}\right\} \tag{J-12}$$

and initial conditions become

$$\left.\begin{aligned}
&\Delta p_a(t=0) = p_{ai} - p_a(t=0) = p_{ai} - p_{ai} = 0 \\
&\Delta p_{r1}(t=0) = p_{r1i} - p_{r1}(t=0) = p_{r1i} - p_{r1i} = 0 \\
&\Delta p_{r2}(t=0) = p_{r2i} - p_{r2}(t=0) = p_{r2i} - p_{r2i} = 0
\end{aligned}\right\} \tag{J-13}$$

Using Equation I-12 in Equations I-9, I-10, and I-11 gives

$$\begin{aligned}
&\alpha_a(p_i - p_{ai} + \Delta p_a) - \alpha_{r1}(p_{ai} - \Delta p_a - p_{r1i} + \Delta p_{r1}) \\
&\qquad - \alpha_{r2}(p_{ai} - \Delta p_a - p_{r2i} + \Delta p_{r2}) = -\kappa_a \frac{d\Delta p_a}{dt}
\end{aligned} \tag{J-14}$$

$$\begin{aligned}
&\alpha_{r1}(p_{ai} - \Delta p_a - p_{r1i} + \Delta p_{r1}) + \alpha_{r12}(p_{r2i} - \Delta p_{r2} - p_{r1i} + \Delta p_{r1}) \\
&\qquad - w_{p,net1} = -\kappa_{r1} \frac{d\Delta p_{r1}}{dt}
\end{aligned} \tag{J-15}$$

$$\begin{aligned}
&\alpha_{r2}(p_{ai} - \Delta p_a - p_{r2i} + \Delta p_{r2}) - \alpha_{r12}(p_{r2i} - \Delta p_{r2} - p_{r1i} + \Delta p_{r1}) \\
&\qquad - w_{p,net2} = -\kappa_{r2} \frac{d\Delta p_{r2}}{dt}
\end{aligned} \tag{J-16}$$

The following definitions can be made to simplify the equations.

$$\left.\begin{aligned} \Delta p_{ac} &= p_i - p_{ai} \\ \Delta p_{r1c} &= p_{ai} - p_{r1i} \\ \Delta p_{r2c} &= p_{ai} - p_{r2i} \\ \Delta p_{rc} &= p_{r2i} - p_{r1i} \end{aligned}\right\} \tag{J-17}$$

Substituting Equation J-17 into Equations J-14, J-15, and J-16 gives

$$\begin{aligned} &\alpha_a(\Delta p_{ac} + \Delta p_a) - \alpha_{r1}(\Delta p_{r1c} - \Delta p_a + \Delta p_{r1}) \\ &\qquad - \alpha_{r2}(\Delta p_{r2c} - \Delta p_a + \Delta p_{r2}) = -\kappa_a \frac{d\Delta p_a}{dt} \end{aligned} \tag{J-18}$$

$$\alpha_{r1}(\Delta p_{r1c} - \Delta p_a + \Delta p_{r1}) + \alpha_{r12}(\Delta p_{rc} - \Delta p_{r2} + \Delta p_{r1}) - w_{p,net1} = -\kappa_{r1} \frac{d\Delta p_{r1}}{dt} \tag{J-19}$$

$$\alpha_{r2}(\Delta p_{r2c} - \Delta p_a + \Delta p_{r2}) - \alpha_{r12}(\Delta p_{rc} - \Delta p_{r2} + \Delta p_{r1}) - w_{p,net2} = -\kappa_{r2} \frac{d\Delta p_{r2}}{dt} \tag{J-20}$$

Equations J-18, J-19, and J-20 can be simplified and rearranged as follows:

$$\begin{aligned} &\kappa_a \frac{d\Delta p_a}{dt} + (\alpha_a + \alpha_{r1} + \alpha_{r2})\Delta p_a - \alpha_{r1}\Delta p_{r1} - \alpha_{r2}\Delta p_{r2} \\ &\qquad = -\alpha_a \Delta p_{ac} + \alpha_{r1}\Delta p_{r1c} + \alpha_{r2}\Delta p_{r2c} \end{aligned} \tag{J-21}$$

$$\begin{aligned} &\kappa_{r1} \frac{d\Delta p_{r1}}{dt} - \alpha_{r1}\Delta p_a + (\alpha_{r1} + \alpha_{r12})\Delta p_{r1} - \alpha_{r12}\Delta p_{r2} \\ &\qquad = w_{p,net1} - \alpha_{r1}\Delta p_{r1c} - \alpha_{r12}\Delta p_{rc} \end{aligned} \tag{J-22}$$

$$\begin{aligned} &\kappa_{r2} \frac{d\Delta p_{r2}}{dt} - \alpha_{r2}\Delta p_a - \alpha_{r12}\Delta p_{r1} + (\alpha_{r2} + \alpha_{r12})\Delta p_{r2} \\ &\qquad = w_{p,net2} - \alpha_{r2}\Delta p_{r2c} + \alpha_{r12}\Delta p_{rc} \end{aligned} \tag{J-23}$$

Applying Laplace transformation (Erdélyi, 1954) to Equations J-21, J-22, and J-23 and using the initial conditions (Equation J-13) gives

$$\begin{aligned} &\kappa_a s\,\overline{\Delta p_a} + (\alpha_a + \alpha_{r1} + \alpha_{r2})\overline{\Delta p_a} - \alpha_{r1}\,\overline{\Delta p_{r1}} - \alpha_{r2}\,\overline{\Delta p_{r2}} \\ &\qquad = \frac{1}{s}(-\alpha_a \Delta p_{ac} + \alpha_{r1}\Delta p_{r1c} + \alpha_{r2}\Delta p_{r2c}) \end{aligned} \tag{J-24}$$

$$\kappa_{r1} s\,\overline{\Delta p_{r1}} - \alpha_{r1}\,\overline{\Delta p_a} + (\alpha_{r1} + \alpha_{r12})\,\overline{\Delta p_{r1}} - \alpha_{r12}\,\overline{\Delta p_{r2}} = \frac{1}{s}\left(w_{p,net1} - \alpha_{r1}\Delta p_{r1c} - \alpha_{r12}\Delta p_{rc}\right) \tag{J-25}$$

$$\kappa_{r2} s\,\overline{\Delta p_{r2}} - \alpha_{r2}\,\overline{\Delta p_a} - \alpha_{r12}\,\overline{\Delta p_{r1}} + (\alpha_{r2} + \alpha_{r12})\,\overline{\Delta p_{r2}} = \frac{1}{s}\left(w_{p,net2} - \alpha_{r2}\Delta p_{r2c} + \alpha_{r12}\Delta p_{rc}\right) \tag{J-26}$$

where

$$\overline{\Delta p_a} = \int_0^\infty e^{-st}\Delta p_a\, d\tau \quad , \quad \overline{\Delta p_{r1}} = \int_0^\infty e^{-st}\Delta p_{r1}\, d\tau \quad , \quad \overline{\Delta p_{r2}} = \int_0^\infty e^{-st}\Delta p_{r2}\, d\tau \tag{J-27}$$

Rearranging J-24, J-25, and J-26 gives

$$(\kappa_a s + \alpha_a + \alpha_{r1} + \alpha_{r2})\,\overline{\Delta p_a} - \alpha_{r1}\,\overline{\Delta p_{r1}} - \alpha_{r2}\,\overline{\Delta p_{r2}} = \frac{1}{s}\left(-\alpha_a\Delta p_{ac} + \alpha_{r1}\Delta p_{r1c} + \alpha_{r2}\Delta p_{r2c}\right) \tag{J-28}$$

$$-\alpha_{r1}\,\overline{\Delta p_a} + (\kappa_{r1} s + \alpha_{r1} + \alpha_{r12})\,\overline{\Delta p_{r1}} - \alpha_{r12}\,\overline{\Delta p_{r2}} = \frac{1}{s}\left(w_{p,net1} - \alpha_{r1}\Delta p_{r1c} - \alpha_{r12}\Delta p_{rc}\right) \tag{J-29}$$

$$-\alpha_{r2}\,\overline{\Delta p_a} - \alpha_{r12}\,\overline{\Delta p_{r1}} + (\kappa_{r2} s + \alpha_{r2} + \alpha_{r12})\,\overline{\Delta p_{r2}} = \frac{1}{s}\left(w_{p,net2} - \alpha_{r2}\Delta p_{r2c} + \alpha_{r12}\Delta p_{rc}\right) \tag{J-30}$$

or

$$\left(s + \frac{\alpha_a + \alpha_{r1} + \alpha_{r2}}{\kappa_a}\right)\overline{\Delta p_a} - \frac{\alpha_{r1}}{\kappa_a}\,\overline{\Delta p_{r1}} - \frac{\alpha_{r2}}{\kappa_a}\,\overline{\Delta p_{r2}} = \frac{1}{s}\left(\frac{-\alpha_a\Delta p_{ac} + \alpha_{r1}\Delta p_{r1c} + \alpha_{r2}\Delta p_{r2c}}{\kappa_a}\right) \tag{J-31}$$

$$-\frac{\alpha_{r1}}{\kappa_{r1}}\overline{\Delta p_a}+\left(s+\frac{\alpha_{r1}+\alpha_{r12}}{\kappa_{r1}}\right)\overline{\Delta p_{r1}}-\frac{\alpha_{r12}}{\kappa_{r1}}\overline{\Delta p_{r2}} = \frac{1}{s}\left(\frac{w_{p,net1}-\alpha_{r1}\Delta p_{r1c}-\alpha_{r12}\Delta p_{rc}}{\kappa_{r1}}\right) \tag{J-32}$$

$$-\frac{\alpha_{r2}}{\kappa_{r2}}\overline{\Delta p_a}-\frac{\alpha_{r12}}{\kappa_{r2}}\overline{\Delta p_{r1}}+\left(s+\frac{\alpha_{r2}+\alpha_{r12}}{\kappa_{r2}}\right)\overline{\Delta p_{r2}} = \frac{1}{s}\left(\frac{w_{p,net2}-\alpha_{r2}\Delta p_{r2c}+\alpha_{r12}\Delta p_{rc}}{\kappa_{r2}}\right) \tag{J-33}$$

By using the definitions (Equation J-34) given below, Equations J-31, J-32, and J-33 can be rewritten as below:

$$\left.\begin{aligned} &a_1=\frac{\alpha_a+\alpha_{r1}+\alpha_{r2}}{\kappa_a},\ a_2=\frac{\alpha_{r1}}{\kappa_a},\ a_3=\frac{\alpha_{r2}}{\kappa_a}\\ &a_4=\frac{-\alpha_a\Delta p_{ac}+\alpha_{r1}\Delta p_{r1c}+\alpha_{r2}\Delta p_{r2c}}{\kappa_a}\\ &a_5=\frac{\alpha_{r1}}{\kappa_{r1}},\ a_6=\frac{\alpha_{r1}+\alpha_{r12}}{\kappa_{r1}},\ a_7=\frac{\alpha_{r12}}{\kappa_{r1}}\\ &a_8=\frac{-\alpha_{r1}\Delta p_{r1c}-\alpha_{r12}\Delta p_{rc}}{\kappa_{r1}},\ a_9=\frac{\alpha_{r2}}{\kappa_{r2}}\\ &a_{10}=\frac{\alpha_{r12}}{\kappa_{r2}},\ a_{11}=\frac{\alpha_{r2}+\alpha_{r12}}{\kappa_{r2}},\ a_{12}=\frac{-\alpha_{r2}\Delta p_{r2c}+\alpha_{r12}\Delta p_{rc}}{\kappa_{r2}} \end{aligned}\right\} \tag{J-34}$$

$$(s+a_1)\overline{\Delta p_a}-a_2\overline{\Delta p_{r1}}-a_3\overline{\Delta p_{r2}}=\frac{1}{s}a_4 \tag{J-35}$$

$$-a_5\overline{\Delta p_a}+(s+a_6)\overline{\Delta p_{r1}}-a_7\overline{\Delta p_{r2}}=\frac{1}{s}\left(\frac{w_{p,net1}}{\kappa_{r1}}+a_8\right) \tag{J-36}$$

$$-a_9\overline{\Delta p_a}-a_{10}\overline{\Delta p_{r1}}+(s+a_{11})\overline{\Delta p_{r2}}=\frac{1}{s}\left(\frac{w_{p,net2}}{\kappa_{r2}}+a_{12}\right) \tag{J-37}$$

The solutions to three equations (Equations J-35, J-36 and J-37) with three unknowns ($\overline{\Delta p_a}, \overline{\Delta p_{r1}}, \overline{\Delta p_{r2}}$) can be obtained by using Cramer's rule (Kreyszig, 1999) as follows:

$$\overline{\Delta p_a} = \frac{D_a}{D} \quad , \quad \overline{\Delta p_{r1}} = \frac{D_{r1}}{D} \quad , \quad \overline{\Delta p_{r2}} = \frac{D_{r2}}{D} \tag{J-38}$$

$$D_a = \begin{vmatrix} \frac{1}{s}a_4 & -a_2 & -a_3 \\ \frac{1}{s}\left(\frac{w_{p,net1}}{\kappa_{r1}} + a_8\right) & (s+a_6) & -a_7 \\ \frac{1}{s}\left(\frac{w_{p,net2}}{\kappa_{r2}} + a_{12}\right) & -a_{10} & (s+a_{11}) \end{vmatrix} \tag{J-39}$$

$$D_{r1} = \begin{vmatrix} (s+a_1) & \frac{1}{s}a_4 & -a_3 \\ -a_5 & \frac{1}{s}\left(\frac{w_{p,net1}}{\kappa_{r1}} + a_8\right) & -a_7 \\ -a_9 & \frac{1}{s}\left(\frac{w_{p,net2}}{\kappa_{r2}} + a_{12}\right) & (s+a_{11}) \end{vmatrix}$$

$$= \frac{w_{p,net1}}{\kappa_{r1}}\frac{1}{s}\left[s^2 + (a_1+a_{11})s + a_1a_{11} - a_3a_9\right] + \frac{w_{p,net2}}{\kappa_{r2}}\frac{1}{s}\left[a_7 s + a_1a_7 + a_3a_5\right]$$

$$+ a_8\, s + \frac{1}{s}\left(a_1a_8a_{11} + a_1a_7a_{12} + a_4a_5a_{11} + a_4a_7a_9 + a_3a_5a_{12} - a_3a_8a_9\right) \tag{J-40}$$

$$+ a_8a_{11} + a_7a_{12} + a_1a_8 + a_4a_5$$

$$D_{r2} = \begin{vmatrix} (s+a_1) & -a_2 & \frac{1}{s}a_4 \\ -a_5 & (s+a_6) & \frac{1}{s}\left(\frac{w_{p,net1}}{\kappa_{r1}} + a_8\right) \\ -a_9 & -a_{10} & \frac{1}{s}\left(\frac{w_{p,net2}}{\kappa_{r2}} + a_{12}\right) \end{vmatrix}$$

$$= \frac{w_{p,net1}}{\kappa_{r1}}\frac{1}{s}\left[a_{10}s + a_1a_{10} + a_2a_9\right] + \frac{w_{p,net2}}{\kappa_{r2}}\frac{1}{s}\left[s^2 + (a_1+a_6)s + a_1a_6 - a_2a_5\right]$$

$$+ a_{12}\, s + \frac{1}{s}\left(a_1a_6a_{12} + a_1a_8a_{10} + a_2a_8a_9 + a_4a_5a_{10} + a_4a_6a_9 - a_2a_5a_{12}\right) \tag{J-41}$$

$$+ a_6a_{12} + a_8a_{10} + a_1a_{12} + a_4a_9$$

$$D = \begin{vmatrix} (s+a_1) & -a_2 & -a_3 \\ -a_5 & (s+a_6) & -a_7 \\ -a_9 & -a_{10} & (s+a_{11}) \end{vmatrix}$$

$$= s^3 + (a_1 + a_6 + a_{11})s^2 + (a_6a_{11} - a_7a_{10} + a_1a_6 + a_1a_{11} - a_2a_5 - a_3a_9)s + a_1a_6a_{11} - a_1a_7a_{10} - a_2a_5a_{11} - a_2a_7a_9 - a_3a_5a_{10} - a_3a_6a_9 \quad \text{(J-42)}$$

Substituting Equations J-40, J-41, and J-42 into Equation J-38 gives

$$\overline{\Delta p_{r1}} = \frac{\left[\begin{array}{l} \frac{w_{p,net1}}{\kappa_{r1}}\frac{1}{s}\left[s^2 + (a_1 + a_{11})s + a_1a_{11} - a_3a_9\right] + \frac{w_{p,net2}}{\kappa_{r2}}\frac{1}{s}\left[a_7 s + a_1a_7 + a_3a_5\right] \\ + a_8\, s + \frac{1}{s}(a_1a_8a_{11} + a_1a_7a_{12} + a_4a_5a_{11} + a_4a_7a_9 + a_3a_5a_{12} - a_3a_8a_9) \\ + a_8a_{11} + a_7a_{12} + a_1a_8 + a_4a_5 \end{array}\right]}{\left[\begin{array}{l} s^3 + (a_1 + a_6 + a_{11})s^2 + (a_6a_{11} - a_7a_{10} + a_1a_6 + a_1a_{11} - a_2a_5 - a_3a_9)s \\ + a_1a_6a_{11} - a_1a_7a_{10} - a_2a_5a_{11} - a_2a_7a_9 - a_3a_5a_{10} - a_3a_6a_9 \end{array}\right]} \quad \text{(J-43)}$$

$$\overline{\Delta p_{r2}} = \frac{\left[\begin{array}{l} \frac{w_{p,net1}}{\kappa_{r1}}\frac{1}{s}\left[a_{10}s + a_1a_{10} + a_2a_9\right] + \frac{w_{p,net2}}{\kappa_{r2}}\frac{1}{s}\left[s^2 + (a_1 + a_6)s + a_1a_6 - a_2a_5\right] \\ + a_{12}\, s + \frac{1}{s}(a_1a_6a_{12} + a_1a_8a_{10} + a_2a_8a_9 + a_4a_5a_{10} + a_4a_6a_9 - a_2a_5a_{12}) \\ + a_6a_{12} + a_8a_{10} + a_1a_{12} + a_4a_9 \end{array}\right]}{\left[\begin{array}{l} s^3 + (a_1 + a_6 + a_{11})s^2 + (a_6a_{11} - a_7a_{10} + a_1a_6 + a_1a_{11} - a_2a_5 - a_3a_9)s \\ + a_1a_6a_{11} - a_1a_7a_{10} - a_2a_5a_{11} - a_2a_7a_9 - a_3a_5a_{10} - a_3a_6a_9 \end{array}\right]} \quad \text{(J-44)}$$

The roots of the cubic equation in Equation J-43 and J-44 are found as follows:

$$Q = \frac{(a_1 + a_6 + a_{11})^2 - 3(a_6 a_{11} - a_7 a_{10} + a_1 a_6 + a_1 a_{11} - a_2 a_5 - a_3 a_9)}{9}$$

$$R = \frac{1}{54}\begin{bmatrix} 2(a_1 + a_6 + a_{11})^3 \\ -9(a_1 + a_6 + a_{11})(a_6 a_{11} - a_7 a_{10} + a_1 a_6 + a_1 a_{11} - a_2 a_5 - a_3 a_9) \\ +27(a_1 a_6 a_{11} - a_1 a_7 a_{10} - a_2 a_5 a_{11} - a_2 a_7 a_9 - a_3 a_5 a_{10} - a_3 a_6 a_9) \end{bmatrix} \quad \text{(J-45)}$$

$$\theta = arc\,cos\left(\frac{R}{\sqrt{Q^3}}\right)$$

$$\mu_1 = 2\sqrt{Q}\,cos\left(\frac{\theta}{3}\right) + \frac{(a_1 + a_6 + a_{11})}{3}$$

$$\mu_2 = 2\sqrt{Q}\,cos\left(\frac{\theta + 2\pi}{3}\right) + \frac{(a_1 + a_6 + a_{11})}{3} \quad \text{(J-46)}$$

$$\mu_3 = 2\sqrt{Q}\,cos\left(\frac{\theta + 4\pi}{3}\right) + \frac{(a_1 + a_6 + a_{11})}{3}$$

Using Equation J-46, the following expression can be written

$$\begin{bmatrix} s^3 + (a_1 + a_6 + a_{11})s^2 \\ +(a_6 a_{11} - a_7 a_{10} + a_1 a_6 + a_1 a_{11} - a_2 a_5 - a_3 a_9)s \\ +a_1 a_6 a_{11} - a_1 a_7 a_{10} - a_2 a_5 a_{11} - a_2 a_7 a_9 - a_3 a_5 a_{10} - a_3 a_6 a_9 \end{bmatrix} = (s + \mu_1)(s + \mu_2)(s + \mu_3) \quad \text{(J-47)}$$

Substituting Equation J-47 into Equations J-43 and J-44 gives

$$\begin{aligned} \overline{\Delta p_{r1}} = {} & \frac{w_{p,net1}}{\kappa_{r1}} \frac{s^2 + (a_1 + a_{11})s + a_1 a_{11} - a_3 a_9}{s(s + \mu_1)(s + \mu_2)(s + \mu_3)} + \frac{w_{p,net2}}{\kappa_{r2}} \frac{a_7 s + a_1 a_7 + a_3 a_5}{s(s + \mu_1)(s + \mu_2)(s + \mu_3)} \\ & + a_8 \frac{s}{(s + \mu_1)(s + \mu_2)(s + \mu_3)} \\ & + \frac{a_1 a_8 a_{11} + a_1 a_7 a_{12} + a_4 a_5 a_{11} + a_4 a_7 a_9 + a_3 a_5 a_{12} - a_3 a_8 a_9}{s(s + \mu_1)(s + \mu_2)(s + \mu_3)} \\ & + \frac{a_8 a_{11} + a_7 a_{12} + a_1 a_8 + a_4 a_5}{(s + \mu_1)(s + \mu_2)(s + \mu_3)} \end{aligned} \quad \text{(J-48)}$$

$$\overline{\Delta p_{r2}} = \frac{w_{p,net1}}{\kappa_{r1}} \frac{a_{10}s + a_1a_{10} + a_2a_9}{s(s+\mu_1)(s+\mu_2)(s+\mu_3)} + \frac{w_{p,net2}}{\kappa_{r2}} \frac{s^2 + (a_1 + a_6)s + a_1a_6 - a_2a_5}{s(s+\mu_1)(s+\mu_2)(s+\mu_3)}$$
$$+ a_{12} \frac{s}{(s+\mu_1)(s+\mu_2)(s+\mu_3)}$$
$$+ \frac{a_1a_6a_{12} + a_1a_8a_{10} + a_2a_8a_9 + a_4a_5a_{10} + a_4a_6a_9 - a_2a_5a_{12}}{s(s+\mu_1)(s+\mu_2)(s+\mu_3)}$$
$$+ \frac{a_6a_{12} + a_8a_{10} + a_1a_{12} + a_4a_9}{(s+\mu_1)(s+\mu_2)(s+\mu_3)} \qquad \text{(J-49)}$$

In order to find the values of Δp_{r1} and Δp_{r2} in real space, inverse Laplace transform of Equations J-48 and J-49 are obtained as follows:

$$\Delta p_{r1} = L^{-1}\left\{\overline{\Delta p_{r1}}\right\} = \frac{w_{p,net1}}{\kappa_{r1}} L^{-1}\left\{\frac{s^2 + (a_1 + a_{11})s + a_1a_{11} - a_3a_9}{(s+0)(s+\mu_1)(s+\mu_2)(s+\mu_3)}\right\}$$
$$+ \frac{w_{p,net2}}{\kappa_{r2}} L^{-1}\left\{\frac{a_7s + a_1a_7 + a_3a_5}{(s+0)(s+\mu_1)(s+\mu_2)(s+\mu_3)}\right\}$$
$$+ a_8 L^{-1}\left\{\frac{s}{(s+\mu_1)(s+\mu_2)(s+\mu_3)}\right\} \qquad \text{(J-50)}$$
$$+ a_{13} L^{-1}\left\{\frac{1}{(s+0)(s+\mu_1)(s+\mu_2)(s+\mu_3)}\right\}$$
$$+ a_{14} L^{-1}\left\{\frac{1}{(s+\mu_1)(s+\mu_2)(s+\mu_3)}\right\}$$

$$\Delta p_{r2} = L^{-1}\left\{\overline{\Delta p_{r2}}\right\} = \frac{w_{p,net1}}{\kappa_{r1}} L^{-1}\left\{\frac{a_{10}s + a_1a_{10} + a_2a_9}{(s+0)(s+\mu_1)(s+\mu_2)(s+\mu_3)}\right\}$$
$$+ \frac{w_{p,net2}}{\kappa_{r2}} L^{-1}\left\{\frac{s^2 + (a_1 + a_6)s + a_1a_6 - a_2a_5}{(s+0)(s+\mu_1)(s+\mu_2)(s+\mu_3)}\right\}$$
$$+ a_{12} L^{-1}\left\{\frac{s}{(s+\mu_1)(s+\mu_2)(s+\mu_3)}\right\} \qquad \text{(J-51)}$$
$$+ a_{15} L^{-1}\left\{\frac{1}{(s+0)(s+\mu_1)(s+\mu_2)(s+\mu_3)}\right\}$$
$$+ a_{16} L^{-1}\left\{\frac{1}{(s+\mu_1)(s+\mu_2)(s+\mu_3)}\right\}$$

where

$$
\begin{aligned}
a_{13} &= a_1a_8a_{11} + a_1a_7a_{12} + a_4a_5a_{11} + a_4a_7a_9 + a_3a_5a_{12} - a_3a_8a_9 \\
a_{14} &= a_8a_{11} + a_7a_{12} + a_1a_8 + a_4a_5 \\
a_{15} &= a_1a_6a_{12} + a_1a_8a_{10} + a_2a_8a_9 + a_4a_5a_{10} + a_4a_6a_9 - a_2a_5a_{12} \\
a_{16} &= a_6a_{12} + a_8a_{10} + a_1a_{12} + a_4a_9
\end{aligned}
\tag{J-52}
$$

Inverse Laplace transform of the term of $\frac{s^2 + (a_1 + a_{11})s + a_1a_{11} - a_3a_9}{(s+0)(s+\mu_1)(s+\mu_2)(s+\mu_3)}$ in Equation J-50 is obtained by separation of the terms as follows:

$$
\frac{s^2 + (a_1 + a_{11})s + a_1a_{11} - a_3a_9}{(s+0)(s+\mu_1)(s+\mu_2)(s+\mu_3)} = \frac{B_1}{(s+0)} + \frac{B_2}{(s+\mu_1)} + \frac{B_3}{(s+\mu_2)} + \frac{B_4}{(s+\mu_3)} \tag{J-53}
$$

$$
B_1 = lim_{s\to 0}\,(s+0)\frac{s^2 + (a_1 + a_{11})s + a_1a_{11} - a_3a_9}{(s+0)(s+\mu_1)(s+\mu_2)(s+\mu_3)} = \frac{a_1a_{11} - a_3a_9}{\mu_1\mu_2\mu_3} \tag{J-54}
$$

$$
\begin{aligned}
B_2 &= lim_{s\to -\mu_1}\,(s+\mu_1)\frac{s^2 + (a_1 + a_{11})s + a_1a_{11} - a_3a_9}{(s+0)(s+\mu_1)(s+\mu_2)(s+\mu_3)} \\
&= -\frac{\mu_1^2 - (a_1 + a_{11})\mu_1 + a_1a_{11} - a_3a_9}{\mu_1(\mu_2 - \mu_1)(\mu_3 - \mu_1)}
\end{aligned}
\tag{J-55}
$$

$$
\begin{aligned}
B_3 &= lim_{s\to -\mu_2}\,(s+\mu_2)\frac{s^2 + (a_1 + a_{11})s + a_1a_{11} - a_3a_9}{(s+0)(s+\mu_1)(s+\mu_2)(s+\mu_3)} \\
&= -\frac{\mu_2^2 - (a_1 + a_{11})\mu_2 + a_1a_{11} - a_3a_9}{\mu_2(\mu_1 - \mu_2)(\mu_3 - \mu_2)}
\end{aligned}
\tag{J-56}
$$

$$
\begin{aligned}
B_4 &= lim_{s\to -\mu_3}\,(s+\mu_3)\frac{s^2 + (a_1 + a_{11})s + a_1a_{11} - a_3a_9}{(s+0)(s+\mu_1)(s+\mu_2)(s+\mu_3)} \\
&= -\frac{\mu_3^2 - (a_1 + a_{11})\mu_3 + a_1a_{11} - a_3a_9}{\mu_3(\mu_1 - \mu_3)(\mu_2 - \mu_3)}
\end{aligned}
\tag{J-57}
$$

$$L^{-1}\left\{\frac{s^2+(a_1+a_{11})s+a_1a_{11}-a_3a_9}{(s+0)(s+\mu_1)(s+\mu_2)(s+\mu_3)}\right\}=L^{-1}\left\{\frac{B_1}{(s+0)}+\frac{B_2}{(s+\mu_1)}+\frac{B_3}{(s+\mu_2)}+\frac{B_4}{(s+\mu_3)}\right\}$$

$$=B_1\,L^{-1}\left\{\frac{1}{(s+0)}\right\}+B_2\,L^{-1}\left\{\frac{1}{(s+\mu_1)}\right\}+B_3\,L^{-1}\left\{\frac{1}{(s+\mu_2)}\right\}+B_4L^{-1}\left\{\frac{1}{(s+\mu_3)}\right\} \quad \text{(J-58)}$$

$$L^{-1}\left\{\frac{1}{(s+0)}\right\}=1\ ,\ \ L^{-1}\left\{\frac{1}{(s+\mu_1)}\right\}=exp(-\mu_1 t)$$
$$L^{-1}\left\{\frac{1}{(s+\mu_2)}\right\}=exp(-\mu_2 t)\ ,\ \ L^{-1}\left\{\frac{1}{(s+\mu_3)}\right\}=exp(-\mu_3 t) \quad \text{(J-59)}$$

Using Equation J-59 in Equation J-58 gives

$$L^{-1}\left\{\frac{s^2+(a_1+a_{11})s+a_1a_{11}-a_3a_9}{(s+0)(s+\mu_1)(s+\mu_2)(s+\mu_3)}\right\}=B_1+B_2\,exp(-\mu_1 t)$$
$$+B_3\,exp(-\mu_2 t)+B_4\,exp(-\mu_3 t) \quad \text{(J-60)}$$

Inverse Laplace transform of the term of $\frac{a_7s+a_1a_7+a_3a_5}{(s+0)(s+\mu_1)(s+\mu_2)(s+\mu_3)}$ in Equation J-50 is obtained by separation of the terms as follows:

$$\frac{a_7s+a_1a_7+a_3a_5}{(s+0)(s+\mu_1)(s+\mu_2)(s+\mu_3)}=\frac{C_1}{(s+0)}+\frac{C_2}{(s+\mu_1)}+\frac{C_3}{(s+\mu_2)}+\frac{C_4}{(s+\mu_3)} \quad \text{(J-61)}$$

$$C_1=lim_{s\to 0}\,(s+0)\frac{a_7s+a_1a_7+a_3a_5}{(s+0)(s+\mu_1)(s+\mu_2)(s+\mu_3)}=\frac{a_1a_7+a_3a_5}{\mu_1\mu_2\mu_3} \quad \text{(J-62)}$$

$$C_2=lim_{s\to -\mu_1}\,(s+\mu_1)\frac{a_7s+a_1a_7+a_3a_5}{(s+0)(s+\mu_1)(s+\mu_2)(s+\mu_3)}$$
$$=-\frac{-a_7\mu_1+a_1a_7+a_3a_5}{\mu_1(\mu_2-\mu_1)(\mu_3-\mu_1)} \quad \text{(J-63)}$$

$$C_3=lim_{s\to -\mu_2}\,(s+\mu_2)\frac{a_7s+a_1a_7+a_3a_5}{(s+0)(s+\mu_1)(s+\mu_2)(s+\mu_3)}$$
$$=-\frac{-a_7\mu_2+a_1a_7+a_3a_5}{\mu_2(\mu_1-\mu_2)(\mu_3-\mu_2)} \quad \text{(J-64)}$$

$$C_4 = lim_{s\to -\mu_3}(s+\mu_3)\frac{a_7 s + a_1 a_7 + a_3 a_5}{(s+0)(s+\mu_1)(s+\mu_2)(s+\mu_3)}$$
$$= -\frac{-a_7\mu_3 + a_1 a_7 + a_3 a_5}{\mu_3(\mu_1-\mu_3)(\mu_2-\mu_3)} \qquad \text{(J-65)}$$

$$L^{-1}\left\{\frac{a_7 s + a_1 a_7 + a_3 a_5}{(s+0)(s+\mu_1)(s+\mu_2)(s+\mu_3)}\right\} = L^{-1}\left\{\frac{C_1}{(s+0)} + \frac{C_2}{(s+\mu_1)} + \frac{C_3}{(s+\mu_2)} + \frac{C_4}{(s+\mu_3)}\right\}$$
$$= C_1 L^{-1}\left\{\frac{1}{(s+0)}\right\} + C_2 L^{-1}\left\{\frac{1}{(s+\mu_1)}\right\} + C_3 L^{-1}\left\{\frac{1}{(s+\mu_2)}\right\} + C_4 L^{-1}\left\{\frac{1}{(s+\mu_3)}\right\} \qquad \text{(J-66)}$$

Substituting Equation J-59 into Equation J-66 gives

$$L^{-1}\left\{\frac{a_7 s + a_1 a_7 + a_3 a_5}{(s+0)(s+\mu_1)(s+\mu_2)(s+\mu_3)}\right\} = C_1 + C_2\, exp(-\mu_1 t) + C_3\, exp(-\mu_2 t) + C_4\, exp(-\mu_3 t) \qquad \text{(J-67)}$$

Inverse Laplace transform of the term of $\frac{s}{(s+\mu_1)(s+\mu_2)(s+\mu_3)}$ in Equations J-50 and J-51 is obtained by separation of the terms as follows:

$$\frac{s}{(s+\mu_1)(s+\mu_2)(s+\mu_3)} = \frac{D_1}{(s+\mu_1)} + \frac{D_2}{(s+\mu_2)} + \frac{D_3}{(s+\mu_3)} \qquad \text{(J-68)}$$

$$D_1 = lim_{s\to -\mu_1}(s+\mu_1)\frac{s}{(s+\mu_1)(s+\mu_2)(s+\mu_3)} = -\frac{\mu_1}{(\mu_2-\mu_1)(\mu_3-\mu_1)} \qquad \text{(J-69)}$$

$$D_2 = lim_{s\to -\mu_2}(s+\mu_2)\frac{s}{(s+\mu_1)(s+\mu_2)(s+\mu_3)} = -\frac{\mu_2}{(\mu_1-\mu_2)(\mu_3-\mu_2)} \qquad \text{(J-70)}$$

$$D_3 = lim_{s\to -\mu_3}(s+\mu_3)\frac{s}{(s+\mu_1)(s+\mu_2)(s+\mu_3)} = -\frac{\mu_3}{(\mu_1-\mu_3)(\mu_2-\mu_3)} \qquad \text{(J-71)}$$

$$L^{-1}\left\{\frac{s}{(s+\mu_1)(s+\mu_2)(s+\mu_3)}\right\} = L^{-1}\left\{\frac{D_1}{(s+\mu_1)} + \frac{D_2}{(s+\mu_2)} + \frac{D_3}{(s+\mu_3)}\right\}$$
$$= D_1 L^{-1}\left\{\frac{1}{(s+\mu_1)}\right\} + D_2 L^{-1}\left\{\frac{1}{(s+\mu_2)}\right\} + D_3 L^{-1}\left\{\frac{1}{(s+\mu_3)}\right\} \qquad \text{(J-72)}$$

Substituting Equation J-59 into Equation J-72 gives

$$L^{-1}\left\{\frac{s}{(s+\mu_1)(s+\mu_2)(s+\mu_3)}\right\} = D_1\, exp(-\mu_1 t) + D_2\, exp(-\mu_2 t) + D_3\, exp(-\mu_3 t) \tag{J-73}$$

Inverse Laplace transform of the term of $\frac{1}{(s+0)(s+\mu_1)(s+\mu_2)(s+\mu_3)}$ in Equations J-50 and J-51 is obtained by separation of the terms as follows:

$$\frac{1}{(s+0)(s+\mu_1)(s+\mu_2)(s+\mu_3)} = \frac{E_1}{(s+0)} + \frac{E_2}{(s+\mu_1)} + \frac{E_3}{(s+\mu_2)} + \frac{E_4}{(s+\mu_3)} \tag{J-74}$$

$$E_1 = lim_{s\to 0}\,(s+0)\frac{1}{(s+0)(s+\mu_1)(s+\mu_2)(s+\mu_3)} = \frac{1}{\mu_1\mu_2\mu_3} \tag{J-75}$$

$$E_2 = lim_{s\to -\mu_1}\,(s+\mu_1)\frac{1}{(s+0)(s+\mu_1)(s+\mu_2)(s+\mu_3)} = -\frac{1}{\mu_1(\mu_2-\mu_1)(\mu_3-\mu_1)} \tag{J-76}$$

$$E_3 = lim_{s\to -\mu_2}\,(s+\mu_2)\frac{1}{(s+0)(s+\mu_1)(s+\mu_2)(s+\mu_3)} = -\frac{1}{\mu_2(\mu_1-\mu_2)(\mu_3-\mu_2)} \tag{J-77}$$

$$E_4 = lim_{s\to -\mu_3}\,(s+\mu_3)\frac{1}{(s+0)(s+\mu_1)(s+\mu_2)(s+\mu_3)} = -\frac{1}{\mu_3(\mu_1-\mu_3)(\mu_2-\mu_3)} \tag{J-78}$$

$$\begin{aligned} L^{-1}\left\{\frac{1}{(s+0)(s+\mu_1)(s+\mu_2)(s+\mu_3)}\right\} &= L^{-1}\left\{\frac{E_1}{(s+0)} + \frac{E_2}{(s+\mu_1)} + \frac{E_3}{(s+\mu_2)} + \frac{E_4}{(s+\mu_3)}\right\} \\ &= E_1\, L^{-1}\left\{\frac{1}{(s+0)}\right\} + E_2\, L^{-1}\left\{\frac{1}{(s+\mu_1)}\right\} + E_3\, L^{-1}\left\{\frac{1}{(s+\mu_2)}\right\} + E_4 L^{-1}\left\{\frac{1}{(s+\mu_3)}\right\} \end{aligned} \tag{J-79}$$

Substituting Equation J-59 into Equation J-79 gives

$$\begin{aligned} L^{-1}\left\{\frac{1}{(s+0)(s+\mu_1)(s+\mu_2)(s+\mu_3)}\right\} &= E_1 + E_2\, exp(-\mu_1 t) \\ &\quad + E_3\, exp(-\mu_2 t) + E_4\, exp(-\mu_3 t) \end{aligned} \tag{J-79}$$

Inverse Laplace transform of the term of $\frac{1}{(s+\mu_1)(s+\mu_2)(s+\mu_3)}$ in Equations J-50 and J-51 is obtained by separation of the terms as follows:

$$\frac{1}{(s+\mu_1)(s+\mu_2)(s+\mu_3)} = \frac{F_1}{(s+\mu_1)} + \frac{F_2}{(s+\mu_2)} + \frac{F_3}{(s+\mu_3)} \tag{J-80}$$

$$F_1 = lim_{s\to-\mu_1}(s+\mu_1)\frac{1}{(s+\mu_1)(s+\mu_2)(s+\mu_3)} = \frac{1}{(\mu_2-\mu_1)(\mu_3-\mu_1)} \tag{J-81}$$

$$F_2 = lim_{s\to-\mu_2}(s+\mu_2)\frac{1}{(s+\mu_1)(s+\mu_2)(s+\mu_3)} = \frac{1}{(\mu_1-\mu_2)(\mu_3-\mu_2)} \tag{J-82}$$

$$F_3 = lim_{s\to-\mu_3}(s+\mu_3)\frac{1}{(s+\mu_1)(s+\mu_2)(s+\mu_3)} = \frac{1}{(\mu_1-\mu_3)(\mu_2-\mu_3)} \tag{J-83}$$

$$\begin{aligned} L^{-1}\left\{\frac{1}{(s+\mu_1)(s+\mu_2)(s+\mu_3)}\right\} &= L^{-1}\left\{\frac{F_1}{(s+\mu_1)} + \frac{F_2}{(s+\mu_2)} + \frac{F_3}{(s+\mu_3)}\right\} \\ &= F_1\,L^{-1}\left\{\frac{1}{(s+\mu_1)}\right\} + F_2\,L^{-1}\left\{\frac{1}{(s+\mu_2)}\right\} + F_3 L^{-1}\left\{\frac{1}{(s+\mu_3)}\right\} \end{aligned} \tag{J-84}$$

Substituting Equation J-59 into Equation J-84 gives

$$L^{-1}\left\{\frac{1}{(s+\mu_1)(s+\mu_2)(s+\mu_3)}\right\} = F_1\,exp(-\mu_1 t) + F_2\,exp(-\mu_2 t) + F_3\,exp(-\mu_3 t) \tag{J-85}$$

Inverse Laplace transform of the term of $\frac{a_{10}s + a_1a_{10} + a_2a_9}{(s+0)(s+\mu_1)(s+\mu_2)(s+\mu_3)}$ in Equation J-51 is obtained by separation of the terms as follows:

$$\frac{a_{10}s + a_1a_{10} + a_2a_9}{(s+0)(s+\mu_1)(s+\mu_2)(s+\mu_3)} = \frac{G_1}{(s+0)} + \frac{G_2}{(s+\mu_1)} + \frac{G_3}{(s+\mu_2)} + \frac{G_4}{(s+\mu_3)} \tag{J-86}$$

$$G_1 = lim_{s\to0}(s+0)\frac{a_{10}s + a_1a_{10} + a_2a_9}{(s+0)(s+\mu_1)(s+\mu_2)(s+\mu_3)} = \frac{a_1a_{10} + a_2a_9}{\mu_1\mu_2\mu_3} \tag{J-87}$$

$$G_2 = lim_{s\to -\mu_1}(s+\mu_1)\frac{a_{10}s + a_1a_{10} + a_2a_9}{(s+0)(s+\mu_1)(s+\mu_2)(s+\mu_3)}$$
$$= -\frac{-a_{10}\mu_1 + a_1a_{10} + a_2a_9}{\mu_1(\mu_2-\mu_1)(\mu_3-\mu_1)} \quad \text{(J-88)}$$

$$G_3 = lim_{s\to -\mu_2}(s+\mu_2)\frac{a_{10}s + a_1a_{10} + a_2a_9}{(s+0)(s+\mu_1)(s+\mu_2)(s+\mu_3)}$$
$$= -\frac{-a_{10}\mu_2 + a_1a_{10} + a_2a_9}{\mu_2(\mu_1-\mu_2)(\mu_3-\mu_2)} \quad \text{(J-89)}$$

$$G_4 = lim_{s\to -\mu_3}(s+\mu_3)\frac{a_{10}s + a_1a_{10} + a_2a_9}{(s+0)(s+\mu_1)(s+\mu_2)(s+\mu_3)}$$
$$= -\frac{-a_{10}\mu_3 + a_1a_{10} + a_2a_9}{\mu_3(\mu_1-\mu_3)(\mu_2-\mu_3)} \quad \text{(J-90)}$$

$$L^{-1}\left\{\frac{a_{10}s + a_1a_{10} + a_2a_9}{(s+0)(s+\mu_1)(s+\mu_2)(s+\mu_3)}\right\} = L^{-1}\left\{\frac{G_1}{(s+0)} + \frac{G_2}{(s+\mu_1)} + \frac{G_3}{(s+\mu_2)} + \frac{G_4}{(s+\mu_3)}\right\}$$
$$= G_1\,L^{-1}\left\{\frac{1}{(s+0)}\right\} + G_2\,L^{-1}\left\{\frac{1}{(s+\mu_1)}\right\} + G_3\,L^{-1}\left\{\frac{1}{(s+\mu_2)}\right\} + G_4L^{-1}\left\{\frac{1}{(s+\mu_3)}\right\} \quad \text{(J-91)}$$

Substituting Equation J-59 into Equation J-91 gives

$$L^{-1}\left\{\frac{a_{10}s + a_1a_{10} + a_2a_9}{(s+0)(s+\mu_1)(s+\mu_2)(s+\mu_3)}\right\} = G_1 + G_2\,exp(-\mu_1 t) + G_3\,exp(-\mu_2 t) + G_4\,exp(-\mu_3 t) \quad \text{(J-92)}$$

Inverse Laplace transform of the term of $\frac{s^2 + (a_1+a_6)s + a_1a_6 - a_2a_5}{(s+0)(s+\mu_1)(s+\mu_2)(s+\mu_3)}$ in Equation J-51 is obtained by separation of the terms as follows:

$$\frac{s^2 + (a_1+a_6)s + a_1a_6 - a_2a_5}{(s+0)(s+\mu_1)(s+\mu_2)(s+\mu_3)} = \frac{H_1}{(s+0)} + \frac{H_2}{(s+\mu_1)} + \frac{H_3}{(s+\mu_2)} + \frac{H_4}{(s+\mu_3)} \quad \text{(J-93)}$$

$$H_1 = lim_{s\to 0}(s+0)\frac{s^2 + (a_1+a_6)s + a_1a_6 - a_2a_5}{(s+0)(s+\mu_1)(s+\mu_2)(s+\mu_3)} = \frac{a_1a_6 - a_2a_5}{\mu_1\mu_2\mu_3} \quad \text{(J-94)}$$

$$H_2 = lim_{s\to -\mu_1}\,(s+\mu_1)\frac{s^2+(a_1+a_6)s+a_1a_6-a_2a_5}{(s+0)(s+\mu_1)(s+\mu_2)(s+\mu_3)}$$
$$= -\frac{\mu_1^2-(a_1+a_6)\mu_1+a_1a_6-a_2a_5}{\mu_1(\mu_2-\mu_1)(\mu_3-\mu_1)} \qquad \text{(J-95)}$$

$$H_3 = lim_{s\to -\mu_2}\,(s+\mu_2)\frac{s^2+(a_1+a_6)s+a_1a_6-a_2a_5}{(s+0)(s+\mu_1)(s+\mu_2)(s+\mu_3)}$$
$$= -\frac{\mu_2^2-(a_1+a_6)\mu_2+a_1a_6-a_2a_5}{\mu_2(\mu_1-\mu_2)(\mu_3-\mu_2)} \qquad \text{(J-96)}$$

$$H_4 = lim_{s\to -\mu_3}\,(s+\mu_3)\frac{s^2+(a_1+a_6)s+a_1a_6-a_2a_5}{(s+0)(s+\mu_1)(s+\mu_2)(s+\mu_3)}$$
$$= -\frac{\mu_3^2-(a_1+a_6)\mu_3+a_1a_6-a_2a_5}{\mu_3(\mu_1-\mu_3)(\mu_2-\mu_3)} \qquad \text{(J-97)}$$

$$L^{-1}\left\{\frac{s^2+(a_1+a_6)s+a_1a_6-a_2a_5}{(s+0)(s+\mu_1)(s+\mu_2)(s+\mu_3)}\right\} = L^{-1}\left\{\frac{H_1}{(s+0)}+\frac{H_2}{(s+\mu_1)}+\frac{H_3}{(s+\mu_2)}+\frac{H_4}{(s+\mu_3)}\right\}$$
$$= H_1\,L^{-1}\left\{\frac{1}{(s+0)}\right\}+H_2\,L^{-1}\left\{\frac{1}{(s+\mu_1)}\right\}+H_3\,L^{-1}\left\{\frac{1}{(s+\mu_2)}\right\}+H_4L^{-1}\left\{\frac{1}{(s+\mu_3)}\right\} \qquad \text{(J-98)}$$

Substituting Equation J-59 into Equation J-98 gives

$$L^{-1}\left\{\frac{s^2+(a_1+a_6)s+a_1a_6-a_2a_5}{(s+0)(s+\mu_1)(s+\mu_2)(s+\mu_3)}\right\} = H_1+H_2\,exp(-\mu_1 t) + H_3\,exp(-\mu_2 t)+H_4\,exp(-\mu_3 t) \qquad \text{(J-99)}$$

Substituting Equations J-60, J-67, J-73, J-79, and J-85 into Equation J-50, and substituting Equations J-73, J-79, J-85, J-92, and J-99 into Equation J-51 gives

$$\Delta p_{r1}(t) = L^{-1}\left\{\overline{\Delta p_{r1}}\right\} = \frac{w_{p,net1}}{\kappa_{r1}}\left[B_1 + B_2\, exp(-\mu_1 t) + B_3\, exp(-\mu_2 t) + B_4\, exp(-\mu_3 t)\right]$$
$$+ \frac{w_{p,net2}}{\kappa_{r2}}\left[C_1 + C_2\, exp(-\mu_1 t) + C_3\, exp(-\mu_2 t) + C_4\, exp(-\mu_3 t)\right]$$
$$+ a_8\left[D_1\, exp(-\mu_1 t) + D_2\, exp(-\mu_2 t) + D_3\, exp(-\mu_3 t)\right]$$
$$+ a_{13}\left[E_1 + E_2\, exp(-\mu_1 t) + E_3\, exp(-\mu_2 t) + E_4\, exp(-\mu_3 t)\right]$$
$$+ a_{14}\left[F_1\, exp(-\mu_1 t) + F_2\, exp(-\mu_2 t) + F_3\, exp(-\mu_3 t)\right] \qquad \text{(J-100)}$$

$$\Delta p_{r2}(t) = L^{-1}\left\{\overline{\Delta p_{r2}}\right\} = \frac{w_{p,net1}}{\kappa_{r1}}\left[G_1 + G_2\, exp(-\mu_1 t) + G_3\, exp(-\mu_2 t) + G_4\, exp(-\mu_3 t)\right]$$
$$+ \frac{w_{p,net2}}{\kappa_{r2}}\left[H_1 + H_2\, exp(-\mu_1 t) + H_3\, exp(-\mu_2 t) + H_4\, exp(-\mu_3 t)\right]$$
$$+ a_{12}\left[D_1\, exp(-\mu_1 t) + D_2\, exp(-\mu_2 t) + D_3\, exp(-\mu_3 t)\right]$$
$$+ a_{15}\left[E_1 + E_2\, exp(-\mu_1 t) + E_3\, exp(-\mu_2 t) + E_4\, exp(-\mu_3 t)\right]$$
$$+ a_{16}\left[F_1\, exp(-\mu_1 t) + F_2\, exp(-\mu_2 t) + F_3\, exp(-\mu_3 t)\right] \qquad \text{(J-101)}$$

or

$$\Delta p_{r1}(t) = \frac{w_{p,net1}}{\kappa_{r1}}\left[B_1 + B_2\, exp(-\mu_1 t) + B_3\, exp(-\mu_2 t) + B_4\, exp(-\mu_3 t)\right]$$
$$+ \frac{w_{p,net2}}{\kappa_{r2}}\left[C_1 + C_2\, exp(-\mu_1 t) + C_3\, exp(-\mu_2 t) + C_4\, exp(-\mu_3 t)\right]$$
$$+ exp(-\mu_1 t)\left[a_8 D_1 + a_{13} E_2 + a_{14} F_1\right]$$
$$+ exp(-\mu_2 t)\left[a_8 D_2 + a_{13} E_3 + a_{14} F_2\right]$$
$$+ exp(-\mu_3 t)\left[a_8 D_3 + a_{13} E_4 + a_{14} F_3\right]$$
$$+ a_{13} E_1 \qquad \text{(J-102)}$$

$$\Delta p_{r2}(t) = \frac{w_{p,net1}}{\kappa_{r1}}\left[G_1 + G_2\, exp(-\mu_1 t) + G_3\, exp(-\mu_2 t) + G_4\, exp(-\mu_3 t)\right]$$
$$+ \frac{w_{p,net2}}{\kappa_{r2}}\left[H_1 + H_2\, exp(-\mu_1 t) + H_3\, exp(-\mu_2 t) + H_4\, exp(-\mu_3 t)\right]$$
$$+ exp(-\mu_1 t)\left[a_{12} D_1 + a_{15} E_2 + a_{16} F_1\right]$$
$$+ exp(-\mu_2 t)\left[a_{12} D_2 + a_{15} E_3 + a_{16} F_2\right]$$
$$+ exp(-\mu_3 t)\left[a_{12} D_3 + a_{15} E_4 + a_{16} F_3\right]$$
$$+ a_{15} E_1 \qquad \text{(J-103)}$$

or

$$\Delta p_{r1}(t)=\frac{w_{p,net1}}{\kappa_{r1}}\left[\begin{array}{l}\dfrac{a_1a_{11}-a_3a_9}{\mu_1\mu_2\mu_3}-\dfrac{\mu_1^2-(a_1+a_{11})\mu_1+a_1a_{11}-a_3a_9}{\mu_1(\mu_2-\mu_1)(\mu_3-\mu_1)}exp(-\mu_1 t)\\ -\dfrac{\mu_2^2-(a_1+a_{11})\mu_2+a_1a_{11}-a_3a_9}{\mu_2(\mu_1-\mu_2)(\mu_3-\mu_2)}exp(-\mu_2 t)\\ -\dfrac{\mu_3^2-(a_1+a_{11})\mu_3+a_1a_{11}-a_3a_9}{\mu_3(\mu_1-\mu_3)(\mu_2-\mu_3)}exp(-\mu_3 t)\end{array}\right]$$

$$+\frac{w_{p,net2}}{\kappa_{r2}}\left[\begin{array}{l}\dfrac{a_1a_7+a_3a_5}{\mu_1\mu_2\mu_3}+\dfrac{a_7\mu_1-a_1a_7-a_3a_5}{\mu_1(\mu_2-\mu_1)(\mu_3-\mu_1)}exp(-\mu_1 t)\\ +\dfrac{a_7\mu_2-a_1a_7-a_3a_5}{\mu_2(\mu_1-\mu_2)(\mu_3-\mu_2)}exp(-\mu_2 t)\\ +\dfrac{a_7\mu_3-a_1a_7-a_3a_5}{\mu_3(\mu_1-\mu_3)(\mu_2-\mu_3)}exp(-\mu_3 t)\end{array}\right]$$

$$+exp(-\mu_1 t)\left[-\frac{a_8\mu_1^2-a_{14}\mu_1+a_{13}}{\mu_1(\mu_2-\mu_1)(\mu_3-\mu_1)}\right]exp(-\mu_2 t)\left[-\frac{a_8\mu_2^2-a_{14}\mu_2+a_{13}}{\mu_2(\mu_1-\mu_2)(\mu_3-\mu_2)}\right]$$

$$+exp(-\mu_3 t)\left[-\frac{a_8\mu_3^2-a_{14}\mu_3+a_{13}}{\mu_3(\mu_1-\mu_3)(\mu_2-\mu_3)}\right]+\frac{a_{13}}{\mu_1\mu_2\mu_3}$$

(J-104)

$$\Delta p_{r2}(t)=\frac{w_{p,net1}}{\kappa_{r1}}\left[\begin{array}{l}\dfrac{a_1a_{10}+a_2a_9}{\mu_1\mu_2\mu_3}+\dfrac{a_{10}\mu_1-a_1a_{10}-a_2a_9}{\mu_1(\mu_2-\mu_1)(\mu_3-\mu_1)}exp(-\mu_1 t)\\ +\dfrac{a_{10}\mu_2-a_1a_{10}-a_2a_9}{\mu_2(\mu_1-\mu_2)(\mu_3-\mu_2)}exp(-\mu_2 t)\\ +\dfrac{a_{10}\mu_3-a_1a_{10}-a_2a_9}{\mu_3(\mu_1-\mu_3)(\mu_2-\mu_3)}exp(-\mu_3 t)\end{array}\right]$$

$$+\frac{w_{p,net2}}{\kappa_{r2}}\left[\begin{array}{l}\dfrac{a_1a_6-a_2a_5}{\mu_1\mu_2\mu_3}-\dfrac{\mu_1^2-(a_1+a_6)\mu_1+a_1a_6-a_2a_5}{\mu_1(\mu_2-\mu_1)(\mu_3-\mu_1)}exp(-\mu_1 t)\\ -\dfrac{\mu_2^2-(a_1+a_6)\mu_2+a_1a_6-a_2a_5}{\mu_2(\mu_1-\mu_2)(\mu_3-\mu_2)}exp(-\mu_2 t)\\ -\dfrac{\mu_3^2-(a_1+a_6)\mu_3+a_1a_6-a_2a_5}{\mu_3(\mu_1-\mu_3)(\mu_2-\mu_3)}exp(-\mu_3 t)\end{array}\right]$$

$$+exp(-\mu_1 t)\left[-\frac{a_{12}\mu_1^2-a_{16}\mu_1+a_{15}}{\mu_1(\mu_2-\mu_1)(\mu_3-\mu_1)}\right]+exp(-\mu_2 t)\left[-\frac{a_{12}\mu_2^2-a_{16}\mu_2+a_{15}}{\mu_2(\mu_1-\mu_2)(\mu_3-\mu_2)}\right]$$

$$+exp(-\mu_3 t)\left[-\frac{a_{12}\mu_3^2-a_{16}\mu_3+a_{15}}{\mu_3(\mu_1-\mu_3)(\mu_2-\mu_3)}\right]+\frac{a_{15}}{\mu_1\mu_2\mu_3}$$

(J-105)

The shallow and deep reservoirs pressures as a function of production time are obtained by using Equations J-104 and J-105 as below.

$$
\begin{aligned}
p_{r1}(t) = p_{r1i} - \Bigg\{ & \frac{w_{p,net1}}{\kappa_{r1}} \left[\begin{array}{l} \dfrac{a_1 a_{11} - a_3 a_9}{\mu_1 \mu_2 \mu_3} - \dfrac{\mu_1^2 - (a_1 + a_{11})\mu_1 + a_1 a_{11} - a_3 a_9}{\mu_1 (\mu_2 - \mu_1)(\mu_3 - \mu_1)} exp(-\mu_1 t) \\ - \dfrac{\mu_2^2 - (a_1 + a_{11})\mu_2 + a_1 a_{11} - a_3 a_9}{\mu_2 (\mu_1 - \mu_2)(\mu_3 - \mu_2)} exp(-\mu_2 t) \\ - \dfrac{\mu_3^2 - (a_1 + a_{11})\mu_3 + a_1 a_{11} - a_3 a_9}{\mu_3 (\mu_1 - \mu_3)(\mu_2 - \mu_3)} exp(-\mu_3 t) \end{array} \right] \\
& + \frac{w_{p,net2}}{\kappa_{r2}} \left[\begin{array}{l} \dfrac{a_1 a_7 + a_3 a_5}{\mu_1 \mu_2 \mu_3} + \dfrac{a_7 \mu_1 - a_1 a_7 - a_3 a_5}{\mu_1 (\mu_2 - \mu_1)(\mu_3 - \mu_1)} exp(-\mu_1 t) \\ + \dfrac{a_7 \mu_2 - a_1 a_7 - a_3 a_5}{\mu_2 (\mu_1 - \mu_2)(\mu_3 - \mu_2)} exp(-\mu_2 t) \\ + \dfrac{a_7 \mu_3 - a_1 a_7 - a_3 a_5}{\mu_3 (\mu_1 - \mu_3)(\mu_2 - \mu_3)} exp(-\mu_3 t) \end{array} \right] \\
& + exp(-\mu_1 t) \left[- \frac{a_8 \mu_1^2 - a_{14} \mu_1 + a_{13}}{\mu_1 (\mu_2 - \mu_1)(\mu_3 - \mu_1)} \right] \\
& + exp(-\mu_2 t) \left[- \frac{a_8 \mu_2^2 - a_{14} \mu_2 + a_{13}}{\mu_2 (\mu_1 - \mu_2)(\mu_3 - \mu_2)} \right] \\
& + exp(-\mu_3 t) \left[- \frac{a_8 \mu_3^2 - a_{14} \mu_3 + a_{13}}{\mu_3 (\mu_1 - \mu_3)(\mu_2 - \mu_3)} \right] \\
& + \frac{a_{13}}{\mu_1 \mu_2 \mu_3}
\end{aligned}
\Bigg\}
$$

(J-106)

$$
p_{r2}(t) = p_{r2i} - \left\{ \begin{array}{l}
\dfrac{w_{p,net1}}{\kappa_{r1}} \left[\begin{array}{l}
\dfrac{a_1 a_{10} + a_2 a_9}{\mu_1 \mu_2 \mu_3} + \dfrac{a_{10}\mu_1 - a_1 a_{10} - a_2 a_9}{\mu_1 (\mu_2 - \mu_1)(\mu_3 - \mu_1)} exp(-\mu_1 t) \\
+ \dfrac{a_{10}\mu_2 - a_1 a_{10} - a_2 a_9}{\mu_2 (\mu_1 - \mu_2)(\mu_3 - \mu_2)} exp(-\mu_2 t) \\
+ \dfrac{a_{10}\mu_3 - a_1 a_{10} - a_2 a_9}{\mu_3 (\mu_1 - \mu_3)(\mu_2 - \mu_3)} exp(-\mu_3 t)
\end{array} \right] \\
+ \dfrac{w_{p,net2}}{\kappa_{r2}} \left[\begin{array}{l}
\dfrac{a_1 a_6 - a_2 a_5}{\mu_1 \mu_2 \mu_3} - \dfrac{\mu_1^2 - (a_1 + a_6)\mu_1 + a_1 a_6 - a_2 a_5}{\mu_1 (\mu_2 - \mu_1)(\mu_3 - \mu_1)} exp(-\mu_1 t) \\
- \dfrac{\mu_2^2 - (a_1 + a_6)\mu_2 + a_1 a_6 - a_2 a_5}{\mu_2 (\mu_1 - \mu_2)(\mu_3 - \mu_2)} exp(-\mu_2 t) \\
- \dfrac{\mu_3^2 - (a_1 + a_6)\mu_3 + a_1 a_6 - a_2 a_5}{\mu_3 (\mu_1 - \mu_3)(\mu_2 - \mu_3)} exp(-\mu_3 t)
\end{array} \right] \\
+ exp(-\mu_1 t) \left[- \dfrac{a_{12}\mu_1^2 - a_{16}\mu_1 + a_{15}}{\mu_1 (\mu_2 - \mu_1)(\mu_3 - \mu_1)} \right] \\
+ exp(-\mu_2 t) \left[- \dfrac{a_{12}\mu_2^2 - a_{16}\mu_2 + a_{15}}{\mu_2 (\mu_1 - \mu_2)(\mu_3 - \mu_2)} \right] \\
+ exp(-\mu_3 t) \left[- \dfrac{a_{12}\mu_3^2 - a_{16}\mu_3 + a_{15}}{\mu_3 (\mu_1 - \mu_3)(\mu_2 - \mu_3)} \right] \\
+ \dfrac{a_{15}}{\mu_1 \mu_2 \mu_3}
\end{array} \right\}
$$

(J-107)

AUTOBIOGRAPHY

Hulya Sarak graduated with 3rd highest GPA among senior class from Petroleum Engineering Department of Istanbul Technical University in 1993. She has taken M.Sc. degree from Petroleum and Natural Gas Engineering Department of Istanbul Technical University in 1997. She has received 3rd rank at M.Sc. division at Annual Student Paper Contest of Society of Petroleum Engineers Turkey section in 1997. She has been rewarded to attend the 1998 Geothermal Institute Diploma Course under funding from the New Zealand Ministry of Foreign Affairs and Trade through the Geothermal Institute of the University of Auckland. She is a research assistant in Department of Petroleum and Natural Gas Engineering at Istanbul Technical University since 1995. Her research interests include natural gas and geothermal reservoir engineering.